Progress in the Chemistry of Organic Natural Products

A. Douglas Kinghorn
Heinz Falk
Simon Gibbons
Jun'ichi Kobayashi *Editors*

104

Progress in the Chemistry of Organic Natural Products

Springer

Progress in the Chemistry of Organic Natural Products

More information about this series at http://www.springer.com/series/10169

A. Douglas Kinghorn • Heinz Falk •
Simon Gibbons • Jun'ichi Kobayashi
Editors

Progress in the Chemistry of Organic Natural Products

Volume 104

With contributions by

H. Falk · K. Wolkenstein

J. L. Ávila · G. Delgado · M. Del-Ángel · A. León

Springer

Editors
A. Douglas Kinghorn
Division of Medicinal Chemistry &
Pharmacognosy, College of Pharmacy
The Ohio State University
Columbus, Ohio
USA

Heinz Falk
Institute of Organic Chemistry
Johannes Kepler University Linz
Linz, Austria

Simon Gibbons
Research Department of Pharmaceutical
and Biological Chemistry
UCL School of Pharmacy
London, United Kingdom

Jun'ichi Kobayashi
Graduate School of Pharmaceutical Science
Hokkaido University
Sapporo, Japan

ISSN 2191-7043 ISSN 2192-4309 (electronic)
Progress in the Chemistry of Organic Natural Products
ISBN 978-3-319-45616-4 ISBN 978-3-319-45618-8 (eBook)
DOI 10.1007/978-3-319-45618-8

Library of Congress Control Number: 2017931072

Printed on acid-free paper

This Springer imprint is published by Springer Nature
The registered company is Springer International Publishing AG
The registered company address is: Gewerbestrasse 11, 6330 Cham, Switzerland

Contents

Natural Product Molecular Fossils

Heinz Falk and Klaus Wolkenstein

Contents

H. Falk (✉)
Institute of Organic Chemistry, Johannes Kepler University, Altenbergerstraße 69, 4040 Linz, Austria
e-mail: heinz.falk@jku.at; heinz@fa.lk

K. Wolkenstein (✉)
Department of NMR Based Structural Biology, Max Planck Institute for Biophysical Chemistry, Am Fassberg 11, 37077 Göttingen, Germany
e-mail: kwolken@gwdg.de

A.D. Kinghorn, H. Falk, S. Gibbons, J. Kobayashi (eds.), *Progress in the Chemistry of Organic Natural Products, Vol. 104*, DOI 10.1007/978-3-319-45618-8_1

1 Introduction

The living world of today is teeming with organic molecules called "natural products". These are produced by living organisms within their primary or secondary metabolism. In the realm of primary metabolism, these compounds are essential to the survival of the organism, whereas the secondary metabolites mostly have an extrinsic function that may also affect other organisms. About 170,000 natural products may be traced by browsing through the Internet (as e.g. [1]) and a cornucopia of these is described and illustrated in the more than hundred volumes of this "Progress in the Chemistry of Organic Natural Products" series.

One might safely infer that this natural product ensemble is not only characteristic of our times, but has been in place throughout the eons since life has begun on earth, with organisms continuously producing a multitude of compounds. Thus, one may ask which compounds or their diagenetic derivatives from these vast amounts of ancient natural products have survived to the present day, thereby resulting in natural product molecular fossils?

The first steps to answer this question were taken rather late within the historical realms of organic and natural product chemistry when, in the 1930s, Alfred Treibs (1899–1983), from the Technical University of Munich, characterized desoxophylloerythroetioporphyrin (**1**) and its vanadium and iron complexes and also deuteroetioporphyrin (**2**) from oil shales and certain coals (Fig. 1). He hypothesized that these compounds originated from the diagenetic transformations of chlorophyll a (**3**) and hemin (**4**), commonly referred to as the "Treibs Scheme" [2].

This finding has served as the origin of a novel area of research called "organic geochemistry", which studies the fate of organic materials in the different compartments of the geosphere through time. Accordingly, Alfred Treibs is considered as the "father" of this discipline. Interestingly enough, the compounds that can be isolated from sediments, oils, and micro- or macrofossils are not only of significance for scientific reasons, but are also quite important for commercial applications, in particular in the oil industry. Geological biomarkers constitute a subgroup of molecular fossils. These can be traced to a particular biological origin and are a vivid area of research.

In this contribution, the authors have aimed to provide an overview of molecular fossils in general and biomarkers in particular together with their bioprecursors, but without attempting to provide a complete inventory of these compounds. Methods used to identify molecular fossils and processes encountered for natural products during the ages will be described. For further reading, the comprehensive textbook "The Biomarker Guide" by Peters, Walters, and Moldowan [3] and the more historically focused work "Echoes of Life" by Gaines, Eglinton, and Rullkötter [4], are recommended.

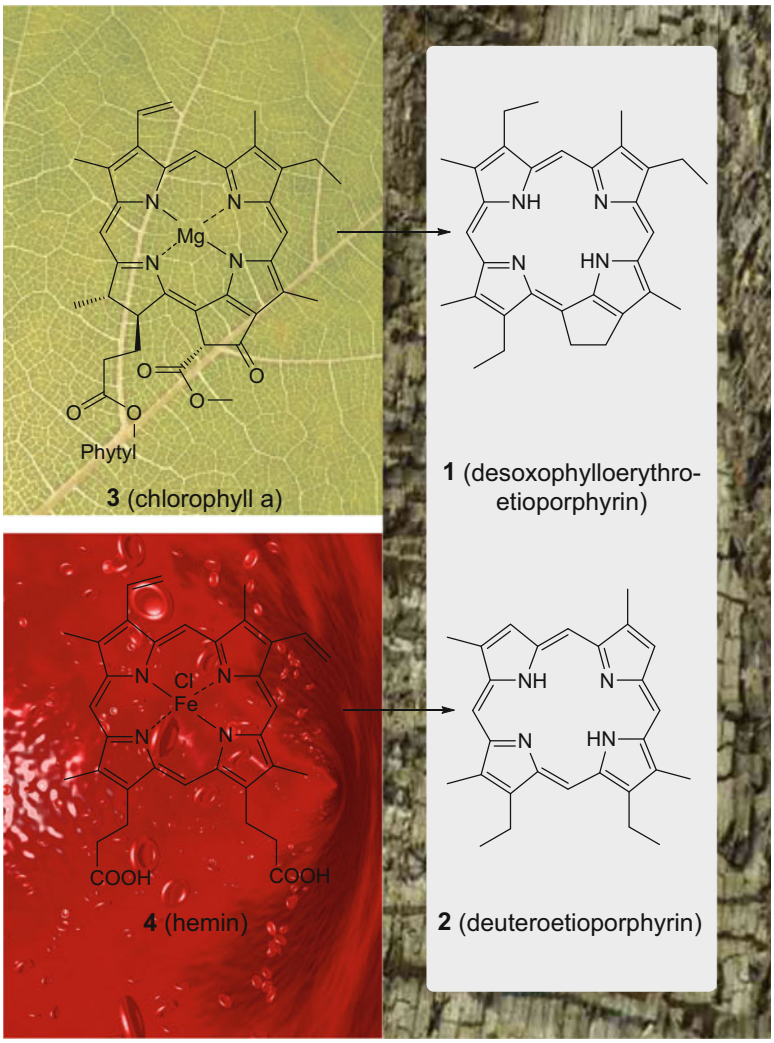

Fig. 1 The molecular fossils **1** and **2** produced from the natural products **3** and **4**: the "Treibs Scheme" hypothesis

2 Molecular Fossils and Their Bioprecursors

From a standpoint of organic chemistry, the molecular fossils found in sediments or micro- and macrofossils are divisible into apolar and polar compounds. For the first group, these substances are subdivided into linear and branched alkanes, alkenes, alicyclic compounds, and aromatic and heterocyclic systems. Within the polar compound class, structural systems of the apolar class bearing functional groups

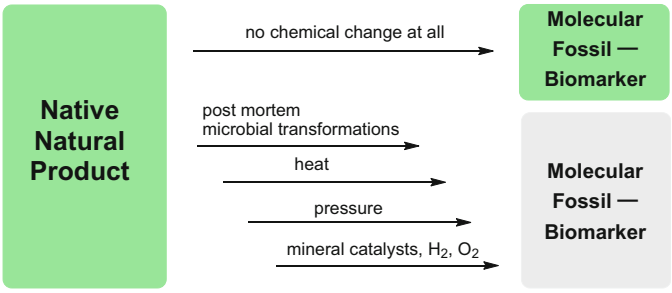

Fig. 2 From natural product to molecular fossil. Note that natural products and the molecular fossils remaining unchanged during geological times are color-coded with a light green background. Molecular fossils are color-coded with a gray background even when they form biomarkers

occur. Thus, among the polar molecular residues of long deceased organisms, ethers, alcohols, phenols, carbonyl compounds, quinones, and acids are evident. Finally, polymers of diverse polarities are found. All of these compounds are derived from their respective bioprecursors through the effects of diagenetic processes, and, accordingly, these precursors can be related to their fossilized compounds that can be isolated.

The ways in which the original natural products have been transformed during the ages are summarized in Fig. 2. For convenience, a geological time scale is provided in Fig. 108. Accordingly, a given native natural product can undergo no chemical transformation at all and occur in an unchanged form at the present time. Alternatively, such a natural product can undergo microbial transformations after the organism has died and become embedded into the sediment, or it could be transformed during diagenetic processes involving heat and pressure, involving mainly catalysis by accompanying minerals for oxidation, reduction, or fragmentation processes. The latter reactions may also involve secondary microbial products. These processes will be described in some depth in Sect. 4.

2.1 Apolar Compounds

Most of the apolar compounds to be discussed in this section were isolated from sediments in connection with oil exploration, or they may be constituents of petroleum. These apolar molecular fossils, which to some extent serve also as biomarkers, are of high importance in evaluating the source rock, age, and maturity of samples, but are also very interesting for the investigation of paleontological questions.

2.1.1 Linear Alkanes

Linear alkanes from methane through tetradecane are main constituents of gas and petroleum [5]. Although most of these are thought to be of biological origin, their sources are not able to be traced back, due to cracking processes that are mostly driven by thermodynamic equilibrations catalyzed by surrounding mineral catalysts. However, there are also non-biological geochemical sources of these hydrocarbons [6].

Interestingly enough, the molecular fossils with a carbon atom content from pentadecane (**5**) to pentatriacontane (**15**) (Fig. 3) display significantly higher ratios of odd- versus even-numbered alkanes [7]. This preference is also observed for present-day *n*-alkanes or their functional derivatives in the natural product area, which, of course, may point to the corresponding biosynthesis pathways (e.g. decarboxylation of even carbon-numbered fatty acids formed via the acetate pathway). It may be mentioned that a Fischer-Tropsch-type abiotic model synthesis starting from aqueous oxalic acid also produces homologous *n*-alkanes. However, no preference for even- or odd-numbered representatives occurs in this case [8].

The *n*-alkane molecular fossils can serve as biomarkers for both biological origin and depositional environment. Thus, **5**–**7** are characteristic for lacustrine or marine phytoplankton [9], but are found also in certain tropical marine environments [10]. Non-marine lacustrine algae contain mostly **9**–**13** [11], whereas terrestrial higher plants are rich in **11**–**13** stemming mainly from leaf waxes [9]. In red or green algae, a preponderance of **6** has been observed, whereas brown algae are rich

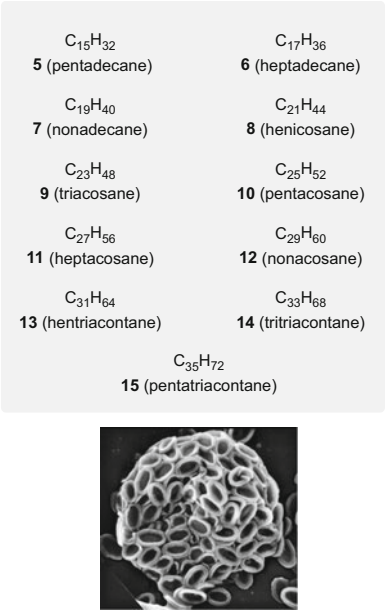

Fig. 3 Linear alkanes: molecular fossils and biomarkers **5**–**15**. Bottom: *Pleurochrysis carterae*, scanning electron microscopic image of coccosphere (Ø ≈ 10 μm) from a culture, courtesy of J. R. Young (UCL, London, UK)

in **5**. The coccolithophoride alga *Pleurochrysis carterae* (formerly known as *Syracosphaera carterae*) (Fig. 3) produces mainly **6** [7].

The relative amounts of certain linear alkanes have been used to calculate indices that correlate to some extent with the distribution of their sources. Thus, for example, the terrigenic/aquatic ratio as given by TAR = ([**11**] + [**12**] + [**13**])/([**5**] + [**6**] + [**7**]) [12], and is a measure to evaluate the weight of land (TAR >1) versus aquatic flora (TAR <1) contributing to an *n*-alkane mixture obtained from a certain sediment. This index is particularly useful in assigning environmental changes in a series of layers. However, care should be exercised as a result of the sensitivity of this index to thermal processes and biodegradation.

With respect to the use of linear alkane biomarkers, a recent detailed survey of modern plants [13] has shown that the distribution of leaf waxes is indicative for certain plants, but extreme care has to be exercised because of the very high annual variability in chain-length distribution. Only for *Sphagnum* (peat mosses) is a predominance of **9** and **10** characteristic. It is noteworthy that **9**, **10**, **11**, and **12** have been detected both in the Early Triassic horsetail *Equisetum brongniarti* from the Northern Vosges, France and in the extant *Equisetum sylvaticum* [14].

A useful distinction of sources can be derived from carbon isotope analysis conducted on terrestrial plant-derived *n*-alkanes. It turns out that $\delta^{13}C = [([^{13}C]/[^{12}C])_{sample}/([^{13}C]/[^{12}C])_{standard} - 1]\cdot 1000‰$ amounts to <–30‰ for C_3-plants like trees, and >–25‰ for C_4-plants like grasses [15].

The original natural products that gave rise to the *n*-alkane fossils may be unchanged leaf waxes or *n*-alkanes that are biosynthesized also by many other organisms in small quantities. Otherwise, they originate from diagenetic processes involving defunctionalization of fatty alcohols or decarboxylation of fatty acids.

2.1.2 Branched Alkanes

Branched alkanes of the *iso*- and *anteiso*-methyl types (Fig. 4) are found in crude oils. However, they do not constitute true biomarkers as they cannot be assigned unequivocally to molecular and organismic origins, because they can be also formed by abiogenic reactions like isomerizations and thermal cracking [16, 17]. In part, these branched alkanes may be derived from the decarboxylation of C_{15}–C_{25} *iso*- and *anteiso*-fatty acids characteristic of demosponges [18].

Cyanobacteria synthesize monomethyl alkanes that bear the methyl group at a further "inside" position. Thus, 4- to 8-methyl alkanes are produced, as exemplified

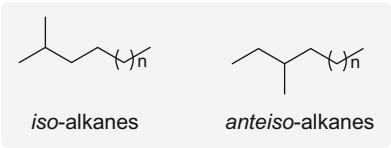

Fig. 4 *iso*- and *anteiso*-Alkanes (n = 9–19)

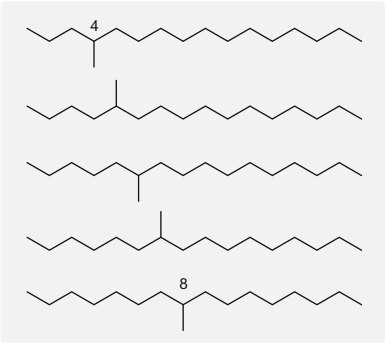

Fig. 5 The 4- to 8-methylhexadecane isomers produced by cyanobacteria

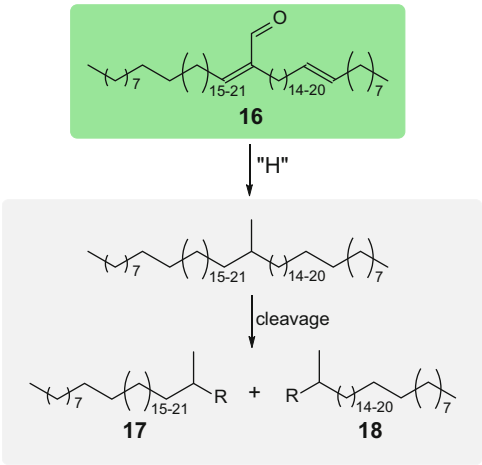

Fig. 6 Formation of monomethylalkanes **17** and **18** from botryals **16**

by the methylhexadecanes shown in Fig. 5 up to the series of methylhenicosanes [19]. These are found in rather recent sediments associated with microbial mats [20], but can be traced also down to the Infracambrian [21].

A rather unusual homologous series of the methyl-*n*-alkanes **17** and **18** occurred in the extractable matter of Permian to Carboniferous torbanites, which represent sediments rich in organic materials. These sediments, in particular, those of Glen Davis in the Permian Sydney basin, contain high levels (≈90%) of the fossil remains of the colonial cellular alga *Botryococcus braunii* (for a picture of this organism, see Fig. 13) [22]. The methyl alkanes extracted from these sediments are characterized by chain lengths from 23 to 31 carbon atoms with the methyl group at positions 2, 3, 4, etc. Since modern *B. braunii* contains large amounts of the so-called botryals (**16**), it was hypothesized that the two homologous series are derived from **16** by microbial/diagenetic transformations, as shown in Fig. 6, thereby generating these biomarkers of *B. braunii*.

Monosubstituted alkane series reminiscent of the letter T, i.e. chains substituted with residues larger than methyl, were found in crude oils [23]. Altogether, 163 isomers have been identified, comprising compounds with a single *n*-alkyl branch in the range of the C_{10}–C_{20} isomers, together with C_{21}–C_{25} isomers containing one ethyl branch. However, these seem to be more products of thermodynamic equilibration processes rather than organisms, and thus cannot be used as biomarkers.

Rather rare branched series of *n*-alkanes were detected in Early Cretaceous black shales, but also in deep-sea hydrothermal waters, and in addition, in a variety of shales covering at least 800 million years, and thereby appear to be rather widespread in the geological record [24]. These series consist of 2,2-dimethylalkanes with even carbon numbers between 16 and 26, and 3,3- and 5,5-diethylalkanes with odd carbon numbers from 15 to 29, obviously being characteristic of products of biosynthesis. The source compounds and organisms are unknown for these *geminally* substituted compounds, which possess a quaternary carbon atom that is not found commonly in organic natural products. The paleogeographic distribution of these molecular fossils suggests non-photosynthesizing sulfide-oxidizing organisms as their source.

Most multiply methyl branched *n*-alkanes isolated from oil or sediments are recognized readily as molecular fossils of isoprenoids because of their skeletal patterns. The first group of linear isoprenoid compounds to be mentioned are the regular head-to-tail linked isoprenoids. When the phytol chain of chlorophylls a or b (mostly used by phototropic organisms like land plants or algae), bacteriochlorophylls c or d (characteristic of purple sulfur bacteria), or phytanyl ethers of methanogens, is hydrolyzed, the resulting phytol (**16**) can be transformed further by diagenesis (Fig. 7) [25]. Within oxic environments on the one hand, pristane (**17**) is formed by oxidation to phytenic acid (**18**), which decarboxylates to pristene (**19**) and is reduced eventually to **17** (Fig. 7a) On the other hand, suboxic saline environments yield phytane (**20**) via dihydrophytol (**21**) as delineated in Fig. 7b. Accordingly, the ratio between **17** and **20** may be used as an indicator of oxic versus suboxic depositional environments [25]. However, they cannot be used as biomarkers in a more specific way than pointing to photosynthesizing organisms within a certain environment.

Interestingly enough, it has turned out that pristane (**17**) can be produced also by reductive cleavage of a common antioxidant, α-tocopherol (**22**), found in plants and algae [26]. This route commences with a thermal electrocyclic ring opening as shown in Fig. 8. However, the preponderance of chlorophylls over **22** in the biota (the ratio [**22**]/[**3**] in photosynthesizing organisms is in the order of 0.01–0.12 [27]) would perhaps make this a rather minor source. Another source of **17** in marine sediments could result from the metabolic transformation of phytol (**16**) biosynthesized by the zooplankton *Calanus hyperboreus* (Fig. 7). This organism uses **16** because of its low density (0.85 g/cm^3) to adjust its buoyancy in the water column [28].

Regular head-to-tail linear isoprenoids with a carbon content from 13 to 20 are often encountered in crude oils and source rock extracts. However, a specific source cannot be assigned. Such compounds could either originate from farnesyl residues

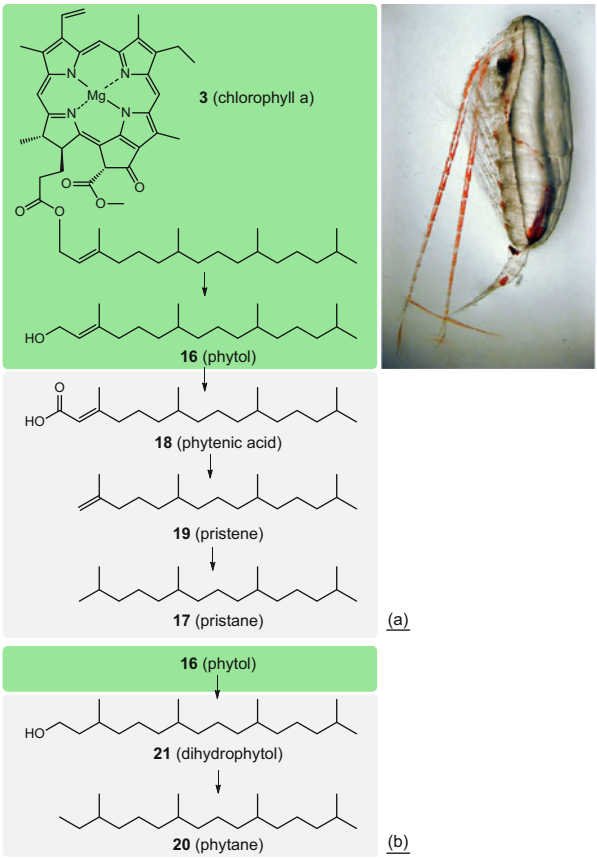

Fig. 7 Formation of pristane (**17**) and phytane (**20**) from e.g. chlorophyll a (**3**) in (**a**) oxic and (**b**) suboxic environments. Right: *Calanus hyperboreus* (length ~8 mm), which produces **16** for better buoyancy; photograph: S. Kwasniewski, WoRMS

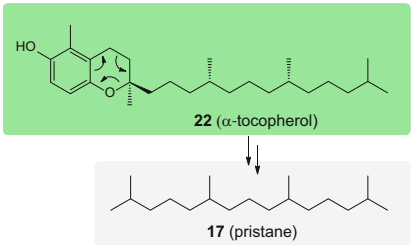

Fig. 8 Formation of pristane (**17**) from α-tocopherol (**22**)

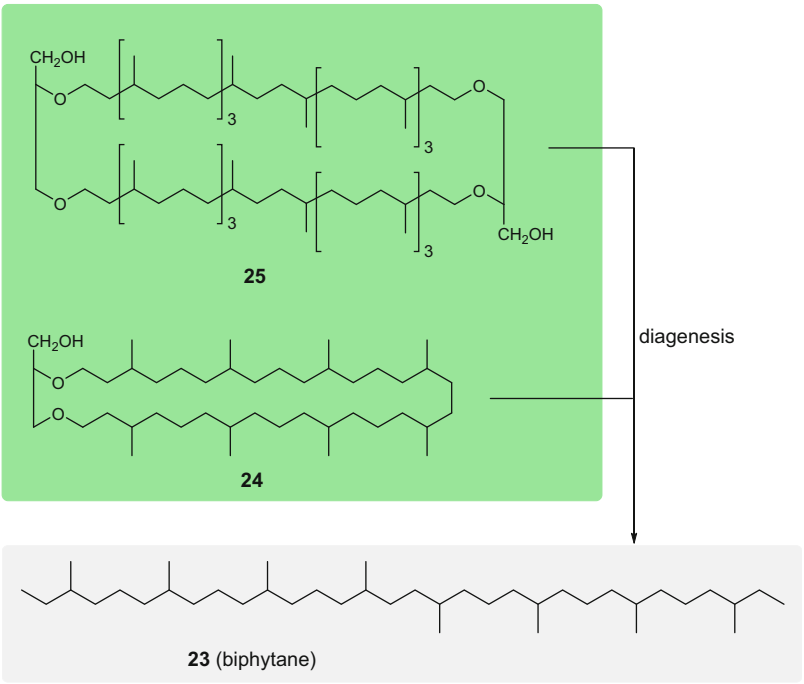

Fig. 9 The archaean biomarker biphytane (**23**), an irregular head-to-head isoprenoid and its biogenic precursor lipids **24** and **25**

or certain isoprenoid aldehydes and ketones. Sometimes the ratio of individual components is used to assess the correlation of oil sources [29]. Regular linear isoprenoids with carbon numbers higher than 20 are used to diagnose saline environments, as in e.g. a C_{25} isoprenoid hydrocarbon that has been reported [30]. The latter compound is likely to be derived from halophilic Archaea [31].

The second group of linear isoprenoid compounds to be mentioned contains the irregular head-to-head and tail-to-tail linked isoprenoids. Such head-to-head linear isoprenoids ranging in carbon numbers from 28 to 39 were found, for example, in Jurassic oils from Siberia [32]. The series consist of representatives formed by head-to-head linking of either pristane (**17**) or phytane (**20**) to units composed of 28–40 carbon atoms. The members of these series are highly specific biomarkers for Archaea as exemplified by biphytane (**23**), which originates from the glycerol diether (**24**) or tetraether lipids (**25**) that form structural elements of archaean membranes (Fig. 9).

In the realm of the irregular tail-to-tail isoprenoids, crocetane (**26**), which is derived by diagenetic reduction of the archaean-produced crocetene (**27**), is used as a biomarker for anaerobic methanotrophic and methanogenic Archaea as e.g. reported in [33]. 2,6,10,19-Tetramethylicosane (**28**) is also indicative of

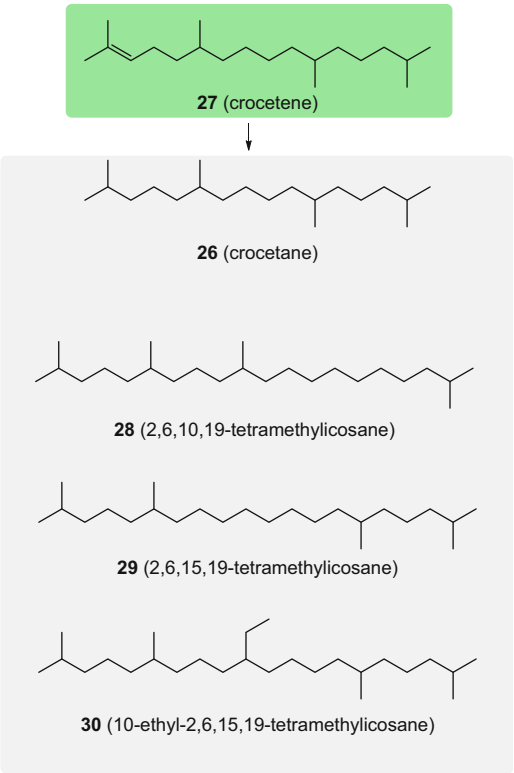

Fig. 10 Irregular tail-to-tail isoprenoids: crocetane (**26**), crocetene (**27**), and alkyl substituted icosanes **28**–**30**

methanotrophic and methanogenic Archaea. It occurs, for example, in the Maastrichtian-Danian (Late Cretaceous–Early Paleocene) shale of the Californian Moreno Formation. Whether or not this hydrocarbon is genuine or derived from a functional precursor is unknown [34]. The structurally related 2,6,15,19-tetramethylicosane (**29**) was identified in sediments from the Albian (Early Cretaceous) black Niveau Paquier shale from southeastern France. Its biological origin is unknown hitherto as is the case for the concomitant 10-ethyl-2,6,15,19-tetramethylicosane (**30**) [35] (Fig. 10).

Squalane (**31**) was identified from crude oil [36], but its ubiquitously occurring precursor squalene (**32**) makes it hardly a specific biomarker. However, high concentrations of **31** in sediments that are also rich in 2,6,10,19-tetramethylicosane (**28**) point to an archaean origin [37]. Two tetramethylsqualanes, 3,7,18,22- (**33**) and 3,7,11,14-tetramethylsqualene (**34**), were isolated from Sumatran crude oil of the Miocene to Pleistocene Duri and Minas wells of the central basin. These are highly specific for *Botryococcus braunii* and a lacustrine origin [38]. Anoxic conditions in lacustrine sediments like those of the famous German Eocene Messel

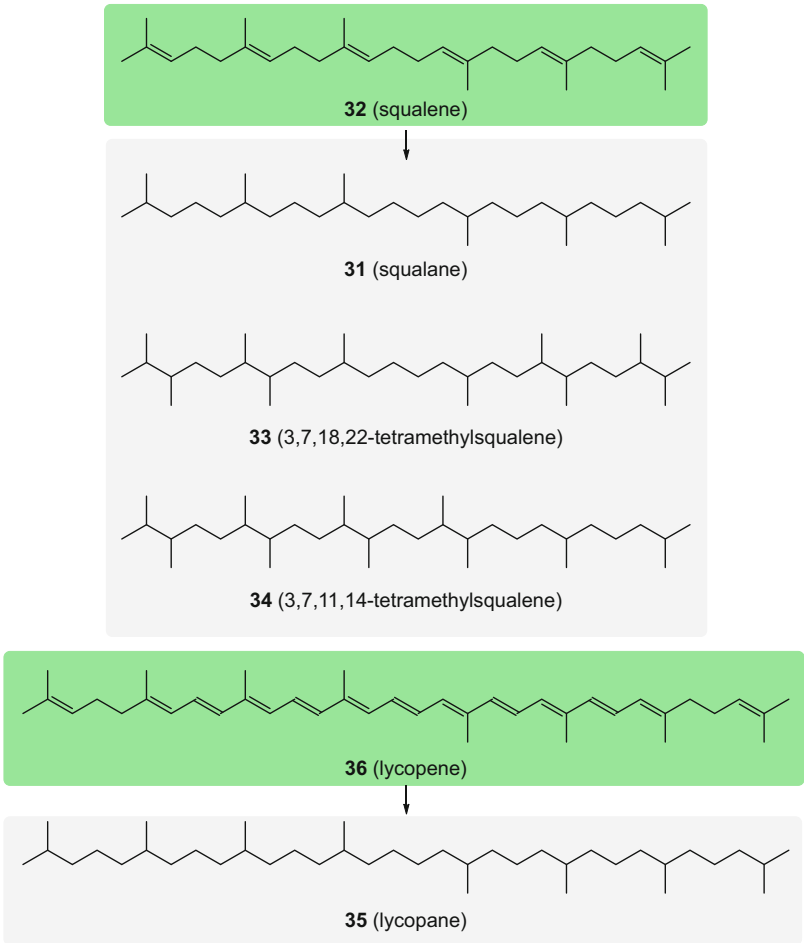

Fig. 11 Irregular tail-to-tail isoprenoids **31–36**

and Australian Miocene Condor oil shales lead to the abundant lycopane (**35**) [39] (Fig. 11). The most obvious source of **35** is the carotenoid lycopene (**36**), which is found in many microorganisms and plants. Thus, **35** also has rather low organismic specificity.

Highly branched isoprenoids are possible diatom markers in Quaternary down to Jurassic source rocks and the corresponding oils [40–42]. The three most prominent types **37**−**39** are characterized by C_{20}, C_{25}, and C_{30} carbon contents (Fig. 12). The biological origin of the highly branched isoprenoids is nicely corroborated by finding various C_{25} and C_{30} unsaturated derivatives in cultures of the diatoms *Haslea ostrearia* and *Rhizosolenia setigera* [43]. Trienes, tetraenes, and pentaenes are preferentially produced [44], as exemplified by (5*E*,9*E*,12*E*,16*E*)-2,6,10,14,18-

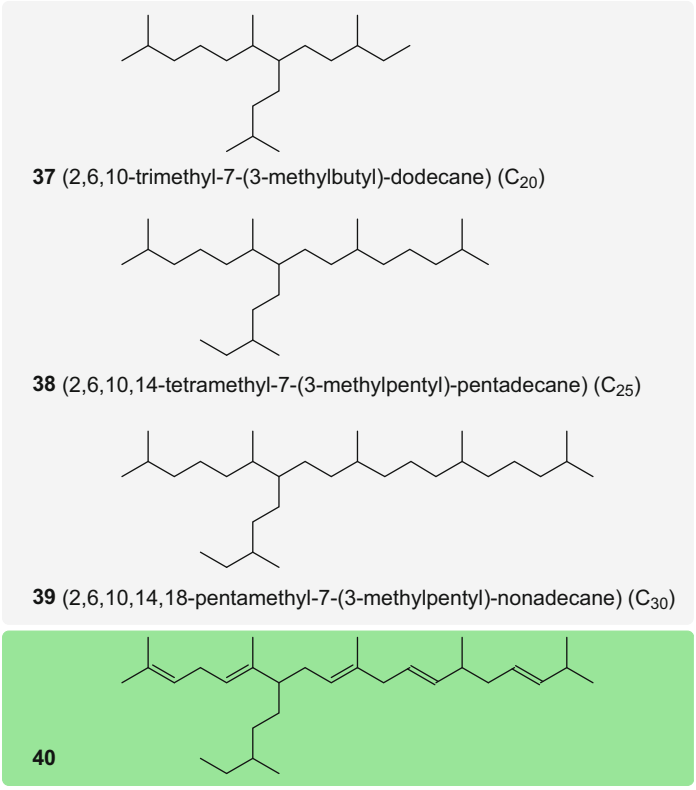

Fig. 12 Highly branched isoprenoids **37**–**39** and the pentaene **40**. Bottom: *Haslea ostrearia*; photograph courtesy of K. Wenderoth (Ebsdorfergrund, Germany)

pentamethyl-7-(3-methylpentyl)nonadeca-2,5,9,12,16-pentaene (**40**) (Fig. 12). These unsaturated derivatives readily reduce diagenetically to saturated compounds. Since diatoms evolved in the Jurassic period, such highly branched isoprenoids can be used to clarify age-related questions or assist in chemostratigraphic investigations [44].

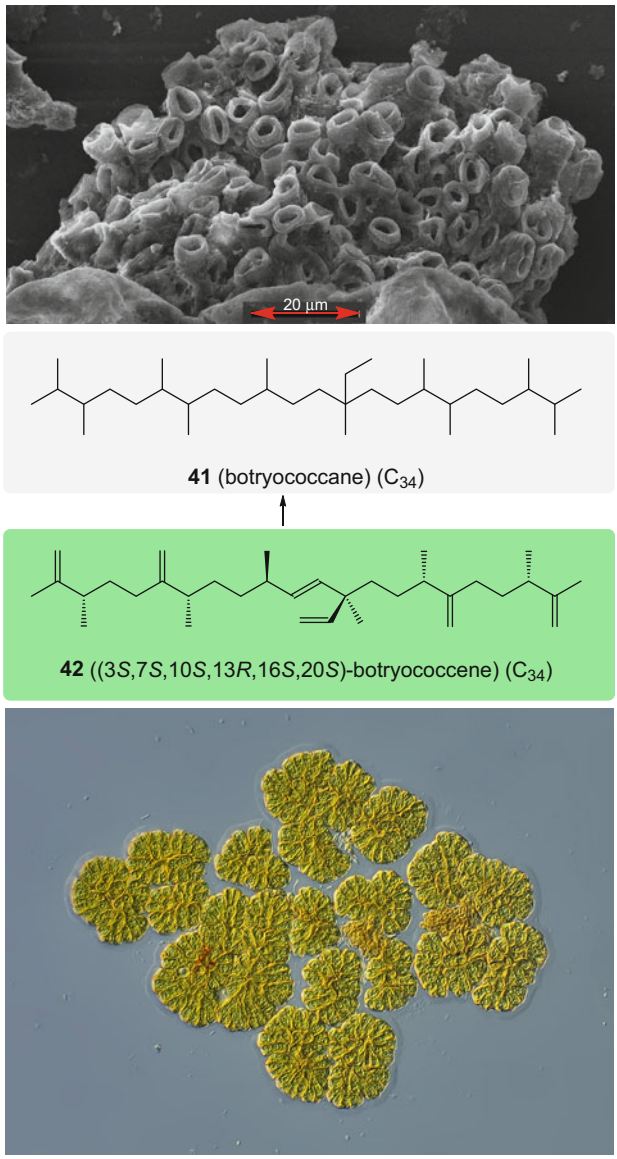

Fig. 13 Botryococcane (**41**) and botryococcene (**42**). Top: scanning electron microscopic image of a Late Visean (Carboniferous) *Botryococcus* sp. colony from Roncador creek, Parnaíba Basin, NE Brazil; photograph courtesy of M. di Pascquo (National Research Council of Argentina, Laboratorio de Palinología y Paleobotánica, Entre Rios, Argentina). Bottom: colony of extant *Botryococcus braunii*; photograph courtesy of M. Plewka (Gevelsberg, Germany, plingfactory.de)

The irregular C_{34}-isoprenoid botryococcane (**41**) (Fig. 13), which can be found in association with fossil colonies of *Botryococcus braunii* from the Late Proterozoic up to the Quaternary period (e.g. [22]), derives diagenetically from the

only known producer of botryococcene (**42**), the fresh to brackish water alga *B. braunii* [45, 46]. In addition, sixteen C_{30}–C_{37} botryococcenes could be characterized from this organism [47]. The first, C_{34} botryococcene, was found in a wild strain from an English lake [48]. It should be mentioned that botryococcene was characterized completely with respect to its absolute configuration as (3*S*,7*S*,10*S*,13*R*,16*S*,20*S*)-**42** [49] (Fig. 13). Note that compounds **41** and **42** display an unusual differentially functionalized quaternary carbon atom at C-10, which is rather rare for this class of natural products.

2.1.3 Alicyclic Compounds

The molecular fossils to be discussed in this section are either simple alkyl substituted cycloalkanes or belong to the terpenoids, steroids, and carotenoids—groups containing vast numbers of compounds.

Alkyl Substituted Alicycles

Alkyl substituted cycloalkanes may be traced in sediments and crude oils stemming from nearly all geological times. Although they mostly are not able to be assigned to specific biomolecular sources, they nevertheless constitute a heritage of past living organisms [50]. These molecular fossils are likely the products of thermal processes during petroleum catagenesis [51].

An extremely interesting example of an ensemble of alkyl cycloalkanes comes from an investigation of the sediments of the Cretaceous/Paleogene boundary at Kawaruppu, Hokkaido, Japan [52]. More than sixty alkyl cycloalkanes could be identified in the layers above, within, and below the famous Cretaceous/Paleogene boundary. Thus, the homologous series of alkyl cyclohexanes **43**–**61**, the dialkylcyclohexanes **62**–**67**, the methylalkylcyclohexanes **68**–**82**, the di- to tetramethylcyclohexanes **83**–**85** (Fig. 14), the homologous series of alkylcyclopentanes **86**–**103**, the decalin derivatives **104** and **105**, and finally even the bicyclic hydrocarbon bicyclo[3.3.1]nonane (**106**) could be characterized (Fig. 15). It is quite intriguing that the distributions of these compounds vary between the sediment layers corresponding to the Cretaceous and Paleogene periods, and thus are related in some way to the famous mass extinction event at the end of the Cretaceous period, which also led to the extinction of the dinosaurs [53].

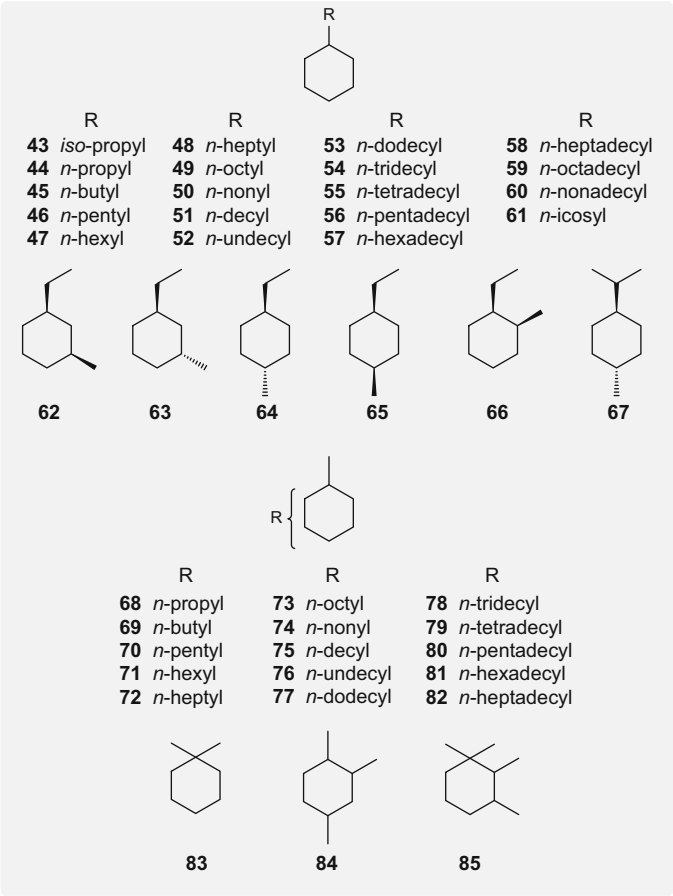

Fig. 14 Alkylcyclohexanes **43-85**

Interestingly, a non-isoprenoid macrocyclic alkane series from cyclopentadecane through cyclotetratriacontane (**107**) with a maximal abundance of cyclohenicosane and a series of monomethylated homologs from cycloheptadecane through cyclohexacosane (**108**) (Fig. 15) was found in a Carboniferous torbanite rich in *Botryococcus braunii* fossils [54]. It is apparent that these compounds originated from this organism.

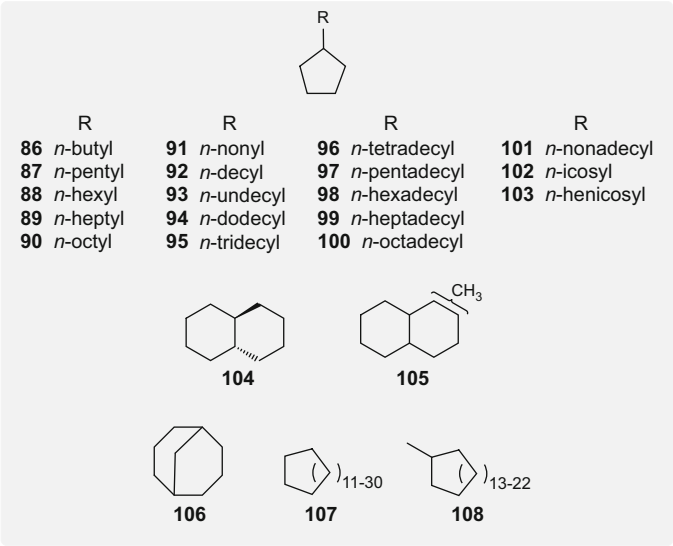

Fig. 15 Alkylcyclopentanes **86–103**, decalins **104** and **105**, bicyclo[3.3.1]nonane (**106**), and the cycloalkanes **107** and methylcycloalkanes **108**

Cyclic Sesquiterpanes

There are only few examples of cyclic sesquiterpanes found as molecular fossils. Thus, two bicyclic sesquiterpanoids, drimane (**109**) and 4β-eudesmane (**110**) (Fig. 16), clearly related to prokaryotic, and, in particular, higher plant terpenes, were identified in oils of the Cretaceous Cormorant Field in the Gippsland Basin, east of Melbourne, Victoria, Australia [55]. Several other sesquiterpene derivatives inclusive of **111** and **112** have been traced in sediments, lignites, or petroleum, but their origin does not seem to be specific for specific organisms [56].

Cyclic Diterpanoids

The monocyclic diterpenoid cembrene (**113**) (Fig. 17) and related compounds were reported to be products of the mild alkaline hydrolysis of kerogen from a lacustrine sediment of the Nördlinger Ries in southern Germany [57]. Most probably, resinous plants containing cembrene derivatives (esters), characteristic of a semiarid climate, were the sources.

The bicyclic diterpane molecular fossils are represented by cadinane (**114**) and two bicadinane isomers **115** and **116** (Fig. 18) found in Miocene Southeast Asian rock extracts and oils [58–61]. Cadinane (**114**) is thought to originate from gymnosperm dammar resins [62], making it a true biomarker for these plants. It was found together with the bicadinanes **115** and **116** in Late Triassic–Middle Jurassic oils from the Perth Basin, Western Australia [63].

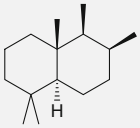

109 (drimane)

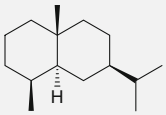

110 (4*β*-eudesmane)

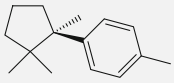

111 ((*R*)-1-methyl-4-(1,2,2-trimethylcyclopentyl)benzene)

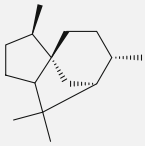

112 ((3*R*,3a*S*,6*S*,7*S*)-3,6,8,8-tetramethyloctahydro-1*H*-3a,7-methanoazulene)

Fig. 16 Drimane (**109**), 4*β*-eudesmane (**110**), and sesquiterpane derivatives **111** and **112**

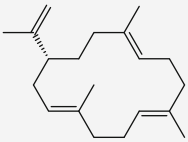

113 (cembrene)

Fig. 17 Cembrene (**113**)

From the tricyclic diterpanes, fichtelite (**117**) is the most prominent member. It was first described in 1841 as a rare organic mineral (Nickel-Strunz class 10.BA.05) accompanying pine wood residues found in peat bogs in the area of the Bavarian Fichtelgebirge (Germany), and named according to its geographical source [64]. Its structure was solved by the chemistry Nobel Prize winner Leopold Ruzicka, in the course of his fundamental studies of isoprenoids [65]. This biomarker is clearly the diagenetic product of the main pine resin component, the tricyclic diterpene abietic acid (**118**) (Fig. 19). From the partial to the de novo syntheses, the elegant preparation of (±)-**117** by Taber and Saleh should be mentioned [66] (Fig. 20).

Related organic minerals derived from conifer diterpanes and found together with **117** in conifer resin fossils are simonellite (**119**) (Nickel-Strunz class 10.

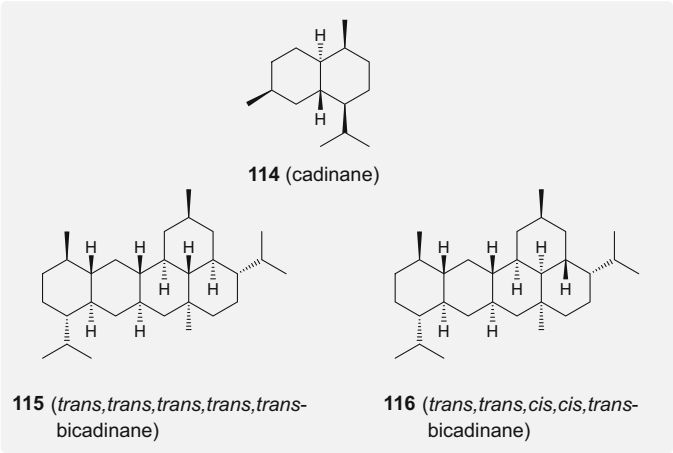

Fig. 18 Cadinane (**114**) and the bicadinanes **115** and **116**

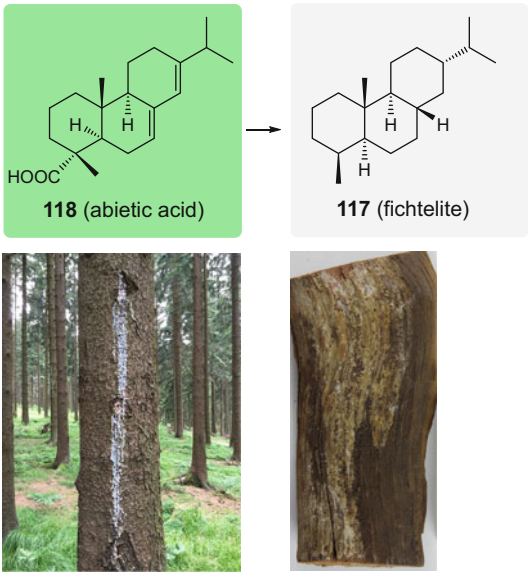

Fig. 19 Fichtelite (**117**) and abietic acid (**118**). Right plate: **117**, Redwitz, Germany; Mineral Collection of the Museum of Natural History, Vienna; photograph courtesy of Vera Hammer. Left plate: its tree source *Picea abies*, producing pitch with its main constituent abietic acid (**118**); photograph: H. Falk

BA.45; Fig. 21), named after its discoverer Vittorio Simonelli [67], and retene, also named phylloretine (**120**) (Nickel-Strunz class 10.BA.35) [68]. The latter seems to be indicative of wood fires. The extremely rare organic mineral dinite (**121**) (Nickel-Strunz class 10.BA.15) accompanying bituminous fossil wood, coal, and

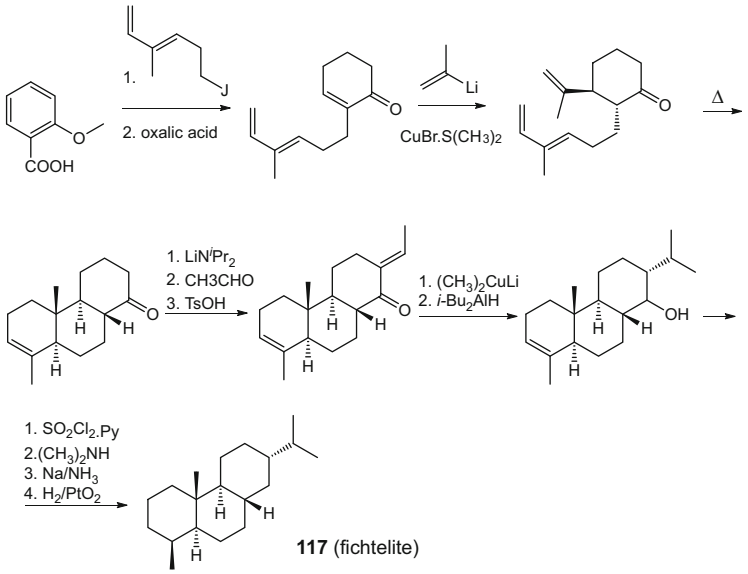

Fig. 20 Synthesis of fichtelite (**117**)

river sediments has been found in Castelnuovo di Garfagna, Tuscany, Italy (Late Miocene) [69]. Together with fichtelite (**117**) the latter was also identified along with a wealth of other bicyclic diterpanes (**122**–**127**) in crude oil and source rock of the Late Cretaceous Gippsland Basin, Australia, but in this case **121** was named isopimarane [70] (Fig. 21).

From the last-mentioned source, several tetracyclic diterpanoids **128**–**135** were also identified besides the bicyclic diterpanoids mentioned [70–73] (Fig. 22). These terpanes are related to diterpanes of conifer leaf resins from the families Podocarpaceae, Araucariaceae, and Cupressaceae. Phyllocladanes **131** and **132** are typical of resins from the genera *Podocarpus* and *Dacrydium*, while the kauranes **129** and **130** were found in *Agathis*. All of these markers were also identified in the Early Carboniferous Gondwana coal of Niger [74]. It comes as no surprise that such tetracyclic diterpenes are widely distributed, for example, as described by Simoneit et al. [75]. This group investigated samples of a Devonian coal from Luquan, Yunnan Province, People's Republic of China, with respect to the fact that their skeleton is closely related to the gibberellins, which are ubiquitous plant hormones. Since the Gymnospermae did not yet occur in the Devonian period, it is thought that the tetracyclic terpanes could be of microbial, fungal, or lower plant origin. Beyerane (**128**) occurs as a main terpane component in coals of the Saarland whereas Ruhr coal (both Germany) contains higher proportions of kauranes **129** and **130** [76]. These coals originated in the Carboniferous period before the families Podocarpaceae, Araucariaceae, and Cupressaceae had evolved. Thus, these diterpanes may be derived from early conifers of the order Voltziales

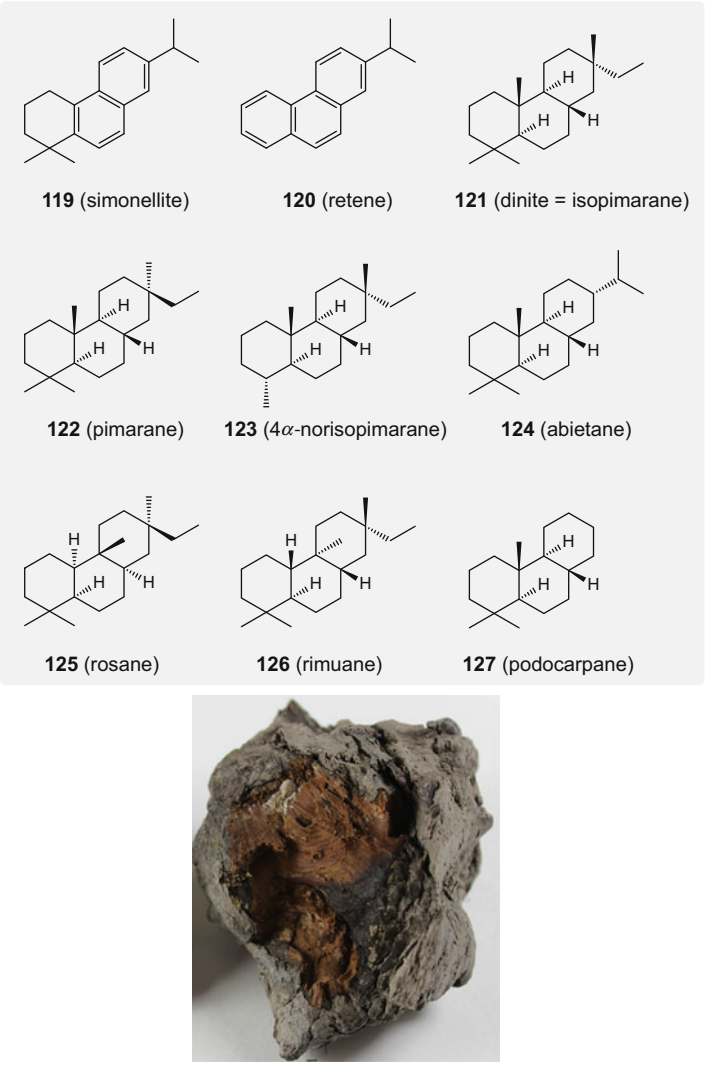

Fig. 21 Tricyclic diterpane biomarkers **119**-**127**. Bottom: simonellite (**119**), Monte Pulciano, Toscana, Italy, Mineral Collection of the Museum of Natural History, Vienna, inv. no. J6938; photograph courtesy of Vera Hammer (NHM, Vienna)

already present during this period. In addition to this suite of compounds, the tetracyclic organic mineral hartite (**136**) (Nickel-Strunz class 10.BA.10) (Fig. 22) was described 1841 and named by its discoverer Wilhelm von Haidinger after the Oberhart coal mine in Lower Austria [77]. As judged from its structure and the

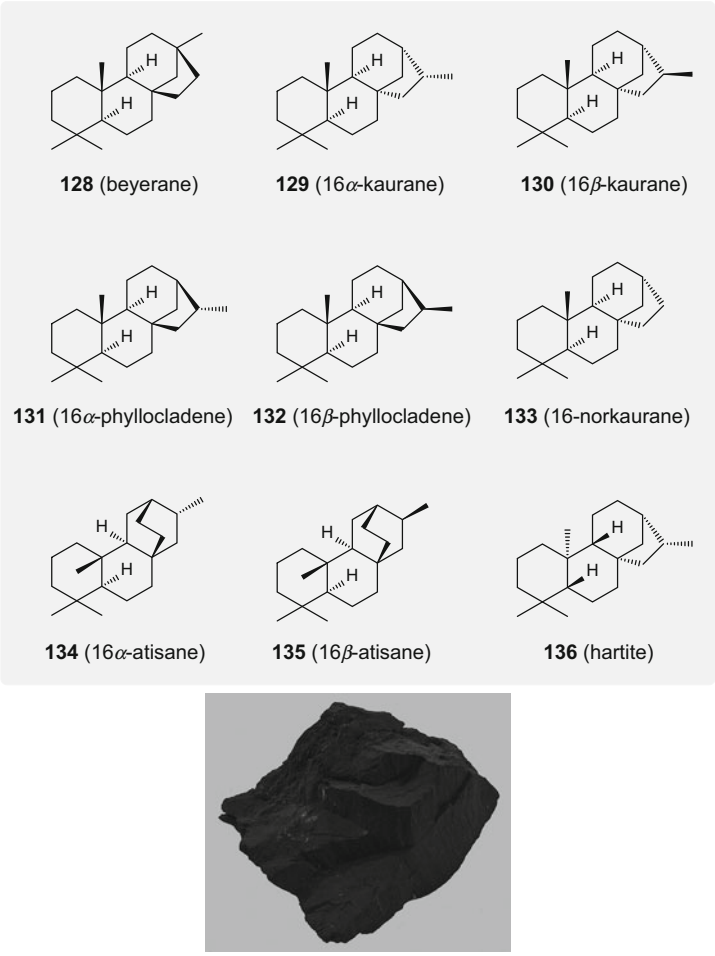

Fig. 22 Tetracyclic diterpanes **128–136**. Bottom: hartite (**136**) forming white specks on coal from Oberhart near Gloggnitz, Austria; photograph: Ra'ike, Mineralogical Museum University Bonn, Germany, Wikimedia Commons

accompanying macrofossils, the organic mineral component **136** also originates from wood.

Tricyclic Sesterterpanoids

This group of tricyclic terpanes, called the cheilanthanes (the name is derived from the fern *Cheilanthes farinosa*), occurs as a series of compounds up to C_{45}, and was identified from Paleogene Californian oil [78], with the main member being **137**. Others, like **138** and **139**, were isolated from oil sand [79], and the unsaturated

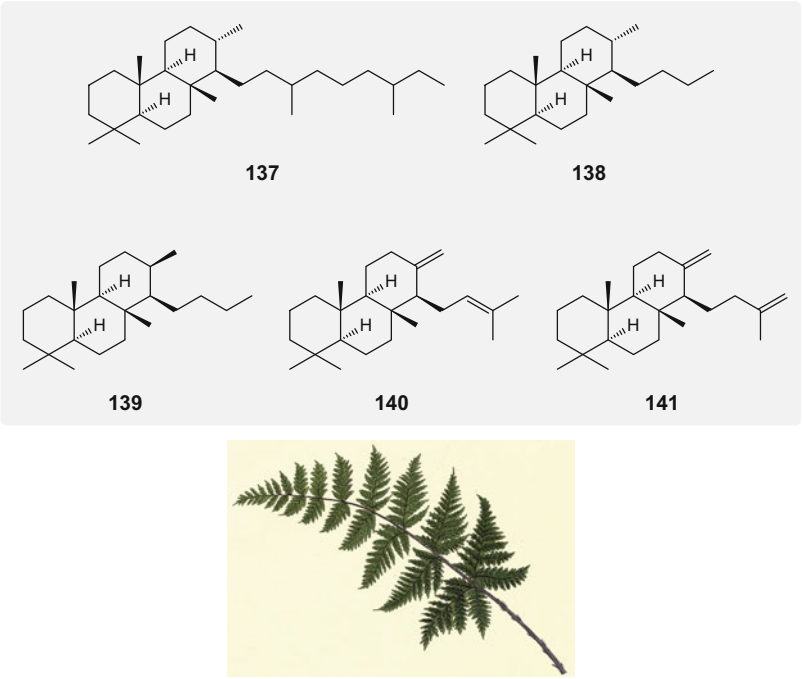

Fig. 23 Tricyclic sesterterpanoids (cheilanthanes) **137–141**. Bottom: *Cheilanthes farinosa*, Plate 6 in "Album of Indian ferns" by C. E. von Baynes; picture: Wikimedia Commons

compounds **140** and **141** (Fig. 23) could be characterized in recent Lake Cadagno sediments of Switzerland [80]. As biological sources, plant-derived di-(*E*)-poly-(*Z*)-polyprenols are possible, but there is also a wealth of over fifty other cheilanthanes occurring in diverse marine organisms [81], which might also have contributed to these molecular fossils.

Pentacyclic Triterpanoids

The parent hydrocarbon of the hopanoids is the pentacyclic triterpane hopane (**142**) (Fig. 24). Its name derives from the *Hopea* tree native to present-day Myanmar, which produces the famous dammar resin. This tree was named in honor of the British botanist John Hope (1725–1786) [82]. Organisms synthesize hopanoids because they fit well into cell membrane bilayers to provide them with rigidity. Due to their importance, the many hopane molecular fossils derived from higher plants, lichens, ferns, microbes, and other organisms are termed "geohopanes". They are distributed globally in sediments and oils, with there having been more than 200 derivatives identified so far. In his survey, Guy Ourisson, one of the pioneers of geochemistry, estimated the content of geohopanoids on earth to be in the order of 10^{12} tons, making these compounds one of the most abundant groups of molecular fossils [83].

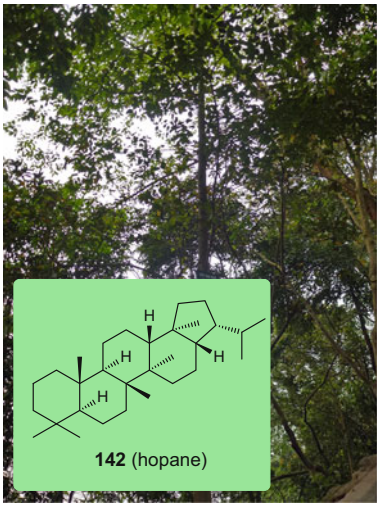

Fig. 24 The geohopanoid parent, the pentacyclic triterpane hopane (**142**) in front of *Hopea odorata* (white thingan); photograph: Hungda, Wikimedia Commons

Geohopanes come in structural variations ranging from C_{27} and C_{29}–C_{35} with rather rare members higher than C_{35} also occurring. Typical examples will be described in the following paragraphs.

28,30-Bisnorhopane (**143**) and 25,28,30-trisnorhopane (**144**) (Fig. 24) have been found in petroleum source rocks deposited under clay-poor anoxic conditions, as exemplified by the Late Cretaceous source rocks of the continental margin of Brazil [84]. These compounds are probably of chemoautotrophic bacterial origin. 18α,30-Norneohopane (**145**), together with 17α-diahopane (**146**), a rearranged hopane of probably bacterial provenance, was characterized in oil from the Permian-Cretaceous Prudhoe Bay field, Alaska, USA [85] (Fig. 25).

The ratio of hopane diastereomers with respect to positions 17 and 21 (for atomic numbering, see Fig. 25) is indicative of the thermal history of sediments, shales, coal, lignites, and oils [86]. Thus, young immature sediments contain mainly 17βH,21βH-hopane (**142**) and older ones are rich in 17βH,21αH-hopane, also named moretane (**147**). A preponderance of 17αH,21βH-hopane (**148**) points to older and deeply buried thermally conditioned sediments. A universal force field estimate using the "Avogadro" program [87] clearly indicates that this behavior is caused by the relative thermodynamic stabilities of the diastereomers, with **148** and **142** the most and least stable, and **147** in between (Fig. 26) [88]. The equilibration seems to be dependent on suited clay catalysts contained in the sediments [89]. The thermodynamically highly stable hopane **148** may be used as a sediment biomarker of methanotrophic bacteria, which produce the unsaturated hopane diploptene (**149**) (Fig. 27) [90].

The C_{31}–C_{35} homohopanes **151**–**156** (also called "extended hopanes") originate diagenetically from bacteriohopanetetrol (**150**) and other C_{35} hopanoids

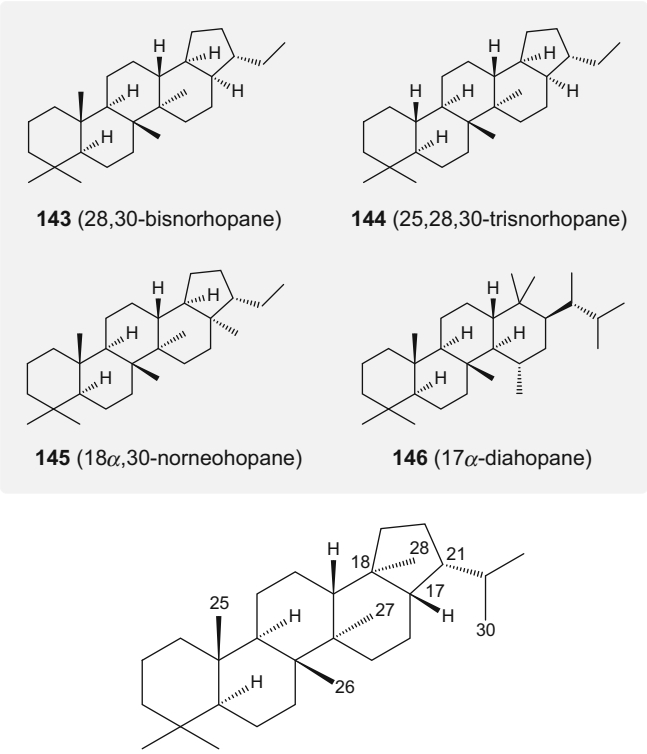

Fig. 25 Geohopane derivatives **143-146**. Bottom: pertinent numbering of hopane (**142**)

characteristic of prokaryotic microorganisms [91] (Fig. 28). These homohopanes **151**–**156** are indicative of anaerobic and highly reducing marine conditions during deposition. The homohopane index given by [**156**]/([**151**]–[**156**]) is sometimes used to define oil from certain source rocks and its thermal maturity [92]. Another thermal maturity parameter is derived from the thermodynamically controlled isomerization of the respective (22*R*)- to the more stable (22*S*)-diastereomer [86]. Interestingly, homohopanes consisting of up to 40 carbon atoms were found in bitumen from the Thornton quarry, south of Chicago, Illinois, USA, deposited under highly reducing conditions in Silurian Niagara dolomite [93]. However, their precursor compounds and organisms of origin have remained unidentified.

It is quite exciting that using a type of homohopane fingerprinting, the origin of the asphalt used in the embalming of ancient Egyptian mummies could be determined [94]. In this manner, it turned out that asphalt had to be imported to Egypt for this purpose from the Dead Sea area because Egypt itself is devoid of any open oil sources.

The 2α-methylhopanes (**158**–**163**) are highly specific for oxygen-producing cyanobacteria [95]. Their biological precursor is 2β-methylbacteriohopanetetrol (**157**), which is abundant in extant cyanobacteria (Fig. 29). The 2α-methylhopanes **158**–**163** were found in 1640 Ma-old shale samples of the Mesoproterozoic Barney

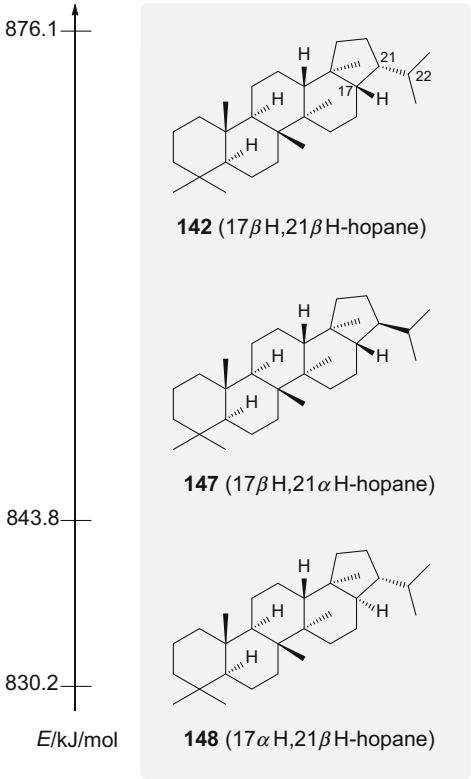

Fig. 26 Relative thermodynamic stabilities (estimated by means of force field calculations) of hopane diastereomers **142**, **147**, and **148**

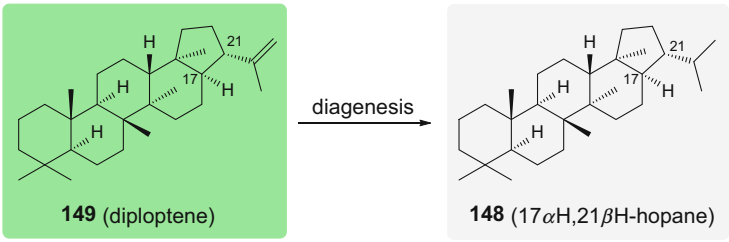

Fig. 27 Diploptene (**149**) and its diagenesis to yield 17αH,21βH-hopane (**148**)

Creek Formation of the McArthur Basin of Northern Australia and in numerous further sediments rich in organic material throughout the eons [96]. Accordingly, the methylhopanoids are suitable biomarkers to look into the origins of oxygenic photosynthesis. However, methylhopanoids extracted from ~2700 Ma-old shales from the Pilbara Craton, Australia turned out to be not indigenous and thus did not provide evidence for the existence of eukaryotes and cyanobacteria in the Archean

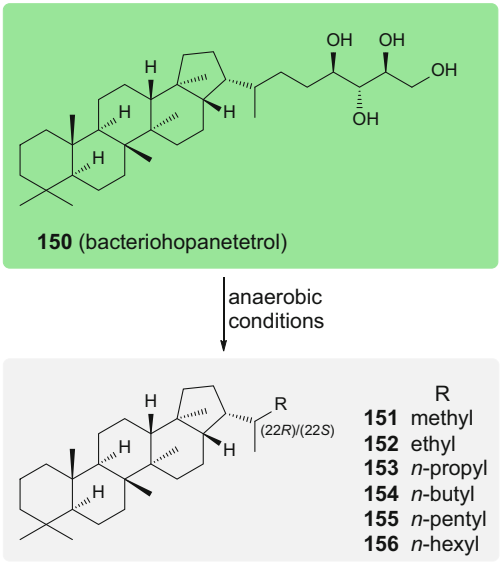

Fig. 28 The homohopanes **151–156** produced by diagenesis of bacteriohopanetetrol (**150**)

Eon [97]. The diastereomerization of the 2β-methyl to the 2α-methyl isomer during diagenesis clearly is due to the unfavorable high-energetic transanular 1,3-interaction of the two methyl groups at positions C-2 and C-10 of the 2β-methyl derivative **157**.

The 3β-methylhopanes **165–170** stemming diagenetically from 3β-methylhopanetetrol (**164**) (Fig. 30) are typical of various organisms, and, in particular, of methanotrophic bacteria and acidophilic Archaea [98]. The hopanes **165–170** and even higher homologs were found, for example, in the Pleistocene bacterial mats intercalated with sandstone in the unique deposit of the Be'eri sulfur mine, which is located on the southwestern Mediterranean coastal plain of Israel [99]. From this source, two tetracyclic terpanoid hydrocarbons, 17α,18-dimethyl-*des*-E-hopane (**171**) and 3β,17α,18-dimethyl-*des*-E-hopane (**172**), obviously resulting from the cleavage of the C-20−C-21 bond of hopanes, were isolated [99] (Fig. 30).

Fernenols like **173** or fernenes occur in ferns, as suggested by their names, but there seem to be other organisms that can also produce these (Fig. 31) [100]. These natural products are diagenetically transformed to fernane (**174**). Thus, all told, **174** is an indicator of both floral input and the Carboniferous to Triassic periods when Gymnospermopsida dominated the flora.

Possible natural product precursors of lupane (**178**) are common to various higher plant lupanes, like betulin (**175**), betulinic acid (**176**), and lupeol (**177**), which may also be called β-visciol (Fig. 32). Lupane (**178**) is found in coals, lignites, and oils [101]. The demethylated derivatives **179** and **180** (Fig. 32) could also originate from higher plant precursors [102].

Hexahydrobenzohopanes **181** containing 32–35 carbon atoms were characterized from crude oils and their sulfur-rich evaporitic carbonate-anhydrite sequences

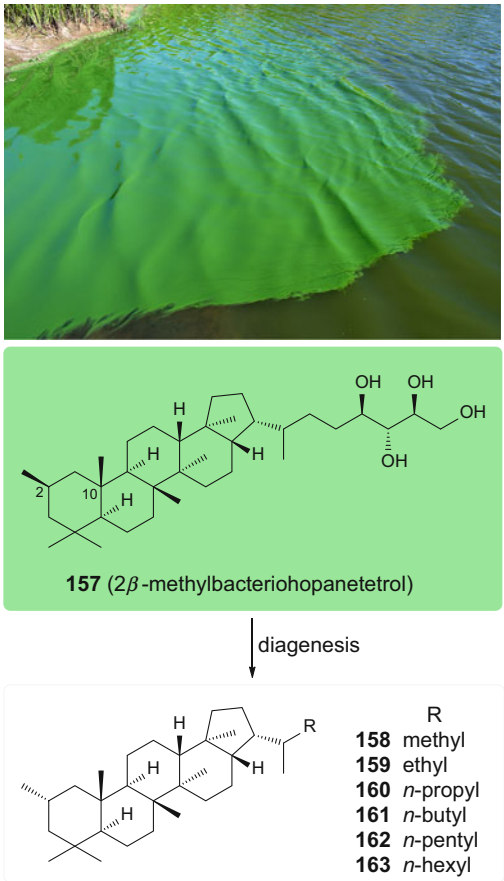

Fig. 29 2-Methylgeohopanes **158–163** and its biological precursor 2β-methylbacteriohopanetetrol (**157**). Top: bloom of cyanobacteria; photograph: C. Fischer, Wikimedia Commons

(Fig. 33). These seem to be characteristic of drastically biodegraded oil in a highly anoxic paleoenvironment, but are not correlated with specific organisms [103]. It might be mentioned that they seem not to be defined with respect to their stereochemistry at the hexahydrobenzene ring and the additional alkyl substituents.

Members of very unusual series of C(14α)-*homo*-26-*nor*-17α-hopanes having C_{27}–C_{35} carbons (**182**–**190**) were characterized from biodegraded petroleum from the marine sandstone of the Late Cretaceous to Early Eocene Loufika outcrop in Congo, revealing an as yet unknown hopane skeletal transposition (Fig. 34) [104]. Although the organismic source is unknown, it has been speculated that these derivatives are formed via oxidation of the C-26 methyl group of the hopane skeleton followed by rearrangement and migration of the C-8–C-14 bond.

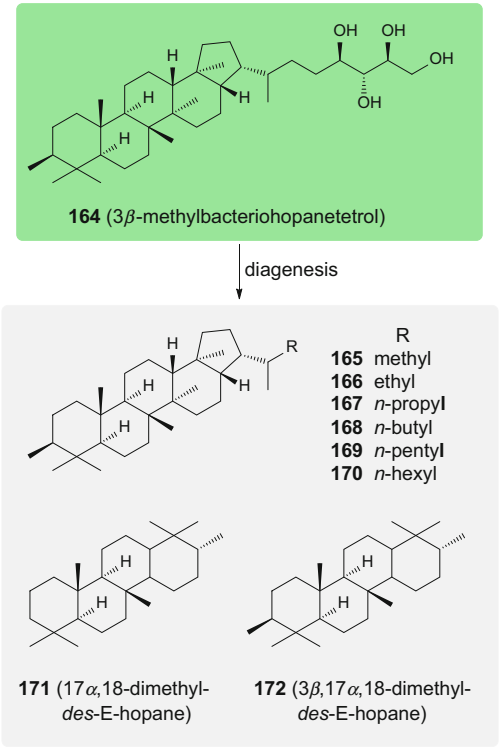

Fig. 30 3β-Methylhopanes **165–170**, its biological precursor 3β-methylbacteriohopanetetrol (**164**) and the *des*-E-hopanes **171** and **172**

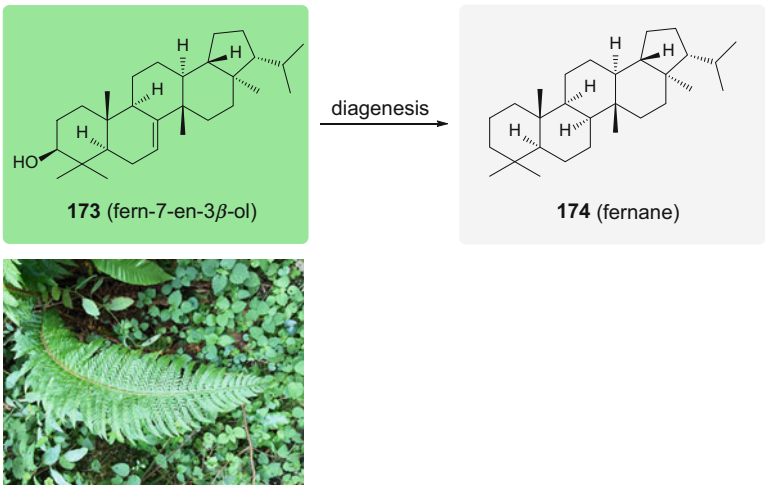

Fig. 31 Diagenesis of fern-7-en-3β-ol **173** to fernane (**174**) and a leaf of *Pteridium aquilinum* (eagle fern); photograph: H. Falk

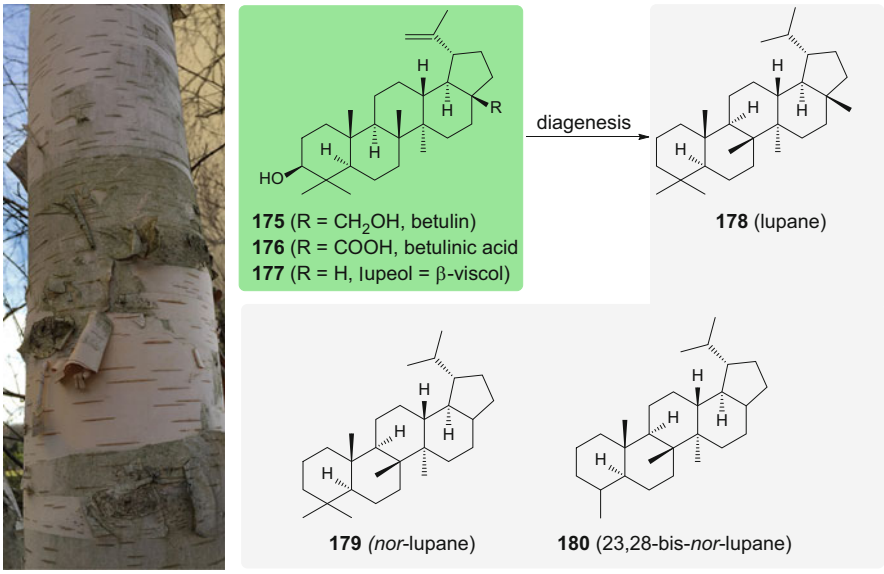

Fig. 32 Lupane derivatives **178–180** and their biological precursors **175–177**. Left: Birch tree (*Betula* sp.), of which the bark is rich in **175** and **176**; photograph: H. Falk

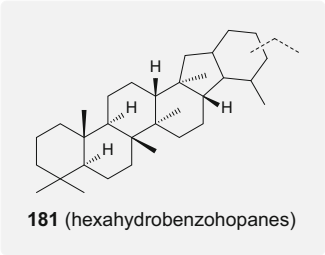

Fig. 33 Hexahydrobenzohopanes (**181**)

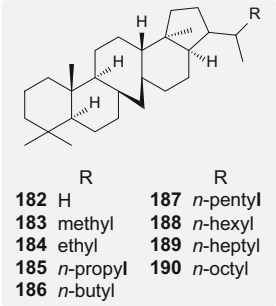

Fig. 34 C(14α)-*homo*-26-*nor*-17α-Hopanes **182–190**

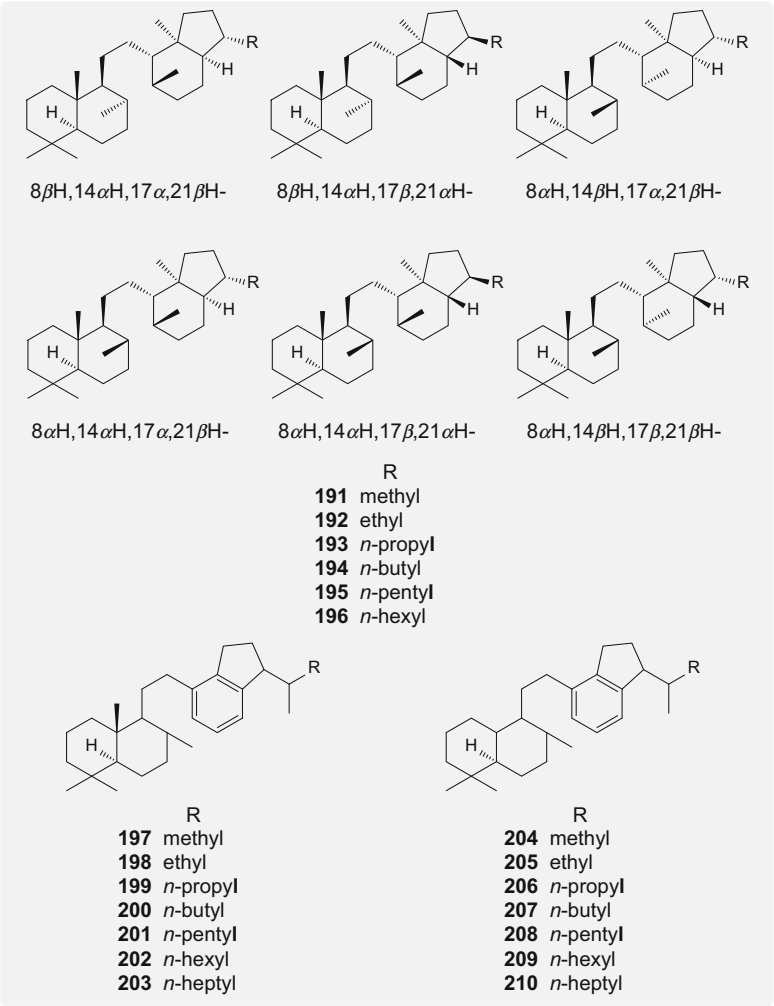

Fig. 35 8,14-*seco*-Hopane diastereomers 8βH,14αH,17α,21βH-, 8βH,14αH,17β,21αH-, 8αH,14βH,17α,21βH-, 8αH,14αH,17α,21βH-, 8αH,14αH,17β,21βH-, 8αH,14βH,17β,21βH-**191** to 8βH,14αH,17α,21βH-, 8βH,14αH,17β,21αH-, 8αH,14βH,17α,21βH-, 8αH,14αH,17α,21βH-, 8αH,14αH,17β,21βH-, 8αH,14βH,17β,21βH-**196**, and monoaromatic *seco*-hopane series **197**–**203** and **204**–**210**

In biodegraded oils from seeps in Pakistan, 8,14-*seco*-hopanes (**191**–**196**) were characterized as a homologous series of a diastereomeric ensemble of six isomers of configurations, 8βH,14αH,17α,21βH, 8βH,14αH,17β,21αH, 8αH,14βH,17α,21βH, 8αH,14αH,17α,21βH, 8αH,14αH,17β,21βH, and 8αH,14βH,17β,21βH [105] (Fig. 35). As these compounds seem to be highly bioresistant, and also occur in non-biodegraded Paleogene brown coal from the Zhoujing mine, Baise Basin, in

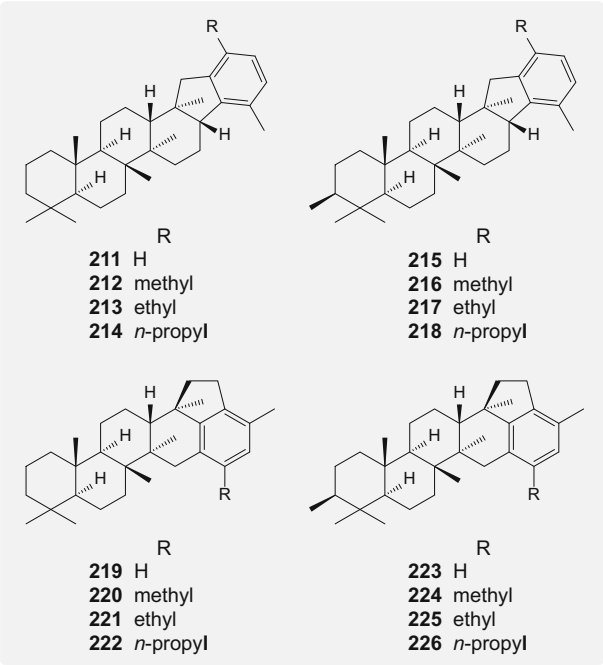

Fig. 36 Linearly and angularly benzo-condensed hopanes **211–218** and 3β-methylhopanes **219–226**

southern mainland China [106], these molecular fossils may either have a direct biological precursor or may have formed during early diagenesis. In addition to these saturated compounds, several demethylated monoaromatic and monoaromatic C-28 demethylated 8,14-*seco*-hopanoids series (C_{28}–C_{34}) (**197**–**203** and **204**–**210**) were detected in biodegraded oil from the Permian-Triassic Oseberg area, Norway (Fig. 35) [107].

Pleistocene bacterial mats intercalated with sandstone in the unique deposit of the Be'eri sulfur mine mentioned above also contain interesting examples of linearly and angularly benzo-condensed hopane and 3β-methylhopane derivatives (**211**–**226**) [99] (Fig. 36). These may result from rearrangement/cyclization/dehydration processes of the bacterial mat hopanoids brought about by the presence of sulfur.

18α-Oleanane (**227**) is a highly specific biomarker of angiosperms, the flowering land plants. This compound derives mainly from betulins like **175** or taraxar-14-ene (**228**) and other pentacyclic triterpenoids (Fig. 37) [108]. This biomarker is also characteristic of a geological time threshold, because flowering plants only started to evolve in the Early Cretaceous period. Thus, screening of the oleanane (**227**) content of numerous source rocks indicated that starting with Early Cretaceous samples, the amounts of **227** began to appear and then increased in abundance nearly exponentially into the Tertiary period [109]. The diastereomeric 18β-

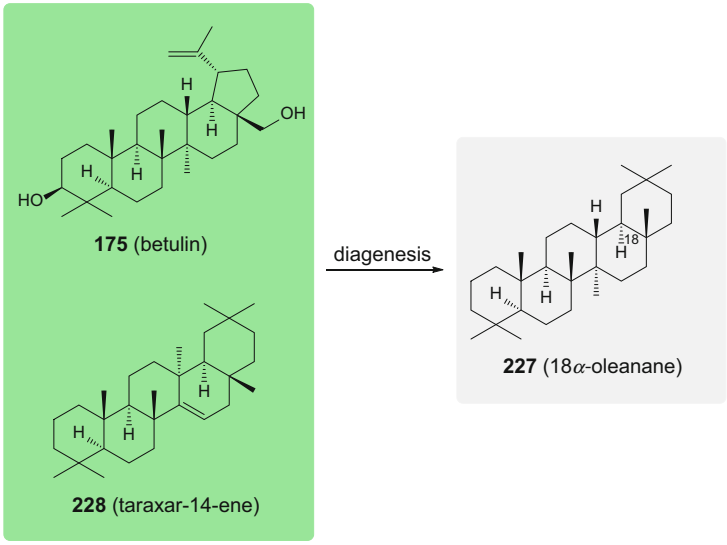

Fig. 37 Diagenetic formation of 18α-oleanane (**227**) from **175** or **228**

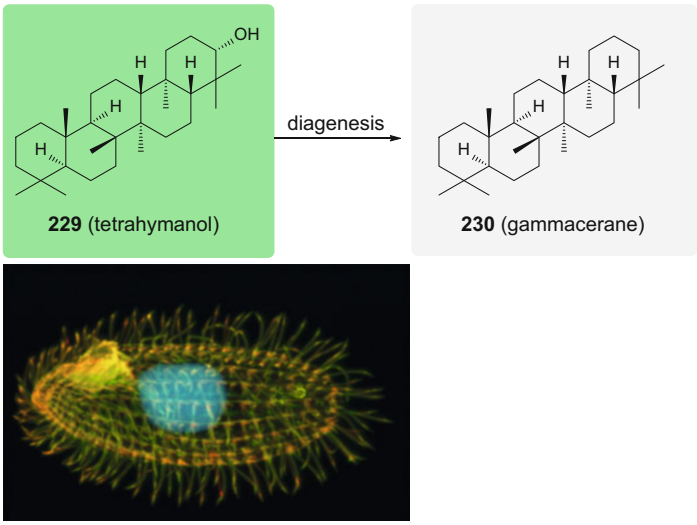

Fig. 38 Formation of gammacerane (**230**) from tetrahymanol (**229**). Bottom: *Tetrahymena thermophila*; photograph: R. Robinson, Wikimedia Commons

oleanane was also recognized in petroleum—but it seems to be thermodynamically less stable than the α-diastereomer **227** [110].

Tetrahymanol (**229**) is a lipid that may substitute for steroids like cholesterol in the membranes of several protozoa like *Tetrahymena thermophila* (Fig. 38) [111, 112]. Its molecular fossil is gammacerane (**230**), which is used as a biomarker

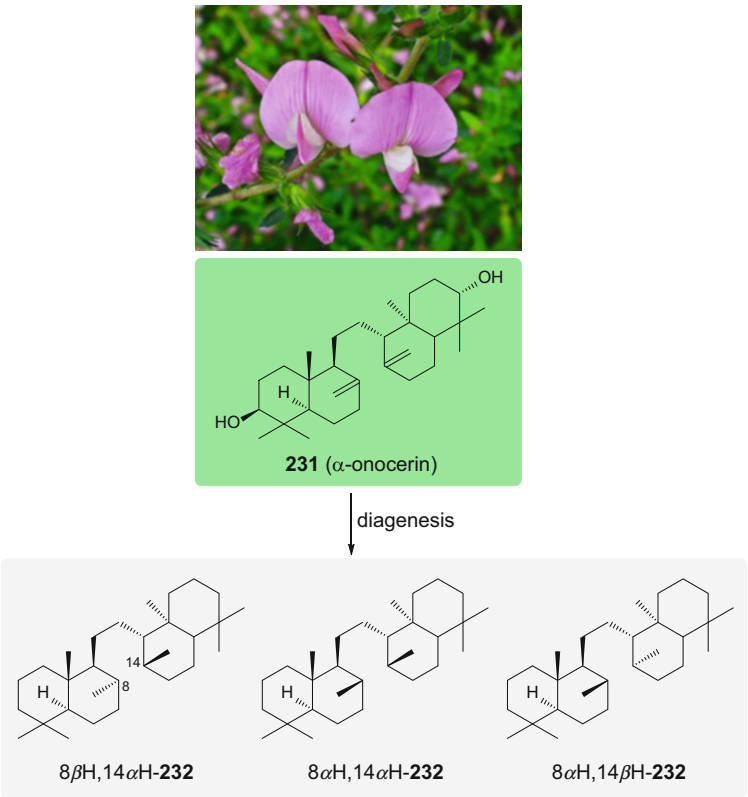

Fig. 39 Diastereomers of onocerane (**232**) diagenetically formed from α-onocerin (**231**). Top: *Ononis spinosa*, spiny restharrow, a producer of **231**; photograph: H. Zell, Wikimedia Commons

for bacterivorous ciliates accumulating in a stratified water column caused by hypersalinity (Fig. 38) [111, 113]. Gammacerane (**230**) was identified in the Miocene Gessoso-Solfifera and Early Jurassic Allgäu formations [111].

The onocerane diastereomers 8*β*H,14*α*H-, 8*α*H,14*α*H-, and 8*α*H,14*β*H-**232** seem to be diagenetic products from α-onocerin (**231**), which is synthesized by both flowering plants and ferns (Fig. 39). The molecular fossils **232** were found in Cretaceous sediments and also in younger samples [114, 115].

Polyprenoids

In addition to a series of linearly and angularly benzo-condensed hopane and 3*β*-methylhopane derivatives (**211–226**) [99] (see Fig. 36), which stem from complex diagenetic processes of hopanoids, several higher regular monoaromatic polyprenols (**233–235**) (Fig. 40) were detected in an extract of the Eocene Messel shale, Germany [116]. Although a specific biological precursor of these molecules

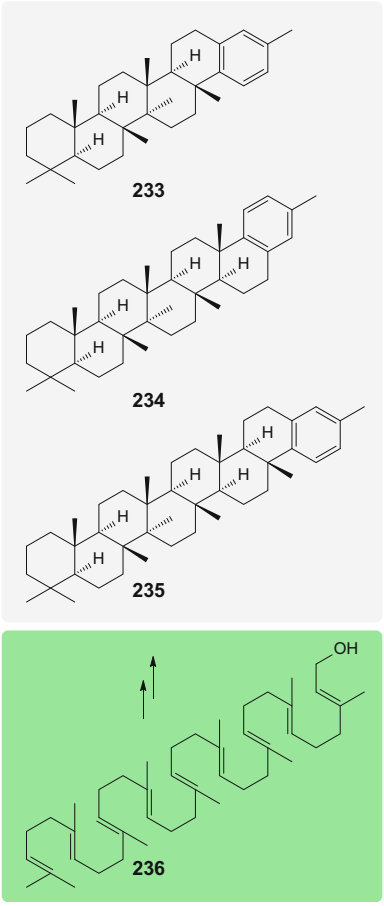

Fig. 40 Polyprenoids **233–235**, and genesis of **235** from long-chain isoprenol **236**

has not been specified, the hexa-, hepta-, and octacyclic isoprenoids could result from the enzymatic cyclization and diagenetic aromatization of long-chain isoprenols. For example, compound **236** may result in the octacyclic system **235** (Fig. 40), but whatever these processes are in detail, the homochirality and all-*trans* ring junction configuration clearly affirm their biological origin. Parallel to the monobenzenoid polyprenoids, the corresponding saturated derivatives have also been traced to the Messel shale and Late Cretaceous sediments of the Lameignére quarry of Orthez, France. Hexacyclic saturated compounds of this type were found to be abundant in extracts from the Early Cretaceous Ostracode zone in southeastern Alberta, Canada [117]. Besides algal and marine remains, this material contains rather large amounts of ostracodes, and therefore it has been suggested to use these "Q-compounds" as biomarkers of this zone, although no natural product source could be specified.

Steroids

Terpenoids are usually discussed in the chemical literature separating them from the triterpenoid steroids (see, for example, monographs on isoprenoids [118, 119], versus those on steroids [120] or the content structure of a typical textbook on the chemistry of natural products [121]). Accordingly, this overall classification method is followed for the molecular fossils described in this chapter.

The most abundant sterol in the eukaryotic living world of both yesterday and today is cholesterol (**237**). Its saturated catabolized derivative coprostanol (**238**) occurs in mammalian feces. Under diagenetic influence, compounds **237** and **238** give rise to cholestane (**239**), its heavily backbone-rearranged diasterane (**240**) (Fig. 41), and mono- and triaromatic steroids; the latter two compound types will be discussed below. However, it should be mentioned that in addition to diagenetic transformation products, intact sterols have been found in a crustacean fossil from the Devonian Gogo Formation, Australia [122]. Interestingly, it has been shown that under laboratory

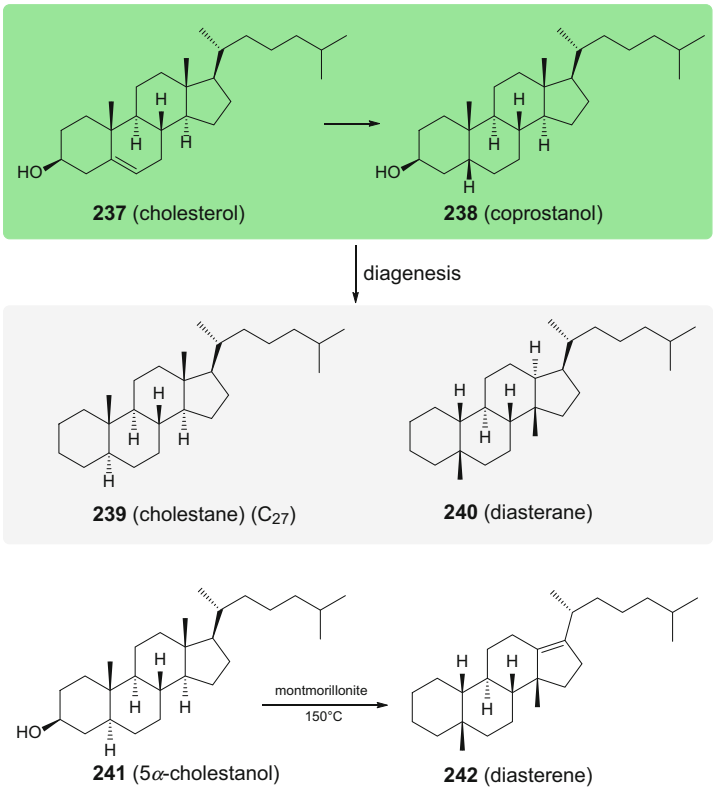

Fig. 41 Formation of cholestane (**239**) and diasterane (**240**) from cholesterol (**237**) or coprostanol (**238**), and as a model reaction for the initial diagenetic transformation the montmorillonite catalyzed rearrangement of 5α-cholestanol (**241**) to diasterene (**242**)

conditions, 5α-cholestanol (**241**) catalyzed by the phyllosilicate clay montmorillonite at 150°C, rearranges to diasterene (**242**) (Fig. 41) [123]. Upon diagenesis under reducing conditions, the latter would yield **240**, thus very nicely corroborating its cholesterolic origin. It should be pointed out that, in general, diasteranes are thought to be thermally more stable than the steranes [124]. However, an estimation by a force field calculation using the "Avogadro" program [87] resulted in diasterane (**240**) being determined as thermodynamically less stable by about 400 kJ/mol than cholestane (**239**) [88].

The 24-alkylcholesterols **243**–**246** are metabolites of diatoms and red algae (brassicasterol (**243**) and double bond homologs), green algae, and higher land plants (sitosterol and ergosterol (**244**)), pelagophytes (**245**), and sponges (**246**). Their molecular fossils are the 24-alkyl-cholestanes **247**–**250** and the corresponding 24-alkyl-diasteranes **251**–**254** (Fig. 42). For the latter compounds, all possible configuration combinations have been observed at the C-20 and C-24 stereocenters. Thus, for example, in a standard crude oil (Stanford-1) sample originating from clay-rich shale source rocks, the (20*S*,24*S*)-, (20*S*,24*R*)-, (20*R*,24*S*)-, and (20*R*,24*R*)-diastereomers of **251**–**254** have been detected [124]. The configurations at the other stereocenters are strongly dependent on age and maturity throughout the

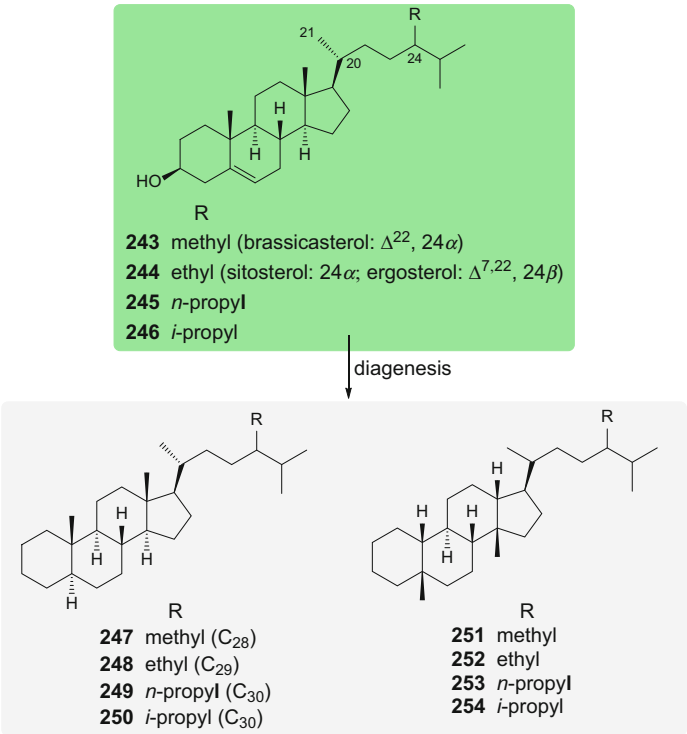

Fig. 42 24-Alkylcholesterols **243**–**246** and their molecular fossils, the 24-alkyl-cholestanes **247**–**250** and the corresponding 24-alkyl-diasteranes **251**–**254**

sterane series, and rearrangement and isomerization reactions are known to take place to some extent [122, 125–127].

It has turned out that the relative abundance of the C_{27} to C_{29} steranes in a given sample is indicative of its provenance. In addition, the relationships between C_{27}, C_{28}, and C_{29} steranes have been used to distinguish younger crudes derived from the Cretaceous and Paleogene periods from those of the Paleozoic Era and older crudes [128]. An age-related parameter may be obtained by comparing the contents of C_{28} with C_{29} of a sample, i.e. by determining the ratio $[C_{28}]/[C_{29}]$. The lower this value, the older the sample of a marine source rock [128]. Thus, for an Early Paleozoic or older oil $[C_{28}]/[C_{29}] < 0.5$, a value of 0.4–0.7 is characteristic of the Late Paleozoic to Early Jurassic, and a value of >0.7 indicates Late Jurassic to Miocene oils. The increase in the phytoplankton diversification with dinoflagellates, coccolithophores, and diatoms in the Jurassic and Cretaceous period obviously caused this increase of the C_{28} steranes.

The so-called sterane index as given by $[C_{30}]/([C_{27}]–[C_{30}])$ is highly specific of marine matter input. The content in C_{30} (**249**) derives from chrysophyte algae, which synthesize 24-*n*-propyl-cholesterol (**245**) [129]. A screening of sediments and oils throughout the Phanerozoic Eon revealed that the C_{30} steranes appeared between the Early Ordovician and Devonian periods, and, accordingly, their source algae evolved during this time. Furthermore, the preponderance of the C_{30} *i*-propyl derivative **250** content over that of the *n*-propyl derivative **249** seems to be age-specific [130], with the *i*-propyl derivative **250** occurring for the first time in the Proterozoic Eon. With respect to the source of **250** it has been speculated that Demospongiae were the main contributors [131]. However, this "sponge biomarker" quality of **250** was questioned and pelagophyte algae were also considered as a probable source [132]. Modern sponges produce **246** in abundance.

The C_{28}–C_{30} 4α-methylsteranes **255–257** and the dinosterane **258** are highly specific to dinoflagellates and certain bacteria. These molecular fossils originate from the 4α-methylsterols that are mainly produced by dinoflagellates, but also by methylotrophic bacteria [133] (Fig. 43).

Two pseudo homologous series of carbon content C_{28}–C_{30} obviously result from the bacterial alkylation of Δ^2-sterenes, which yields 2α- (**259–262**) and 3β-methylsteranes (**263–266**) (Fig. 43) [134]. In addition, 3β-alkylsteranes (**267**) with β-alkyl residues at position C-3 ranging from methyl to *n*-undecyl and also one with an isopentyl side chain were identified in crude oils and rock extracts from the Precambrian to the Miocene [135].

In addition to the normal steranes, demethylated steranes generally occur in much smaller quantities. Nevertheless, the norsteranes can serve as age-related markers. Of these, three series of C_{26}-norcholestanes have been encountered: 21-, 24-, and 27-norcholestane (**268–270**) (Fig. 44). Whereas there is only a single diastereomer of the 5α,14α,17αH- and 5α,14β,17βH-21-norcholestanes (**268**), the (20*R*)- and (20*S*)-diastereomers of the 5α,14α,17αH- and 5α,14β,17βH-24-norcholestanes and 27-norcholestanes have been identified. Traces of the 24- and 27-norcholestanes (**269**, **270**) can be found back to the Proterozoic Eon [136], but the relative concentration levels of the 24-norcholestanes increase in the Cretaceous and

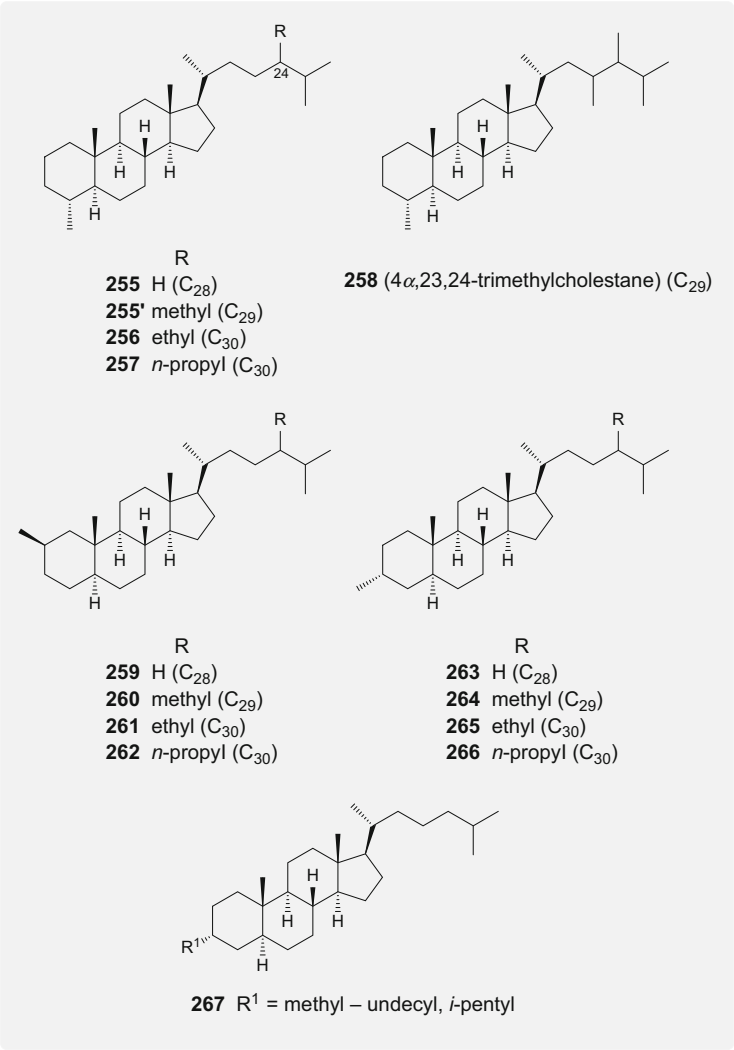

Fig. 43 4-Methylsteranes **255–257**, dinosterane **258**, 2- and 3-methylsteranes **259–266**, and 3-alkylsteranes **267**

Miocene and can thus be used as the age parameter NCR = Σ(([24-*nor*])/(Σ([24-*nor*]) + Σ([27-*nor*])) [137]. In addition to the norcholestanes, the corresponding series of the rearranged nordiacholestanes such as **271** are found and can be used for the same purpose with the analogous parameter NDR = Σ(([24′-*nor*])/(Σ([24′-*nor*]) + Σ([27′-*nor*])) [136]. The evolution of phytoplankton is the cause of this age-related signal: diatoms producing 24-norcholestane precursors were first observed for the Jurassic period and became more and more abundant in the Cretaceous and Paleogene periods. The origin of the 24-norcholestane diastereomers **269** from 24-norcholesta-5,22-dien-

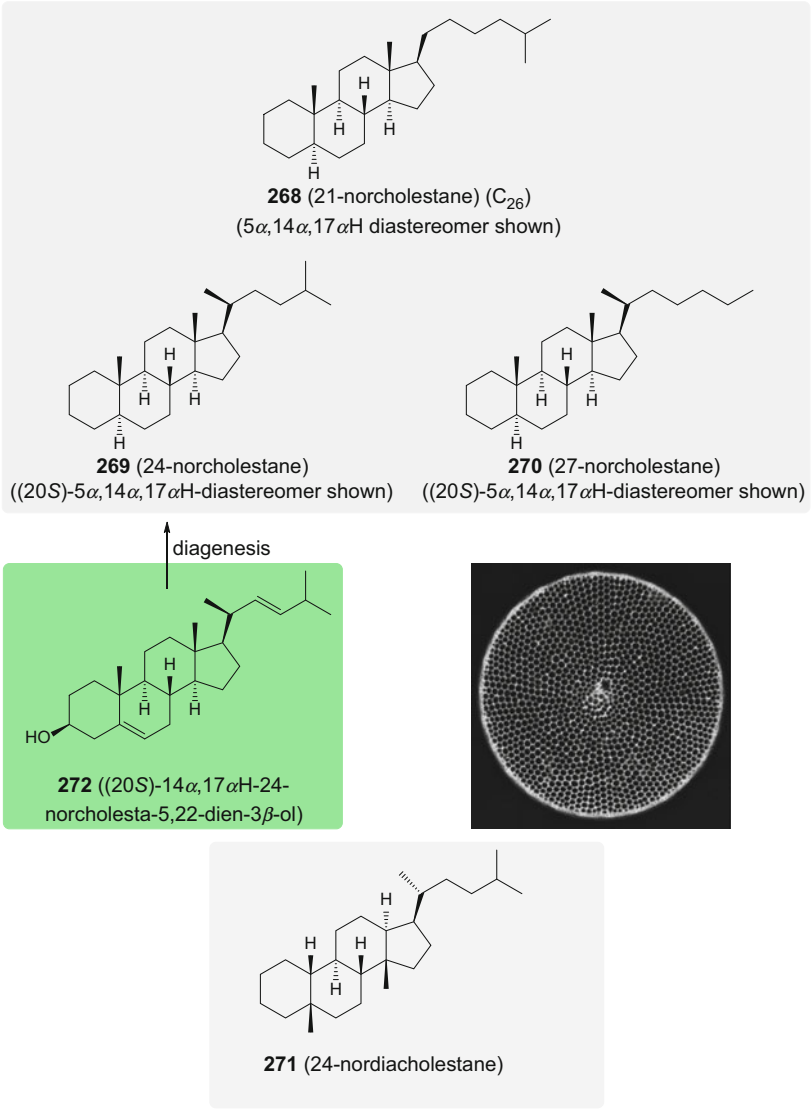

Fig. 44 Norcholestanes **268**–**270**, source cholestadienol **272** and the nordiacholestane **271**. Image of the diatom *Thalassosira* sp. Eocene/Oligocene, Oamaru, New Zealand; photograph stacked from eleven microphotographs with slightly different focal distances by A. Gleich, Wikimedia Commons

3β-ol (**272**) has been traced to the diatom *Thalassiosira* aff. *antarctica* and to a lesser extent the dinoflagellate *Gymnodinium simplex* [138].

Monoaromatic steroids with aromatization of ring C and concomitant loss of the methyl group at position C-18 occur for most of the molecular fossils and biomarkers

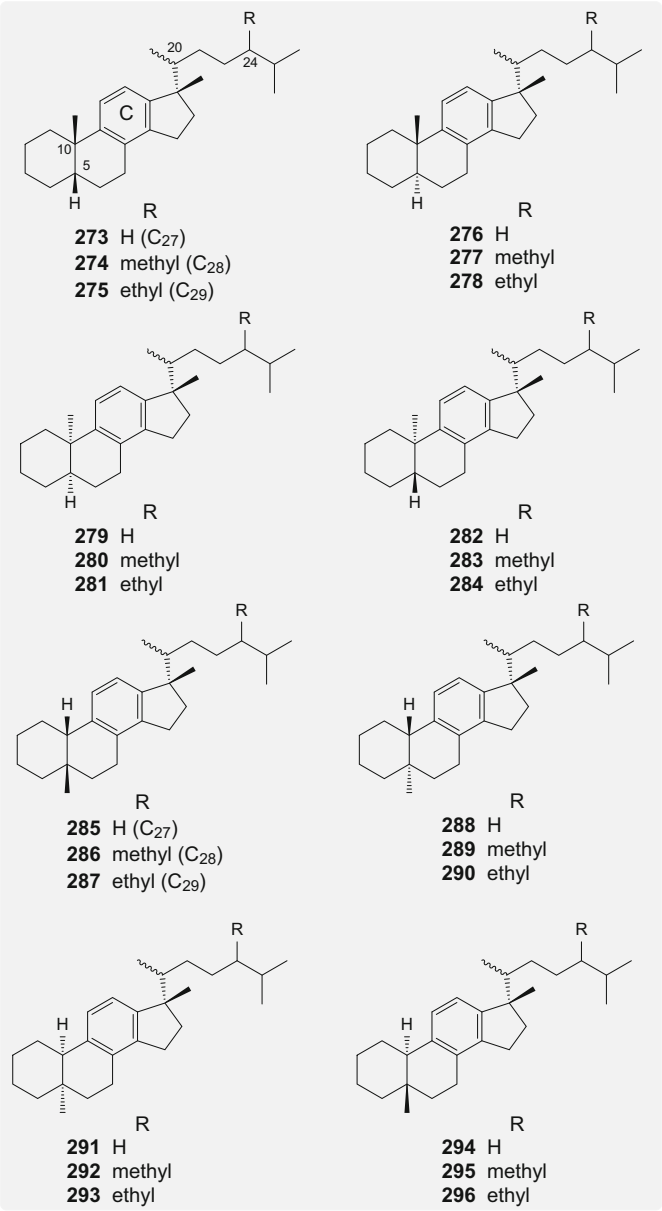

Fig. 45 Sterenes and diasterenes with an aromatic ring C: **273–296**

discussed above. These have been isolated as a series of derivatives substituted at position C-24 and display combinatorial stereochemistry at their remaining chiral centers. Thus, the (20*R*)- and (20*S*)-diastereomers of the 5*β*H,10*β*-, 5*α*H,10*β*-, 5*α*H,10*α*-, and 5*β*H,10*α*-isomers (**273**–**284**) were identified (Fig. 45) [139–141]. In

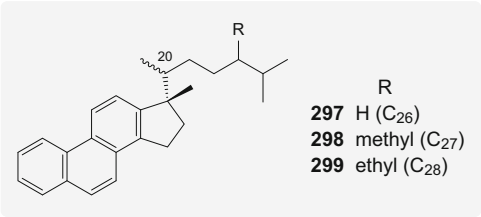

Fig. 46 Triaromatic sterenes **297–299**

addition, the corresponding rearranged diasterene (20*R*)- and (20*S*)-diastereomers **285–296** have been found. Several specific ratios of these isomers were used to characterize source-rock depositional environments, to achieve correlations between sources, and as indicators of eukaryotic species contribution [142]. However, the heavy diagenetic and catagenetic transformations, which these aromatic systems underwent during diagenesis, make them less suited to serve as organismic markers.

Complete aromatization of the monoaromatic C_{27}–C_{29} derivatives discussed above then leads to the C_{26}–C_{28} triaromatic sterenes, which in the course of this process have lost an additional methyl group. For these, the (20*R*)- and (20*S*)-diastereomers of **297–299** (Fig. 46) have been observed as widespread constituents of sediments and petroleum [143]. However, as in the case of the monoaromatic molecular fossils, for which the specificity with respect to organisms is low, the organismic specificity of the triaromatic systems becomes even lower.

Carotenoids

Planktonic green sulfur bacteria (Chlorobiaceae), which reside in the lacustrine and marine subsurface volume, biosynthesize in a unique manner the aromatic C_{40} carotenoid isorenieratene (**300**), which, upon partial diagenetic hydrogenations, yields isorenieratane (**301**) (Fig. 47). Isorenieratane (**301**) and other derivatives of this kind indicate photic zone anoxia in the depositional environment and have been identified in a number of sedimentary rocks ranging from the Ordovician to the Miocene [144]. As the Chlorobiaceae use the reverse citric cycle of carbon fixation, there is an enrichment of ^{13}C (about 15‰) observed in these molecular fossils. Otherwise, the ubiquitous β-carotene (**302**) gives rise diagenetically to β-isorenieratene (**303**), a compound also produced by Chlorobiaceae, and, by further diagenesis, **303** yields β-isorenieratane (**304**). Isorenieratene (**300**) can also result in a wide range of derivatives produced by Diels-Alder cyclizations, aromatization, and

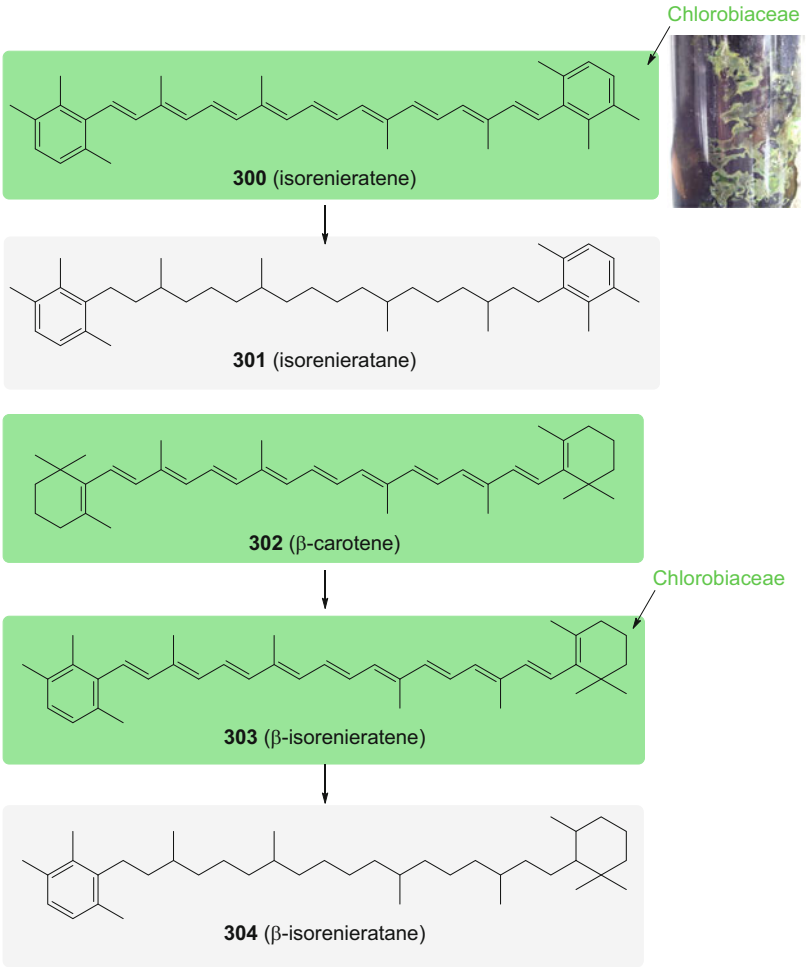

Fig. 47 Carotenoids **300–304** and a Chlorobiaceae culture; photograph: J. Werther, Wikimedia Commons

elimination reactions involving also intermediate sulfurization during diagenesis, as shown by the examples **305–309** in Fig. 48 [144]. The biotic crisis at the end of the Permian period, the most severe mass extinction of the past 500 million years, was accompanied by an oceanic anoxic event with widespread photic zone euxinic conditions. During this time, the Chlorobiaceae grew abundantly and, accordingly, their biomarker **301** has been used to trace this event in a drilling core acquired from the Perth Basin, Western Australia [145].

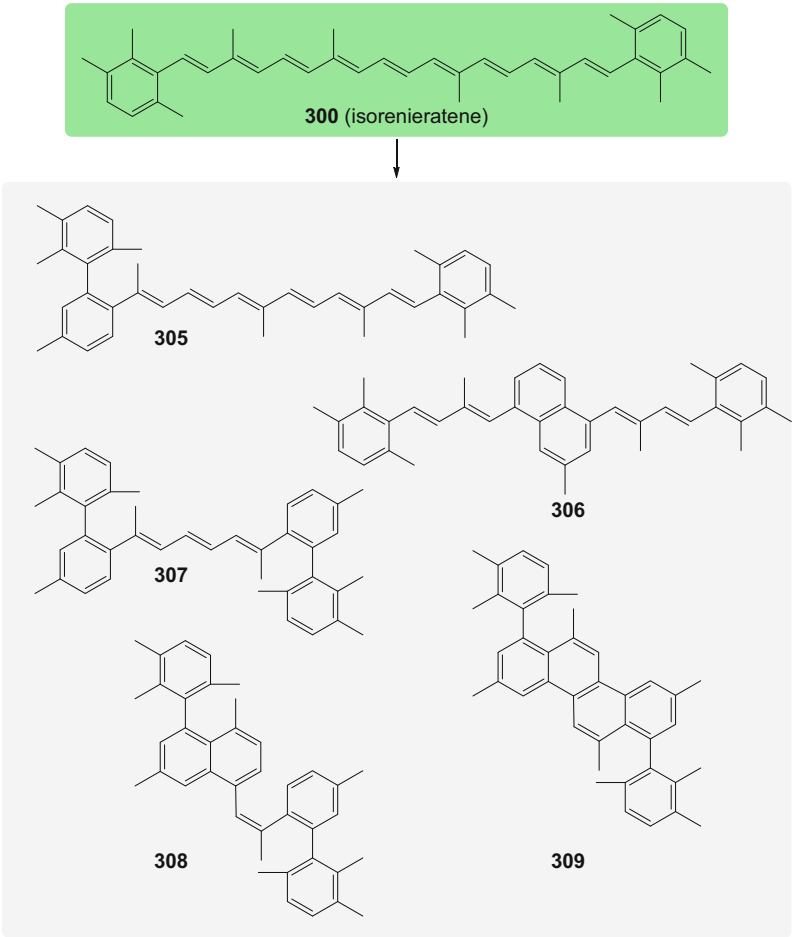

Fig. 48 Diagenetic products of isorenieratene (**300**)

Another carotenoid typical of green sulfur bacteria is chlorobactene (**310**), which through diagenesis yields chlorobactane (**311**) (Fig. 49), and is found together with **301**, for example, in the 1640 million-year-old Precambrian Barney Creek Formation carbonates in the McArthur Basin, Australia [146].

Typical of the planktonic purple sulfur bacteria (Chromatiaceae), which reside in the surface region, is okenone (**312**). The latter is transformed diagenetically into okenane (**313**) (Fig. 49), and is encountered e.g. as a main carotenoid fossil in the above-mentioned Barney Creek Formation [146]. In addition to these compounds, renierapurpurane (**314**), β-renierapurpurane (**315**), palaerenieratane (**316**), and additionally cyclized derivatives like **317** have been identified (Fig. 49) [146].

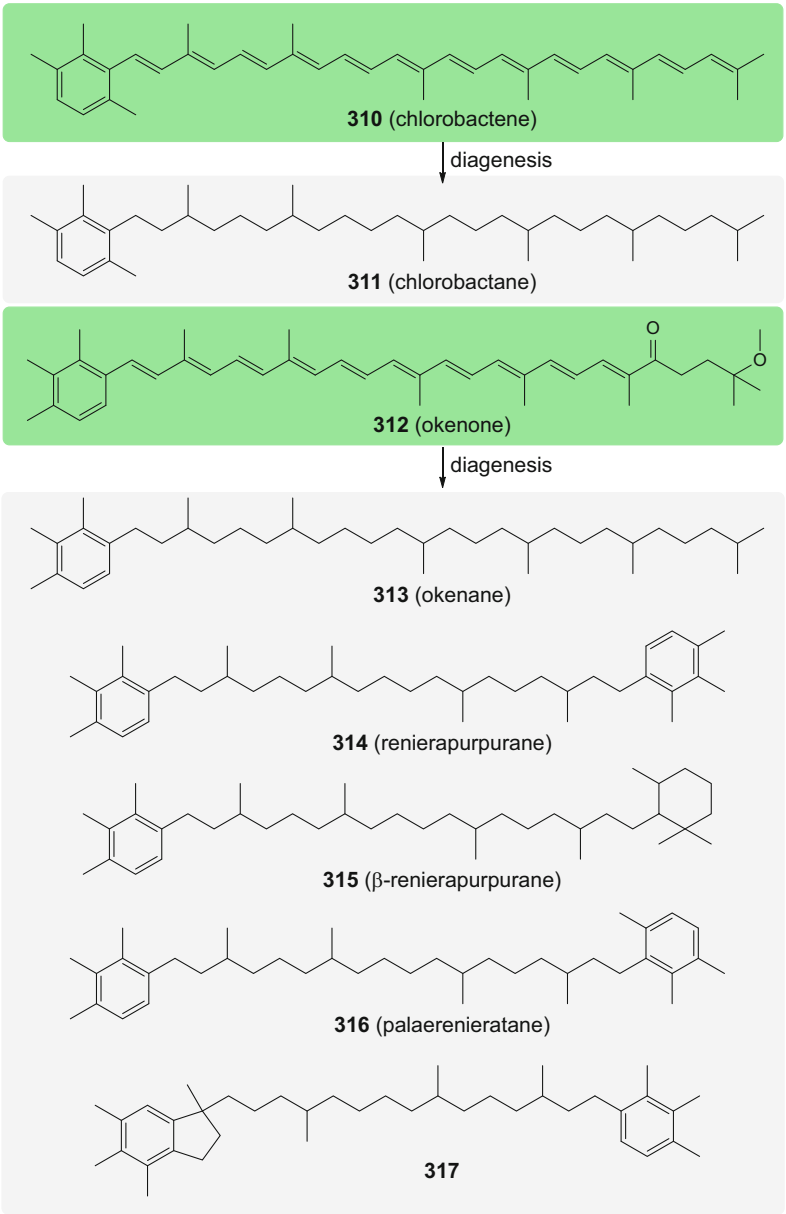

Fig. 49 Carotenoids **310** and **312** and their molecular fossils **311** and **313**, and additional biomarkers **314–317** of green and purple sulfur bacteria

It should be mentioned that under anoxic conditions, carotenoids may be preserved in an unaltered form in sediments. The oldest intact carotenoids found so far are from the Miocene. Isorenieratene (**300**) has been reported from a Messinian

marl from Italy and an unspecified diaromatic carotenoid was documented from a Lower Miocene clay from the Blake-Bahama basin in the western North Atlantic Ocean [147].

2.1.4 Other Aromatic and Heterocyclic Compounds

From Simple Aromatic Compounds to Polyaromatic Hydrocarbons

From the molecular fossils with an aromatic unit not yet described within one of the above sections, the first group that will discussed are the phenyl alkanes. Owing to the nearly ubiquitous presence of linear alkyl sulfonate detergents in the geosphere, these compounds have to be treated with caution when considering them as molecular fossils. Nevertheless, in the particular case of Australian crude oils and sediments, it has been demonstrated beyond doubt that phenyl alkane **318**, substituted at positions C-2–C-6 and with carbon numbers between 13 and 35 (Fig. 50), are indeed authentic descendants of ancient life [148], since contemporary phenyl alkane detergents display alkane lengths in the range of only ten to fourteen carbon atoms. There is good evidence that the phenyl alkane **318** originates in algal species like *Botryococcus braunii* or organisms related to extant *Thermoplasma acidophilum* bacteria.

As a more recent example, *n*-alkanes of chain lengths up to 25 carbon atoms substituted at position C-1 with either 1- or 2-naphthyl moieties (**319**, **320**) (Fig. 50) were found in Cretaceous sedimentary source rocks of the onshore Songliao Basin in northeastern mainland China [149]. These might be attributed to microbial and land terpenoid sources but could also be due to ring isomerizations and transalkylation processes with increasing maturity [150].

1,2,7-Trimethylnaphthalene (**322**) together with 1,2,5-trimethylnaphthalene (**323**) are derived diagenetically from oleanene-type triterpenoids like β-amyrin (**321**) thereby indicating angiosperm input (as, for example, from dandelion, *Taraxacum officinale*) (Fig. 50) [151]. In certain oils, 1,3,6,7-tetramethylnaphthalene (**324**) (Fig. 50) is encountered but seems to be derived from bacterial sources [152].

Five very interesting isohexyl-alkylnaphthalenes (**325**–**329**) were identified in a suite of crude oils from the Cambrian to the Paleogene from around the world (Fig. 51) [153]. The concomitant benzene derivative **330** has been encountered from the Permian period onward, indicating both bacterial or algal and higher plant origin, whereas the alkylnaphthalenes **325**–**329** are associated exclusively with higher plant di- and triterpenoid precursors.

The structural features of the precursors necessary to produce these products by ring opening, as shown in Fig. 52, are: first, a terpenoid A–B ring system with a *geminal* dimethyl group at position C-4, and second, an *angular* methyl group at

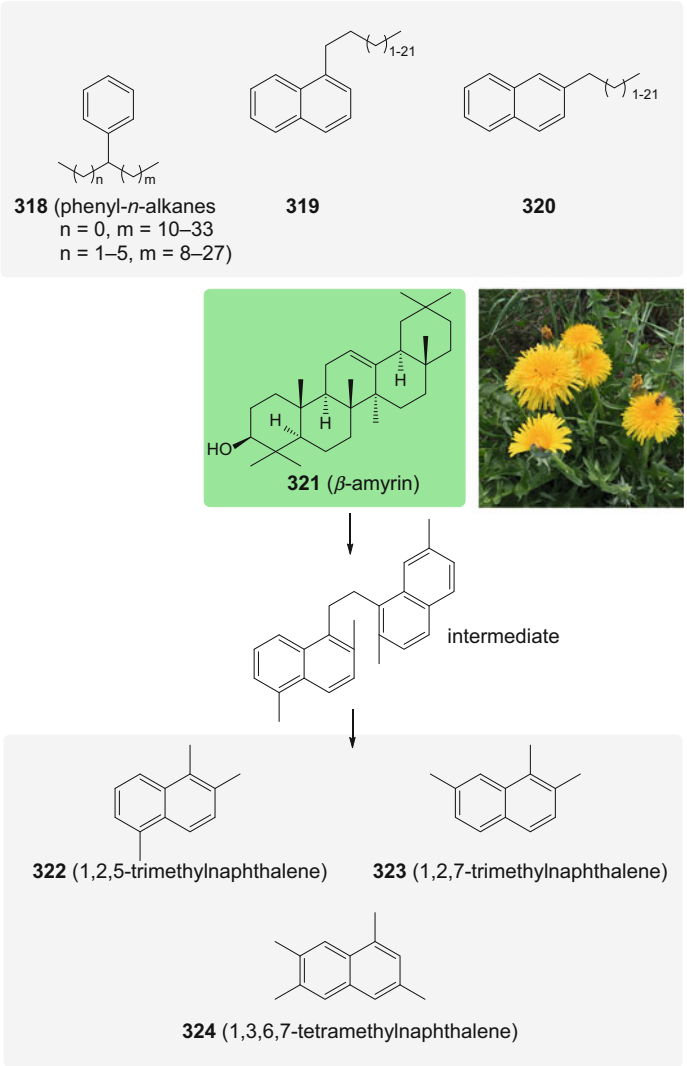

Fig. 50 Phenyl- and naphth-1- and 2-yl-*n*-alkanes **318** and **319** and **320**. Trimethylnaphthalenes **322** and **323** derive from *β*-amyrin (**321**) (with one of its sources, *Taraxacum officinale*; photograph: H. Falk); 1,3,6,7-tetramethylnaphthalene (**324**)

position C-10. This was demonstrated by means of model reactions using the natural products phyllocladene (**331**) and olean-18-ene (**332**) as the educts [153].

From Devonian to Cretaceous crude oils and from coals that are partially saturated, condensed aromatic compounds comprising methyltetralin and methylindan isomers were identified (Fig. 53) [154]. Although these are clearly of biological origin, they are not attributable to a specific source. In the case of 1- and 2-methyltetralin (**333** and

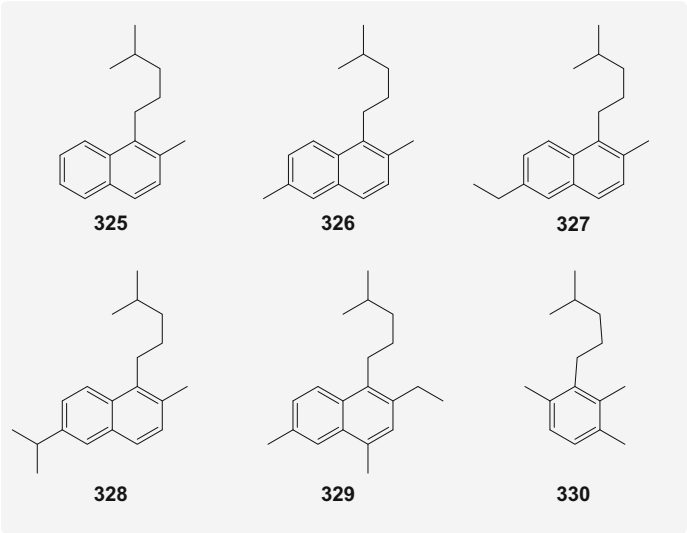

Fig. 51 Isohexyl aromatic molecular fossils: 2-methyl-1-(4-methylpentyl)naphthalene (**325**), 2,6-dimethyl-1-(4-methylpentyl)naphthalene (**326**), 6-ethyl-2-methyl-1-(4-methylpentyl)naphthalene (**327**), 6-*i*-propyl-2-methyl-1-(4-methylpentyl)naphthalene (**328**), 2-ethyl-4,6-dimethyl-1-(4-methylpentyl)naphthalene (**329**), and 1,2,4-trimethyl-3-(4-methylpentyl)benzene (**330**)

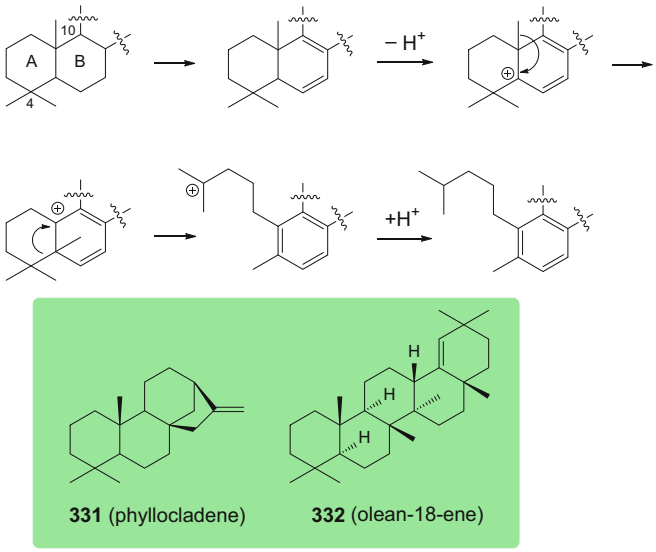

Fig. 52 Mechanistic details of the ring opening of terpenes to yield isohexyl substituted benzenes and naphthalenes with natural products **331** and **332** showing the respective prerequisites

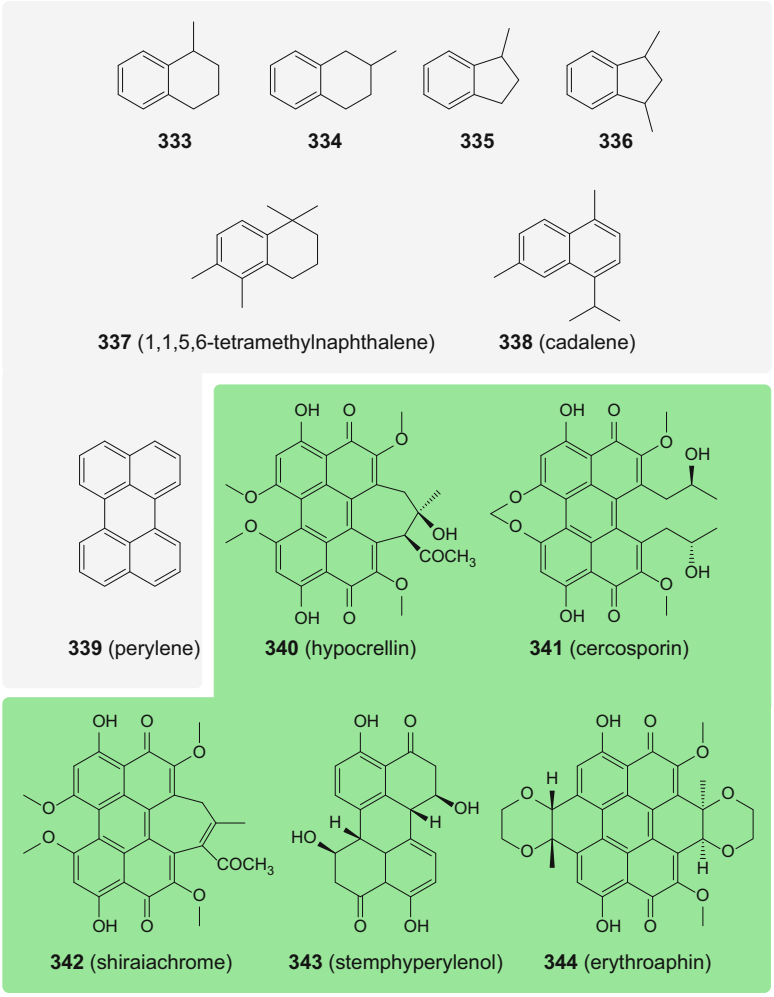

Fig. 53 Tetralin and indan derivatives **333–337**, cadalene (**338**), perylene (**339**), and perylene-containing natural products **340–344**

334), the isomers were found to be racemic, which was also the case with the 1-methyl- and 1,3-dimethylindans **335** and **336**. 2-Methyltetralin (**334**) concentrations were found to be about twice of those of 1-methyltetralin (**333**). In the case of the indans, the *cis*-**336** isomer was found to be in slight excess (52–70%) over the *trans*-**336** isomer. 1,1,5,6-Tetramethylnaphthalene (**337**) and cadalene (**338**) originating from cadinane (**114**), a marker for dammar resin-producing gymnosperms, are general biomarkers for higher plants [155].

Phenanthrene molecular fossils like fichtelite (**117**) (see Fig. 19), simonellite (**119**), and retene (**120**) (see Fig. 21), derived from abietic acid (**118**), were

discussed above in Sect. 2.1.3. It may be pointed out that **120** could not only originate from conifers, but may also result from ancient algal and bacterial biomass forms [156]. In the course of the present description, fluorene and phenanthrene (named as organic minerals kratochvilite and ravatite—Strunz classifications 10.BA.25 and 10.BA.40) may be set aside, because as molecular fossils they cannot be attributed to specific natural products and might also be of abiogenic origin. Thus, on proceeding to higher polyaromatic systems, perylene (**339**) should be dealt with initially (Fig. 53). This highly condensed compound is a common and abundant sediment constituent. A study of Saanich Inlet in British Columbia Holocene coastal marine anoxic basin, revealed that perylene (**339**) is present in both marine- and land-derived strata [157]. It is formed by microbial mediated diagenesis and it is yet unclear as to which specific organisms provide the precursor(s), because it can be derived from both aquatic and terrestrial organic matter or by additional microbial processes. However, a concomitant study of Late Triassic to Middle Jurassic sediments in the Northern Carnarvon Basin, Australia showed that at a diagenetic origin of about 0.6 ppm, compound **339** may be traced to mostly terrestrial sources like fungi [158]. These organisms may biosynthesize binaphthyls or perylenequinones like hypocrellin (**340**), cercosporin (**341**), shiraiachrome (**342**), stemphyperylenol (**343**), or erythroaphin (**344**) (Fig. 53) [158, 159]. A very detailed more recent study of this somewhat controversial issue involving a Holocene sediment profile from the Qingpu trench, Yangtze River Delta, People's Republic of China, and of sediment samples down to the Devonian, has made it clear that the concentration of **339** was closely related to the occurrence of wood-degrading fungi [160].

Sediments, coal deposits, and crude oils contain commonly varying, but significant amounts of polyaromatic hydrocarbons (**345–355**) (Fig. 54), as, for example, described in an earlier report [158]). These can be derived either by extensive chemical transformations of organic natural products, combustion, or thermal processes of organic material, or else stem from non-biogenic processes, like the "zigzag process" involving acetylene and butadiene radical additions to yield the thermodynamically most favorable polyaromatic hydrocarbons (Fig. 55) [161, 162]. Thus, such polyaromatic hydrocarbons constitute in part molecular fossils, but these compounds also may be derived from non-biogenic sources. Contrary to this situation for most of the polyaromatic hydrocarbons, 1,2,3,4,5,6-hexahydrophenanthro[1,10,9,8-*opqra*]perylene (**356**) (Fig. 54) is a highly specific diagenetic molecular fossil and thus a biomarker of hypericinoids, which will be discussed in Sect. 2.2.3. A synthesis and X-ray structural analysis of **356** to define its identity were described [163], and its spatial structure, which displays rather distorted saturated rings due to steric strain, is shown at the bottom of Fig. 54.

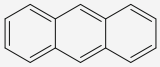

345 (anthracene)

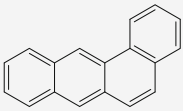

346 (benzo[*a*]anthracene)

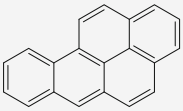

347 (benzo[*a*]pyrene)

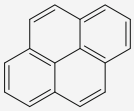

348 (pyrene)

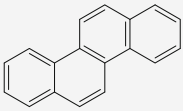

349 (chrysene)

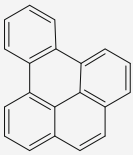

350 (benzo[*e*]pyrene)

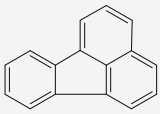

351 (fluoranthene)

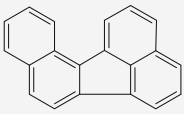

352 (benzo[*j*]fluoranthene)

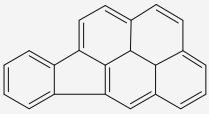

353 (indeno[*cd*-123]pyrene)

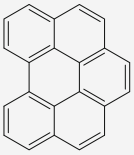

354 (benzo[*ghi*]perylene)

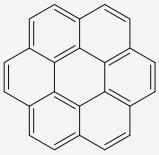

355 (coronene)

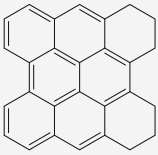

356 (1,2,3,4,5,6-hexahydrophenanthro[1,10,9,8-*opqra*]perylene)

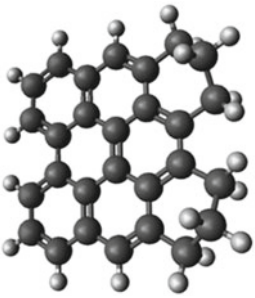

Fig. 54 Polyaromatic hydrocarbons **345**–**356** and bottom: X-ray analytical structure of **356** [163]

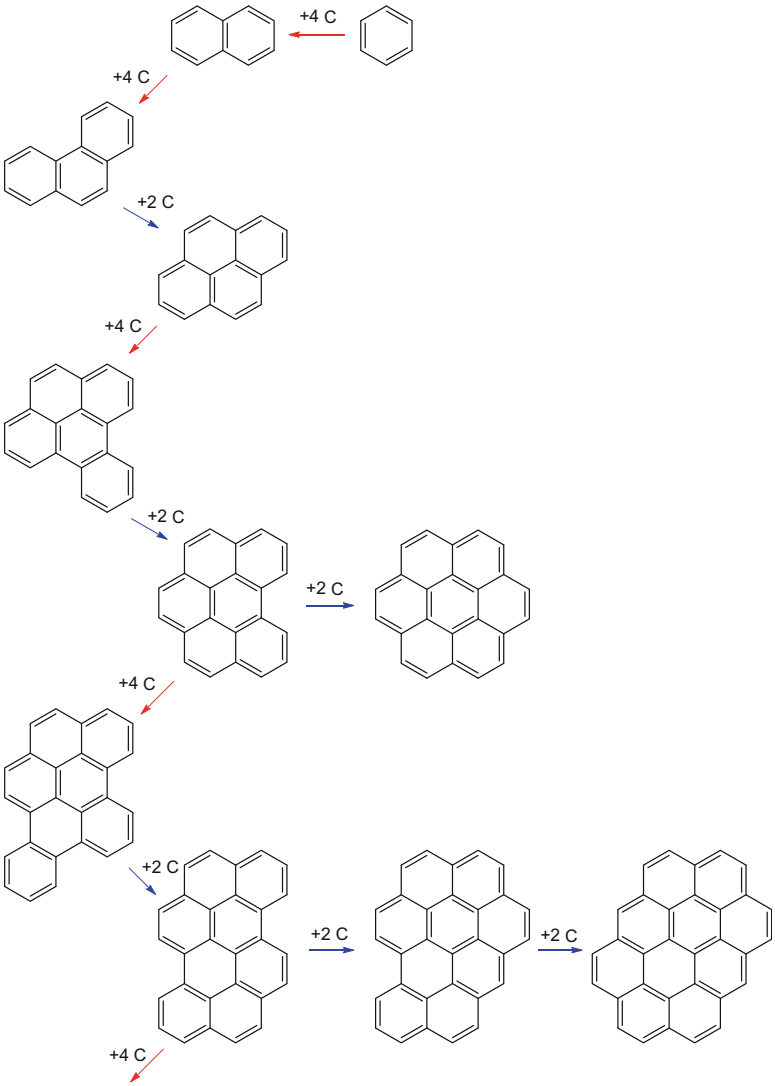

Fig. 55 "Zigzag" formation of polyaromatic hydrocarbons

Porphyrins

Since the pioneering studies [164] and ideas of Alfred Treibs mentioned earlier in Sect. 1 [2], investigations on porphyrins, or "geoporphyrins" as they are usually called, have evolved significantly. In particular, this topic matured in the last few decades of

the last century, when structural analysis by modern methods (HPLC, NMR) became available [165], but this field is still flowering in the early twenty-first century (e.g. [166]). Geoporphyrins are found globally in sediments, coals, and oils deposited in various geological periods: classic sources with abundant porphyrins mentioned in chronological order (see Fig. 106) are the Devonian Henryville beds of the New Albany oil shale [167], the Permian Kupferschiefer in Germany [168], the Triassic Serpiano oil shale in Switzerland [169], the Toarcian (Jurassic) shales of Europe [170], the Cretaceous Julia Creek deposits in Queensland, Australia [171], the Eocene Messel lacustrine shale in Germany [172], the Eocene Green River Formation of the western USA [173], the Miocene Monterey Formation in California, USA [174], and the Pliocene Willershausen lacustrine deposits in Germany [175]. Porphyrin derivatives were even suggested as potential ideal biomarkers in the search for extraterrestrial life [176]. Two series of the nearly one hundred geoporphyrins presently known are encountered. The first is derived diagenetically from heme, cytochrome, and other naturally occurring cyclic tetrapyrroles, and the second from the diverse chlorophylls of photosynthesizing organisms [177].

When starting from the natural products, heme (**357**) or the cytochromes, the first step is detachment of the porphyrin from the protein, resulting in hemin (**4**) (Figs. 1 and 56). The latter is then transformed diagenetically into a plethora of differently substituted porphyrin derivatives and their various metal complexes, thereby expanding dramatically the "Treibs Scheme" that ended with deuteroetioporphyrin (**2**) [2]. Figure 56 displays a route leading via dealkylation/hydrogenation to **361** [178], then by successive decarboxylations to **362** [179], and finally to **2** [2], with all possible intermediates identified in various sediments and oils. Another branch commences with **357** by hydrogenation to mesoporphyrin IX (**358**) and its metal (Ni, Fe,) complexes [180] (from which even a gallium complex was identified in a Middle Triassic pink calcite from the hydrothermal region of Deutsch-Altenburg in Austria [181]). Then, monodecarboxylation results in the two monopropionic acids **359** [182], and finally, decarboxylation yields etioporphyrin III (**360**) and its metal (Fe, Ni, V) complexes. However, the latter could also be derived from chlorophyll [183]. Besides these porphyrins, various others were identified, as exemplified by **363** as the main constituent of gilsonit (synonym: uintahite) from the Eocene bitumen mines of the Uinta Basin in Utah, USA [184, 185], octamethylporphyrin and its Ni complex (**364**) [186], and the monopropionic acid **365** and its Ni complex [167]. It should be mentioned that hemoglobin-derived porphyrins have also been found preserved in a blood-engorged mosquito of the Middle Eocene Kihenehn Formation of Montana, USA, as suggested by mass spectrometric data [187].

With respect to the chlorophyll-derived porphyrins, a boundary is encountered, as there is some evidence that **363** may not only be derived from **357** but also from plant material, as indicated earlier [183]. Three main pathways are available to describe the fate of chlorophylls until they become molecular fossils or biomarkers. For all three, the first step is hydrolysis of the phytyl and methyl esters of chlorophyll (**3**) to yield the diacid pheophorbide a (**366′**), which is found in modern (down to 500 years) sediments of Lake Baikal [188], and methyl pheophorbide a (**366**), which has even

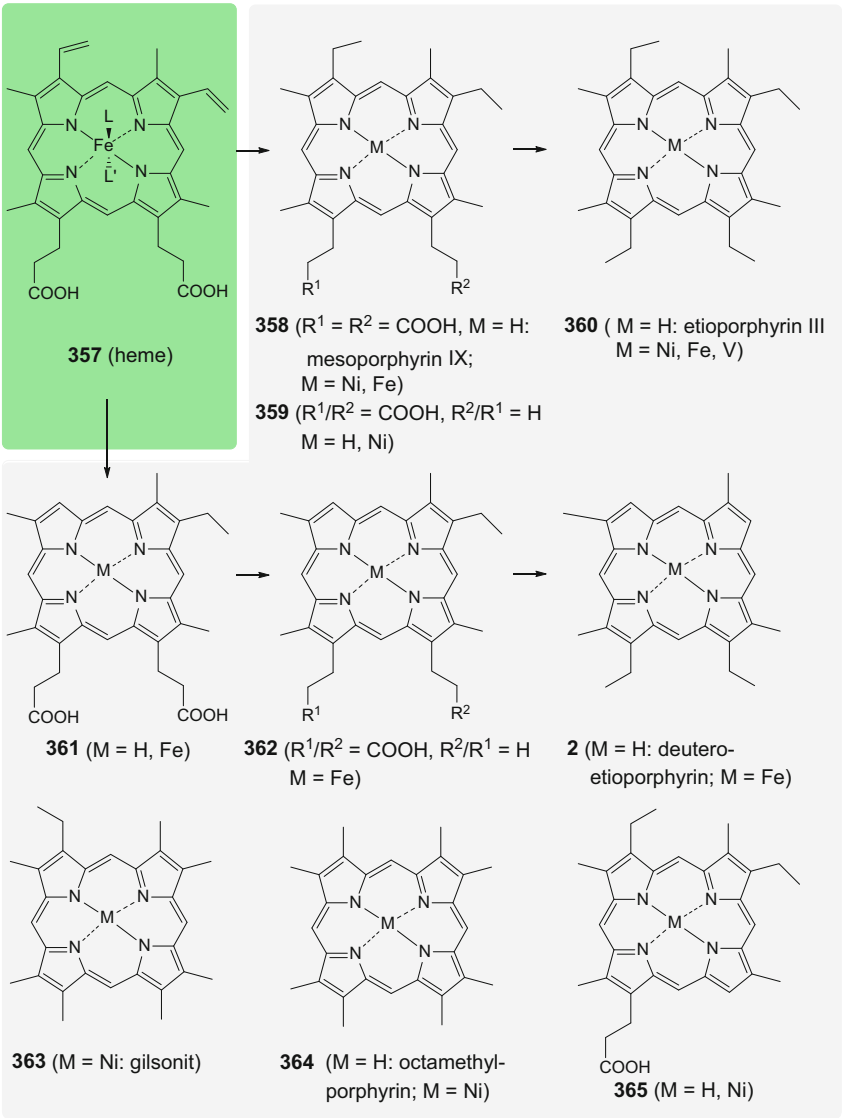

Fig. 56 Geoporphyrins **2** and **358–365** originating from heme (**357**)

been found in still green-colored fossil *Zelkova*, *Celtis*, and *Ulmus* leaves of the Miocene Succor Creek Flora from Oregon, USA [189–191] and in Eocene brown coal from Geiseltal, Germany, containing green-colored angiosperm leaves [191].

On the first pathway (Fig. 57), **366**, upon decarboxylation, results in pyropheophorbide a (**367**), which is encountered in the bottom sediments of an eutrophic lake [192]. Hydrogenation of the C-3 vinyl group leads to the major

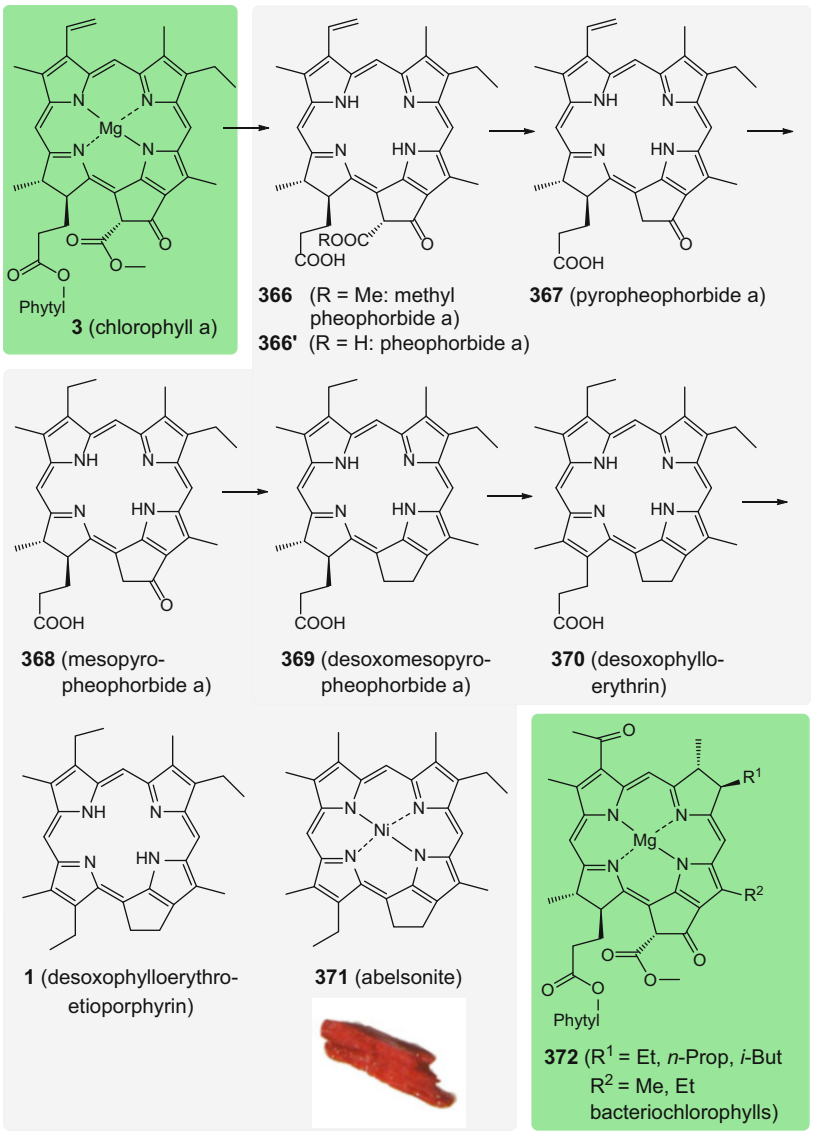

Fig. 57 Molecular fossils **366–371** of chlorophyll a (**3**) and bacteriochlorophylls **372**. Bottom: abelsonite crystal, length 1.8 mm, Green River Formation, Uintah County, Utah, USA; photograph: T. Witzke, Wikimedia Commons

chlorin in the Eocene Messel oil shale, mesopyropheophorbide a (**368**), identified as being present as its nickel complex [193]. Reduction of the exocyclic ring carbonyl group of **368** yields desoxomesopyropheophorbide a (**369**), identified in the Late Pliocene lacustrine sediment of Willershausen, Germany [175]. Finally,

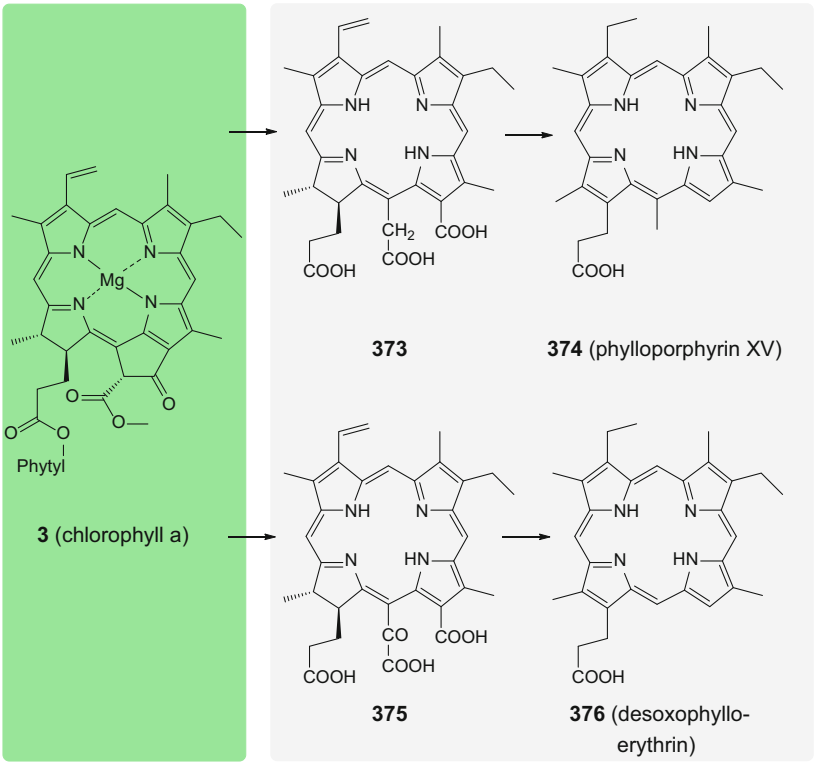

Fig. 58 Molecular fossils **373–376** of chlorophyll a (**3**)

dehydrogenation of ring D of **369** results in desoxophylloerythrin (**370**), and its decarboxylation ends with desoxophylloerythroetioporphyrin (**1**), as already realized by Treibs [2, 164]. The nickel complex of the 2-desmethyl derivative is found as the mineral abelsonite (**371**) (Nickel-Strunz classification 10.CA.20; named in honor of the U.S. physicist Philip H. Abelson (1913–2004)) [194, 195], known, for example, from the Parachute Creek Member of the Eocene Green River Formation. Analogous pigments are derived from chlorophyll b and the bacteriochlorophylls **372** [179].

The second pathway (Fig. 58) is characterized by a splitting of the exocyclic ring to yield the intermediates **373** and **375**, which then by decarboxylation give rise to phylloporphyrin XV (**374**) and desoxophylloerythrin (**376**) [179].

The third pathway (Fig. 59) involves cyclization to yield the seven-membered ring of 13^2,17^3-cyclopheophorbide enol (**377**), which was identified in 1999 in surface sediments of the Black Sea, the Mediterranean Sea, and the Peru coastal margin as one of the most abundant pigments [196]. Interestingly, this compound

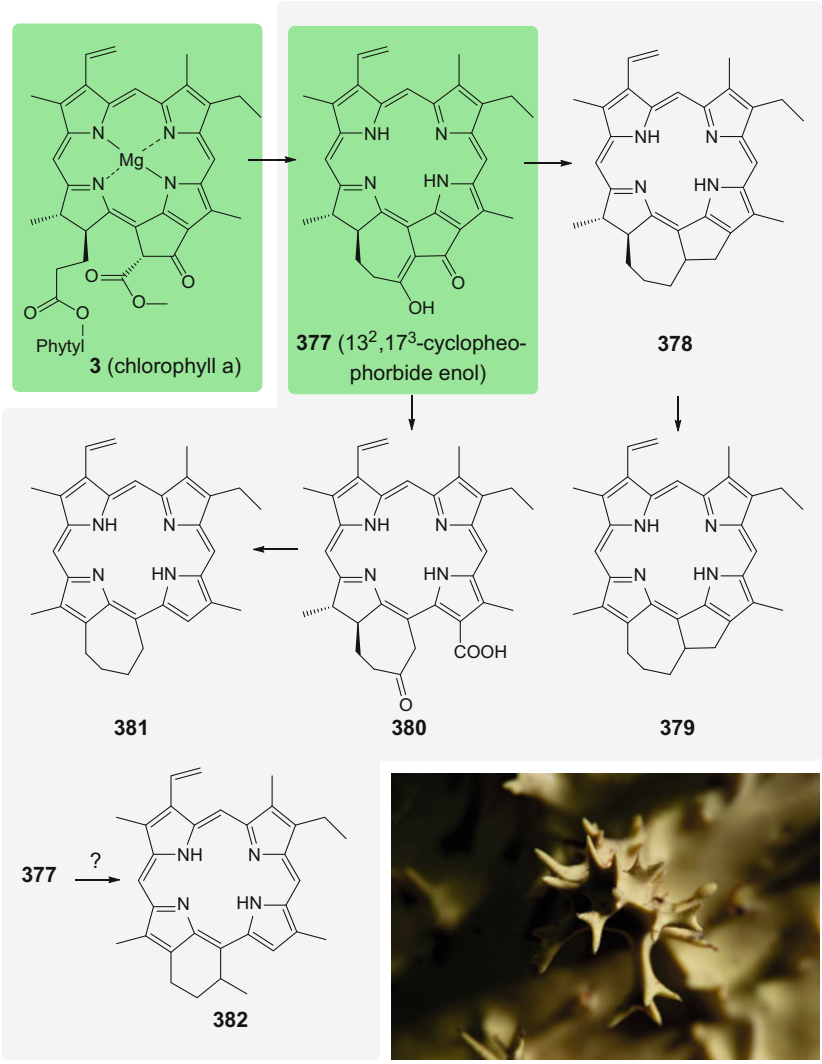

Fig. 59 Molecular fossils **377**–**382** of chlorophyll a (**3**). Bottom: *Darwinella oxeata* from Middle Arch, Poor Knights Marine Reserve, New Zealand, which produces **377**; photograph courtesy of Richard Robinson (www.depth.co.nz)

was also isolated as a natural product from the sponge *Darwinella oxeata* (Fig. 59) [197] in 1986 and the clam *Venerupis philippinarum* (formerly *Ruditapes philippinarum*) in 1990 [198]. As **377** was produced by chemical synthesis as early as 1971 [199], this is a rare case when a natural compound was synthesized before it could be determined as being a natural product. $13^2,17^3$-Cyclopheophorbid-enol (**377**) is a prominent precursor of the molecular fossil

five- and seven-membered exocyclic ring systems. Thus, it leads after reduction to **378** [175] and eventually by dehydrogenation to the fully unsaturated porphyrin nucleus of **379**, which is documented from the Late Pliocene lacustrine sediments of Willershausen (Germany) [175]. Otherwise, **377** can be ring opened to give **380** and after reduction the exocyclic seven-membered ring derivative **381**, as found in Eocene Messel oil shale [179]. Under ring contraction, **377** may also yield the six-membered analogue **382**, which has been isolated as its vanadium complex from the Triassic Serpiano oil shale (Switzerland) [200].

Heterocyclic Compounds

Nitrogen Heterocycles

The products of heme catabolism, biliverdin (**383**) and protoporphyrin (**384**) (Fig. 60), are known to be responsible for the coloration of certain bird eggs (see Fig. 60 for an emu egg colored by **383**). Both compounds have been detected in subfossil eggshells of extinct moa species from New Zealand. Whereas the bile pigment **383** has been found in blue green-colored eggshells of the upland moa *Megalapteryx didinus*, **384** has been detected in beige-colored eggs of the North Island moa *Euryapteryx curtus* and an undetermined South Island moa species [201]. Since bile pigments are quite unstable and are easily cleaved and oxidized to the respective pyrrole compounds, the preservation of these compounds over time is remarkable. Even more interesting is that biliverdin (**383**) and protoporphyrin (**384**) recently have also been detected in Late Cretaceous eggshells (*Macroolithus yaotunensis*) from mainland China, presumably laid by the oviraptorid dinosaur *Heyuannia huangi* [202]. Evidently, the inorganic/biopolymeric matrix of eggshells can effectively protect the embedded pigments, probably by calcium salt formation. One may add that various gastropod shells contain organic pigments like **383**, and that corresponding color patterns have been retained down to the Triassic [203]. However, no reliable chemical data on these fossils are available.

In connection with the diagenesis of chlorins and porphyrins, the maleimides have to be mentioned as their diagenetic end products. Given the stability of the chlorins and porphyrins due to their 18 π-electron aromatic anulene system, it seems that only in rather rare instances would substituted maleimides be derived by a non-enzymatic diagenetic process. Porphyrins in animals and chlorins in plants or algae are enzymatically catabolized within their source organisms or via photooxidation in the water column to yield bile pigments like biliverdin (**383**) (Fig. 60) [204–208]. Mammalian and plant bile pigments are quite unstable and are easily cleaved and oxidized to the respective pyrrole compounds. Thus, the molecular fossils involving maleimides are likely due to this route. An extensive study of the Permian Kupferschiefer of the lower Rhine Basin (Germany) and the Middle Triassic Serpiano shale of Monte San Giorgio

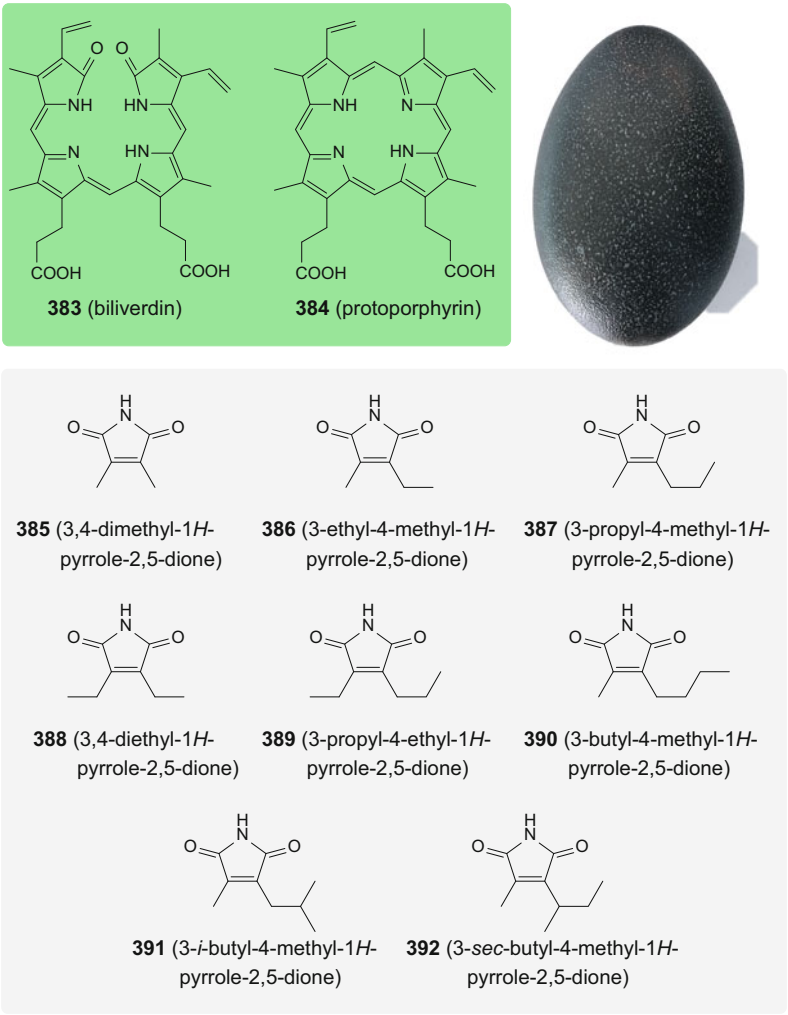

Fig. 60 Biliverdin (**383**), protoporphyrin (**384**), a biliverdin-colored egg shell of extant *Dromaius novaehollandiae* (emu), and dialkyl substituted maleimides **385**–**392**; photograph: H. Falk

(Switzerland) [209, 210] revealed the presence of the eight maleimides **385**–**392** shown in Fig. 60. The substitution pattern of the most abundant 3-ethyl-4-methyl-1*H*-pyrrole-2,5-dione (**386**) clearly points to an origin from chlorophyll a (**3**), which provides a link to either phytoplankton consisting of cyanobacteria or algae, or higher plants. Otherwise, the substituents of 3-propyl-4-methyl-1*H*-pyrrole-2,5-dione (**387**) and 3-*i*-butyl-4-methyl-1*H*-pyrrole-2,5-dione (**391**) are typical of the bacteriochlorophylls c, d, or e of the Chlorobiaceae, the anoxygenic green sulfur bacteria.

Oxygen Heterocycles

Several chromanes (**393–397**) (Fig. 61) were identified in various sediments and oils ranging from the Permian to the Pleistocene [211, 212]. The source of these compounds is somewhat uncertain: they have been discarded as likely precursors, although tocopherols like **22** seem to be related to the molecular fossils **393–397** with respect to their isoprenoid structures. These might originate from bacterial or

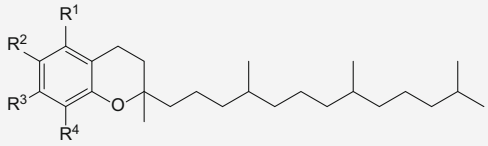

393 ($R^1 = R^2 = R^3 = H$, $R^4 = Me$: 2,8-dimethyl-2-(4,8,12-trimethyltridecyl)chromane)
394 ($R^1 = R^2 = H$, $R^3 = R^4 = Me$: 2,7,8-trimethyl-2-(4,8,12-trimethyltridecyl)chromane)
395 ($R^1 = R^3 = H$, $R^2 = R^4 = Me$: 2,7,8-trimethyl-2-(4,8,12-trimethyltridecyl)chromane)
396 ($R^1 = H$, $R^2 = R^3 = R^4 = Me$: 2,6,7,8-tetramethyl-2-(4,8,12-trimethyltridecyl)chromane)
397 ($R^2 = H$, $R^1 = R^3 = R^4 = Me$: 2,5,7,8-tetramethyl-2-(4,8,12-trimethyltridecyl)chromane)

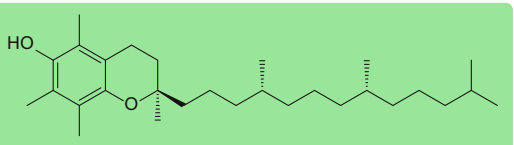

22 (α-tocopherol)

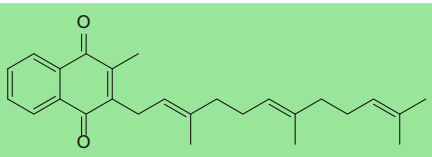

398 (menaquinone-3)

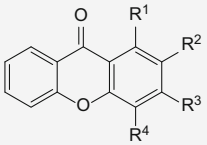

399 $R^1 = R^2 = R^3 = R^4 = H$
400 $R^1 = Me$, $R^2 = R^3 = R^4 = H$
401 $R^2 = Me$, $R^1 = R^3 = R^4 = H$
402 $R^3 = Me$, $R^1 = R^2 = R^4 = H$
403 $R^4 = Me$, $R^1 = R^2 = R^3 = H$

Fig. 61 Isoprenoid chromanes **393–397**, α-tocopherol (**22**), menaquinone-3 (**398**), and xanthones **399–403**

archaean isoprenoid quinones like **398** and are indicative of mesosaline deposition conditions. A hypothesis (condensation of alkylated phenols with pristene or phytol [213]) of their origin has been proposed, but shown to be very unlikely [214].

Xanthone (**399**) and its related methylxanthones **400–403** (Fig. 61) were detected in Cenozoic crude oils from offshore Norway [215]. Their origin is still unknown, but it is speculated that they may be formed by oxidation of xanthenes or originate by geosynthesis from aromatic compounds.

Sulfur Heterocycles

In many shales and crude oils that are derived from a saline origin with a high content of elemental sulfur, various sulfur-containing molecular fossils are found [50, 216–221]. The main group is those of the substituted thiophenes, their saturated derivatives, and sulfoxides of the latter. A large ensemble of substituted thiophenes has been found, as in Late Jurassic carbonates from Germany [212], with several homologous series of alkyl thiophenes occurring. The first of these series **404** starts with 2-methylthiophene and may include octyl to hexacosyl residues. The second comprises 2-methyl-5-alkylthiophenes **405**, whereas the third (**406**) has a 2-ethyl residue instead of the methyl group. The fourth group contains mid-chain thiophene series, **407** and **408** (Fig. 62).

A few derivatives with branched side chains were also identified, such as 2-methyl-5-(4-methyltridecyl)thiophene (**409**) [212]. In addition to this compound and the members of the above-mentioned series, several isoprenoid thiophenes like **410–413** could be identified (Fig. 63). To these branched chain derivatives may be added an ensemble of highly branched isoprenoid thiophenes like **414–417**, which

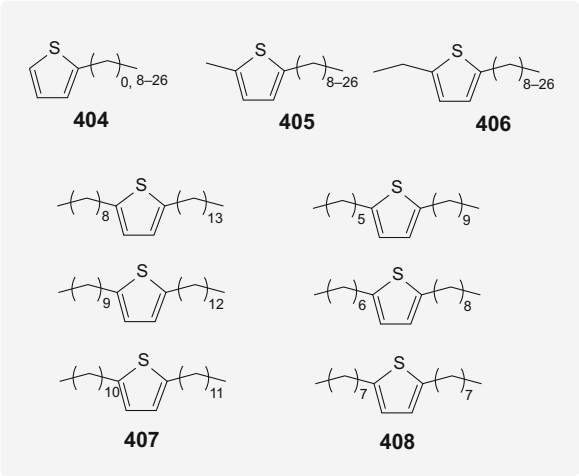

Fig. 62 Alkylthiophene series **404–408**

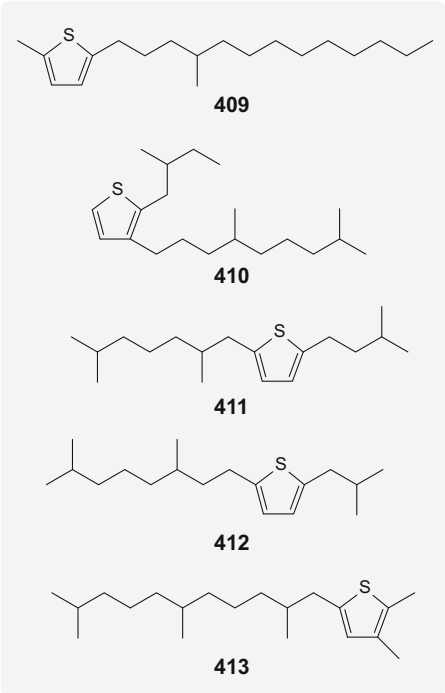

Fig. 63 Branched alkylthiophenes **409–413**

were isolated from lacustrine sediments and oils like those of the Miocene Ribesalbes shales from the southern European rift system [220]. From these localities, the thiolanes **418** and **420** and sulfoxides **419** and **421** derived from **415** and **416** (Fig. 64) were identified. They are analogous to the sulfur derivatives from immature sediments [217].

Interestingly, hopanoids with a thiophene ring in the side chain could also be characterized [217, 221]. Besides these thiophenes, thiolanes, and thiolane sulfoxides comparable with **418–421** are also present. The configurational situation in the C-17 and C-21-hopane positions is the same as encountered already with the geohopanes described in Sect. 2.1.3. Two representative examples are the thiophene hopane **422** and the thiolane hopane **423**, as shown in Fig. 65.

With respect to the formation of all these sulfur-containing systems it is necessary that the depositional conditions are characterized by high sulfur concentrations. The reaction between a natural product containing a 1,3-diene moiety upon reaction with sulfur will then yield the thiophene ring as exemplified by the transformation of **424** to **415** (Fig. 66) [220]. It is worth mentioning that a reaction of this type can be used for the industrial production of thiophene starting from gaseous sulfur and 1,3-butadiene [222]. From this information, it is clear that sulfur-

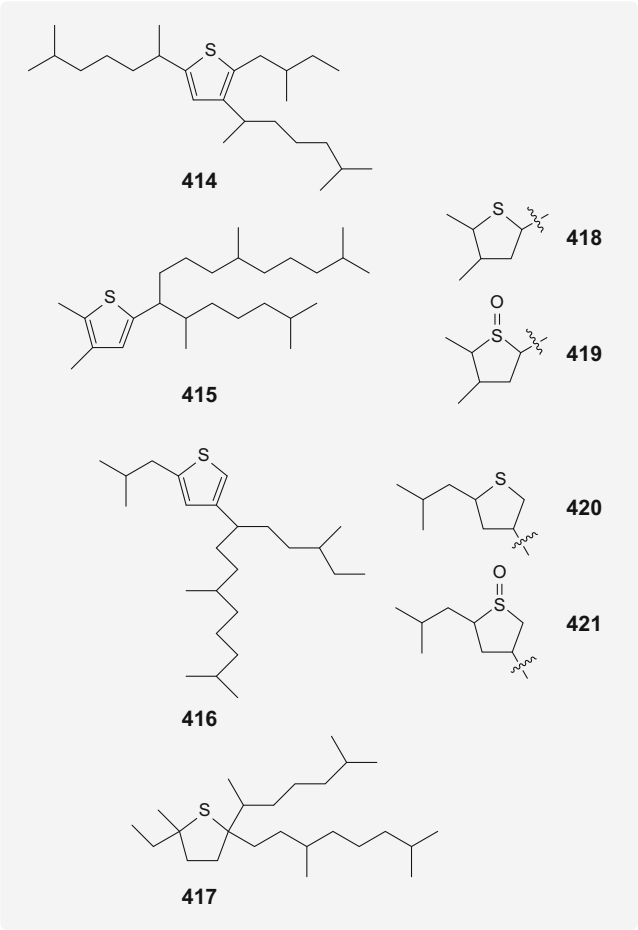

Fig. 64 Highly branched alkylthiophenes **414**–**416**, the respective thiolane and sulfoxide derivatives **418**–**421**, and the tetra-alkylated thiolane **417**

containing compounds of the kind discussed above originate from addition processes of the genuine natural products, or their partially diagenetically altered derivatives in the presence of elemental sulfur. Thus, these molecular fossils can serve to some extent as biomarkers of their biological precursors, but in addition, they are also indicators of sulfur-rich paleoenvironmental conditions.

Complementary to the mono-ring sulfur heterocycles one should also mention that oil shales, as exemplified from the Eocene Green River Formation, can contain isoprenoid 2,4-dialkyl-benzo[*b*]thiophenes like **425** (Fig. 66) [50, 218].

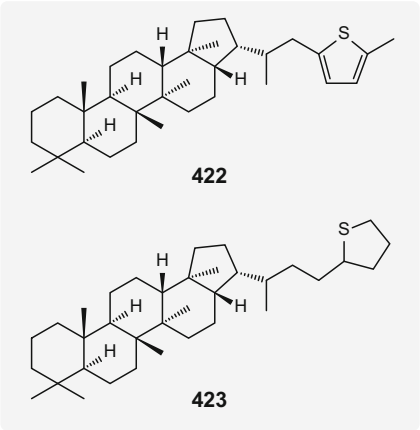

Fig. 65 Sulfurated hopanes **422** and **423**

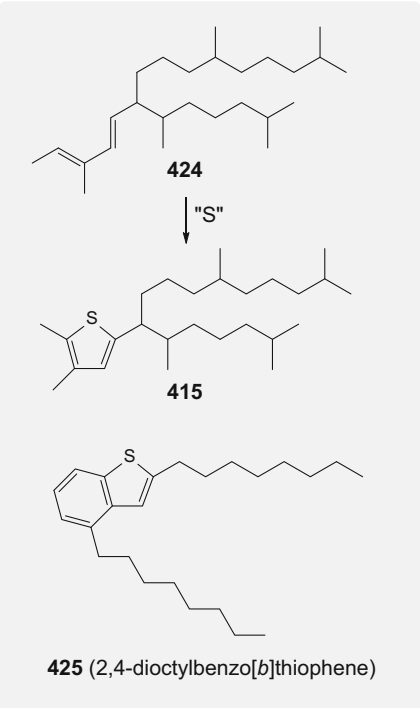

Fig. 66 Addition of a sulfur species "S" to a 1,3-diene precursor **424** to yield the highly branched terpenoid thiophene **415** and the benzo-condensed compound 2,4-dioctylbenzo[*b*]thiophene (**425**)

2.2 Polar Compounds

The apolar molecular fossils described so far may be extracted readily from their geological samples. In most cases for the polar compounds, which are characterized as having mainly the same skeletons as the apolar examples, samples may be generated only with a considerable experimental effort and under rather harsh conditions. In addition, the analytical methodology necessary to solve the rather complicated structures involved has become available recently. Thus, examples of polar molecular fossils only began to be elucidated during the last few decades.

2.2.1 Ethers

The remarkable main components of archaean membranes are diether or tetraether lipids. These consist of glycerol and various isoprenoids or long chain equivalents [223–227]. Such lipids may be considered as analogs of the diglycerides of bacteria and eukaryotes; they impose a much higher stability and rigidity on the membranes, which is necessary to protect organisms against extreme temperatures and acidity conditions.

In the typical archaean diether lipids, glycerol is etherified to C_{20}, C_{25}, and C_{40} isoprenoid alcohols, resulting in open chain lipids **426–428** and the cyclic diether **24** (Fig. 67). As the ether bond in general is of high stability, not only diagenetically

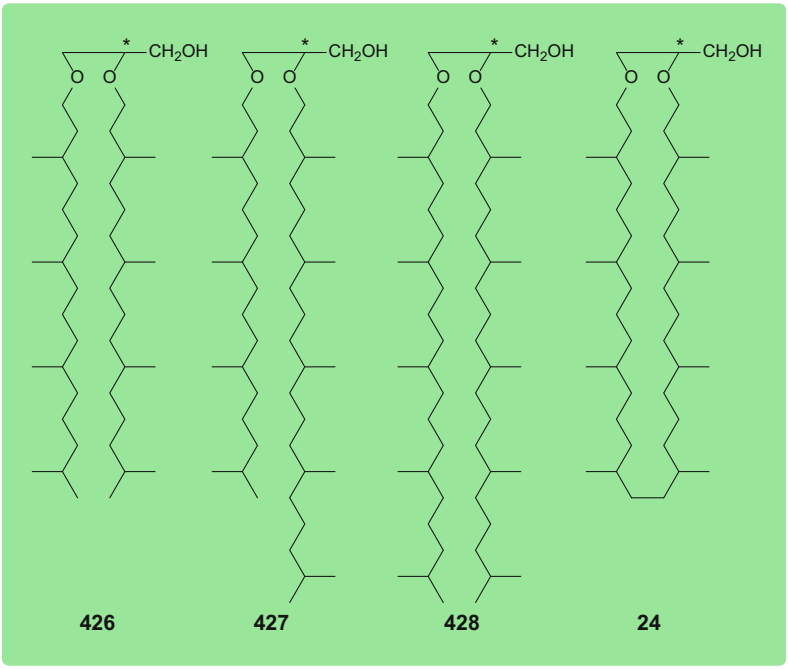

Fig. 67 Archaean glycerol dialkyl diether lipids **426–428** and cyclic glycerol diether **24**

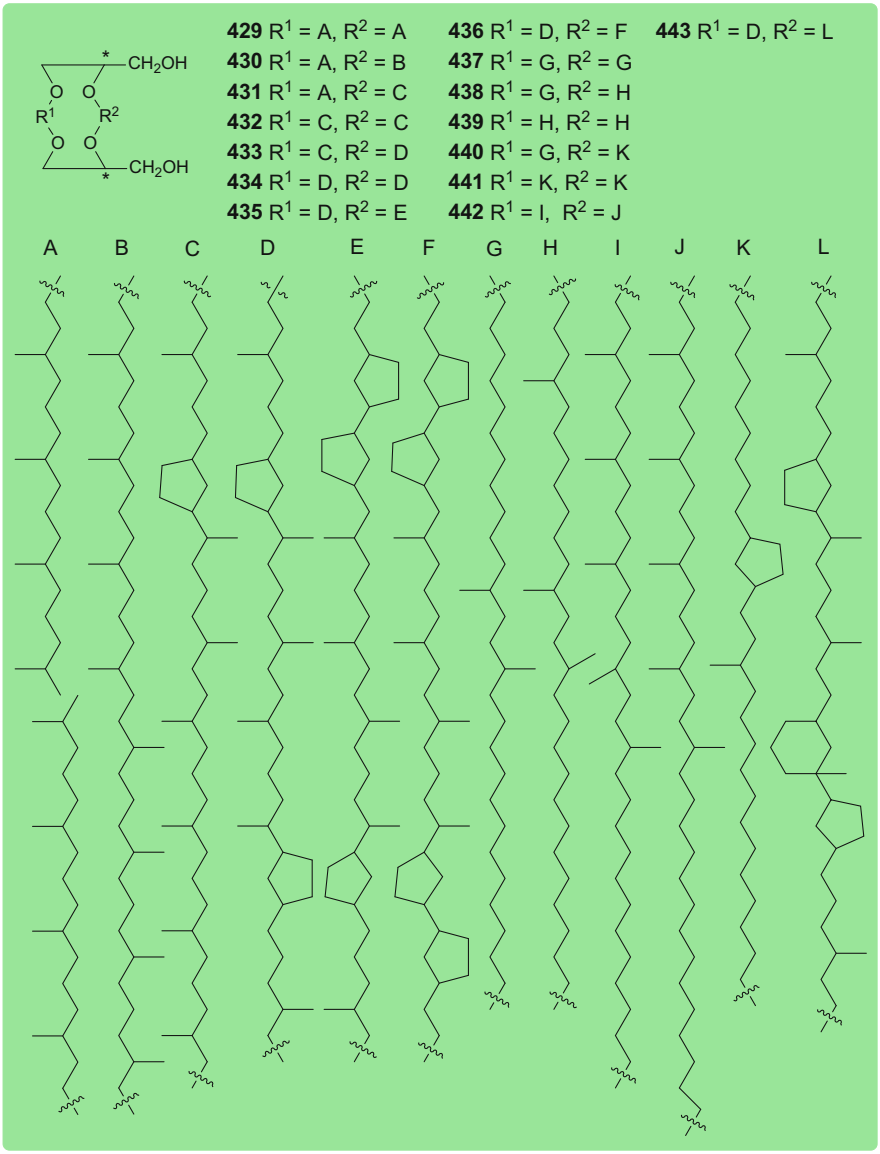

Fig. 68 Archaean diglycerol dialkyl tetraethers **429–443**

degraded alkanes like biphytane (**23**) are present in certain sediments (Fig. 9), but also the intact ethers have been found, as shown from the comparatively modern surroundings of Mediterranean cold seeps [228], methanogenic sediments [229, 230], or surface soils [231] to the Eocene lacustrine Messel oil shale [232]. The lipids **426–428** and **24** possess an asymmetric carbon atom at the glycerol moiety (indicated by an asterisk in Fig. 67). Accordingly, these molecules

are chiral in addition to the terpenoid chirality of the chains, but no convincing data seem to be available if such compounds are racemic or a pure enantiomer. The unspecified chiral centers of the glycerol di- and tetraether molecules are obviously due to the shortcomings of the analytical methods used to address structural details, principally those based on mass spectrometry.

The structural variety of the tetraethers is much larger than detailed above, because, in addition to their rather simple non-terpenoidal moieties, isoprenoid chains A or B and G–J are encountered, chains with embedded pentacyclic rings C–F and K, and even L containing a hexacyclic ring (Fig. 68). These chains are etherified at two glycerol units to form open chain lipids **429** and **430** or macrocyclic ring systems as exemplified with **431**–**443** [227, 233]. Due to the presence of two chiral centers at the glycerol units (indicated by asterisks in Fig. 68) these lipids occur as *meso*- or *racem*-diastereomers [237], and again information on the chiral center configurations or diastereomerism of the tetraethers is not well defined.

The isoprenoid glycerol dialkyl glycerol tetraethers occur in both recent and ancient sediments [225, 234–236], back to the mid-Cretaceous [237]. A tetraether index was defined using compounds consisting of 86 carbon atoms (TEX_{86}), and can be used as a proxy for sea surface temperatures [231, 238]. It is interesting to note that large portions of the cyclic structures occur in the lipids from organisms adapted to extreme conditions. Whereas **433** is characteristic of methanogenic organisms, most other ethers of the series are found in the Caldariella group of extremely thermoacidophilic Archaea, *Thermoplasma* sp. and *Sulfolobus solfaticarus*, or hyperthermophiles of low-temperature marine sediments such as *Methanosarcina barkeri*. The additional hexacyclic ring of crenarcheol (**443**) is found exclusively in Thaumarchaeota (formerly Crenarchaeota), psychotrophic marine organisms, in which they seem to stabilize the membranes at low temperatures [225]. With respect to further structural variations, one of the glycerol units of the tetraethers can be replaced by a nonitol [224]. Even non-isoprenoid chains containing a three-membered ring occur in dialkyl glycerol diethers from cold-seep carbonate crusts of Mediterranean mud volcanos that contain *Thermodesulfobacterium commune*, *Ammonifex degensii*, and *Aquifex pyrophilus* [239].

2.2.2 Alcohols and Phenols

Alcohols

The simplest alcohols found in the fossil record are *n*-alkanols with chain lengths between 22 and 34 carbon atoms and a strong preponderance of the even-numbered members (**444**–**450**) over the odd-numbered ones (Fig. 69) [240]. This general observation points to the involvement of the acetate biosynthesis pathway, which is typical for leaf waxes of plants. Since these compounds can still be found in present-day plants, it appears that they have remained unchanged for millions of years. The molecular fossils (in this case true biomarkers) **444**–**450** were identified in fossil plant leaves from the Miocene Clarkia lake deposit in northwestern Idaho, USA

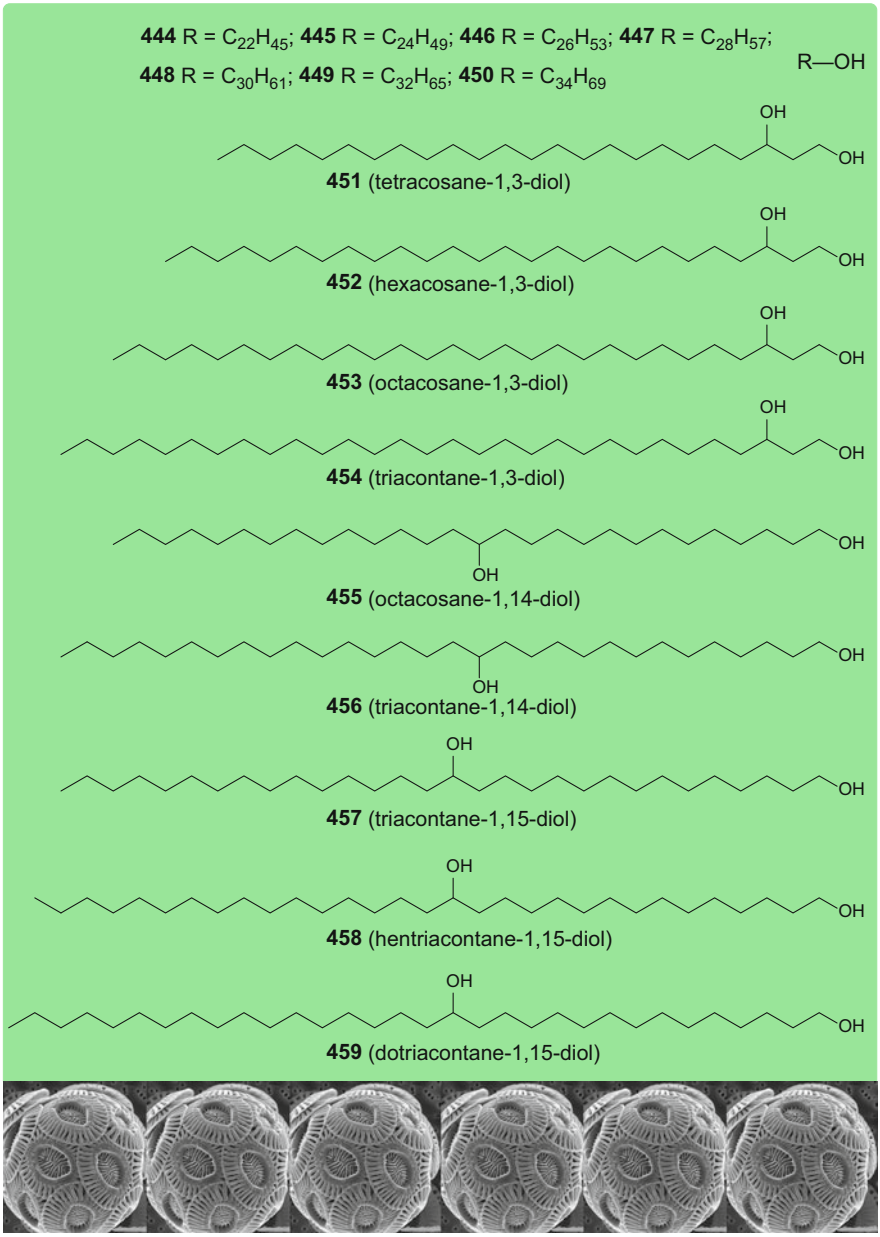

Fig. 69 *n*-Alkanols **444–450** and *n*-alkanediols **451–459**; Bottom: *Emiliana huxleyi*; picture: collage of scanning electron micrographs of a single cell; photograph: A. R. Taylor, Wikimedia Commons

(17–20 Ma), and to a much lesser extent in surrounding sediments [240]. Most species were found to be enriched in **448**, whereas a *Sequoia* sp. (redwood) and a *Fagus* sp. (beech tree) had a preponderance of **447** and **445**. *Quercus rubra* (red oak) showed

high concentration levels of **448** together with **449**; a *Platanus* sp. (plane tree) **446** as the most abundant compound, and a *Taxodium* sp. (cypress) was richest in **447**. Thus, a chemotaxonomic classification of the various fossil leaves using principal component analysis became possible [240]. Leaf fossils and the enclosing sediments of the Miocene Clarkia deposit also were found to contain even-numbered homologous 1,3-*n*-alkanediols (**451**–**454**), with chain lengths from 24 to 32 carbon atoms [241] (Fig. 69).

Several *n*-alkanediols with chain lengths of 28 to 32 carbon atoms were detected in various sediments that were deposited in the Quaternary period [242]. Thus, long-chain 1,14-diols with chain lengths of 28 and 30 carbon atoms (**455** and **456**; Fig. 69) were found to be typical of *Proboscia* diatoms [243]. Young sediments (several thousand years) from the Gulf of St. Lawrence, Canada, and the Black Sea were shown to contain 1,15-diols (**457**–**459**) (Fig. 69), with chain lengths of 30–32 carbon atoms [244, 245]. These latter biomarkers are specific to the coccolithophore *Emiliana huxleyi* (Fig. 69) or yellow-green algae (Eustigmatophytes). A critical review discussed the general use of the mid-chain diols in assessing paleoenvironmental information like identifying fresh water influx [246].

Several α,ω-diols were characterized from various sediments that also contain cyclic biphytane tetraethers like **433** and the hydrocarbon biphytane **23** together with its mono to tricyclic analogs [234]. On first sight, the acyclic and cyclic biphytanyldiols **460**–**463** (Fig. 70) seem to originate from the corresponding cyclic

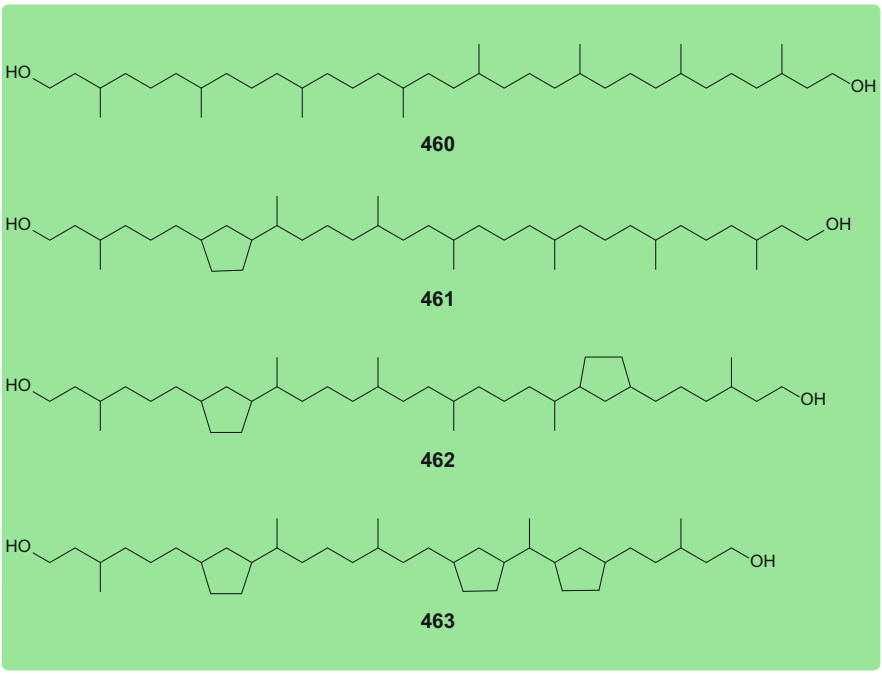

Fig. 70 Biphytanediols **460**–**463**

diglycerol tetraethers shown in Fig. 68, which are characteristic of Archaea. However, diagenetic splitting of ether bonds is rather unreasonable and, in particular, the co-occurrence of different chain structure distributions in the cyclic ether versus those of the diols points to an independent formation of the latter. It is hypothesized that the poorly studied planktonic Archaea may biosynthesize such diols [234].

Phenols

Simple alkylphenols are common in crude oils. Thus, analysis of SRM 1580 standard crude oil revealed the presence of the alkylphenols **464–486** (Fig. 71) [247]. The organismic source of these molecular fossils remains obscure, but the information extracted from the distribution of the isomers can be used to analyze migration processes of oils [248] or to judge biodegradation and water washings of the oil in question [249].

The bark remnants found in Eocene brown coal from Geiseltal (Germany) are addressed as "Affenhaar" (laticifers). These contain mono- and triaromatic phenolic triterpenoid derivatives of the oleanane (**487**, **491**), lupane (**488**, **489**, **492**), and ursane (**490**) series (Fig. 72) [250]. The precursor of all these molecular fossils is hypothesized to be the natural product α-amyrin (**493**) (Fig. 72) found, for example, in dandelion plants (*Taraxacum officinale*, see Fig. 50).

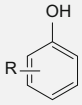

464 R = 2-Me
465 R = 3-Me
466 R = 4-Me
467 R = 2 Et
468 R = 3-Et
469 R = 4-Et
470 R = 2-*n*-Prop
471 R = 4-*n*-Prop
472 R = 2-*i*-Prop
473 R = 3-*i*-Prop
474 R = 4-*i*-Prop

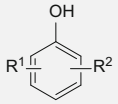

475 R^1 = 2-Me, R^2 = 3-Me
476 R^1 = 2-Me, R^2 = 4-Me
477 R^1 = 2-Me, R^2 = 5-Me
478 R^1 = 2-Me, R^2 = 6-Me
479 R^1 = 3-Me, R^2 = 4-Me
480 R^1 = 3-Me, R^2 = 5-Me
481 R^1 = 2-*i*-Prop, R^2 = 4-Me
482 R^1 = 2-Me, R^2 = 5-*i*-Prop

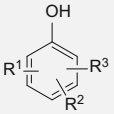

483 R^1 = 2-Me, R^2 = 3-Me, R^3 = 5-Me
484 R^1 = 2-Me, R^2 = 3-Me, R^3 = 6-Me
485 R^1 = 2-Me, R^2 = 4-Me, R^3 = 6-Me
486 R^1 = 3-Me, R^2 = 4-Me, R^3 = 5-Me

Fig. 71 Alkylphenols **464–486**

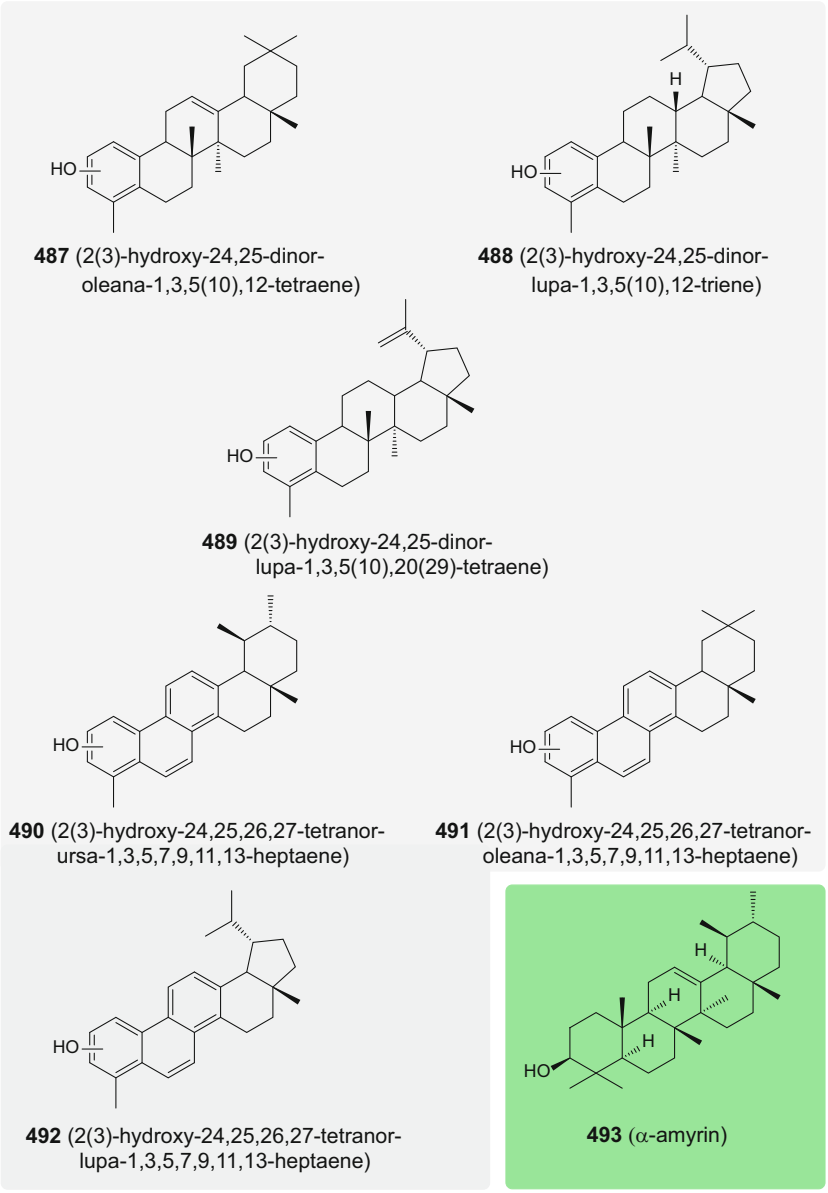

Fig. 72 Hydroxytriterpenoids **487–492** and the natural product α-amyrin (**493**)

From conifer fossils of Eocene and Miocene origins, the three phenolic terpenoids **494–496** (Fig. 73) were isolated [251]. Thus, both Eocene *Taxodium balticum* (from clays of the Zeitz Formation, Germany) and Miocene *Glyptostrobus oregonensis* (from the Clarkia Formation, USA) seed cones contain ferruginol

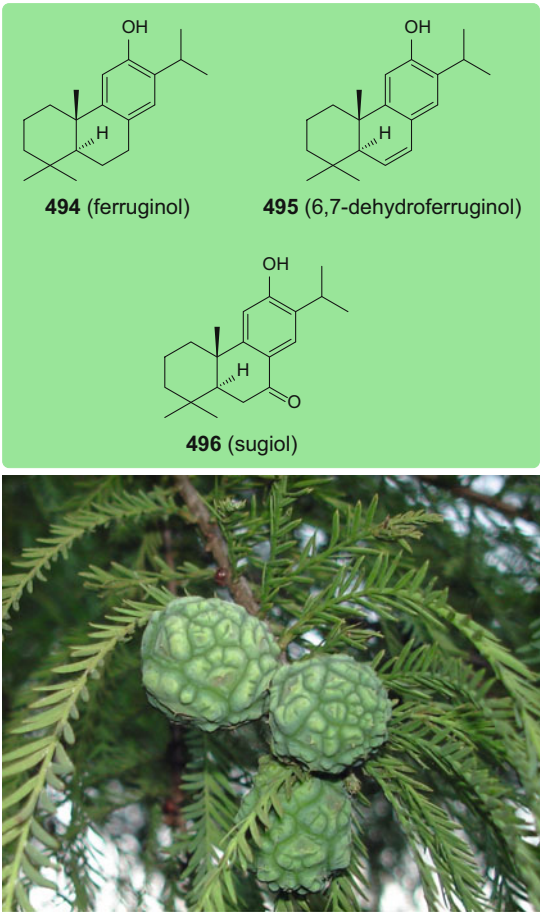

Fig. 73 Phenolic terpenoids **494**–**496**. Bottom: extant *Taxodium distichum* cones (bald cypress, related to fossilized *Taxodium balticum*); photograph: CarTick at en.wikipedia

(**494**), 6,7-dehydroferruginol (**495**), and sugiol (**496**). These terpenes are also found in the corresponding extant conifers, such as the bald cypress *Taxodium distichum* (Fig. 73), and accordingly remained unchanged within the deposits for up to 50 million years.

2.2.3 Carbonyl Compounds, Flavonoids, and Quinones

In this section, three functional systems involving carbonyl compounds are described. The first of these deals with aldehydes and ketones, the second refers to flavonoids, and the third is dedicated to quinoid compounds.

Carbonyl Compounds

Long-chain *n*-alkanals are rather rare and their origin is unclear. For example, a series (**497**) with unimodal distribution ranging from 22 to 32 carbon atoms (with C_{28} as the maximum) was reported in 10,000-year-old sediments of Le Voua de la Motte, a small lake south of Lake Geneva (Fig. 74) [252]. These may be associated with straight-chain lipids of terrestrial origin.

In contrast to the unclear origin of alkanals, it is evident that long-chain *n*-alken-2(3)-ones of chain lengths between 35 and 41 carbon atoms and between one and four double bonds with the thermodynamically most stable (*E*)-configuration (the most important unchanged natural products **498–506** are shown in Fig. 75), are produced by the genera *Emiliania, Chrysotila,* and *Isochrysis* of the Gephyrocapsaceae algal family [253, 254] (for a representation of *Emiliania huxleyi*, see Fig. 69). Several of these compounds had been found in older sediments [255], with the oldest dating from the Early Aptian (Early Cretaceous, 120.5 Ma), which were deposited during an oceanic anoxic event [256].

Alkenone-producing organisms respond to changes in their environment, in particular to temperature changes, resulting in the alteration of the relative amounts of different alkenones. The higher the temperature of the water in which these organisms grow, the greater becomes the relative proportion of the less unsaturated alkenones. Thus, the alkenones are important to indicate paleotemperatures and to some degree also salinity [257]. The unsaturation index as a measure of temperature was defined as $U^{K}_{37} = [\mathbf{498}]/([\mathbf{498}]+[\mathbf{499}])$ [258]; it may be correlated to the temperature by $T = (U^{K}_{37} - 0.044)/0.033°C$ [242]. With respect to salinity the ratio of the alkenone chain lengths K_{37}/K_{38} increases with decreasing salinity [257]. Summaries of paleotemperature determination using alkenones have been published [259, 260]. As suggested earlier [261], the alkenones are used by the producing organisms primarily for metabolic storage.

It should be noted that the bifunctional 1-hydroxyalkan-15-ones **507** (Fig. 75), containing 30–32 carbon atoms, have been found in Black Sea sediments up to 7000 years of age [245]. However, it is not clear which organisms may have produced these molecular fossils.

Several aromatic ketones with unmethylated or methylated anthracen-9(10*H*)-one (**508–510**) or 7*H*-benzo[*de*]anthracen-7-one (**511–513**) structures (Fig. 76) were isolated from Cretaceous sediments from the lower Indus basin, Pakistan, and Devonian sediments from Canning Basin, Western Australia [162]. It is

497

Fig. 74 *n*-Alkanal series **497**

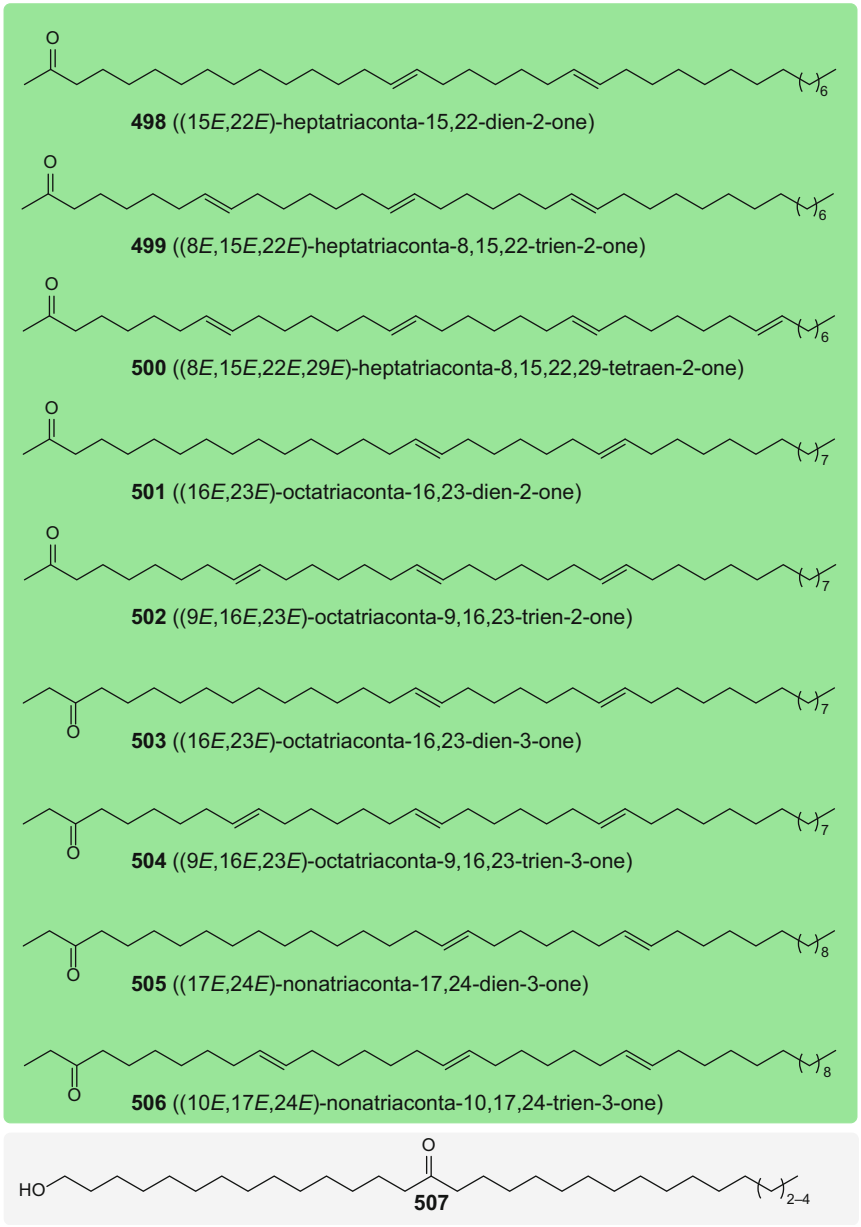

Fig. 75 Alkenones **498–506** from Gephyrocapsaceae, which also constitute their unchanged molecular fossils, and the 1-hydroxyalkan-15-one series **507**

interesting to note that the latter compounds **511–513** display a stabilizing quinone methide system. The aromatic carbonyl compounds might be derived from quinone precursors like **340–344** (see Fig. 53), but they may also constitute oxidation

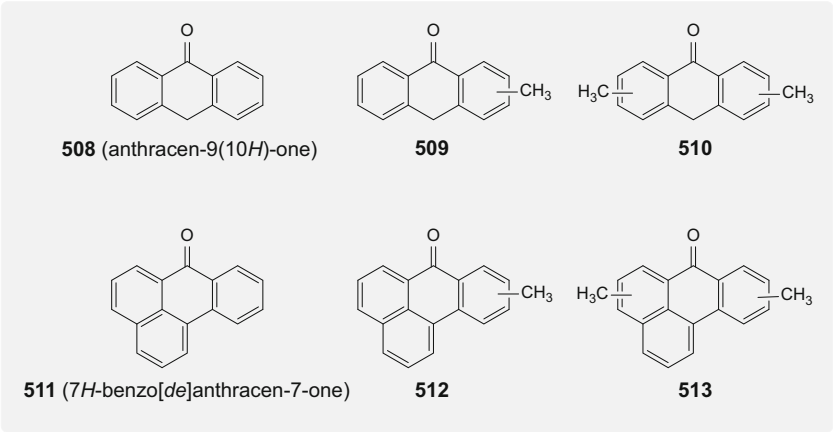

Fig. 76 Aromatic ketones **508–513**

products from condensed aromatic systems. Another carbonyl compound already mentioned as a phenol derivative is sugiol (**496**) (see Fig. 73), which was isolated from Miocene *Glyptostrobus oregonensis* seed cones (from the Clarkia Formation, USA) [251].

Flavonoids

The flavonoid aglycones kaempferol (**514**) and dihydrokaempferol (**515**) (Fig. 77) have been isolated from green-colored leaves of *Zelkova* of the Miocene Succor Creek Flora from Oregon, USA [190]. Leaves of *Celtis* and *Ulmus* from the Succor Creek Flora also yielded flavonoids in their glycosidic form [191]. Whereas 3-*O*-glycosides of quercetin (**516**) occur in *Ulmus*, the apigenin and luteolin *C*-glycosides vitexin (**518**) and orientin (**519**) as well as isovitexin (**520**) and isoorientin (**521**) have been found in *Celtis*. Furthermore, apigenin and luteolin diglycosides have been reported.

The preservation of the *O*-glycosides is particularly notable, since such compounds hydrolyze readily under acidic conditions. Flavonoids and flavonoid glycosides have also been isolated from angiosperm leaves of the Miocene Clarkia Flora from Idaho, USA. A fossilized *Platanus* sp. yielded the flavonoid aglycones kaempferol (**514**) and quercetin (**516**) as well as kaempferol and quercetin arabinosides, galactosides, and glucosides linked at position C-3 (**522–526**) [262]. Quercetin-3-*O*-arabinoside (**522**) and quercetin-3-*O*-glucoside (**524**) have been isolated from *Pseudofagus* [263], and kaempferol-3-*O*-glucoside (**523**) and quercetin-3-*O*-glucoside (**524**) and the flavonoid diglycosides kaempferol-3-*O*-rutinoside (**527**) and quercetin-3-*O*-rutinoside (**528**) from *Liriodendron* leaf fossils [264]. The biflavonoids 5-*O*-methylginkgetin (**530**) and its methoxy derivative **531** have been detected in the leaves of Cretaceous *Ginkgo coriacea*, closely resembling

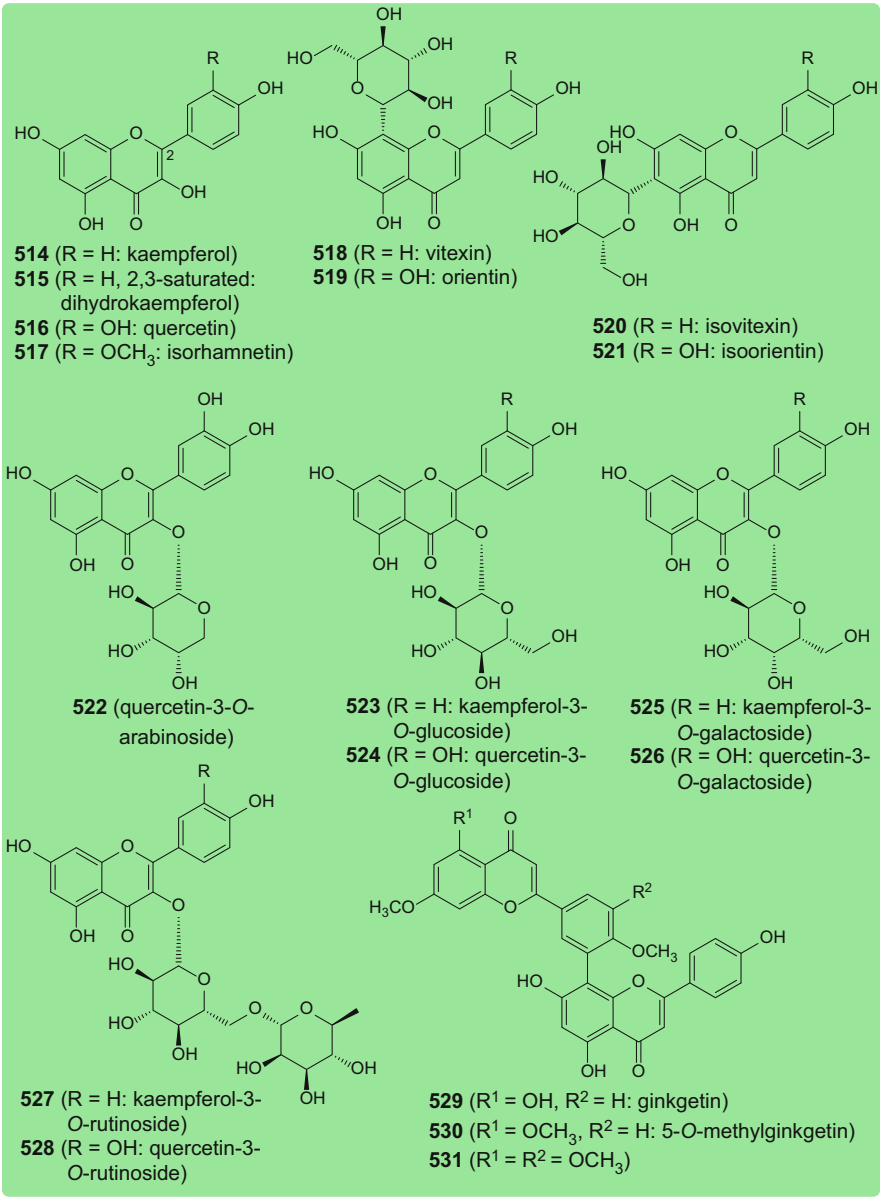

Fig. 77 Flavonoid aglycones **514–517**, flavonoid *C*-glycosides **518–521**, flavonoid *O*-glycosides **522–526**, flavonoid *O*-diglycosides **527** and **528**, and diflavonoids **529–531**

ginkgetin (**529**) present in the extant *Ginkgo biloba* [265]. Whereas the fossil flavonoids **530** and **531** have been identified by their UV spectra and HPLC-MS, identification of **514–528** was performed only by two-dimensional paper

chromatography and UV spectroscopic comparison to currently available reference compounds. Thus, the identifications of the latter compounds may be regarded as tentative.

Quinones

Anthraquinone (**532**) (Fig. 78) was discovered in a burning coal seam as an organic mineral in 1922 at the now abandoned Mt. Pyramiden coal mine of Svalbard (Spitsbergen, Norway) [266]. It was named hoelite (Nickel-Strunz classification 10.CA.15) after the Norwegian geologist Adolf Hoel (1879–1964), who led the expedition [267]. This compound was later found in the Permian–Carboniferous Kladno [268] and the Kateňna coal mines [269] in Bohemia, and in Germany in the Carola mine (Freital near Dresden, Late Carboniferous; see Fig. 78) [270]. Hoelite (**532**) occurs rather rarely in coal fire environments and is associated frequently with elemental sulfur. Thus, its organismic origin is uncertain.

Brick-red smears in the shale of the Saxony Ölsnitz coal mine (Late Carboniferous) were detected by Kolbeck and analyzed by Treibs as two forms of an organic mineral, graebeit a and graebeit b (**533**) (Fig. 78), named in honor of the German Carl Graebe, a pioneer of anthracene chemistry (1841–1927) [271, 272]. According to their analytical data, these two minerals are the hexahydroxyanthraquinones **533** bearing side chains of uncertain structures. They may be derived from coal-forming plant material in which hydroxyanthraquinones frequently occur [273].

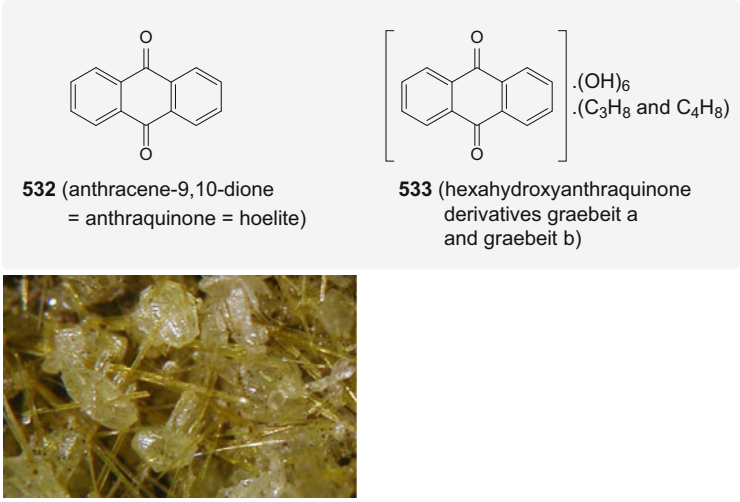

Fig. 78 Anthraquinone (**532**) and its hexahydroxy derivatives **533**. Picture: hoelite needles among sulfur grains, Carolaschacht mine, Freital, Saxony, Germany; photograph: T. Witzke, Wikimedia Commons

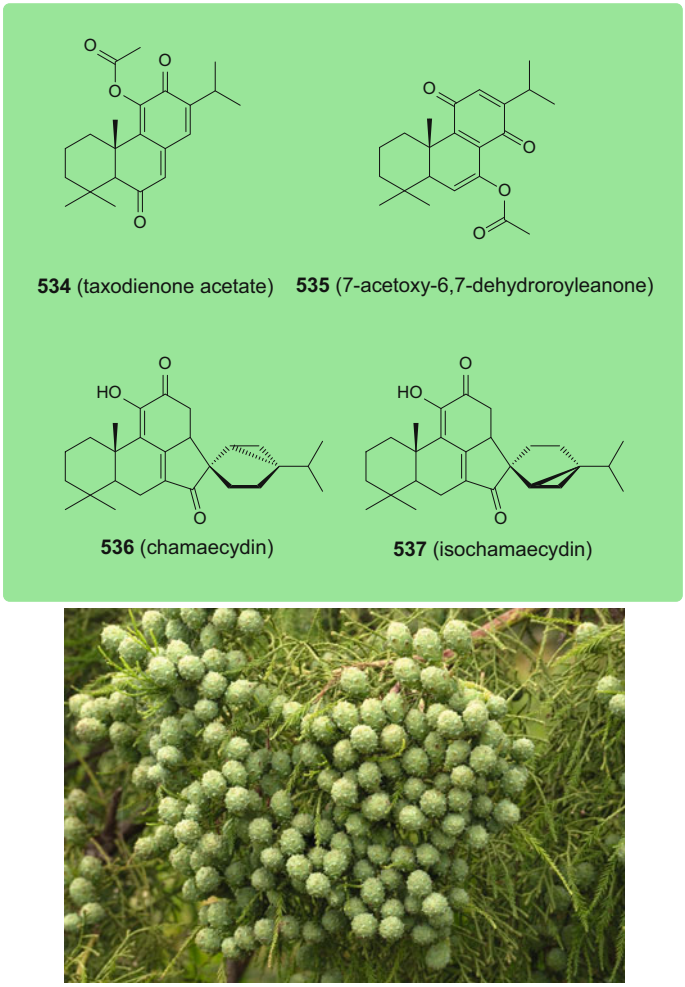

Fig. 79 Quinoid conifer biomarkers taxodienone acetate (**534**), 7-acetoxy-6,7-dehydroroyleanone (**535**), chamaecydin (**536**), and isochamaecydin (**537**). Bottom: *Glyptostrobus pensilis* seed cones; photograph: T. Rodd, Creative Commons

The resins from the Miocene Clarkia flora from Emerald Creek, Idaho, USA, yielded, in addition to the phenolic compounds **494**–**496** (Fig. 73) described in Sect. 2.2.2, several unchanged terpenoids with vinylogous quinoid (**534**, **536**, **537**) or quinone (**535**) structures (Fig. 79) [251, 274]. Thus, in Miocene *Taxodium dubium* seed cones, taxodienone acetate (**534**) and 7-acetoxy-6,7-dehydroroyleanone (**535**) were identified, whereas the Miocene *Glyptostrobus oregonensis* seed cones contained only **534** [274]. In addition, two further quinoid systems with a spirocyclic system, chamaecydin (**536**) and isochamaecydin (**537**), were characterized [251]. All these compounds (**534**–**537**) are also found in the related extant conifers *Taxodium*

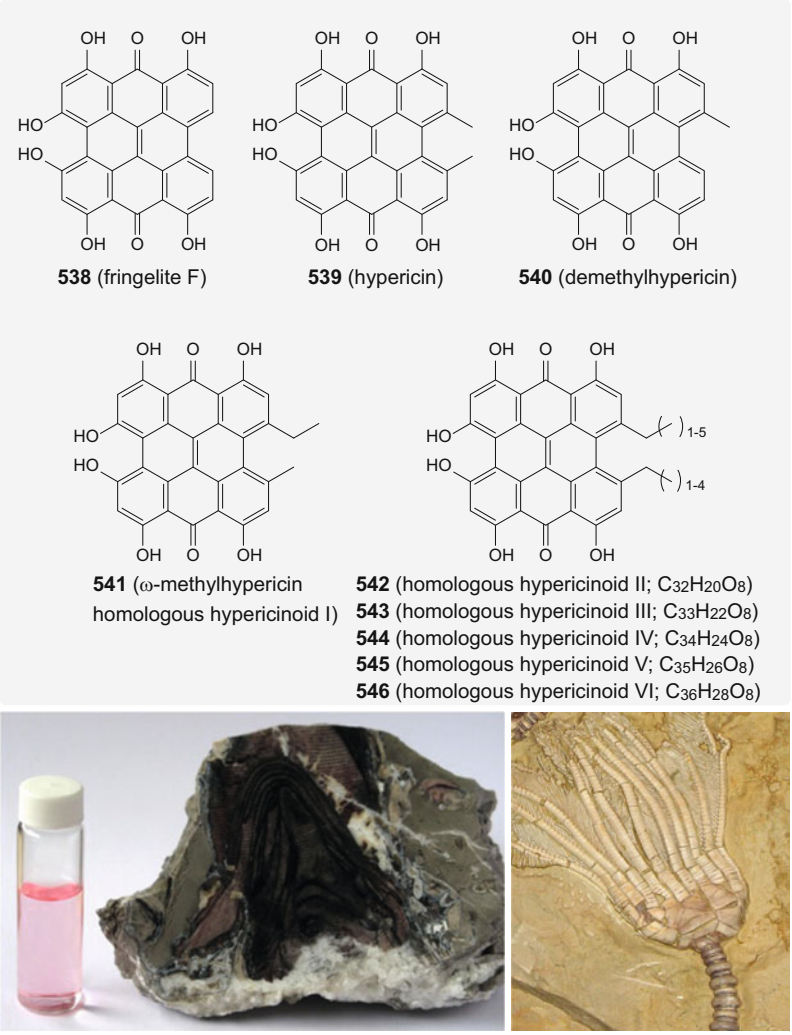

Fig. 80 Hypericinoid molecular fossils **538–546**. Bottom left: Jurassic *Liliocrinus munsterianus* root from Liesberg, Switzerland (collection of Staatliches Museum für Naturkunde, Stuttgart), and extract of hypericinoids. Bottom right: Middle Triassic *Carnallicrinus carnalli* from Freyburg/Unstrut, Germany, specimen with hypericinoid-colored stalk from Museum of Natural History, Vienna, Austria; photographs: K. Wolkenstein

distichum (Fig. 73) and *Glyptostrobus pensilis* (Fig. 79) [251] making these compounds true unchanged biomarkers of these trees.

In a series of papers, Max Blumer (1923–1977), also one of the pioneers of the study of organic geochemistry, reported on his investigations of purple pigments obtained from fossil sea lilies (*Liliocrinus* sp., formerly *Millericrinus* sp.) of the Jurassic age [275–278]. This type of coloration of fossil Echinodermata specimens has been observed since the nineteenth century [279–282] (Fig. 80). Blumer named

the pigments "fringelites" after a prominent location where such fossil crinoids are found: Fringeli in Northern Switzerland. Using diffuse reflectance spectrometry screening, a much wider distribution of fringelites in the fossil record became evident [283, 284]. However, only the application of modern structural analytical methodology, and in particular HPLC-MS, made it possible to gain insight into defined structures and their distribution. Thus, it turned out that from the fringelites D−H Blumer proposed, only fringelite F (**538**) "survived" structural scrutiny, and instead of the other fringelites, hypericin (**539**), demethylhypericin (**540**), and a series of homologous hypericinoid compounds (**541–546**) were characterized (Fig. 80) [285, 286]. In addition, the completely defunctionalized hydrocarbon **356** (Fig. 54), already described in Sect. 2.1.4, was identified [285–288].

Further to the elucidation of their structures, knowledge of the distribution of the hypericinoids **538–546** among various species and within different geological periods has become considerably more extensive [285–289]. Thus, it turned out that these biomarkers occur in numerous fossil crinoid species from the Triassic and Jurassic periods of Europe and the Jurassic of the Middle East and East Africa, including representatives from four (Millericrinida, Comatulida, Isocrinida, and Encrinida) of the eight post-Paleozoic crinoid orders.

The characteristic skeleton of the hypericinoid compounds is phenanthro[1, 10,9,8-*opqra*]perylene-7,14-dione. The structural and chemical aspects of the most well-known derivative, hypericin (**539**), have been reviewed thoroughly [290], but the main issues important for its occurrence as a molecular fossil should be delineated in this context.

First, due to the very short and therefore strong hydrogen bond in the *bay*-region that stabilizes the hypericinate ion (**539**$^-$), and, in addition, the presence of a vinylogous carboxylic acid subsystem involving the *peri*-region(s), hypericinoids with two *bay*-hydroxy groups display a rather high acidity. This has been characterized with a pK_a value of about 1.8 making it about 1000-fold more acidic than acetic acid (p$K_a \approx 4.8$) (Fig. 81; the vinylogous carboxylate is indicated in red) [291]. Second, due to steric strain in the *bay*-regions, the molecule becomes twisted, thus displaying atropisomerism. The rather low inversion barrier of the enantiomeric molecular propellers, estimated experimentally and by quantum chemical and force field calculations to be in the order of 80 kJ/mol [290], results in the presence of the racemate (*M*)-**539** + (*P*)-**539** in solution and in the crystalline state (Fig. 81) [292].

Hypericin (**539**) biosynthesis in extant *Hypericum* species has been established as involving two consecutive reaction cascades (Fig. 82). The first consists of the biosynthesis of two anthraquinone halves of the targeted octahydroxyphenanthroperylene quinone on the acetate malonate pathway, starting with one molecule of acetyl coenzyme A and seven molecules of malonyl coenzyme A, which yields the octaketide **547**. The latter undergoes multiple aldol cyclizations to form emodin anthrone (**548**) [159]. Emodin anthrone (**548**) is then dimerized enzymatically in a regiospecific manner to afford **539** [293]. Otherwise, abiotic simply base-catalyzed oxidative dimerization would yield a mixture of **539** and isohypericin (**549**) [294].

All the above-mentioned findings lead to the question of the biological precursors of the molecular fossils **538–546**. Extant crinoids contain a series of

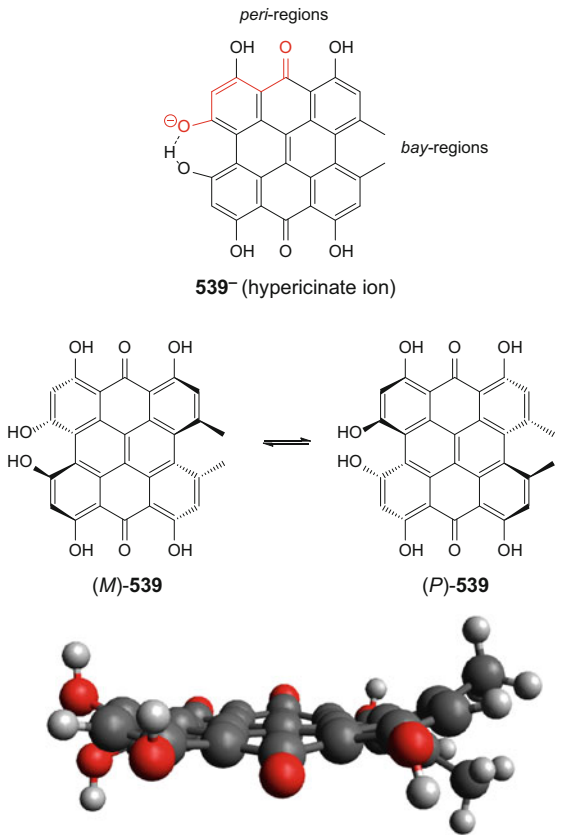

Fig. 81 The hypericinate ion (**539**⁻) and the equilibrium between the atropisomers (*M*)- and (*P*)-**539**. Bottom: ball and stick model ("Avogadro" [87]) of (*P*)-**539** to illustrate its helically twisted structure

brominated hypericinoid compounds, gymnochromes A–F (**550–555**) and additional derivatives (Fig. 83) [289, 295, 296]. Thus, a persistent and widespread spatial and taxonomic occurrence of hypericinoid pigments since the Mesozoic Era has been observed. While there is a recently published report that Paleozoic (Mississippian) crinoids also contain quinone-like compounds [297], these results are questionable on methodological grounds [298]). Obviously, these compounds have had a general functional importance (e.g. antiviral, cytotoxicity, feed repellant activities) for the evolutionary success of the Crinoidea. It is interesting to note that bromination of natural products as observed for the gymnochromes occurs throughout the living world and in particular in those of marine organisms [299]. However, no brominated molecular fossils are yet known, indicating that the carbon-bromine bond might be too labile to survive within even a short geological period.

It should be mentioned that the skeleton of the hypericinoids is also found in other organisms like the protist *Stentor coeruleus*. In this organism, stentorin (**556**) (Fig. 83) serves as a photoreceptor.

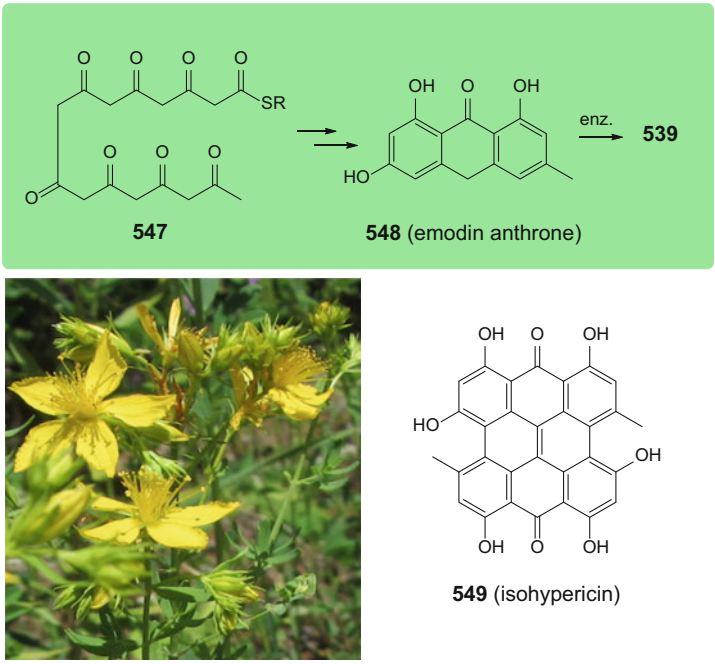

Fig. 82 Biosynthesis of hypericin (**539**). Bottom: *Hypericum perforatum* (St. John's Wort); photograph: H. Falk; isohypericin (**549**)

These results point to a diagenetic reaction cascade (Fig. 84) in which the natural pigments of gymnochromic structures are transformed by debromination steps, dealkylation (yielding the homologous series of hypericinoids **541**–**546**, hypericin (**539**) its dealkylation products **540** and **538**), and eventually reduction to the aromatic hydrocarbon **356**.

A further aspect is the extremely long preservation of the hypericinoids of in some cases up to 240 Ma, thus representing the oldest polyketides known thus far [285]. Two of the reasons are on the one hand the possibility that they form salts with respect to the highly acidic *bay*-region mentioned above and on the other hand the formation of chelates at the *peri*-positions occurs, as illustrated for the calcium salt of **539** in Fig. 85 [300].

The fossil calcareous red alga *Solenopora jurassica* displays a striking pink coloration (Fig. 86). This fossil is well known from the Jurassic of France [301] and from the "Beetroot Stone" from the Jurassic of Great Britain [302]. The pigments contained in the regularly alternating bands that have been interpreted as seasonal growth structures are of endogenous origin, because no traces of these could be found in the surrounding sediments [303]. Initial speculations assigned the coloration to porphyrins [302] or hypericinoids [283]. However, using HPLC-MS, circular dichroism, ^{11}B NMR spectroscopy, solvolysis, and H/D-exchange reactions, it was shown that these pigments form a series of spiroborates with two phenolic ligands [304]. Only by work-up of a quite large quantity of a fossil sample

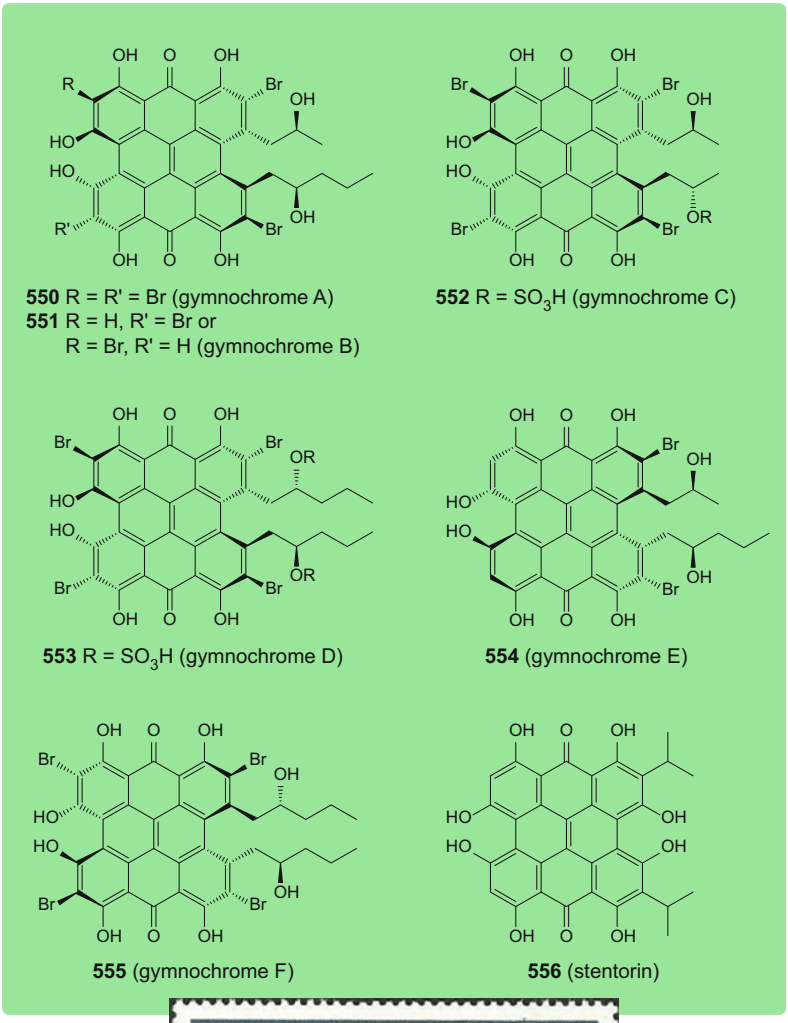

Fig. 83 Gymnochromes **550–555** and stentorin (**556**). Bottom: New Caledonian stamp from 1988 displaying the stalked deep-water crinoid *Gymnocrinus richeri*. It celebrated the discovery of this "living fossil" at a depth of 520 m in the bathial zone off the coast of New Caledonia in 1986 by Bertrand Richer de Forges. Engraving: Baillais

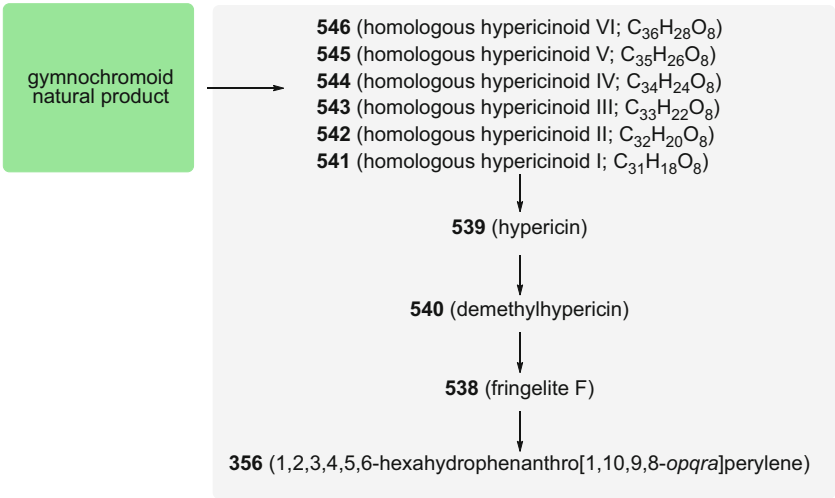

Fig. 84 Diagenetic degradation of gymnochromic natural products to yield the hypericinoid compounds cascade **546–538** and **356**

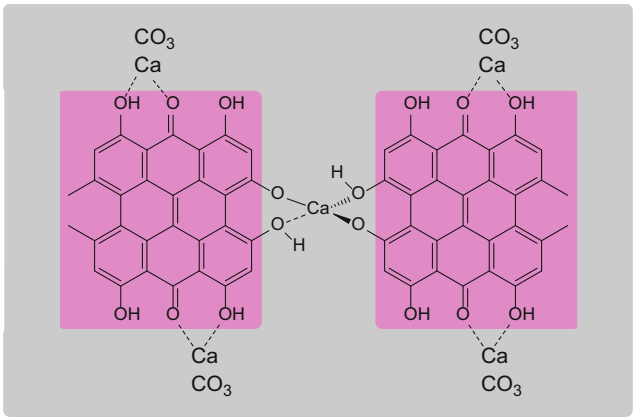

Fig. 85 Calcium salt of hypericin (**539**) involving the *bay*-position and chelate formations with the surrounding calcite matrix at *peri*-positions

(0.8 kg), could 6–57 μg of the individual pigments **557–569** (Fig. 86) be isolated. Their complete structural details including their rather complex stereochemistry were elucidated by means of microcryoprobe NMR spectroscopy, circular dichroism, and density functional theory calculations [305].

The fundamental skeleton of the ligands is the pentacyclic benzo[*g*,*h*]tetraphenone, which is substituted with isopropyl or (2*S*)-methylbutyryl residues, one methyl group, and varying numbers of hydroxy groups. The benzo[*gh*] tetraphene scaffold was hitherto only recently encountered in the natural organic compound clostrubin (**570**) (Fig. 87). This compound was isolated from the

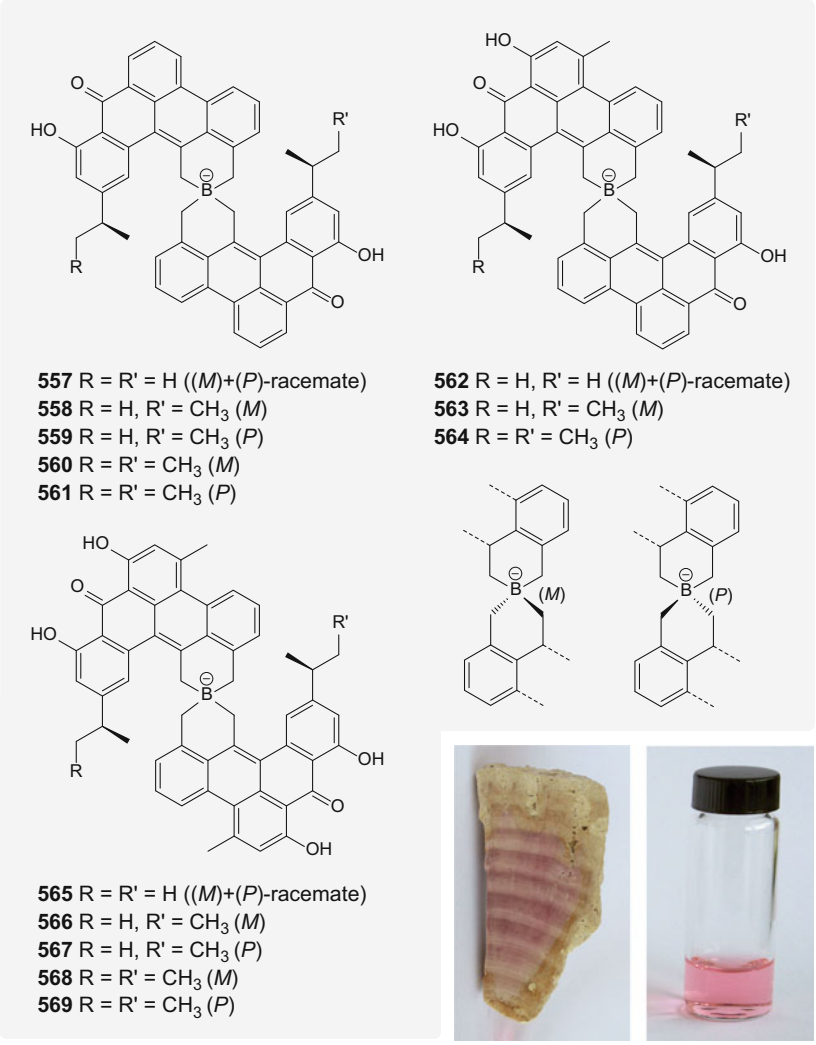

Fig. 86 Borolithochromes A (**565**), B1 (**566**), B2 (**567**), C1 (**568**), C2 (**569**), D (**562**), E (**563**), F (**564**), G (**557**), H1 (**558**), H2 (**559**), I1 (**560**), and I2 (**561**). Bottom: slab of *Solenopora jurassica* and pigment extract; photograph: K. Wolkenstein

bacterium *Clostridium beijerinckii* and shown to be biosynthesized via a polyketide cascade [306]. Accordingly, the biosynthesis of the borolithochrome ligands is envisaged to follow also a polyketide path starting from (2*S*)-methylbutyryl-coenzyme A (Fig. 87), resulting in, for example, the borolithochrome C ligand **571** [305].

The structural details and occurrence of the borolithochromes point to the intriguing question of their organismic source. Generally, *Solenopora jurassica* is assigned to the solenoporaceans, a now extinct, but once widespread group of

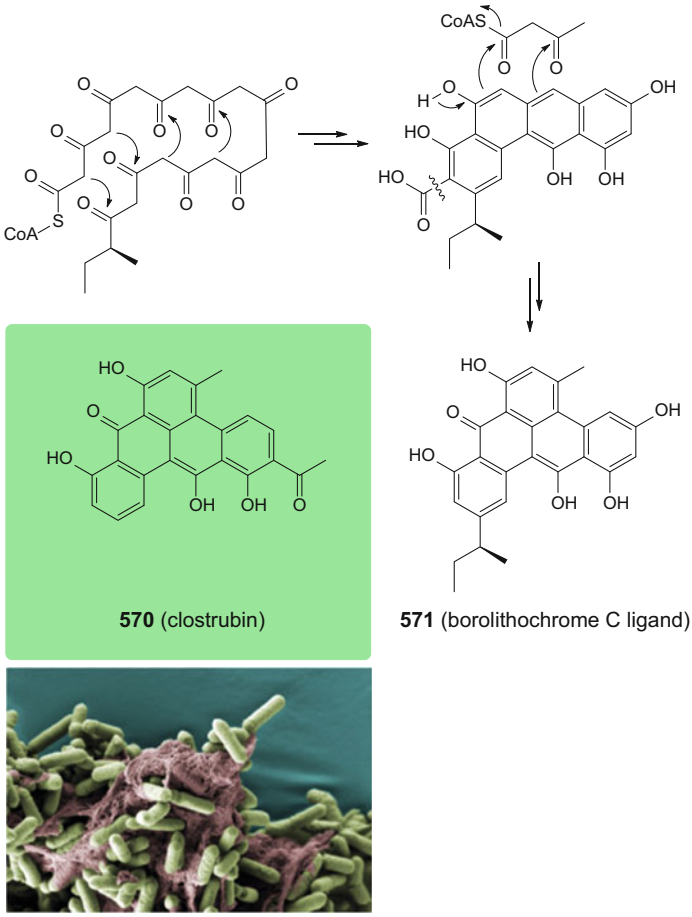

Fig. 87 Biosynthesis of the borolithochrome ligands exemplified with **571** and the natural product clostrubin (**570**) together with a false-colored scanning electron microscopic image of *Clostridium beijerinckii*; length of the bacteria 1–2 μm. Picture courtesy of K. Cross (Institute of Food Research, Norwich, UK) and B. Stegmann (University of Ulm, Germany)

corraline red algae (Rhodophyta). Currently, the solenoporaceans are considered as a heterogeneous group also containing Early Paleozoic forms that have been interpreted as chaetetid sponges [307]. The rather similar structures of the borolithochrome ligands and clostrubin (**570**) suggest that the borolithochromes may have been produced by bacteria [305]. The amazing preservation of the pigments that are thought to be only slightly degraded by diagenesis (perhaps dealkylation and dehydroxylation as encountered in the hypericinoids), might be due to the fact that these compounds are borate anions (see Fig. 86) that have to be intrinsically bound by salt formation to the calcareous matrix with Ca(II) as already encountered for the hypericinoids (see Fig. 85).

It should be added that boron-containing natural products are very rare, and found mostly as borates esterified to *vicinal cis*-diols as is the case with boromycin and related boronated polyketides [308, 309]. It is possible that this observed rarity might in part be due to the experimental work-up conditions used typically for marine natural products.

A pink phyllosilicate fibrous clay mineral of the palygorskite group occurs as a surface deposit near Quincy sur Cher in the Mehun-sur-Yèvre basin of central France and was named accordingly as quincyte (quincyite, quinciite) [310, 311] (Fig. 88). This sepiolite ($Mg_4Si_6O_{15}(OH)_2.6H_2O$) is found dispersed in limestone laid down by a large Eocene lake [312, 313].

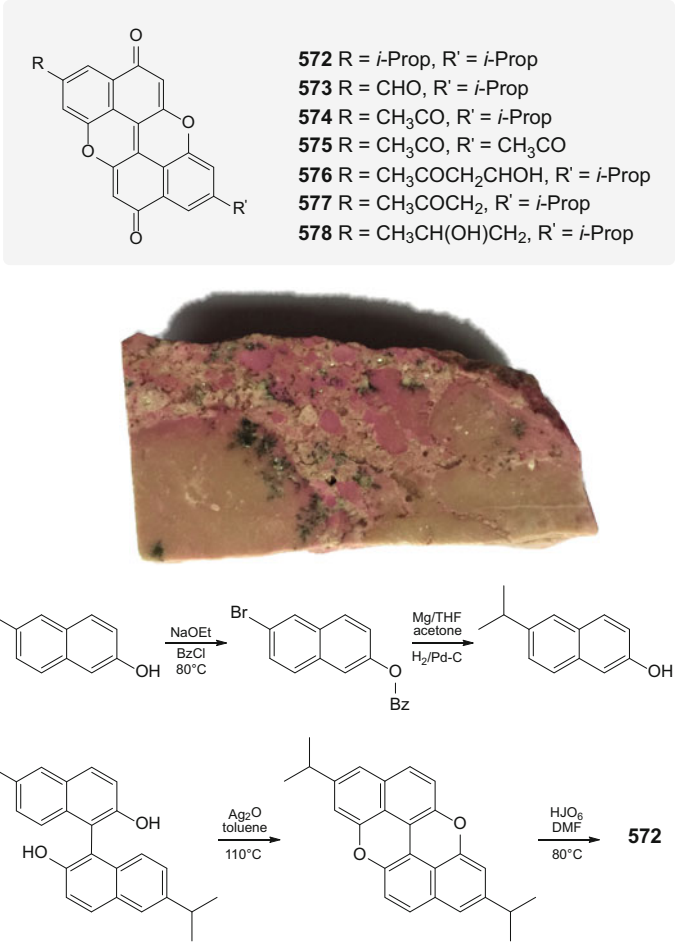

Fig. 88 Quincyte pigments **572–578**. Middle: a slab of limestone containing sepiolite colored with quincyte pigments, width 5 cm, Eocene, Mehun-sur-Yèvre, France; photograph: H. Falk. Bottom: structure confirmation by independent synthesis of **572** [315]

The pigments responsible for the pink coloration may be extracted only after HF-dissolution of the silicate matrix. There have been several attempts to establish the structures, as, for example, by Treibs [314]. However, the individual constituents of the isolated quincyte pigment mixture were able to be derived only by the use of modern instrumental analysis. These consist of the seven substituted *peri*-xanthenoxanthene-4,10-quinone derivatives **572–578** (Fig. 88) [315]. Interestingly, the structure of the major pigment **572** has been confirmed by an independent five-step synthesis starting from 6-bromonaphthalen-2-ol (Fig. 88).

The biological origin of pigments **572–578** is still an open question, because no macro- or microfossils have been detected along with the quincyte. However, given the conditions of deposition and an apparent acetate malonate or terpenoid biosynthesis pathway (as indicated by the *i*-propyl groups), a characteristic of natural quinones found in fungi [315], a fungal origin of **572–578** is plausible.

2.2.4 Acids

Simple aliphatic carboxylic acids from carbon dioxide and formic to caprylic acids are minor constituents in the majority of crude oils, oil field brines, and source rocks [316]. Their concentrations are higher in low-maturity and biodegraded oils [317, 318]. Thus, these molecular fossils seem to be derived by diagenetic oxidative degradation from molecular fossils with higher molecular weights and therefore are not able to be attributed to specific biological sources.

As encountered earlier with functionalized aliphatic derivatives, aliphatic carboxylic acids are biosynthesized mostly from acetyl-coenzyme A, and thus a preference for even carbon-numbered members is observed. The Messinian (Late Miocene, 7.2–5.3 Ma) sedimentary series of the Lorca basin near Murcia in Spain has provided a good example of the occurrence of a large variety of fatty acids, which may serve as bacterial and algal markers [216]. A whole series of acids (**579**) (Fig. 89) from C_{12}–C_{32} has been identified.

Linear carboxylic acids **579** with a carbon number of C_{22}–C_{32} and strong bimodal even/odd predominance are formed mainly via a C_3 type of metabolism and are derived largely from higher plant epicuticular waxes. Those with C_{14}–C_{18} chain lengths are due to the microbial decay of leaf mesophyll, as shown for the Miocene Lake Clarkia, Emerald Creek deposit in Idaho, USA [319].

Unsaturated fatty acids occur very seldom in fossil deposits. Only the sulfur-rich surroundings of the Messinian (Late Miocene) Lorca Basin sediments of Murcia, Spain, have allowed **580** and **581** to survive [216]. These two unsaturated acids are indicative of purple sulfur bacteria.

Branched *iso*- and *anteiso*-fatty acids with 15 and 17 carbon atoms, **582** and **583** and **584** and **585** (Fig. 89), also found in the Lorca sediments, are indicative of sulfate-reducing bacteria [216]. 10-Methylhexadecanoic acid (**586**), sometimes found in sediments, is specific to sulfate-reducing bacteria but may also be due to demosponges [18]. The isoprenoid phytanic acid (**587**) (Fig. 89), isolated also from

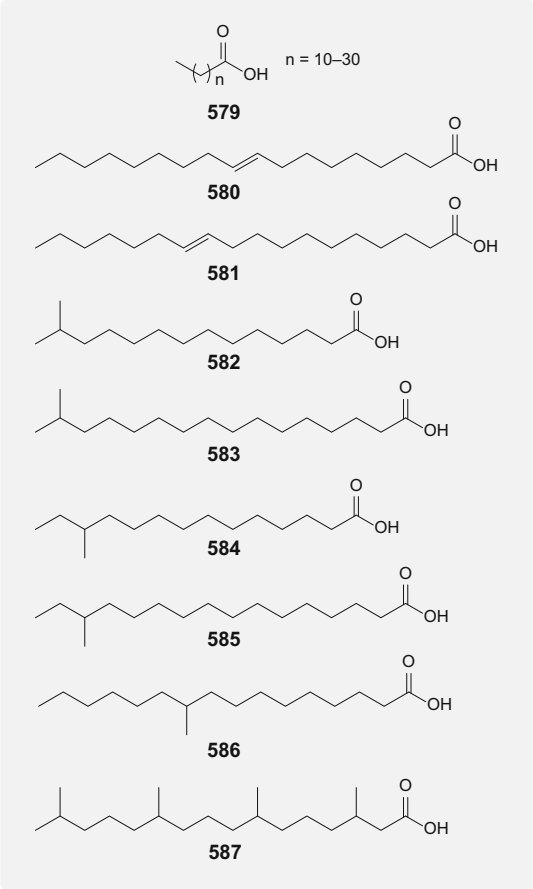

Fig. 89 Carboxylic acids **579–587**

the Lorca deposit [216], derives from the phytyl side chain of chlorophylls and accordingly is a potential marker of algae.

Glyptostrobus oregonensis seed cones contain the bicyclic terpene (*E*)-communic acid (**588**), and the tricyclic terpene acids **589–592** (Fig. 90) were identified in *Cunninghamia chaneyi* seed cones of the Miocene Clarkia deposits mentioned above [274]. Although the tricyclic diterpene conifer resin constituent abietic acid (**118**) is quite easily transformed during diagenesis into fichtelite (**117**) (see Fig. 19), as shown in Sect. 2.1.3, surprisingly it was identified in an unchanged form together with its ferric salt in bituminous coal [320].

The steroidal 5α-cholanic acid (**594**), together with its 5β-diastereomer as the diagenetic products of a bile acid (e.g. animalian cholic acid (**593**)) (Fig. 91), was encountered along with a variety of C_{16}–C_{31} carboxylic acids of undefined structures, in a virgin crude oil from the Midway Sunset field in California, USA of

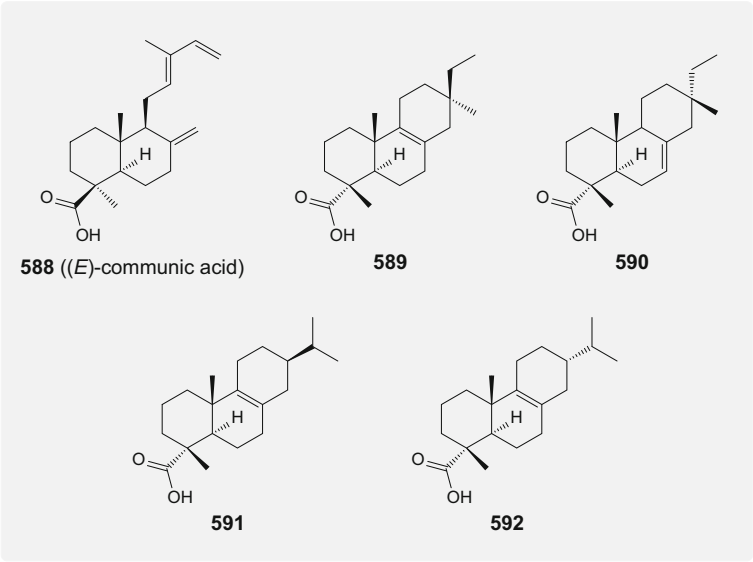

Fig. 90 (*E*)-Communic acid (**588**) and tricyclic terpene carboxylic acids **589–592**

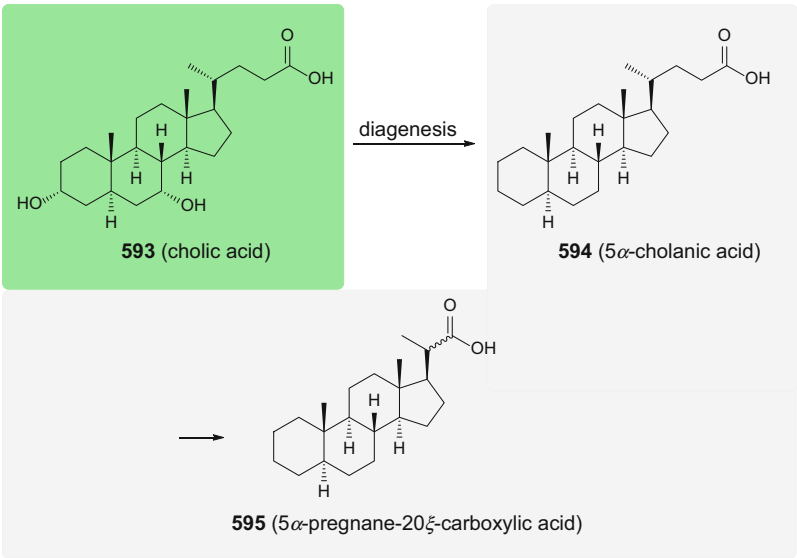

Fig. 91 Fossil steroid carboxylic acids **594** and **595** and their biological precursor, cholic acid (**593**)

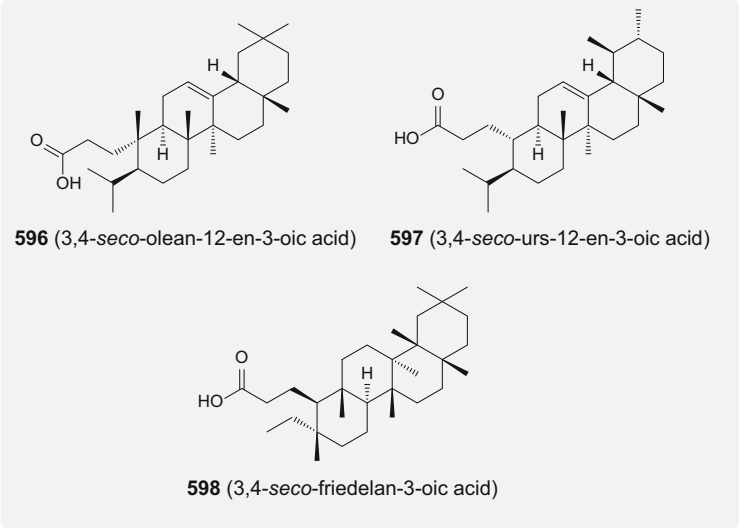

596 (3,4-*seco*-olean-12-en-3-oic acid) **597** (3,4-*seco*-urs-12-en-3-oic acid)

598 (3,4-*seco*-friedelan-3-oic acid)

Fig. 92 Tetracyclic triterpene carboxylic acids **596** and **597** and tetracyclic triterpane carboxylic acid **598**

Pliocene age [321]. In addition, 5α-pregnane-20ξ-carboxylic acid **595** and its 5β-diastereomer were identified.

Within the large set of fossil carboxylic acids from the Miocene Lake Clarkia deposit in Idaho, USA, several tetracyclic terpenoid acids **596–598** (Fig. 92) were isolated [319], which presumably originate by photochemical cleavage of the corresponding pentacyclic 3-hydroxy-triterpenoids of the oleanane-, ursane-, and friedelane types, which are typical of higher plants [322].

This Miocene Lake Clarkia deposit has afforded also a series of hopanoid acids [319]: (22*R*)-17αH,21βH-homohopanoic acid (**599**) and its (22*R*)-17βH,21αH- and (22*R*)-17βH,21βH-diastereomers, (22*R*)-17αH,21βH-bishomohopanoic acid (**600**) and its (22*R*)-17βH,21αH- and (22*R*)-17βH,21βH-diastereomers, (22*R*)-17βH,21βH-trishomohopanoic acid (**601**), and finally (22*R*)-17βH,21βH-tetrakishomohopanoic acid (**602**) (Fig. 93). These geohopane acids are derived from hopanes characteristic of methanotrophic bacteria [83, 319]. (22*R*)-17αH,21βH-Bishomohopanoic acid (**600**) and its (22*R*)-17βH,21αH- and (22*R*)-17βH,21βH-diastereomers, with the latter as the major component, were also found in the Messinian (Late Miocene) sequence of the Lorca Basin, Spain, and were suggested to be heterotrophic prokaryotic markers [216].

Aromatic, hydroaromatic, and heterocyclic carboxylic acids are generally present in crude oils in only rather small amounts, but structural details are missing and there is no obvious correlation to any organismic ancestors [321]. This situation is contrary for the porphyrin carboxylic acids as discussed in some detail in Sect. 2.1.4 for **358**, **359**, **361**, **362**, and **365** (see Fig. 56), which are known from porphyrin-rich deposits.

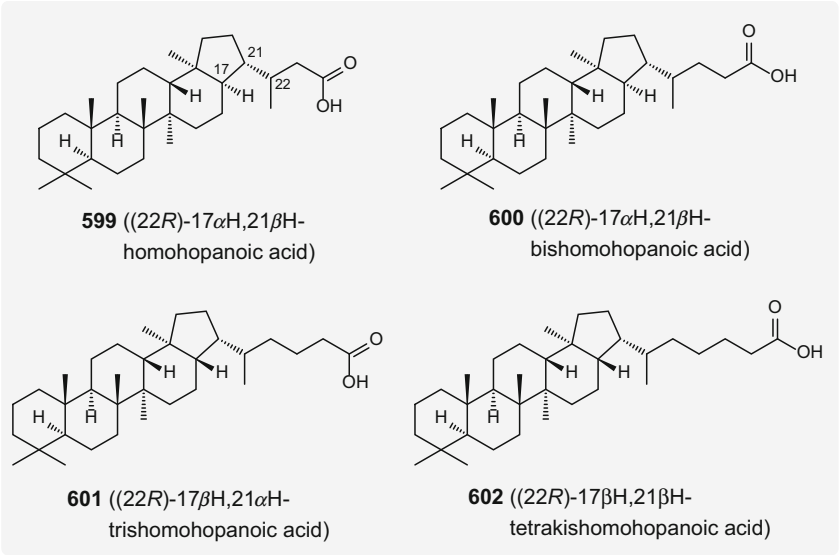

Fig. 93 Pentacyclic hopanoic acids **599–602**

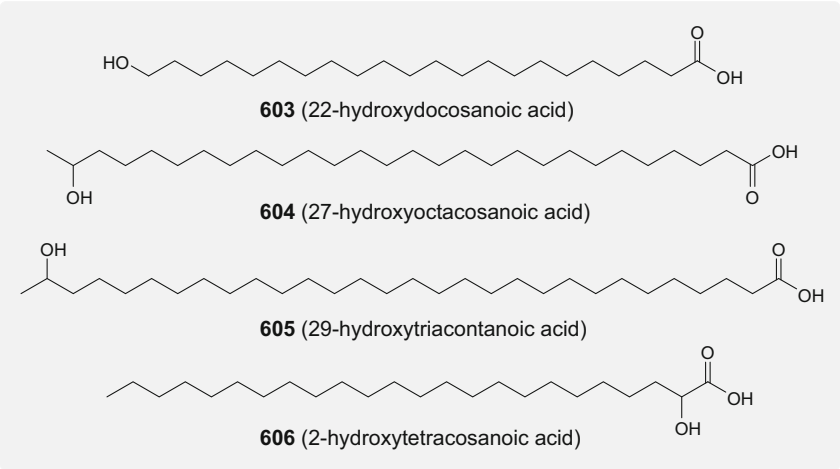

Fig. 94 Hydroxycarboxylic acids **603–606**

A great abundance of the C_{22} member **603** of the ω-hydroxycarboxylic acids (Fig. 94) is found in the Miocene Lake Clarkia deposit mentioned above [319]. It was likely produced by aerobic autotrophs, such algae and cyanobacteria living high up in the water column. This deposit is also rich in the (ω–1)-hydroxycarboxylic acids **604** and **605**, which contain 28 and 30 carbon atoms;

they may result from aquatic photoautotrophs as indicated by their heavy $\delta^{13}C$ values [319]. (ω–1)-Hydroxycarboxylic acids with chain lengths from C_{16}–C_{28} were characterized from a variety of sediments [323]. In addition, 3-hydroxycarboxylic acids characteristic of methanotrophic bacteria were found [324]. Bacterial input to the Late Miocene Lorca basin sediments mentioned above was inferred from the presence of 2-hydroxytetracosanoic acid (**606**) [216].

Proteins in dead organisms are hydrolyzed rapidly to produce amino acids, not least by the action of microorganisms consuming the organismic remains. The homochiral acids are constitutionally more or less stable under diagenetic conditions, but become racemized with time as illustrated with (*S*)-alanine ((*S*)-**607**) in Fig. 95. Hopes have been high in being able to use the presence of optically active amino acids and their stereochemical fate to assess primordial life and timing in billion years old Precambrian cherts [325] and even meteorites [326]. However, it has turned out that contamination of the samples with extant materials imposed an unsurmountable barrier to such expectations.

What has remained from this excitement about the promise of amino acids is the use of (*S*)-isoleucine ((2*S*,3*S*)-**608**) diastereomerization [327] (Fig. 95) or the less

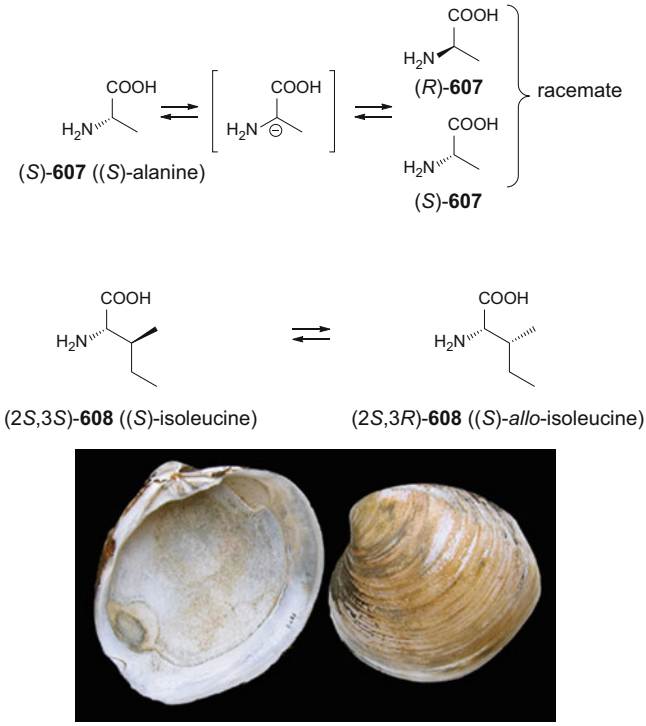

Fig. 95 Racemization of (*S*)-alanine ((*S*)-**607**) and diastereomerization of isoleucine (**608**). Bottom: extant *Arctica islandica*, Ø ≈ 10 cm, Northern Sea. Photograph: J. J. ter Poorten, Wikimedia Commons

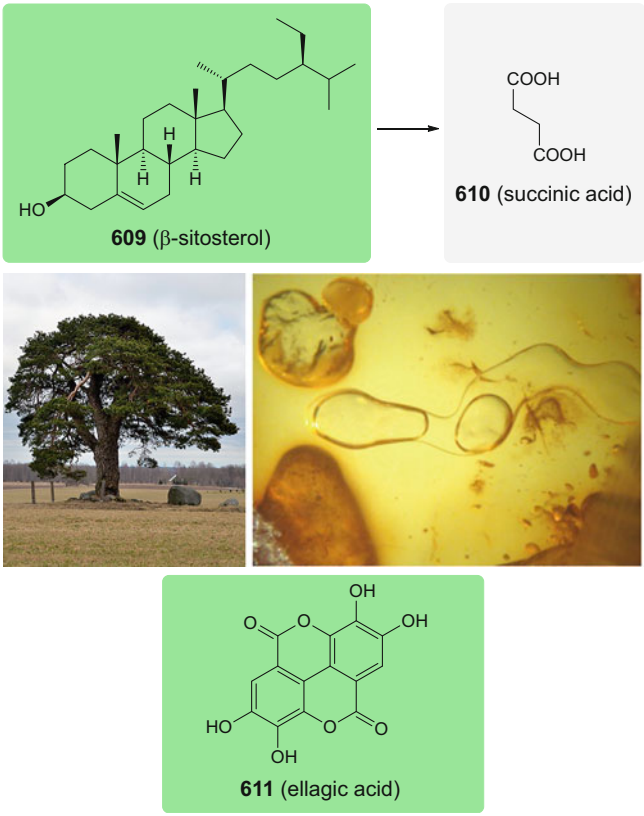

Fig. 96 Succinic acid (**610**), its presumptive biological origin from β-sitosterol (**609**), and ellagic acid (**611**). Left plate: extant *Pinus silvestris*, a producer of **609**; photograph I. Leidus, Wikimedia Commons. Right plate: inclusion droplets containing **610** in Baltic amber from Early Miocene (Eocene origin) found in the former strip mine Goitzsche near Bitterfeld, Germany. Picture width 13 mm; photograph courtesy of A. E. Richter (Augsburg, Germany)

suited racemization of other amino acids [328] to determine paleotemperatures. Such an isoleucine paleothermometer has become possible due to: (a) following kinetic measurements, the equilibrium between the diastereomers (2*S*,3*S*)-**608** = (2*S*,3*R*)-**608** may be established after 2 Ma at 10°C, and (b) an independent determination of fossil age may be obtained using, for example, tandem-accelerated mass spectrometry radiocarbon dating. Thus, climate changes in the Quaternary period (within the last glacial period in the Devensian of Scotland: 100,000–12,000 years) became accessible by investigating the isoleucine/*allo*-isoleucine diastereomer content of the shells of fossil and extant shells of the marine mollusk *Arctica islandica* (Fig. 95) [327].

From dicarboxylic acid molecular fossils, the most important and interesting one is succinic acid (**610**) (Fig. 96). This compound can be isolated from several ambers, in particular from Eocene (44 Ma) succinite (≈8% **610**, accordingly its naming!) from

Bitterfeld, Germany [329]. Knowledge of dry distillation products consisting mainly of succinic acid anhydride dates back to the investigations of Agricola 1546 [330]. Interestingly enough, **610** was also characterized in Baltic amber aqueous inclusion droplets as the main component (Fig. 96) [331]. A fascinating question is, of course, the biological origin of this diacid. As it turns out, **610** is a microbial degradation product from the side chains of typical plant sterols like β-sitosterol (**609**) [332, 333].

An ester bond, for example, in triglycerides does not withstand prolonged basic aqueous or microbial influences. Accordingly, it is quite evident that esters are very rarely encountered as molecular fossils. However, two such esters that survived an extended length of time possibly due to their protection by hydrophobic matrices may be mentioned: the quinones taxodienone acetate (**534**) and 7-acetoxy-6,7-dehydroroyleanone (**535**), occurring in the Miocene seed cones of *Taxodium dubium* and *Glyptostrobus oregonensis*, as discussed in Sect. 2.2.3 (Fig. 79), which both contain an acetate residue [274]. Ellagic acid (**611**), an intramolecular phenol ester, or, in other words, a dilactone, has been found in *Quercus consimilis* from the Miocene Succor Creek flora Oregon, USA (Fig. 96) [334].

2.3 Polymers

On the borderline of true polymers are the more than one hundred different high-molecular weight structures of asphaltenes (carbo- and heterocyclic compounds) contained in the solid fraction of petroleum or in coal. Their molecular architectures recently have been unraveled by a combination of atomic force microscopy and scanning tunneling microscopy [335]. As an example, **612**, reminiscent of a section of a graphene sheet, is displayed in Fig. 97. The origin of these molecules in being recognized as chemically altered fragments of kerogen (see below) is grounded in biogenic carbon compounds, but is still far away from having any defined biogenic ancestor molecules.

As mentioned before with a few exceptions the large biopolymer group of proteins and peptides are hardly ever found as molecular fossils themselves. The

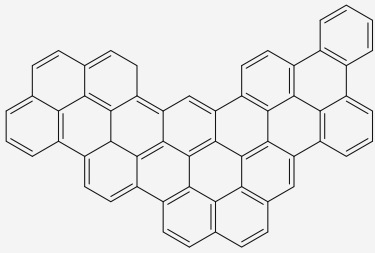

612

Fig. 97 An example of an asphaltene constituent **612**

reason is that they are degraded efficiently to their constituent amino acids by mere hydrolysis or microbial metabolism. However, a recent study using immunofluorescence and high-resolution mass spectrometry did document that structures similar to blood vessels in 80 Ma-old *Brachylophosaurus canadensis* bones contained protein fragments (e.g. the beta-tubulin peptide AVLVDLEPGTMDSVR, which resembles very closely the corresponding peptide of the extant ostrich: AILVDLEPGTMDSVR). These are not consistent with either bacterial, mold, or fungal contamination origin, but display sequences authentic to archosaurian blood vessels [336]. Thus, it has been shown in this manner that modern paleoproteomics becomes feasible if the protein is contained in a tightly sealed rigid structure.

The same structural fragility observed for proteins holds also for the large group of the polysaccharides from cellulose to starches. The resulting monomers in these cases are valuable carbon sources for microbes and thus almost nothing is left of them. However, using pyrolysis-GC-MS the polysaccharide chitin has been detected in the crayfish *Astacus* and in insects from the Pliocene lake sediments of Willershausen, Germany [337] and in beetles from the Oligocene lake sediments of Enspel, Germany [338]. Furthermore, the presence of chitin in *Hyolithellus micans* from the Middle Cambrian of Bornholm [339] and the demosponge *Vauxia gracilenta* from the 505 Ma-old Middle Cambrian Burgess Shale [340] has been verified by detection of its hydrolysate monomer, D-glucosamine. As described in the next sections a few other biopolymers are robust enough to withstand age.

2.3.1 Kerogen

The portion of organic matter in sediments and rocks that is insoluble in normal organic solvents, bases, and non-oxidizing acids, and in having molecular masses beyond 1000 Da, is called kerogen [9]. Its name was designated by the Scottish organic chemist Alexander Crum Brown (1838–1922) in 1906 who derived it from the Greek words κηρός = wax and γένεση = birth. It may be mentioned that the organic matter soluble in the above-mentioned solvents is called bitumen.

Formation of kerogen starts with the breakdown of biopolymers. The products of this transformation then undergo polycondensation. The resulting large, intermediate, and small units are called, in turn, humins, humic acids, and fulvic acids. Under pressure and elevated temperatures these condensates finally result in kerogen by losing hydrogen, oxygen, nitrogen, sulfur, and functional groups, leading to isomerizations and aromatization. Besides the plethora of biomacromolecules that, as indicated above, are easily hydrolyzed, there are several groups of biopolymers resistant to hydrolysis and microbes and thus end up as kerogen constituents (Fig. 98) [341]. Thus, algaenan, a complex biopolymer containing carotenoids, fatty acids, phenylpropanoids, and phenolics, which is the main component of the cell walls of green alga, yields the kerogen alginite. Cutan, forming the cuticles of plants, is a hydrocarbon polymer, which yields cutinite. Lignin, an important structural material of vascular plants and algae, is a highly complex phenol ether polymer, which gives rise to vitrinite and fusinite. Sesqui- and diterpene

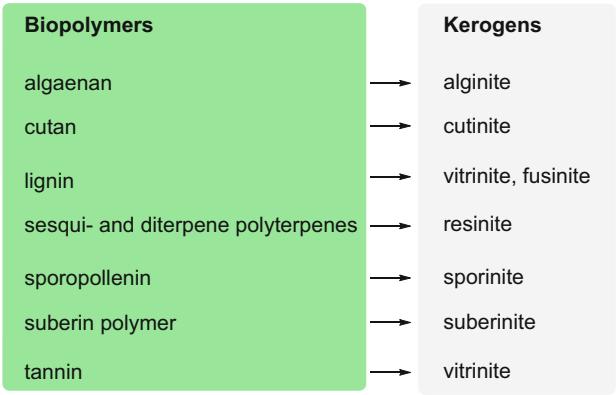

Fig. 98 Biopolymers and their kerogen constituents after diagenesis

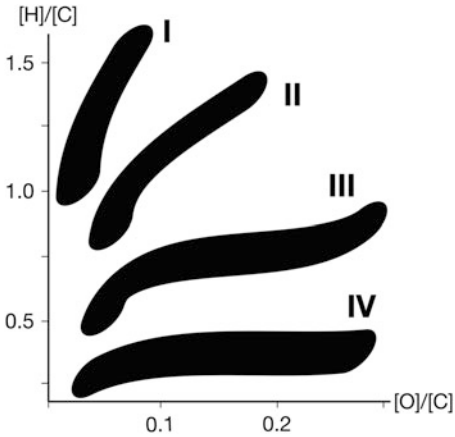

Fig. 99 The van Krevelen diagram with type I–IV kerogens

polyterpenes end up in resinites, and sporopollenin from the outer walls of plant spores and pollen grains, a complex biopolymer, results in sporinite. Suberin, a polyaromatic-polyaliphatic polyester from corky tissues gives suberinite, and the phenolic polyester "tannin" from a variety of plant species results in the kerogen vitrinite.

Of course, it is not possible to assign detailed chemical structures to these fossil polymers although they make up most of the organic carbon in the geosphere. However, by plotting the bulk element content ratios of hydrogen [H], carbon [C], and oxygen [O] into a diagram of [H]/[C] versus [O]/[C] (i.e. the van Krevelen diagram, originally proposed for the evaluation of coals [342]) it is possible to discriminate between the four main structural types of kerogen [342] (Fig. 99), as follows:

- Type I kerogen of the liptinite or alginite type is rather rare and is characterized by [H]/[C] >1 and [O]/[C] <0.1. It derives mainly from lacustrine algae or bacteria and is rich in aliphatic components. Examples are the Eocene Messel shale or the Eocene Green River Formation.
- Type II kerogen of the exinite type is common to most oil shales and originates mainly in marine planktonic organisms as found e.g. in the Toarcian (Early Jurassic) shales of the Paris basin. Its [H]/[C] ratio is in the range of 0.8–1.5 and [O]/[C] of 0.03–0.18. This type of kerogen contains also varying amounts of sulfur and aromatic components.
- Type III kerogen of the vitrinite type derives mainly from fibrous and woody plant material. It is characterized by [H]/[C] <1 and [O]/[C] in the range of 0.03–0.3. An example is from the oil field of the Cretaceous Douala basin in Cameroon.
- Type IV kerogen of the inertite type stems from oxidized and recycled wood debris and displays a [H]/[C] <0.5 and [O]/[C] in the range of 0.02–0.3. It contains high amounts of polycyclic aromatic hydrocarbons and has thus no potential to produce aliphatic hydrocarbons.

2.3.2 Amber

What exactly is meant by "amber", derived from the Arabic "*anbar*", and what the boundaries are to resins or copal, are still issues of discussion [343]. Whatever the precise meaning, besides several low-molecular compounds mentioned in part already (e.g. succinic acid (**610**)), amber contains polymers that are more or less defined, with the oldest examples being from the Carboniferous period. These polymers allow the classification of different types of amber, which are also called resinites [344, 345]. Accordingly, one may define:

- Class I resinites, which are mainly constituted from labdatriene diterpene polymers. Four subgroups are encountered within this class.
  - Class Ia resinites include the most common ambers, the so-called succinites. The polymer consists of a copolymer of communic acid (**588**) and its reduction product communol linked via their terminal vinyl groups, with the resulting chains then cross-linked with succinic acid (**610**) at their communol parts [346], as shown in Fig. 100. A representative is Baltic amber as used in the reconstruction of the famous "Amber Room" in the Catherine Palace near St. Petersburg, Russia.
  - Class Ib resinites contain a communic acid polymer (upper left part of Fig. 100). However, they are not cross-linked with succinic acid (**610**). Cretaceous amber (ambrite) from New Zealand serves as an example for this class.
  - Class Ic resinites contain polymers of the diastereomers of communic acid and communol including ozic acid and zanzibaric acid [347]. This type of amber is found in Mexico, the Dominican Republic (Oligocene-Miocene resinite originating from *Hymenaea protera*; see Fig. 101), and East Africa.

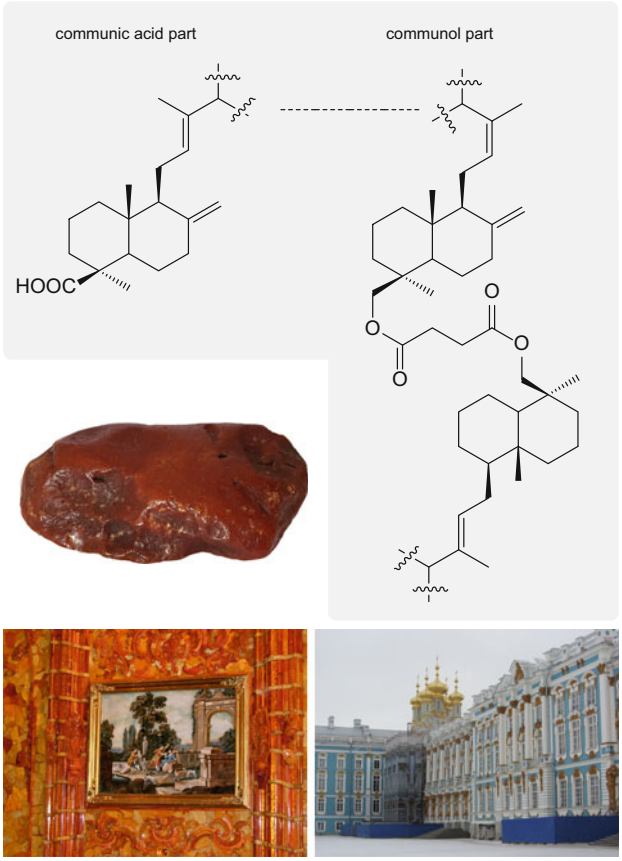

Fig. 100 Polymeric structure of Class Ia resinites; below formula: succinite slab from Early Miocene (Eocene origin) found in the former strip mine Goitzsche near Bitterfeld, Germany; photograph: H. Falk. Bottom left: detail of the "Amber Room" in the Catherine Palace, reconstructed from 350 artificially induced shades of Baltic amber; photograph: Wikimedia Commons. Bottom right: the Catherine Palace, which houses the "Amber Room", Pushkin, near St. Petersburg, Russia; photograph: H. Falk

  – Class Id resinites are made up from polymers based on labdanoid diterpenes with an *enantio* configuration including ozic acid and ozol cross-linked by succinic acid (**610**), as shown in Fig. 102. Such ambers were found in the Eocene fossil forest site of Axel Heiberg Island of the Canadian Arctic Archipelago and two other Canadian localities.

- Class II resinites contain ambers with a polycadinene structure, as illustrated in Fig. 103a. They are less common than Class I resinites and were produced by Dipterocarpaceae species. Extant resins of this type are commercially available under the name "damar".

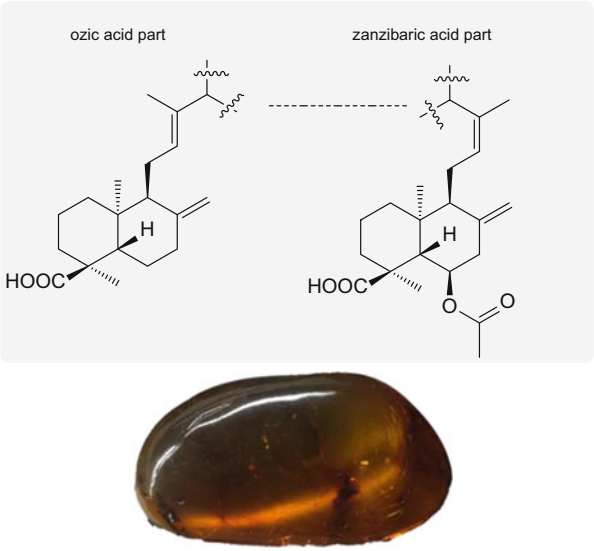

Fig. 101 Polymeric structure of Class Ic resinites involving ozic (left) and zanzibaric acid (right). Bottom: amber from the Dominican Republic (Museum of Natural History, Vienna, Austria, L7918); photograph: H. Falk

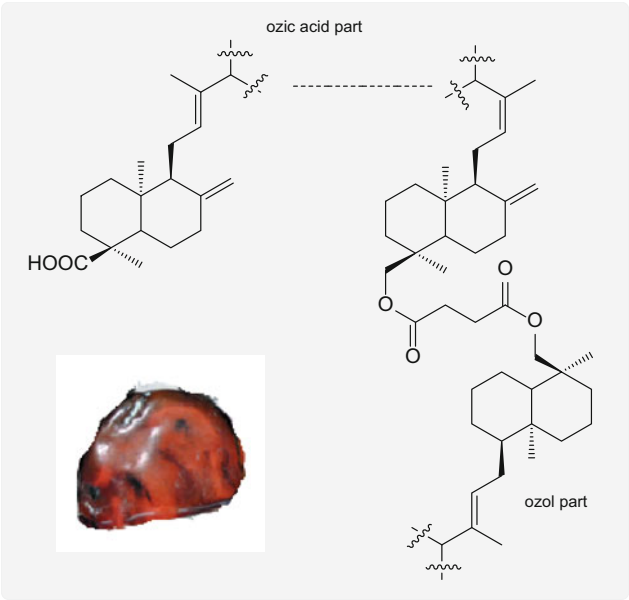

Fig. 102 Polymeric structure of Class Id resinites. Bottom left: Canadian amber; photograph H. Falk

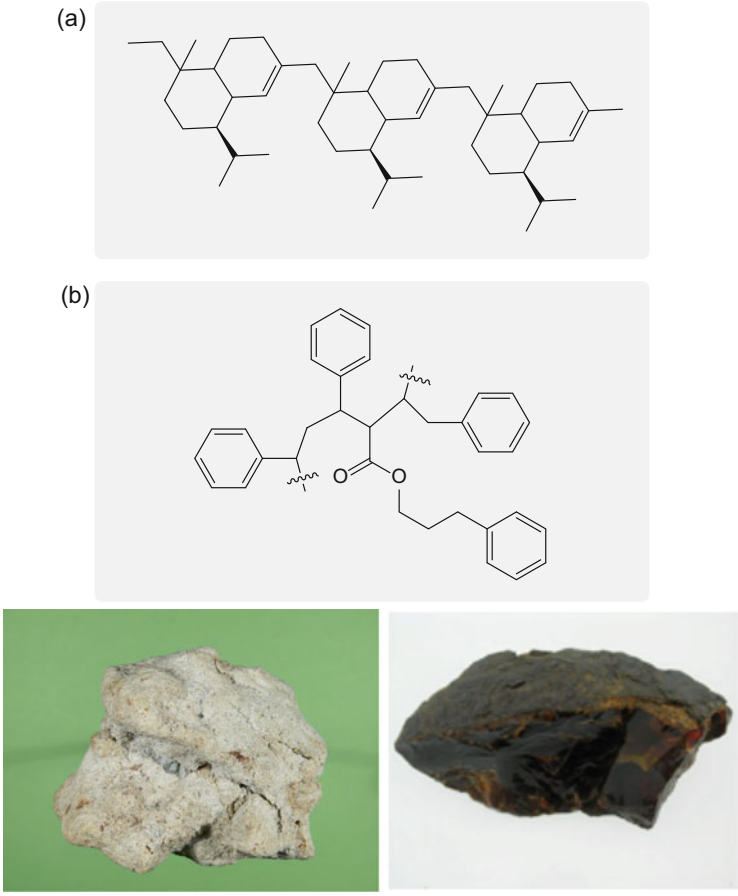

Fig. 103 Polymeric structure of Class II (a) and III (b) resinites. Bottom left: siegburgite amber concretion from Siegburg near Bonn, Germany; photograph: R. Fuhrmann, Wikimedia Commons. Bottom right: resinite from Golling, Austria, Museum of Natural History, Vienna, M2342; photograph courtesy V. Hammer (NHM, Vienna)

- Class III resinites are unique as they consist of natural polystyrene copolymerized with 3-phenylpropanyl cinnamate (Fig. 103b). They originate from Hamamelidaceae spp. and were first discovered near Siegburg, near Bonn in Germany, and accordingly named siegburgite (Fig. 103, bottom left). Siegburgite primarily was formed when resin dropped on sand resulting in concretions, which then underwent diagenesis. It is of the same age as the Eocene Baltic amber succinites with which they sometimes co-occur.
- Class IV resinites are amber-like materials with non-polymer constituents mainly of the cedrene-based sesquiterpenoid type. An example is a resinite from Golling, Salzburg, Austria displayed in Fig. 103, bottom right.

- Class V resinites comprise a mixture of diterpenoid resins and *n*-alkylated compounds.

It should be mentioned that the method of choice to discriminate between the various types of ambers is IR spectrometry, and a large collection of spectra together with photographs of many holotypes has become available recently [348].

2.3.3 Melanin

Melanin (its name derives from the Greek word μέλας = dark, black) is a broad group of ubiquitous pigments found in bacteria, fungi, plants, and animals. Whereas nitrogen-free melanins (allomelanins) occur in bacteria, fungi, and plants, nitrogen-containing melanins are widespread in animals. Animal melanins can be divided in two distinct types: eumelanin (**613**), which is black to brown in color, and pheomelanin (**614**), which has yellow to red hues. Both biopolymers are rather complicated materials with heavy crosslinking and variation of their constituents. They are derived mainly from the amino acids tyrosine and cysteine, and their partial structures are shown in Fig. 104. In both cases, the starting compound is tyrosine, which during biosynthesis of the pigments is converted to DOPA and finally the latter to dopaquinone. To make eumelanins, Nature mainly polymerizes dopaquinone, whereas for pheomelanin, condensation of dopaquinone with cysteine first furnishes a benzothiazine monomer, which eventually polymerizes. These pigments have a variety of functions for various organisms from coloration and radiation shielding to defense. They are embedded in distinct granules that are called eumelanosomes and pheomelanosomes.

Morphological and carbon content data have suggested the presence of melanosomes in a color-banded fossil feather from the Early Cretaceous Crato Formation of Brazil, contrary to earlier investigations that suggested that fossil feathers are preserved as carbonized traces of feather-degrading bacteria [349]. Moreover, based on the morphology of melanosome-like structures (elongate eumelanosomes and subspherical pheomelanosomes), the plumage patterns and even the coloration of the Late Jurassic dinosaur *Anchiornis huxleyi* from mainland China have been reconstructed [350]. However, due care should be exercised to assign specific colors to extinct organisms, especially when based solely on morphological data. The first direct chemical evidence for fossil melanin has been obtained from the chemical characterization of eumelanin in cephalopod ink sacs from the Jurassic of the United Kingdom (for a photograph of a similar specimen from the Early Jurassic of Germany, see Fig. 104) [351]. Using time-of-flight secondary-ion mass spectrometry, eumelanin has also been detected in association with melanosome-like structures in the fossilized skin of extinct marine reptiles: a Paleogene leatherback turtle, a Cretaceous mosasaur, and a Jurassic ichthyosaur [352]. More recently, melanins have been identified by time-of-flight secondary-ion mass spectrometry in further fossil specimens (fish, amphibians, birds, mammals), with the oldest record (Middle Pennsylvanian, 309 Ma) of melanin found in a

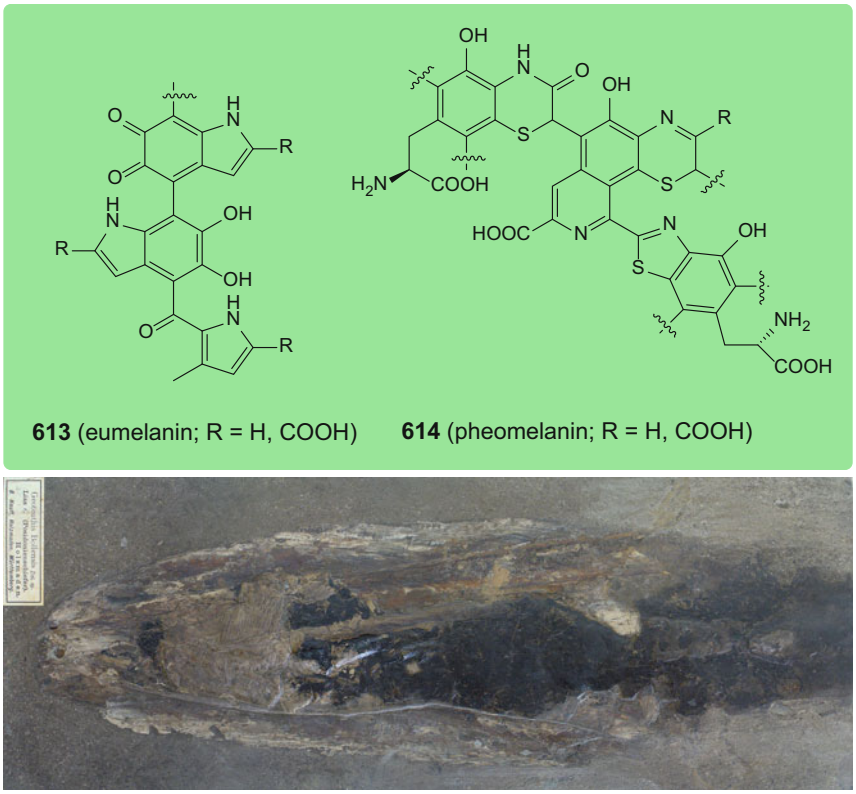

Fig. 104 Partial structures of eumelanin (**613**) and pheomelanin (**614**). Bottom: *Loligosepia aalensis* with preserved ink sac in which fossilized eumelanin is still present; Toarcium (Early Jurassic) Holzmaden, Germany, Staatliches Museum für Naturkunde Karlsruhe, Germany; photograph: H. Zell, Wikimedia Commons

cyclostome (jawless fish) eye from the Francis Creek shale of Mazon Creek (Illinois, USA) [353].

2.3.4 Nucleic Acids

Polynucleotides are most important natural products as they constitute the information base of the living world [354]. Of course, knowledge about organisms living in times long passed seems to be highly important and desirable. Thus, the stakes are quite high to find molecular fossils containing mostly unchanged DNA. Modern analytical methods, and, in particular, the polymerase chain reaction, have made it possible to amplify the tiniest amounts of DNA and to eventually analyze the sequence [355].

However, there are two main practical obstacles encountered in relation to the optimistic hope of being able to analyze the DNA of fossil organisms such as dinosaurs. First, the tremendous amplification of tiny traces of DNA contamination with modern DNA is a very demanding problem, but one that can be solved by extreme care in terms of the extraction and handling procedures used [356]. Second, and most important, DNA decays (by hydrolysis) with time, dependent on temperature and humidity. Thus, the half-life of DNA derived from an investigation of 158 radiocarbon-dated bones of the extinct New Zealand moa bird was estimated as 521 years at 13.1°C for a mitochondrial DNA of 242 base pairs length [357]. This value greatly reduces the time window accessible needed to obtain reasonable results, and in living up to hopes of a "Jurassic Park" type of science fiction.

Nevertheless, analysis of ancient DNA (aDNA) allows the possibility of having a glimpse into several hundred thousand years of the past with respect to evolution, phylogeny, ancient population genetics, geographic phylo-distributions, and ancient genomics in general. As a highlight, one might mention Egyptian mummies [358]. The Neanderthal versus Denisovan and *Homo sapiens* evolution was studied by analyzing the DNA of an 110,000-years-old molar tooth found in the Siberian Denisova cave [359] and comparing it to Neanderthal and extant human genes. A very detailed study of the relationship of Neanderthals and Denisovans with the Middle Pleistocene (about 430,000 years old) Sima de los Huesos hominins showed that the latter were related more closely to the Neanderthals [360]. The celebrated Tyrolean "Ötzi" iceman was investigated with respect to origin and phenotype [361]. Fossil avian egg shell DNA [362] was studied, and the decline of the woolly mammoth (Fig. 105) was deduced by comparing DNA from 4300- and 44,800-year-old Siberian fossils [363].

Fig. 105 Woolly baby mammoth (6–12 months old) (*Mammuthus primigenius*) "Dima" of an age of about 40,000 years, found 1977 in the Magadan area, NE Siberia, Russia. St. Petersburg Zoological Museum; photograph: H. Falk

3 Methodology

Since generally complex mixtures of organic compounds occur, the first step in the investigation of molecular fossils is the separation of mixtures into individual compounds. If the geological sample is a liquid (oil, petroleum), one usually tries to separate fractions by distillation. Otherwise, selective extraction of the pulverized solid sample using different solvents of varying polarity might be an option. In the case of sediments, besides direct Soxhlet or ultrasonic extraction with organic solvents (e.g. [21]), it is usually best to dissolve the matrix initially. For carbonate material, hydrochloric acid is commonly applied (e.g. [305], but there are other non-oxidizing acids like chloroacetic acid), while with silicates hydrofluoric acid would need to be used (e.g. [315]). The residue can then be extracted applying various organic solvents, depending on which fractions (polar, apolar) are desired.

In most cases, a solution of a mixture of organic compounds is obtained. Separation can then follow established methodology. For volatile compounds, gas chromatography would be the first choice, whereas non-volatile compounds may be separated by thin-layer chromatography or high-performance liquid chromatography.

To analyze the compounds with respect to structural details, the common methods of organic natural product structure elucidation are applied. These include the comparison of gas chromatograms with those of authentic materials (e.g. [21]), total synthesis (e.g. [65, 315]), mass spectrometry, inclusive of isotope distribution analysis [364], gas chromatography–mass spectrometry (e.g. [13, 365], and high-performance liquid chromatography–mass spectrometry (e.g. [305]). Also, extremely important are various one- and two-dimensional ^{1}H and ^{13}C nuclear magnetic resonance spectroscopy techniques [366], in particular, micro nuclear magnetic resonance instrumentation (e.g. [305]).

Direct analysis of molecular fossils within the intact matrix can be achieved by time-of-flight secondary-ion mass spectrometry, such as has been described in Ref. [187]. This method allows for two-dimensional resolution of surfaces, which is highly informative for molecular fossils embedded in micro- or macrofossils. Insoluble organic residues may be investigated by pyrolysis-GC-MS, providing useful information on molecules from the characterization of their fragments [337, 338]. Reflectance UV-visible spectroscopy is sometimes an option to screen the surface of colored macrofossils, but, due care must be exercised [283]. Infrared spectrometry can be used to characterize kerogens or coals, but particularly for ambers it offers the possibility of "fingerprinting" the various sources and types [343, 348]. Raman spectroscopy in the micro-reflection mode allows for the determination of chemical phases, which is of high importance for the study of preservation of rather ancient organic material, such as e.g. from Cambrian Burgess shale [367] or even in the astrobiological realm.

4 Diagenetic, Catagenetic, and Metagenetic Processes

Without going into the details of geological processes [9, 368, 369], a short overview of the main reactions that influence the fate of organic natural products and thus their resulting molecular fossils may be presented. A flow diagram is shown in Fig. 106, which is an extension of Fig. 2, and illustrates the molecular evolution from the time the natural product contained in a dying organism is deposited to the development of a molecular fossil and its possible further fate.

The main driving forces of chemical alteration of natural products like lipids, proteins, carbohydrates, lignin, or other metabolites of an organism are metabolism by microbial systems, heat, humidity, oxygenating and reducing agents, mineral catalysts, and pressure exerted by the accumulating mineral deposits. Diagenesis is the process through which the organic contents transform under rather low temperatures (up to 50–100°C) and under microbial influence within a shallow burial (down to about 1000 m). Aerobic organisms in the uppermost sediments consume free oxygen, and organic matter is used as their carbon source. In the deeper layers, anaerobic organisms reduce sulfate for this purpose. Biopolymers are hydrolyzed yielding humin and later on kerogen. Many natural products remain either unchanged or undergo only minor transformations by oxidative or reductive processes, which are occasionally catalyzed by the surrounding mineral matrix. Accordingly, many molecular fossils and biomarkers make it through this stage. When the temperature becomes elevated to about 100–150°C and pressure is rising from deeper burial, catagenesis sets in with thermal degradation of the molecules,

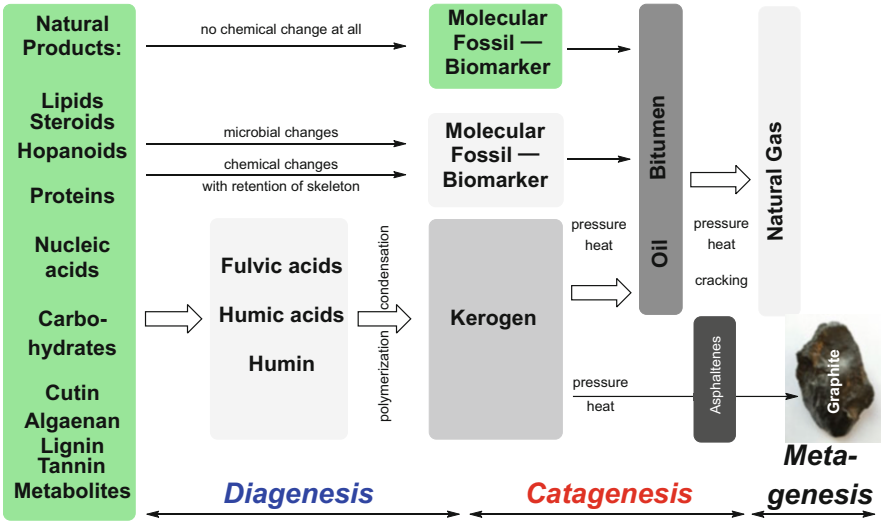

Fig. 106 Diagenesis, catagenesis, and metagenesis of natural products. Paleozoic graphite slab, Kaisersberg, Austria; photograph: H. Falk

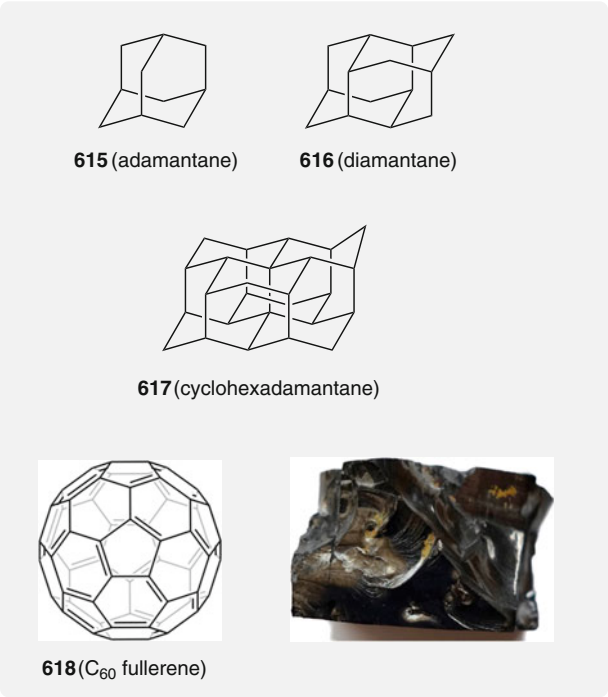

Fig. 107 Adamantane (**615**), diamantane (**616**), cyclohexadamantane (**617**), C_{60} fullerene (**618**), and (bottom right) shungite, Precambrian (600 Ma) Onega Sea, Shun'ga area, Karelia, Russia; photograph: H. Falk

eventually yielding oil and bitumen. Higher temperatures up to 200°C then give rise to cracking processes, providing natural gas. Part of the kerogen can be transformed during metamorphosis by even higher temperatures and pressures via the asphaltenes, as, for example, **612** (see Fig. 97) into graphite. It might be mentioned that virtually all crude oils contain 1–100 ppm diamondoids like adamantane (**615**) or diamantane (**616**) derivatives, and in one case even cyclohexadamantane (**617**) (Fig. 107). A defined biological source is not available, but these compounds can be thought to be formed by cracking and carbocation-mediated rearrangements (governed by thermodynamic stabilization) of biogenic precursors [370, 371]. Interestingly, derivatives of **615** and **616** were also found in the Cretaceous/Paleogene boundary sediments at Kawaruppu, Hokkaido, Japan [52]. Similar arguments may hold for the fullerenes, like **618**, characterized for example in Precambrian non-graphitized shungite-coal [372, 373] (Fig. 107).

Finally, it might be convenient for readers who are not too familiar with geology to consult the chart of Fig. 108 containing the geological time scale. In addition,

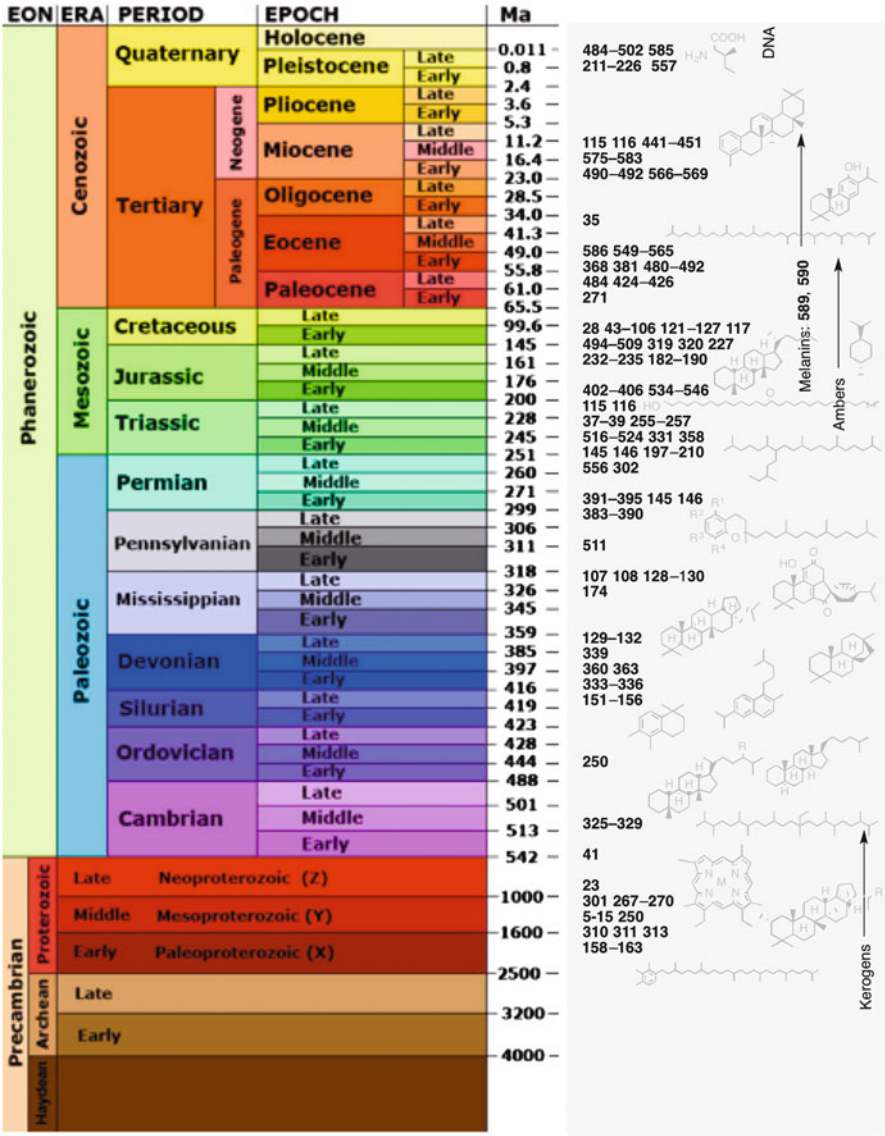

Fig. 108 Geological timescale (US Geological Survey in Wikipedia Commons; it might be noted that Pennsylvanian and Mississippian are taken together as the Carboniferous) and examples of early occurrences of molecular fossils and biomarkers indicated by their formula numbers

examples for the respective early occurrences of molecular fossils are also included along with this timeline to provide an impression of molecular fossil distribution throughout geological times.

Acknowledgments We are grateful to Dr. Vera Hammer (head of the Mineral Collection of the Museum of Natural History, Vienna, Austria) for her assistance with organic minerals, ambers, and their photographs, to Prof. Norbert Vávra (University Vienna) for "amber help", to Dr. Melinda Mayer, Kathryn Cross (Inst. of Food Res., Norwich, UK), and Dr. Benjamin Stegmann (University of Ulm), Dr. Mercedes di Pasquo (National Research Council of Argentinia, Laboratorio de Palinología y Paleobotánica, Entre Rios, Argentina), Michael Plewka (Gevelsberg, Germany, plingfactory.de), Richard Robinson (Underwater Photographer, Auckland, New Zealand, www.depth.co.nz), Dr. Jeremy R. Young (UCL, London, UK), and Dr. Klaus Wenderoth (Ebsdorfergrund, Germany) for permission to use their photographs as indicated in the respective Figures. We are also grateful to Dr. Christoph Etzlstorfer (JKU, Linz) for his help with computations.

References

1. Dictionary of natural products at: http://dnp.chemnetbase.com
2. Treibs A (1936) Chlorophyll - und Häminderivate in organischen Mineralstoffen. Angew Chem 49:682
3. Peters KE, Walters CC, Moldowan JM (2005) The biomarker guide, vol 1 and 2, 2nd edn. Cambridge University Press, New York
4. Gaines SM, Eglinton G, Rullkötter J (2009) Echoes of life. What fossil molecules reveal about earth history. Oxford University Press, Oxford, UK
5. Smith HM (1967) Hydrocarbon constituents of petroleum and some possible lipid precursors. J Am Oil Chem Soc 44:680
6. Ni Y, Dai J (2009) Geochemical characteristics of abiogenic alkane gases. Petrol Sci 6:327
7. Clark RC Jr, Blumer M (1967) Distribution of *n*-paraffins in marine organisms and sediment. Limnol Oceanogr 12:79
8. Rushdi AI, Simoneit BRT (2001) Lipid formation by aqueous Fischer–Tropsch-type synthesis over a temperature range of 100 to 400°C. Orig Life Evol Biosph 31:103
9. Tissot BP, Welte DH (1984) Petroleum formation and occurrence, 2nd edn. Springer, New York
10. Jacobson SR, Hatch JR, Teerman SC, Askin RA (1988) Middle Ordovician organic matter assemblages and their effect on Ordovician-derived oils. Am Assoc Petrol Geol Bull 72:1090
11. Moldowan JM, Seifert WK, Gallegos EJ (1985) Relationship between petroleum composition and depositional environment of petroleum source rocks. Am Assoc Petrol Geol Bull 69:1255
12. Bourbonniere RA, Meyers PA (1996) Sedimentary geolipid records of historical change in the watersheds and productivities of Lakes Ontario and Erie. Limnol Oceanogr 41:352
13. Bush RT, McInerney FA (2013) Leaf wax *n*-alkane distributions in and across modern plants: implications for paleoecology and chemotaxonomy. Geochim Cosmochim Acta 117:161
14. Knoche H, Ourisson G (1967) Organic compounds in fossil plants (*Equisetum*; horsetails). Angew Chem Int Ed 6:1085
15. Rieley G, Collier RJ, Jones DM, Eglinton G, Eakin PA, Fallick E (1991) Sources of sedimentary lipids deduced from stable carbon-isotope analyses of individual compounds. Nature 352:425
16. Klomp UC (1986) The chemical structure of a pronounced series of *iso*-alkanes in South Oman crudes. Org Geochem 10:807
17. Elvert M, Suess E, Whiticar MJ (1999) Anaerobic methane oxidation associated with marine gas hydrates: superlight C-isotopes from saturated and unsaturated C_{20} and C_{25} irregular isoprenoids. Naturwissenschaften 86:295

18. Thiel V, Jenisch A, Wörheide G, Löwenberg A, Reitner J, Michaelis W (1999) Mid-chain branched alkanoic acids from "living fossil" demosponges: a link to ancient sedimentary lipids? Org Geochem 30:1
19. Shiea J, Brassell SC, Ward DM (1990) Mid-chain branched mono- and dimethyl alkanes in hot spring cyanobacterial mats: a direct biogenic source for branched alkanes in ancient sediments? Org Geochem 15:223
20. Robinson N, Eglinton G (1990) Lipid chemistry of Icelandic hot spring microbial mats. Org Geochem 15:291
21. Höld IM, Schouten S, Jellema J, Sininghe Damsté JS (1999) Origin of free and bound mid-chain methyl alkanes in oils, bitumens and kerogens of the marine, Infracambrian Huqf Formation (Oman). Org Geochem 30:1411
22. Audino M, Grice K, Alexander R, Boreham CJ, Kagi RI (2001) Unusual distribution of monomethylalkanes in *Botryococcus braunii*-rich samples: origin and significance. Geochim Cosmochim Acta 65:1995
23. Warton B, Alexander R, Kagi RI (1997) Identification of some single branched alkanes in crude oils. Org Geochem 27:465
24. Kenig F, Simons D-JH, Crich D, Cowen JP, Ventura GT, Rehbein-Khalily T, Brown TC, Anderson KB (2003) Branched aliphatic alkanes with quaternary substituted carbon atoms in modern and ancient geological samples. Proc Natl Acad Sci USA 100:12554
25. Powell TG (1988) Pristane/phytane ratio as environmental indicator. Nature 333:604
26. Goossens H, de Leeuw JW, Schenck PA, Brassell SC (1984) Tocopherols as likely precursors of pristane in ancient sediments and crude oils. Nature 312:440
27. Booth VH (1963) α-Tocopherol, its co-occurrence with chlorophyll in chloroplasts. Phytochemistry 2:421
28. Blumer M, Mullin MM, Thomas DW (1964) Pristane in the marine environment. Helgoländer Wiss Meeresuntersuch 10:187
29. Illich HA (1983) Pristane, phytane, and lower molecular weight isoprenoid distributions in oil. Am Assoc Petrol Geol Bull 67:385
30. Waples DW, Haug P, Welte DH (1974) Occurrence of a regular C_{25} isoprenoid hydrocarbon in Tertiary sediments representing a lagoonal-type, saline environment. Geochim Cosmochim Acta 38:381
31. Grice K, Schouten S, Nissenbaum A, Charrach J, Sininghe Damsté JS (1998) Isotopically heavy carbon in the C_{21} to C_{25} regular isoprenoids in halite-rich deposits from the Sdom formation, Dead Sea Basin, Israel. Org Geochem 28:349
32. Petrov AA, Vorobyova NS, Zemskova ZK (1990) Isoprenoid alkanes with irregular "head-to-head" linkages. Org Geochem 16:1001
33. Barber CJ, Grice K, Bastow TB, Alexander R, Kagi R (2001) The identification of crocetane in Australian crude oils. Org Geochem 32:943
34. Schwartz H, Sample J, Weberling KD, Minisini D, Moore JC (2003) An ancient linked fluid migration system: cold-seep deposits and sandstone intrusions in the Panoche Hills, California, USA. Geo-Mar Lett 23:340
35. Vink A, Schouten S, Sephton S, Sininghe Damsté JS (1998) A newly discovered norisoprenoid, 2,6,15,19-tetramethylicosane, in Cretaceous black shales. Geochim Cosmochim Acta 62:965
36. Gardner PM, Whitehead EV (1972) The isolation of squalane from Nigerian petroleum. Geochim Cosmochim Acta 36:259
37. Brassell SC, Wardroper AMK, Thompson ID, Maxwell JR, Eglinton G (1981) Specific acyclic isoprenoids as biological markers of methanogenic bacteria in marine sediments. Nature 290:693
38. Summons RE, Metzger P, Largeau C, Murray AP, Hope JM (2002) Polymethylsqualanes from *Botryococcus braunii* in lacustrine sediments and oils. Org Geochem 33:99
39. Freeman KH, Hayes JM, Trendel J-M, Albrecht P (1990) Evidence from carbon isotope measurements for diverse origins of sedimentary hydrocarbons. Nature 343:254

40. Yon DA, Maxwell JR, Ryback G (1982) 2,6,10-Trimethyl-7-(3-methylbutyl)-dodecane, a novel sedimentary biological marker compound. Tetrahedron Lett 23:2143
41. Belt ST, Allard WG, Massé G, Robert J-M, Rowland SJ (2000) Highly branched isoprenoids (HBIs): identification of the most common and abundant sedimentary isomers. Geochim Cosmochim Acta 64:3839
42. Sinninghe Damsté JS, Muyzer G, Abbas B, Rampen SW, Masse G, Allard WG, Belt ST, Robert J-M, Rowland SJ, Moldowan JM, Barbanti SM, Fago FJ, Denisevich P, Dahl J, Trindade LAF, Schouten S (2004) The rise of the rhizosolenid diatoms. Science 304:584
43. Volkman JK, Barrett SM, Dunstan GA (1994) C_{25} and C_{30} highly branched isoprenoid alkenes in laboratory cultures of two marine diatoms. Org Geochem 21:407
44. Belt ST, Cooke DA, Robert J-M, Rowland S (1996) Structural characterization of widespread polyunsaturated isoprenoid biomarkers: a C_{25} triene, tetraene and pentaene from the diatom *Haslea ostrearia* Simonsen. Tetrahedron Lett 37:4655
45. Moldowan JM, Seifert WK (1980) First discovery of botryococcane in petroleum. J Chem Soc Chem Commun:912
46. McKirdy DM, Cox RE, Volkman JK, Howell VJ (1986) Botryococcane in a new class of Australian non-marine crude oils. Nature 320:57
47. Metzger P, Largeau C, Casadevall E (1991) Lipids and macromolecular lipids of the hydrocarbon-rich microalga *Botryococcus braunii*. Chemical structure and biosynthesis. Prog Chem Org Nat Prod 57:1
48. Maxwell JR, Douglas AG, Eglinton G, McCormick A (1968) The Botryococcenes – hydrocarbons of novel structure from the alga *Botryococcus braunii*, Kützing. Phytochemistry 7:2157
49. White JD, Somers TC, Reddy GN (1986) Absolute configuration of (–)-botryococcene. J Am Chem Soc 108:5352
50. Ingram LL, Ellis J, Crisp PT, Cook AC (1983) Comparative study of oil shales and shale oils from the Mahogany Zone, Green River Formation (U.S.A.) and Kerosene Creek Seam, Rundle Formation (Australia). Chem Geol 38:185
51. Kissin YV (1990) Catagenesis of light cycloalkanes in petroleum. Org Geochem 15:575
52. Shimoyama A, Yabuta H (2002) Mono- and bicyclic alkanes and diamantoid hydrocarbons in the Cretaceous/Tertiary boundary sediments at Kawaruppu, Hokkaido, Japan. Geochem J 36:173
53. Alvarez LW, Alvarez W, Asaro F, Michel HV (1980) Extraterrestrial cause for the Cretaceous-Tertiary extinction. Science 208:1095
54. Audino M, Grice K, Alexander R, Kagi RI (2001) Macrocyclic-alkanes: a new class of biomarker. Org Geochem 32:759
55. Alexander R, Kagi R, Noble R (1983) Identification of the bicyclic sesquiterpenes drimane and eudesmane in petroleum. J Chem Soc Chem Commun:226
56. Brassell SC, Eglinton G, Maxwell JR (1983) The geochemistry of terpenoids and steroids. Biochem Soc Trans 11:575
57. Barakat AO, Rullkötter J (2005) Gas chromatographic/mass spectrometric analysis of cembrenoid diterpenes in kerogen from a lacustrine sediment. Org Mass Spectrom 28:157
58. van Aarssen BGK, Kruk C, Hessels JKC, de Leeuw JW (1990) *cis-cis-trans*-Bicadinane, an uncommon triterpane family isolated from crude oils. Tetrahedron Lett 31:4645
59. van Aarssen BGK, Cos HC, Hoogendoorn P, de Leeuw JW (1990) A cadinene biopolymer in fossil and extant dammar resins as a source for cadinanes and bicadinanes in crude oils from Southeast Asia. Geochim Cosmochim Acta 54:3021
60. van Aarssen BGK, Hessels JKC, Abbink OA, de Leeuw JW (1992) The occurrence of polycyclic sesqui-, tri-, and oligoterpenoids derived from a resinous polymeric cadinene in crude oils from southeast Asia. Geochim Cosmochim Acta 56:1231
61. Cox HC, de Leeuw JW, Schenck PA, van Koningsveld H, Jansen JC, van de Graaf B, van Geerestein VJ, Kanters JA, Kruk C, Jans AWH (1986) Bicadinane, a C_{30} pentacyclic isoprenoid hydrocarbon found in crude oil. Nature 319:316

62. Simoneit BRT, Grimalt JO, Wang TG, Cox RE, Hatcher PG, Nissenbaum A (1986) Cyclic terpenoids of contemporary resinous plant detritus and of fossil woods, ambers and coals. Org Geochem 10:877
63. Summons RE, Boreham CJ, Foster CB, Murray AP, Gorter JD (1995) Chemostratigraphy and composition of oils in the Perth Basin, Western Australia. Aust Petrol Prod Expl Assoc J 35:613
64. Mineralienatlas: https://www.mineralienatlas.de/lexikon/index.php/MineralData?mineral=Fichtelite
65. Ruzicka L, Waldmann E (1935) Polyterpene und Polyterpenoide XCVI. Zur Konstitution des Fichtelits. Helv Chim Acta 18:611
66. Taber DF, Saleh SA (1980) Intramolecular Diels-Alder route to angularly substituted perhydrophenanthrenes. Synthesis of (±)-fichtelite. J Am Chem Soc 102:5085
67. Mineralienatlas: https://www.mineralienatlas.de/lexikon/index.php/MineralData?mineral=Simonellite
68. Mineralienatlas: https://www.mineralienatlas.de/lexikon/index.php/MineralData?mineral=Reten
69. Mineralienatlas: https://www.mineralienatlas.de/lexikon/index.php/MineralData?mineral=Dinit
70. Noble RA, Knox J, Alexander R Kagi RI (1985) Identification of tetracyclic hydrocarbons in Australian crude oils and sediments. J Chem Soc Chem Commun:32
71. Noble RA, Alexander R, Kagi RI, Knox J (1985) Tetracyclic diterpanoid hydrocarbons in some Australian coals, sediments and crude oils. Geochim Cosmochim Acta 49:2141
72. Noble RA, Alexander R, Kagi RI, Nox JK (1986) Identification of some diterpenoid hydrocarbons in petroleum. Org Geochem 10:825
73. Noble RA (1986) A geochemical study of bicyclic alkanes and diterpenoid hydrocarbons in crude oils, sediments, and coals. PhD Thesis, Department of Organic Chemistry, University of Western Australia, Perth, Australia
74. Disnar JR, Harouna M (1994) Biological origin of tetracyclic diterpanes, *n*-alkanes and other biomarkers in lower carboniferous Gondwana coals (Niger). Org Geochem 21:143
75. Sheng G, Simoneit BRT, Leif RN, Chen X, Fu J (1992) Tetracyclic terpanes enriched in Devonian cuticle humin coals. Fuel 71:523
76. Schulze T, Michaelis W (1990) Structure and origin of terpenoid hydrocarbons in some German coals. Org Geochem 16:1051
77. Haidinger W (1841) Ueber den Hartit, eine neue Species aus der Ordnung der Erdharze. Ann Phys Chem 54:262
78. Moldowan JM, Seifert WK, Gallegos EJ (1983) Identification of an extended series of tricyclic terpanes in petroleum. Geochim Cosmochim Acta 47:1531
79. Dzou LIP, Noble RA, Senftle JT (1995) Maturation effects on absolute biomarker concentration in a suite of coals and associated vitrinite concentrates. Org Geochem 23:681
80. Behrens A, Schaeffer P, Albrecht P (2000) Occurrence of precursors of regular tricyclopolyprenoids in recent sediments. Org Lett 2:361
81. Ungur N, Kulciţki V (2009) Occurrence, biological activity and synthesis of cheilanthane sesterterpenoids. Tetrahedron 65:3815
82. Mills JS, Werner AEA (1955) The chemistry of dammar resin. J Chem Soc:3132
83. Ourisson G, Albrecht P (1992) Hopanoids. 1. Geohopanoids: the most abundant natural products on earth? Acc Chem Res 25:398
84. Mello MR, Koutsoukos EAM, Hart MB, Brassell SC, Maxwell JR (1989) Late Cretaceous anoxic events in the Brazilian continental margin. Org Geochem 14:529
85. Moldowan JM, Fago FJ, Carlson RMK Young DC, van Duvne G, Clardy J, Schoell M, Pillinger CT, Watt DS (1991) Rearranged hopanes in sediments and petroleum. Geochim Cosmochim Acta 55:3333
86. van Dorsselaer A, Albrecht P, Ourisson G (1977) Identification of novel 17α(H)-hopanes in shales, coals, lignites, sediments and petroleum. Bull Soc Chim Fr:165
87. Avogadro, an advanced, free open source molecular editor: http://avogadro.cc/wiki/Main_Page
88. Falk H, Etzlstorfer C, unpublished results

89. French KL, Tosca NJ, Cao C, Summons RE (2012) Diagenetic and detrital origin of moretane anomalies through the Permian-Triassic boundary. Geochim Cosmochim Acta 84:104
90. Rohmer M (1993) The biosynthesis of triterpenoids of the hopane series in Eubacteria: a mine of new enzyme reactions. Pure Appl Chem 65:1293
91. Ourisson G, Albrecht P, Rohmer M (1979) The hopanoids. Palaeochemistry and biochemistry of a group of natural products. Pure Appl Chem 51:709
92. Peters KE, Moldowan JM (1991) Effects of source, thermal maturity, and biodegradation on the distribution and isomerization of homohopanes in petroleum. Org Geochem 17:47
93. Rullkötter J, Philip P (1981) Extended hopanes up to C_{40} in Thornton bitumen. Nature 292:616
94. Rullkötter J, Nissenbaum A (1988) Dead Sea asphalt in Egyptian mummies: molecular evidence. Naturwissenschaften 75:618
95. Rohmer M, Ourisson G (1976) Structure des bactériohopanetétrols d'*Acetobacter xylinum*. Tetrahedron Lett 40:3633
96. Summons RE, Jahnke LL, Hope JM, Logan GA (1999) 2-Methylhopanoids as biomarkers for cyanobacterial oxygenic photosynthesis. Nature 400:554
97. Rasmussen B, Fletcher IR, Brocks JJ, Kilburn MR (2008) Reassessing the first appearance of eukaryotes and cyanobacteria. Nature 455:1101
98. Zundel M, Rohmer M (1985) Procaryotic triterpenoids I. 3β-Methylhopanoids from *Acetobacter* species and *Methylococcus capsulatus*. Eur J Biochem 150:23
99. Burhan RYP, Trendel J-M, Adam P, Wehrung P, Albrecht P, Nissenbaum A (2002) Fossil bacterial ecosystem at methane seeps: origin of organic matter from Be'eri sulfur deposit, Israel. Geochim Cosmochim Acta 23:4085
100. Paull R, Michaelsen BH, McKirdy DM (1998) Fernenes and other triterpenoid hydrocarbons in *Dicroidium*-bearing Triassic mudstones and coals from South Australia. Org Geochem 29:1331
101. Stefanova M, Magnier C, Velinova D (1995) Biomarker assemblage of some Miocene-aged Bulgarian lignite lithotypes. Org Geochem 23:1067
102. Rullkötter J, Leythauser D, Wendisch D (1982) Novel 23,28-bisnorlupanes in Tertiary sediments. Widespread occurrence of nuclear demethylated triterpenes. Geochim Cosmochim Acta 46:2501
103. Connan J, Dessort D (1987) Novel family of hexacyclic hopanoid alkanes (C_{32} C_{35}) occurring in sediments and oils from anoxic paleoenvironments. Org Geochem 11:103
104. Trendel J-M, Graff R, Wehrung P, Albrecht P, Dessort D, Connan J (1993) C(14α)-*homo*-26-*nor*-17α-Hopanes, a novel and unexpected series of molecular fossils in biodegraded petroleum. J Chem Soc Chem Commun:461
105. Fazeelat T, Alexander R, Kagi RI (1995) Molecular structures of sedimentary 8,14-secohopanes inferred from their gas chromatographic retention behaviour. Org Geochem 23:641
106. Wang T-G, Simoneit BRT (1990) Organic geochemistry and coal petrology of Tertiary brown coal in the Zhoujing mine, Baise Basin, South China: 2. Biomarker assemblage and significance. Fuel 69:12
107. Nytoft HP, Bojesen-Koefoed JA, Christiansen FG (2000) C_{26} and $C_{28}-C_{34}$ 28-norhopanes in sediments and petroleum. Org Geochem 31:25
108. ten Haven HL, Rullkötter J (1988) The diagenetic fate of taraxer-14-ene and oleanane isomers. Geochim Cosmochim Acta 52:2543
109. Moldowan JM, Dahl J, Huizinga BJ, Fago FJ, Hickey LJ, Peakman TM, Taylor DW (1994) The molecular fossil record of oleanane and its relation to angiosperms. Science 265:768
110. Riva A, Caccialanza PG, Quagliaroli F (1988) Recognition of 18β(H)-oleanane in several crudes and Tertiary-Upper Cretaceous sediments. Definition of a new maturity parameter. Org Geochem 13:671

111. Sinninghe Damsté JS, Kenig F, Koopmans MP, Köster J, Schouten S, Hayes JM, de Leeuw JW (1995) Evidence for gammacerane as an indicator of water column stratification. Geochim Cosmochim Acta 59:1895
112. Venkatesan MI (1989) Tetrahymenol: its widespread occurrence and geochemical significance. Geochim Cosmochim Acta 53:3095
113. Ourisson G, Rohmer M, Poralla K (1987) Prokaryotic hopanoids and other polyterpenoid sterol surrogates. Annu Rev Microbiol 41:301
114. Kimble BJ, Maxwell JR, Philp RP, Eglinton G (1974) Identification of steranes and triterpanes in geolipid extracts by high-resolution gas chromatography and mass spectrometry. Chem Geol 14:173
115. Pearson MJ, Obaje NG (1999) Onocerane and other triterpenoids in Late Cretaceous sediments from the Upper Benue Trough, Nigeria: tectonic and palaeoenvironmental implications. Org Geochem 30:583
116. Schaeffer P, Poinsot J, Hauke V, Adam P, Wehrung P, Trendel J-M, Albrecht P, Dessort D, Connan J (1994) Novel optically active hydrocarbons in sediments: evidence for an extensive biological cyclization of higher regular polyprenols. Angew Chem Int Ed 33:1166
117. Riediger CL, Fowler MG, Snowdon LR (1997) Organic geochemistry of the Lower Cretaceous ostracode zone, a brackish/non-marine source of some lower Mannville oils in southeastern Alberta. In: Pemberton SG, David PJ (eds) Petroleum geology of the Cretaceous Mannville Group, Western Canada. Can Soc Petrol Geol Mem 18:93
118. Bach T, Rohmer M (eds) (2013) Isoprenoid synthesis in plants and microorganisms. New concepts and experimental approaches. Springer, Heidelberg
119. Concepción MR (ed) (2014) Plant isoprenoids. Springer, Heidelberg
120. Makin HLJ, Gower DB (eds) (2010) Steroid analysis. Springer, Heidelberg
121. Thomson RH (ed) (1993) The chemistry of natural products. Springer, Heidelberg
122. Melendez I, Grice K, Schwark L (2013) Exceptional preservation of Palaeozoic steroids in a diagenetic continuum. Sci Rep 3:2768
123. Rubinstein I, Sieskind O, Albrecht P (1975) Rearranged sterenes in a shale: occurrence and simulated formation. J Chem Soc Perkin Trans I:1833
124. Peters KE, Moldowan JM, LaCroce MV, Kubicki JD (2014) Stereochemistry, elution order and molecular modeling of four diaergostanes in petroleum. Org Geochem 76:1
125. Mackenzie AS, Brassell SC, Eglinton G, Maxwell JR (1982) Chemical fossils: the geological fate of steroids. Science 217:491
126. Brassell SC, McEvoy J, Hoffmann CF, Lamb NA, Peakman TM, Maxwell JR (1984) Isomerisation, rearrangement and aromatisation of steroids in distinguishing early stages of diagenesis. Adv Org Geochem 6:11
127. Mackenzie AS, Lamb NA, Maxwell JR (1982) Steroid hydrocarbons and the thermal history of sediments. Nature 259:223
128. Grantham PJ, Wakefield LL (1988) Variations in the sterane carbon number distributions of marine source rock derived crude oils through geological time. Org Geochem 12:61
129. Moldowan JM, Fago FJ, Lee CY, Jacobson SR, Watt DS, Slogui N-E, Jeganathan A, Young DC (1990) Sedimentary 24-*n*-propylcholestanes, molecular fossils diagnostic of marine algae. Science 247:309
130. McCafferey MA, Moldowan JM, Lipton PA, Summons RE, Peters KE, Jeganathan A, Watt DS (1994) Paleoenvironmental implications of novel C_{30} steranes in Precambrian to Cenozoic age petroleum and bitumen. Geochim Cosmochim Acta 58:529
131. Love GD, Grosjean E, Stalvies C, Fike DA, Grotzinger JP, Bradley AS, Kelly AE, Bhatia M, Meredith W, Snape CE, Bowring SA, Condon DJ, Summons RE (2009) Fossil steroids record the appearance of Desmospongiae during the Cryogenian period. Nature 457:718
132. Antcliffe JB (2013) Questioning the evidence of organic compounds called sponge biomarkers. Palaeontology 56:917
133. Wolff GA, Lamb NA, Maxwell JR (1986) The origin and fate of 4-methyl steroid hydrocarbons. I. Diagenesis of 4-methyl sterenes. Geochim Cosmochim Acta 50:335

134. Dastillung M, Albrecht P (1977) Δ^2-Sterenes as diagenetic intermediates in sediments. Nature 269:678
135. Dahl J, Moldowan JM, Summons RE, McCaffrey MA, Lipton P, Watt DS, Hope JM (1995) Extended 3β-alkyl steranes and 3-alkyl triaromatic steroids in crude oils and rock extracts. Geochim Cosmochim Acta 59:3717
136. Zhang S, Moldowan JM, Li M, Bian L, Zhang B, Wang F, He Z, Wang D (2002) The abnormal distribution of the molecular fossils in the pre-Cambrian and Cambrian: its biological significance. Sci China Ser D 45:193
137. Holba AG, Tegelaar EW, Huizinga BJ, Moldowan JM, Singletary MS, McCaffrey MA, Dzou LIP (1998) 24-Norcholeatanes as age-sensitive molecular fossils. Geology 26:783
138. Rampen SW, Schouten S, Abbas B, Panoto FE, Muyzer G, Campbell CN, Fehling J, Sinninghe Damsté JS (2007) On the origin of 24-norcholestanes and their use as age-diagnostic biomarkers. Geology 35:419
139. Riolo J, Albrecht P (1985) Novel rearranged ring C monoaromatic steroid hydrocarbons in sediments and petroleum. Tetrahedron Lett 26:2701
140. Riolo J, Ludwig B, Albrecht P (1985) Synthesis of C ring monoaromatic steroid hydrocarbons occurring in geological samples. Tetrahedron Lett 26:2697
141. Riolo J, Hussler G, Albrecht P, Connan J (1986) Distribution of aromatic steroids in geological samples: their evaluation as geochemical parameters. Org Geochem 10:981
142. Moldowan JM, Fago FJ (1986) Structure and significance of a novel rearranged monoaromatic steroid hydrocarbon in petroleum. Geochim Cosmochim Acta 50:343
143. Ludwig B, Hussler G, Wehrung P, Albrecht P (1981) C_{26}–C_{29} triaromatic steroid derivatives in sediments and petroleums. Tetrahedron Lett 22:3313
144. Koopmans MP, Köster J, van Kaam-Peters HME, Kenig F, Schouten S, Hartgers WA, de Leeuw JW, Sinninghe Damsté JS (1996) Diagenetic and catagenetic products of isorenieratene: molecular indicators for photic zone anoxia. Geochim Cosmochim Acta 60:4467
145. Grice K, Cao C, Love GD, Böttcher ME, Twitchett RJ, Grosjean E, Summons RE, Turgeon SC, Dunning W, Jin Y (2005) Photic zone euxinia during the Permian-Triassic superanoxic event. Science 307:706
146. Brocks JJ, Schaeffer P (2008) Okenane, a biomarker for purple sulfur bacteria (Chromatiaceae), and other new carotenoid derivatives from the 1640 Ma Barney Creek Formation. Geochim Cosmochim Acta 72:1396
147. Sinninghe Damsté JS, Koopmans MP (1997) The fate of carotenoids in sediments: an overview. Pure Appl Chem 69:2067
148. Ellis L, Langworthy TA, Winans R (1996) Occurrence of phenylalkanes in some Australian crude oils and sediments. Org Geochem 24:57
149. Lu H, Wang L, Song Z, Greenwood P, Yin Q (2011) Occurrence and distribution of series long-chain alkyl naphthalenes in Late Cretaceous sedimentary rocks of the Songliao Basin, China. Geochem J 45:125
150. Radke M, Rullkötter J, Vriend SP (1994) Distribution of naphthalenes in crude oils from the Java Sea: source and maturation effects. Geochim Cosmochim Acta 58:3675
151. Strachan MG, Alexander R, Kagi RI (1986) Trimethylnaphthalenes in crude oils and sediments: effects of source and maturity. Geochim Cosmochim Acta 52:1255
152. van Aarssen BGK, Alexander R, Kagi RI (1996) The origin of Barrow Sub-basin crude oil: a geochemical correlation using land-plant biomarkers. Aust Petrol Prod Expl Assoc J 36:465
153. Ellis L, Singh RK, Alexander R, Kagi RI (1996) Formation of isohexyl alkylaromatic hydrocarbons from aromatization-rearrangement of terpenoids in the sedimentary environment: a new class of biomarker. Geochim Cosmochim Acta 60:4747
154. Berthod A, Wang X, Gahm KH, Armstrong DW (1998) Quantitative and stereoisomeric determination of light biomarkers in crude oil and coal samples. Geochim Cosmochim Acta 62:1619

155. Ellis L, Singh RK, Alexander R, Kagi RI (1995) Identification and occurrence of dihydro-*ar*-curcumene in crude oils and sediments. Org Geochem 23:197
156. Wen Z, Wang R, Radke M, Wu Q, Sheng G, Liu Z (2000) Retene in pyrolysates of algal and bacterial organic matter. Org Geochem 31:757
157. Silliman JE, Meyers PA, Ostrom PH, Ostrom NW, Eadie BJ (2000) Insights into the origin of perylene from isotopic analyses of sediments from Saanich Inlet, British Columbia. Org Geochem 31:1133
158. Jiang C, Alexander R, Kagi RI, Murray AP (2000) Origin of perylene in ancient sediments and its geological significance. Org Geochem 31:1545
159. Gill M, Steglich W (1987) Pigments of fungi (Macromycetes). Prog Chem Org Nat Prod 51:1
160. Grice K, Lu H, Atahan P, Asif M, Hallmann C, Grenwood P, Maslen E, Tulipani S, Williford K, Dodson J (2009) New insights into the origin of perylene in geological samples. Geochim Cosmochim Acta 73:6531
161. Stein SE (1978) On the high temperature chemical equilibria of polycyclic aromatic hydrocarbons. J Phys Chem 82:566
162. Simoneit BRT (2002) Molecular indicators (biomarkers) of past life. Anat Rec 268:186
163. Wolkenstein K, Gross JH, Oeser T, Schöler HF (2002) Spectroscopic characterization and crystal structure of the 1,2,3,4,5,6-hexahydrophenanthro[1,10,9,8-*opqra*]perylene. Tetrahedron Lett 43:1653
164. Treibs A (1934) Über das Vorkommen von Chlorophyllderivaten in einem Ölschiefer aus der oberen Trias. Liebigs Ann Chem 509:103
165. Callot HJ, Ocampo R (2000) Geochemistry of porphyrins. In: Kadish KM, Smith KM, Guilard R (eds) The porphyrin handbook 1. Academic Press, San Diego, p 349
166. Espinosa M, Pacheco US, Leyte F, Ocampo R (2014) Separation and identification of porphyrin biomarkers from a heavy crude oil Zaap-1 offshore well, Sonda de Campeche, México. J Porphyrins Phthalocyanines 18:542
167. van Berkel GJ, Quirke JME, Filby RH (1989) The Henryville Bed of the New Albany shale – I. Preliminary characterization of the nickel and vanadyl porphyrins in the bitumen. Org Geochem 14:119
168. Gibbison R, Peakman TM, Maxwell JR (1995) Novel porphyrins as molecular fossils for anoxygenic photosynthesis. Tetrahedron Lett 36:9057
169. Chicarelli MI, Hayes JM, Popp BN, Eckardt CB, Maxwell JR (1993) Carbon and nitrogen isotopic compositions of alkyl porphyrins from the Triassic Serpiano oil shale. Geochim Cosmochim Acta 57:1307
170. Moldowan JM, Sundararaman P, Schoell M (1986) Sensitivity of biomarker properties to depositional environment and/or source input in the Lower Toarcian of SW-Germany. Org Geochem 10:915
171. Clezy PS, Fookes CJR, Prashar JK, Salek A (1992) The chemistry of pyrrolic compounds. LXVII. A new demethyl analog of DPEP (desoxophylloeythroetioporphyrin). Aust J Chem 45:703
172. Huseby B, Ocampo R (1997) Evidence for porphyrins bound, via ester bonds, to the Messel oil shale kerogen by selective chemical degradation experiments. Geochim Cosmochim Acta 61:3951
173. Wolff GA, Chicarelli MI, Shaw GJ, Evershed RP, Quirke JME, Maxwell JR (1984) Structure analysis of naturally occurring alkyl porphyrins by hydrogen chemical ionization mass spectrometry. Tetrahedron 40:3777
174. Sundararaman P, Hwang RJ, Ocampo R, Boreham CJ, Callot HJ, Albrecht P (1994) Temporal changes in the distribution of C_{33} cycloheptenoDPEP and 17-nor C_{30} DPEP in rocks. Org Geochem 21:1051
175. Keely BJ, Harris PG, Popp BN, Hayes JM, Meischner D, Maxwell JR (1994) Porphyrin and chlorin distributions in a late Pliocene lacustrine sediment. Geochim Cosmochim Acta 58:3691

176. Suo Z, Avci R, Higby Schweitzer MH, Deliorman M (2007) Porphyrin as an ideal biomarker in the search for extraterrestrial life. Astrobiology 7:605
177. Montforts F-P, Glasenapp-Breiling M (2002) Naturally occurring cyclic tetrapyrroles. Prog Chem Org Nat Prod 84:1
178. Bonnett R, Burke PJ, Czechowski F, Reszka A (1984) Porphyrins and metalloporphyrins in coal. Org Geochem 6:177
179. Ocampo R, Bauder C, Callot HJ, Albrecht P (1992) Porphyrins from Messel oil shale (Eocene, Germany): structure elucidation, geochemical and biological significance, and distribution as a function of depth. Geochim Cosmochim Acta 56:745
180. Bonnettt R, Burke PJ, Reszka A (1983) Iron porphyrins in coal. J Chem Soc Chem Commun:1085
181. Bonnett R, Burke PJ, Czechowski F (1987) Metalloporphyrins in lignite, coal, and calcite. In: Filby RH, Branthaver JF (eds) Metal complexes in fossil fuels. ACS Symp Ser 344:173
182. Bauder C, Ocampo R, Callot HJ, Albrecht P (1990) Structural evidence for heme fossils in Messel oil shale (FRG). Naturwissenschaften 77:378
183. Fookes CJR (1985) The etioporphyrins of oil shale: structural evidence for their derivation from chlorophyll. J Chem Soc Chem Commun:706
184. Quirke JME, Eglinton G, Maxwell JR (1979) Petroporphyrins. 1. Preliminary characterization of the porphyrins of gilsonite. J Am Chem Soc 101:7693
185. Mineralienatlas: https://www.mineralienatlas.de/lexikon/index.php/MineralData?mineral=Gilsonit
186. Huseby B, Ocampo R, Bauder C, Callot HJ, Rist K, Barth T (1996) Study of the porphyrins released from the Messel oil shale kerogen by hydrous pyrolysis experiments. Org Geochem 24:691
187. Greenwalt DE, Goreva YS, Siljeström SM, Rose T, Harbach RE (2013) Hemoglobin-derived porphyrins preserved in a Middle Eocene blood-engorged mosquito. Proc Natl Acad Sci USA 110:18496
188. Soma Y, Tanaka A, Soma M, Kawai T (1996) Photosynthetic pigments and perylene in the sediments of southern basin of Lake Baikal. Org Geochem 24:553
189. Niklas KJ, Giannasi DE (1977) Flavonoids and other chemical constituents of fossil Miocene *Zelkova* (Ulmaceae). Science 196:877
190. Giannasi DE, Niklas KJ (1977) Flavonoid and other chemical constituents of fossil Miocene *Celtis* and *Ulmus* (Succor Creek Flora). Science 197:765
191. Dilcher DL, Pavlick RJ, Mitchell J (1970) Chlorophyll derivatives in Middle Eocene sediments. Science 168:1447
192. Keely BJ, Brereton RG, Maxwell JR (1988) Occurrence and significance of pyrochlorins in a lake sediment. Org Geochem 13:801
193. Prowse WG, Keely BJ, Maxwell JR (1990) A novel sedimentary metallochlorin. Org Geochem 16:1059
194. Storm CB, Krane J, Skjetne T, Telnaes N, Branthaver JF, Baker EW (1984) The structure of abelsonite. Science 223:1075
195. Mineralienatlas: https://www.mineralienatlas.de/lexikon/index.php/MineralData?mineral=Abelsonit
196. Ocampo R, Sachs JP, Repeta DJ (1999) Isolation and structure determination of the unstable $13^2,17^3$-cyclopheophorbide *a* enol from recent sediments. Geochim Cosmochim Acta 63:3743
197. Karuso P, Bergquist PR, Buckleton JS, Cambie RC, Clark GR, Rickard CEF (1986) $13^2,17^3$-Cyclopheophorbide enol, the first porphyrin isolated from a sponge. Tetrahedron Lett 27:2177
198. Sakata K, Amamoto K, Ishikawa H, Yagi A, Etoh H, Ina K (1990) Chlorophyllone-a, a new pheophorbide-a related compound isolated from *Ruditapes philippinarum* as an antioxidative compound. Tetrahedron Lett 31:1165
199. Falk H, Hoornaert G, Isenring HP, Eschenmoser A (1975) Über Enolderivate der Chlorophyllreihe. Darstellung von $13^2,17^3$-Cyclopheophorbid-enolen. Helv Chim Acta 58:2347

200. Chicarelli MI, Wolff GA, Murray M, Maxwell JR (1984) Porphyrins with a novel exocyclic ring system in an oil shale. Tetrahedron 40:4033
201. Igic B, Greenwood D, Palmer D, Cassey P, Gill B, Grim T, Brennan PR, Bassett S, Battley P, Hauber M (2010) Detecting pigments from colourful eggshells of extinct birds. Chemoecology 20:43
202. Wiemann J, Yang T, Sander PNN, Schneider M, Engeser M, Kath-Schorr S, Müller CE, Sander PM (2015) The blue-green eggs of dinosaurs: how fossil metabolites provide insights into the evolution of bird reproduction. PeerJ PrePrints 3:e1323. doi:10.7287/peerj.preprints.1080v1
203. Tichy G (1980) Colour retention in Triassic gastropods. Verh Geol BA 1980:175
204. Falk H (1989) The chemistry of linear oligopyrroles and bile pigments. Springer, Vienna
205. Lightner DA (2013) Bilirubin: Jekyll and Hyde pigment of life. Prog Chem Org Nat Prod 98:1
206. Kräutler B (2008) Chlorophyll catabolites. Prog Chem Org Nat Prod 89:1
207. Kräutler B (2016) Breakdown of chlorophyll in higher plants—phyllobilins as abundant, yet hardly visible signs of ripening, senescence, and cell death. Angew Chem Int Ed 55:4882
208. Troxler RF, Smith KM, Brown SB (1980) Mechanism of the photo-oxidation of bacteriochlorophyll-c derivatives. Tetrahedron Lett 21:491
209. Grice K, Gibbison R, Atkinson JE, Schwark L, Eckardt CB, Maxwell JR (1996) Maleimides (1*H*-pyrrole-2,5-diones) as molecular indicators of anoxygenic photosynthesis in ancient water columns. Geochim Cosmochim Acta 60:3913
210. Grice K, Schaeffer P, Schwark L, Maxwell JR (1997) Changes in palaeoenvironmental conditions during deposition of the Permian Kupferschiefer (lower Rhine Basin, northwest Germany) inferred from molecular and isotopic compositions of biomarker components. Org Geochem 26:677
211. Sinninghe Damsté JS, Kock-van Dalen ACK, de Leeuw JW, Schenck PA, Guoying S, Brassell SC (1987) The identification of mono-, di- and trimethyl 2-methyl-(4,8,12-trimethyltridecyl)chromans and their occurrence in the geosphere. Geochim Cosmochim Acta 51:2393
212. Schwark L, Vliex M, Schaeffer P (1998) Geochemical characterization of Malm Zeta laminated carbonates from the Franconian Alb, SW-Germany. Org Geochem 29:1921
213. Li M, Larter SR, Taylor P, Jones DM, Bowler B, Bjorøy M (1995) Comments on "Biomarkers or not biomarkers? A new hypothesis for the origin of pristane involving derivation from methyltrimethyltridecylchromans (MTTCs) formed during diagenesis form chlorophyll and alkylphenols. Org Geochem 23:159
214. Sinninghe Damsté JS, de Leeuw JW (1996) Comments on "Biomarkers or not biomarkers. A new hypothesis for the origin of pristane involving derivation from methyl-trimethyltridecylchromans (MTTCs) formed during diagenesis from chlorophyll and alkylphenols" from M Li, S. R. Larter, P. Taylor P, D. M. Jones, B Bowler, M Bjorøy. Org Geochem 23:1085
215. Oldenburg TBP, Wilkes H, Horsfield B, van Duin ACT, Stoddart D, Wilhelms A (2002) Xanthones – novel aromatic oxygen-containing compounds in crude oils. Org Geochem 33:595
216. Russell M, Grimalt JO, Hartgers WA, Taberner C, Rouchy JM (1997) Bacterial and algal markers in sedimentary organic matter deposited under natural sulphurization conditions (Lorca Basin, Murcia, Spain). Org Geochem 26:605
217. Sinninghe Damsté JS, Rijpstra WIC, de Leeuw JW, Schenck PA (1989) The occurrence and identification of organic sulphur compounds in oils and sediment extracts: II. Their presence in samples from hypersaline and non-hypersaline palaeoenvironments and possible application as source, palaeoenvironmental and maturity indicators. Geochim Cosmochim Acta 53:1323
218. Grimalt JO, Grifoll M, Solanas AM, Albaigés J (1991) Microbial degradation of marine evaporitic crude oils. Geochim Cosmochim Acta 55:1903

219. Sinninghe Damsté JS, Kock-van Dalen AC, de Leeuw JW, Schenck PA (1987) The identification of 2,3-dimethyl-5-(2,6,10-trimethylundecyl)thiophene, a novel sulphur containing biological marker. Tetrahedron Lett 28:957
220. Xavier F, De Las HC, Grimalt JO, Lopez JF, Albaigés J, Sinninghe Damsté JS, Schouten S, De Leeuw JW (1997) Free and sulphurized hopanoids and highly branched isoprenoids in immature lacustrine oil shales. Org Geochem 27:41
221. Valisolalao J, Perakis N, Chappe B, Albrecht P (1984) A novel sulfur containing C_{35} hopanoid in sediments. Tetrahedron Lett 25:1183
222. Wei S (2005) Process and production system for thiophene manufacturing from butadiene and sulfur. Chinese Patent CN 1420116
223. Rosa M (1991) Archaebacteria: lipids, membrane structures, and adaption to environmental stresses. In: di Prisco G (ed) Life under extreme conditions. Springer, Heidelberg, p 61
224. de Rosa M, de Rosa S, Gambacorta A (1977) Lipid structures in the *Caldariella* group of extreme thermoacidophile bacteria. J Chem Soc Chem Commun:514
225. Schouten S, Hopmans EC, Pancost RD, Sinninghe Damsté JS (2000) Widespread occurrence of structurally diverse tetraether membrane lipids: evidence for the ubiquitous presence of low-temperature relatives of hyperthermophiles. Proc Natl Acad Sci USA 97:14421
226. Hopmans EC, Schouten S, Pancost RD, van der Meer MTJ, Sinninghe Damsté JS (2000) Analysis of intact tetraether lipids in archaeal cell material and sediments by high performance liquid chromatography/atmospheric pressure chemical ionization mass spectrometry. Rapid Commun Mass Spectrom 14:585
227. Hoefs MJL, Schouten S, de Leeuw JW, King LL, Wakeham SG, Sinninghe Damsté JS (1997) Ether lipids of planktonic Archaea in the marine water column. Appl Environ Microbiol 63:3090
228. Pancost RD, Hopmans EC, Sinninghe Damsté JS, MEDINAUT Shipboard Scientific Party (2001) Archaean lipids in Mediterranean cold seeps: molecular proxies for anaerobic methane oxidation. Geochim Cosmochim Acta 65:1611
229. Pauly GG, van Vleet ES (1986) Archaebacterial ether lipids: natural tracers of biogeochemical processes. Org Geochem 10:859
230. Nichols PD, Mancuso CA, White DC (1987) Measurement of methanotroph and methanogen signature phospholipids for use in assessment of biomass and community structure in model systems. Org Geochem 11:451
231. Yang H, Pancost RD, Jia C, Xie S (2016) The response of archaeal tetraether membrane lipids in surface soils to temperature: a potential palaeothermometer in paleosols. Geomicrobiol J 33:98
232. Chappe B, Michaelis W, Albrecht P, Ourisson G (1979) Fossil evidence for a novel series of archaebacterial lipids. Naturwissenschaften 66:522
233. Michaelis W, Albrecht P (1979) Molecular fossils of archaebacteria in kerogen. Naturwissenschaften 66:420
234. Schouten S, Hoefs MJL, Koopmans MP, Bosch H-J, Sinninghe Damsté JS (1998) Structural characterization, occurrence and fate of archeal ether-bound acyclic and cyclic biphytanes and corresponding diols in sediments. Org Geochem 29:1305
235. Sinninghe Damsté JS, Schouten S (1997) Is there evidence for a substantial contribution of prokaryotic biomass to organic carbon in Phanerozoic carbonaceous sediments? Org Geochem 26:517
236. Ajioka T, Yamamoto M, Murase J (2014) Branched and isoprenoid glycerol dialkyl tetraethers in soils and lake/river sediments in Lake Biwa basin and implications for MBT/CBT proxies. Org Geochem 73:70
237. Kuypers MMM, Blokker P, Erbacher J, Kinkel H, Pancost RD, Schouten S, Sinninghe Damsté JS (2001) Massive expansion of marine Archaea during a Mid-Cretaceous oceanic anoxic event. Science 293:9286

238. Ho SL, Mollenhauer G, Fietz S, Martinez-Garcia A, Lamy F, Rueda G, Schipper K, Méheust M, Rosell-Melé SR, Tiedemann R (2014) Appraisal of TEX86 and thermometries in subpolar and polar regions. Geochim Cosmochim Acta 131:213
239. Pancost RD, Bouloubassi I, Aloisi G, Sinninghe Damsté JS, MEDINAUT Shipboard Scientific Party (2001) Three series of non-isoprenoidal dialkyl glycerol diethers in cold-seep carbonate crusts. Org Geochem 32:695
240. Lockheart MJ, van Bergen PF, Evershed RP (2000) Chemotaxonomic classification of fossil leaves from the Miocene Clarkia lake deposit, Idaho, USA based on *n*-alkyl lipid distributions and principal component analyses. Org Geochem 31:1223
241. Huang Y, Li T, Lockheart MJ, Peakman TM, Eglinton G (1994) C_{26} to C_{32} 1,3-Alkanediols, a novel series of biological markers identified in miocene (17-20 Ma) leaf fossils and sediment. Nat Prod Lett 4:15
242. Versteegh GJM, Jansen JHF, de Leeuw JW, Schneider RR (2000) Mid-chain diols and keto-ols in SE Atlantic sediments: a new tool for tracing past surface water masses? Geochim Cosmochim Acta 64:1879
243. Rampen SW, Schouten S, Schefuß E, Sinninghe Damsté JS (2009) Impact of temperature on long chain diol and mid-chain hydroxy methyl alkanoate compositions in *Proboscia* diatoms: results from culture and field studies. Org Geochem 40:1124
244. Nichols PD, Johns RB (1986) The lipid chemistry of sediments from the St. Lawrence estuary. Acyclic unsaturated long chain ketones, diols and ketone alcohols. Org Geochem 9:25
245. de Leeuw JW, Rijpstra C, Schenck PA (1981) The occurrence and identification of C_{30}, C_{31} and C_{32} alkan-1,15-diols and alkan-15-one-1-ols in Unit I and Unit II Black Sea sediments. Geochim Cosmochim Acta 45:2281
246. Versteegh GJM, Bosch H-J, de Leeuw JW (1997) Potential palaeoenvironmental information of C_{24} to C_{36} mid-chain diols, keto-ols and mid-chain hydroxy fatty acids; a critical review. Org Geochem 27:1
247. Rolfes J, Andersson JT (2001) Determination of alkylphenols after derivatization to ferrocenecarboxylic acid esters with gas chromatography-atomic emission detection. Anal Chem 73:3073
248. Larter SR, Bowler BFJ, Li M, Chen M, Brincat D, Bennett B, Noke K, Donohoe P, Simmons D, Kohnen M, Telnaes N, Horstad I (1996) Molecular indicators of secondary oil migration distances. Nature 383:593
249. Taylor P, Bennett B, Jones M, Larter S (2001) The effect of biodegradation and water washing on the occurrence of alkylphenols in crude oils. Org Geochem 32:341
250. Simoneit BRT, Otto A, Wilde V (2003) Novel biomarker triterpenoids of fossil laticifers in Eocene brown coal from Geiseltal, Germany. Org Geochem 34:121
251. Otto A, White JD, Simoneit BRT (2002) Natural product terpenoids in Eocene and Miocene conifer fossils. Science 297:1543
252. Wünsche L, Mendoza YA, Gülaçar (1988) Lipid geochemistry of a post-glacial lacustrine sediment. Org Geochem 13:1131
253. Marlowe IT, Green JC, Neal AC, Brassell SC, Eglinton G, Course PA (1984) Long chain (n-C_{37}–C_{39}) alkenones in the Prymnesiophyceae. Distribution of alkenones and other lipids and their taxonomic significance. Br Phycol J 19:203
254. Rontani J-F, Prahl FG, Volkman JK (2006) Re-examination of the double bond positions in alkenones and derivatives: biosynthetic implications. J Phycol 42:800
255. de Leeuw JW, van der Meer FW, Rijpstra WIC, Schenck PA (1980) On the occurrence and structural identification of long chain unsaturated ketones and hydrocarbons in sediments. Phys Chem Earth 12:211
256. Brassell SC, Dumitrescu M, ODP Leg 198 Shipboard Scientific Party (2004) Recognition of alkenones in a Lower Aptian porcellanite from the west-central Pacific. Org Geochem 35:181
257. Ono M, Sawada K, Kubota M, Shiraiwa Y (2009) Change of the unsaturation degree of alkenone and alkenoate during acclimation to salinity change in *Emiliana huxleyi* and *Gephyrocapsa oceanica* with reference to palaeosalinity indicator. Res Org Geochem 25:53

258. Prahl FG, Wakeham SG (1987) Calibration of unsaturation patterns in long-chain ketone compositions for palaeotemperature assessment. Nature 330:367
259. Müller PJ, Kirst G, Ruhland G, von Storch I, Rosell-Melé A (1998) Calibration of the alkenone palaeotemperature index based on core-tops from the eastern South Atlantic and the global ocean (60°N–60°S). Geochim Cosmochim Acta 62:1757
260. Herbert TD (2006) Alkenones as palaeotemperature indicators. In: Elderfield H (ed) The oceans and marine geochemistry, volume 6, Holland HD, Turekian KK (eds) Treatise on geochemistry. Elsevier, Amsterdam, p 391
261. Epstein BL, D'Hondt S, Hargraves PE (2001) The possible metabolic role of C_{37} alkenones in *Emiliana huxleyi*. Org Geochem 32:867
262. Rieseberg LH, Soltis DE (1987) Flavonoids of fossil Miocene *Platanus* and its extant relatives. Biochem Syst Ecol 15:109
263. Giannasi DE, Niklas KJ (1981) Comparative paleobiochemistry of some fossil and extant Fagaceae. Am J Bot 68:762
264. Niklas KJ, Giannasi DE, Baghai NL (1985) Paleobiochemistry of North American fossil *Liriodendron* sp. Biochem Syst Ecol 13:1
265. Zhao Y-X, Li C-S, Luo X-D, Wang Y-F, Zhou J (2006) Palaeophytochemical constituents of Cretaceous *Ginkgo coriacea* Florin leaves. J Integr Plant Biol 48:983
266. Oftedahl I (1929) Minerals from the burning coal seam at Mt. Pyramide, Spitsbergen. In: Hoel A (ed) Det norske Videnskaps–Akademi i Oslo, Resultater av de norske statunderstøttede Spitsbergenekspeditioner (Skrifter om Svalbard og Ishavet) 1:9
267. http://www.mindat.org/min-1915.html
268. Záček V, Oplustil S, Mayova A, Meyer FR (1995) Die Mineralien von Kladno in Mittelböhmen, Tschechische Republik. Min Welt 6:13
269. Jirásek J (2001) Thermal changes of the rocks in the dump pile of the Kateňna Colliery in Radvanice (Eastern Bohemi) Ostrava VSB Technical University of Ostrava. Inst Geol Eng 541:69
270. Thalheim K, Reichel W, Witzke T (1991) Die Minerale des Döhlener Beckens. Schriften des Museums für Mineralogie und Geologie zu Dresden, Nr 3
271. Treibs A, Steinmetz H (1933) Über das Vorkommen von Anthrachinon-Farbstoffen im Mineralreich (Graebeït). Ann Chem 506:171
272. Kolbeck F (1934) Ueber das Vorkommen von Anthrachinon-Farbstoffen bei der Gewerkschaft "Gottes Segen" in Oelsnitz (Erzg.). Jb Berg u Hüttenw in Sachsen 108:15
273. Hoffmann-Ostenhof O (1950) Vorkommen und biochemisches Verhalten der Chinone. Prog Chem Org Nat Prod 6:154
274. Otto A, Simoneit BRT, Rember WC (2003) Resin compounds from the seed cones of three fossil conifer species from the Miocene Clarkia flora, Emerald Creek, Idaho, USA, and from related extant species. Rev Palaeobot Palyn 126:225
275. Blumer M (1951) Fossile Kohlenwasserstoffe und Farbstoffe in Kalksteinen (Geochemische Untersuchungen III.). Mikrochemie 36:1048
276. Blumer M (1960) Pigments of a fossil echinoderm. Nature 188:1100
277. Blumer M (1962) The organic chemistry of a fossil – I. The structure of the fringelite-pigments. Geochim Cosmochim Acta 26:225
278. Blumer M (1965) Organic pigments: their long-term fate. Science 149:722
279. Parkinson J (1808) Organic remains of a former world, vol 2. Sherwood, Neely & Jones, London
280. Bather FA (1893) The Crinoidea of Gotland. Part I. The Crinoidea Inadunata. PA Nostedt & Söner, Stockholm
281. Jaekel O (1894) Platte mit *Encrinus carnalli*. Sitz Ber Ges Naturforsch Fr Berlin 155
282. Biese W (1927) Über die Encriniten des unteren Muschelkalkes von Mitteldeutschland. Abh Preuß Geol Landesanst, N F 103:1
283. Falk H, Mayr E, Richter AE (1994) Simple diffuse reflectance UV-vis spectroscopic determination of organic pigments (fringelites) in fossils. Microchim Acta 117:1

284. Falk H, Mayr E (1995) Synthesis and properties of fringelite D (1,3,4,6,8,10,13-octahydroxy-phenanthro[1,10,9,8, *opqra*]perylene-7,14-dione). Monatsh Chem 125:699
285. Wolkenstein K, Gross JH, Falk H, Schöler HF (2006) Preservation of hypericin and related polycyclic quinone pigments in fossil crinoids. Proc R Soc B 273:451
286. Wolkenstein K, Głuchowski E, Gross JH, Marynowski L (2008) Hypericinoid pigments in Millericrinids from the Kimmeridgian of the Holy Cross mountains (Poland). Palaios 23:773
287. Blumer M (1962) The organic chemistry of a fossil – II. Some rare polynuclear hydrocarbons. Geochim Cosmochim Acta 26:228
288. Thomas DW, Blumer M (1964) The organic chemistry of a fossil – III. The hydrocarbons and their geochemistry. Geochim Cosmochim Acta 28:1467
289. Wolkenstein K (2015) Persistent and widespread occurrence of bioactive quinone pigments during post-Paleozoic crinoid diversification. Proc Natl Acad Sci USA 112:2794
290. Falk H (1999) From the photosensitizer hypericin to the photoreceptor stentorin – the chemistry of phenanthroperylene quinones. Angew Chem Int Ed 38:3116
291. Leonhartsberger JG, Falk H (2002) The protonation and deprotonation equilibria of hypericin revisited. Monatsh Chem 133:167
292. Etzlstorfer C, Falk H, Müller N, Schmitzberger W, Wagner UG (1993) Tautomerism and stereochemistry of hypericin: force field, NMR, and X-ray crystallographic investigations. Monatsh Chem 124:751
293. Bais HP, Vepachedu R, Lawrence CB, Stermitz FR, Vivanco JM (2003) Molecular and biochemical characterization of an enzyme responsible for the formation of hypericin in St. John's wort (*Hypericum perforatum* L.). J Biol Chem 278:32413
294. Falk H, Schoppel G (1992) On the synthesis of hypericin by oxidative trimethylemodin anthrone and emodin anthrone dimerization: isohypericin. Monatsh Chem 123:931
295. De Riccardis F, Iorizzi M, Minale L, Riccio R, Richer de Forges B, Debitus C (1991) The gymnochromes: novel marine brominated phenanthroperylenequinone pigments from the stalked crinoid *Gymnocrinus richeri*. J Org Chem 56:6781
296. Kemami Wangun HV, Wood A, Fiorilla C, Reed JK, McCarthy PJ, Wright AE (2010) Gymnochromes E and F, cytotoxic phenanthroperylenequinones from a deep-water crinoid *Holopus rangii*. J Nat Prod 73:712
297. O'Malley CE, Ausich WI, Chin Y-P (2013) Isolation and characterization of the earliest taxon-specific organic molecules (Mississippian, Crinoidea). Geology 41:347
298. Wolkenstein K (2014) Isolation and characterization of the earliest taxon-specific organic molecules (Mississippian, Crinoidea). Comment and author reply. Geology 42:e320, e322
299. Gribble GW (2010) Naturally occurring organohalogen compounds – a comprehensive update. Prog Chem Org Nat Prod 91:1
300. Falk H, Mayr E (1997) Concerning *bay* salt and *peri* chelate formation of hydroxyphenanthroperylene quinones (fringelites). Monatsh Chem 128:353
301. Lemoine P (1927) *Solenopora* from the Jurassic of France. Bull Soc Géol Fr 27:405
302. Harland TL, Torrens HS (1982) A redescription of the Bathonian red alga *Solenopora jurassica* from Gloucestershire, with remarks on its preservation. Palaeontology 25:905
303. Wright VP (1985) Seasonal banding in the alga *Solenopora jurassica* from Middle Jurassic of Gloucestershire, England. J Palaeontol 59:721
304. Wolkenstein K, Gross JH, Falk H (2010) Boron-containing organic pigments from a Jurassic red alga. Proc Natl Acad Sci USA 107:19374
305. Wolkenstein K, Sun H, Falk H, Griesinger C (2015) Structure and absolute configuration of Jurassic polyketide-derived spiroborate pigments obtained from microgram quantities. J Am Chem Soc 137:13460
306. Pidot S, Ishida K, Cyrulies M, Hertweck C (2014) Discovery of clostrubin, an exceptional polyphenolic polyketide antibiotic from a strictly anaerobic bacterium. Angew Chem Int Ed 53:7856
307. Taylor TN, Taylor EL, Krings M (2009) Palaeobotany: the biology and evolution of fossil plants, 2nd edn. Academic Press, Amsterdam

308. Rezanka T, Sigler K (2008) Biologically active compounds of semi-metals. Phytochemistry 69:585
309. Scorei R (2012) Is boron a prebiotic element? A mini-review of the essentiality of boron for the appearance of life on earth. Orig Life Evol Biosph 42:3
310. Berthier MP (1825) Examen de las substance rose de Quincy (département du Cher). Ann Mines 10:272
311. http://www.gemmology.ch/quinciite.html
312. Louis M, Guillemin CJ, Goni JC, Ragot JP (1969) Coloration rose-carmin d'une sépiolite Eocéne, la quincyite, par des pigments organiques. Adv Org Geochem:553
313. Brousse A (2012) La quinciite et l'opale associée des calcaires lacustres de la region du Quincy, Berry (Cher). Saga Inf 316:8
314. Treibs A, Wilhelm R, Jacob K (1981) Der Quincyte-Farbstoff. Ann Chem:842
315. Prowse WG, Arnot KI, Recka JA, Thomson RH, Maxwell JR (1991) The quincyte pigments: fossil quinones in an Eocene clay mineral. Tetrahedron 47:1095
316. Means JL, Hubbard N (1987) Short-chain aliphatic acid anions in deep surface brines: a review of their origin, occurrence, properties, and importance and new data on their distribution and geochemical implications in the Palo Duro Basin, Texas. Org Geochem 11:177
317. Barth T, Andresen B, Iden K, Johansen H (1997) Modelling source rock production potentials for short-chain organic acids and CO_2 – a multivariate approach. Org Geochem 25:427
318. Dias RF, Freeman KH, Lewan MD, Franks SG (2002) δ^{13} of low-molecular-weight organic acids generated by the hydrous pyrolysis of oil-prone source rocks. Geochim Cosmochim Acta 66:2755
319. Huang Y, Lockheart MJ, Logan GA, Eglinton G (1996) Isotope and molecular evidence for the diverse origins of carboxylic acids in leaf fossils and sediments from the Miocene Lake Clarkia deposit, Idaho, USA. Org Geochem 24:289
320. Golumbic C, Hofer LJE, Peebles WC, Orchin M (1950) Detection of abietic acid in bituminous coal. J Soc Chem Ind 69:100
321. Seifert WK (1973) Steroid acids in petroleum – animal contribution to the origin of petroleum. Pure Appl Chem 34:633
322. Simoneit BRT, Xu Y, Neto RR, Cloutier JB, Jaffé R (2009) Photochemical alteration of 3-oxygenated triterpenoids: implications for the origin of 3,4-*seco*-triterpenoids in sediments. Chemosphere 74:543
323. Boon JJ, de Lange F, Schuyl PJW, de Leeuw JW, Schenck PA (1977) Organic geochemistry of Walvis Bay diatomaceous ooze. II. Occurrence and significance of the hydroxy acids. Adv Org Geochem 1975:255
324. Skerratt JH, Nichols PD, Bowman JP, Sly LI (1992) Occurrence and significance of long-chain (ω-1)-hydroxy fatty acids in methane-utilizing bacteria. Org Geochem 18:189
325. Kvenvolden KA, Peterson E, Pollock GE (1969) Optical configuration of amino acids in pre-Cambrian fig tree chert. Nature 221:141
326. Kvenvolden KA, Lawless J, Pering K, Peterson E, Flores J, Ponnamperuma C, Kaplan IR, Moore C (1970) Evidence for extraterrestrial amino acids and hydrocarbons in the Murchinson meteorite. Nature 228:923
327. Miller GH, Jull AJT, Linick T, Sutherland D, Sejrup HP, Brigham JK, Bowen DQ, Mangerud J (1987) Racemization-derived late Devensian temperature reduction in Scotland. Nature 326:593
328. Kimber RWL, Griffin CV (1987) Further evidence of the complexity of the racemization process in fossil shells with implication for amino acid racemization dating. Geochim Cosmochim Acta 51:839
329. Yamamoto S, Otto A, Krumbiegel G, Simoneit BRT (2006) The natural product biomarkers in succinite, glessite and stantienite ambers from Bitterfeld, Germany. Rev Palaeobot Palyn 140:27
330. Agricola G (2006) De natura Fossilium. Handbuch der Mineralogie (1546). Marix Verlag, Wiesbaden
331. Buchberger W, Falk H, Katzmayr MU, Richter AE (1997) On the chemistry of Baltic amber inclusion droplets. Monatsh Chem 128:177
332. Kieslich K (1985) Microbial side-chain degradation of sterols. J Basic Microbiol 25:461

333. Szykuła J, Hebda C, Orpiszewski J, Aichholz R, Szynkiewicz A (1990) Studies on the neutral fraction of baltic amber. Prace Muzeum Ziemi 41:15
334. Niklas KJ, Giannasi DE (1978) Angiosperm paleobiochemistry of the Succor Creek Flora (Miocene) Oregon, USA. Am J Bot 65:943
335. Schuler B, Meyer G, Peña D, Mullins OC, Gross L (2015) Unraveling the molecular structures of asphaltenes by atomic force microscopy. J Am Chem Soc 137:9870
336. Cleland TP, Schroeter ER, Zamdborg L, Zheng W, Lee JE, Tran JC, Bern M, Duncan MB, Lebleu VS, Ahlf DR, Thomas PM, Kalluri R, Kelleher NL, Schweitzer MH (2015) Mass spectrometry and antibody-based characterization of blood vessels from *Brachylophosaurus canadensis*. J Proteome Res 14:5252
337. Briggs DEG, Stankiewicz BA, Meischner D, Bierstedt A, Evershed RP (1998) Taphonomy of arthropod cuticles from Pliocene lake sediments, Willershausen, Germany. Palaios 13:386
338. Stankiewicz BA, Briggs DEG, Evershed RP, Flannery MB, Wuttke M (1997) Preservation of chitin in 25-million-year-old fossils. Science 276:1541
339. Carlisle DB (1964) Chitin in a Cambrian fossil, *Hyolithellus*. Biochem J 90:1C
340. Ehrlich H, Rigby JK, Botting, JP, Tsurkan, MV, Werner C, Schwille, P, Petrášek Z, Pisera A, Simon P, Sivkov VN, Vyalikh DV, Molodtsov SL, Kurek D, Kammer M, Hunoldt S, Born R, Stawski D, Steinhof A, Bazhenov VV, Geisler T (2013) Discovery of 505-million-year old chitin in the basal demosponge *Vauxia gracilenta*. Sci Rep 3: Article number: 3497. doi:10.1038/srep03497
341. Tegelaar EW, de Leeuw JW, Derenne S, Largeau C (1989) A reappraisal of kerogen formation. Geochim Cosmochim Acta 53:3103
342. van Krevelen DW (1950) Graphical-statistical method for the study of structure and reaction processes of coal. Fuel 29:269
343. Vávra N (2009) The chemistry of amber – facts, findings and opinions. Ann Naturhist Mus Wien 111A:445
344. Anderson KB, Winans RE, Botto RE (1992) The nature and fate of natural resins in the geosphere – II. Identification, classification and nomenclature of resinites. Org Geochem 18:829
345. Anderson KB (1994) The nature and fate of natural resins in the geosphere – IV. Middle and Upper Cretaceous amber from the Taimyr Peninsula, Siberia – evidence for a new form of polylabdanoid of resinite and revision of the classification of Class I resinites. Org Geochem 21:209
346. Poulin J, Helwig K (2014) Inside amber: the structural role of succinic acid in Class Ia and Class Id resinite. Anal Chem 86:7428
347. Cunningham A, Gay ID, Oehlschlanger AC, Langenheim JH (1983) ^{13}C NMR and IR analyses of the structure, aging and botanical origin of Dominican and Mexican ambers. Phytochemistry 22:965
348. Kosmowska-Ceranowicz B, Vávra N (2015) Infrared spectra of the World's resins – holotype characteristics. Polska Akademia Nauk Muzeum Ziemi w Warszawie, Warszawa
349. Vinther J, Briggs DEG, Prum RO, Saranathan V (2008) The colour of fossil feathers. Biol Lett 4:522
350. Li Q, Gao K-Q, Vinther J, Shawkey MD, Clarke JA, D'Alba L, Meng Q, Briggs DEG, Miao L, Prum RO (2010) Plumage color patterns of an extinct dinosaur. Science 327:1369
351. Glass K, Ito S, Wilby PR, Sota T, Nakamura A, Bowers CR, Vinther J, Dutta S, Summons R, Briggs DEG, Wakamatsu K, Simon JD (2012) Direct chemical evidence for eumelanin pigment from the Jurassic period. Proc Natl Acad Sci USA 109:10218
352. Lindgren J, Sjovall P, Carney RM, Uvdal P, Gren JA, Dyke G, Schultz BP, Shawkey MD, Barnes KR, Polcyn MJ (2014) Skin pigmentation provides evidence of convergent melanism in extinct marine reptiles. Nature 506:484
353. Colleary C, Dolocan A, Gardner J, Singh S, Wuttke M, Rabenstein R, Habersetzer J, Schaal S, Feseha M, Clemens M, Jacobs BF, Currano ED, Jacobs LL, Sylvestersen RL, Gabbott SE, Vinther J (2015) Chemical, experimental, and morphological evidence for

diagenetically altered melanin in exceptionally preserved fossils. Proc Natl Acad Sci USA 112:12592
354. Egli M, Saenger W (1984) Principles of nucleic acid structure. Springer, Heidelberg
355. Mullis KB, Faloona FA (1987) Specific synthesis of DNA in vitro via a polymerase-catalyzed chain reaction. Meth Enzymol 155:335
356. Pääbo S, Poinar H, Serre D, Jaenicke-Després V, Hebler J, Rohland N, Kuch M, Krause J, Vigilant L, Hofreiter M (2004) Genetic analyses from ancient DNA. Annu Rev Genet 38:645
357. Allentoft ME, Collins M, Harker D, Haile J, Oskam CL, Hale ML, Campos PF, Samaniego JA, Gilbert MTP, Willerslev E, Zhang G, Scofield RP, Holdaway RN, Bunce M (2012) The half-life of DNA in bone: measuring decay kinetics in 158 dated fossils. Proc R Soc B 279:4724
358. Hänni C, Laudet V, Coll J, Stehlin D (1994) An unusual mitochondrial DNA sequence variant from an Egyptian mummy. Genomics 22:487
359. Sawyer S, Renaud G, Viola B, Hublin J-J, Gansauge M-T, Shunkov MV, Derevianko AP, Prüfer K, Kelso J, Pääbo S (2015) Nuclear and mitochondrial DNA sequences from two Denisovan individuals. Proc Natl Acad Sci USA 112:15696
360. Meyer M, Arsuaga J-L, de Filippo C, Nagel S, Aximu-Petri A, Nickel B, Martínez I, Gracia A, de Castro JMB, Carbonell E, Viola B, Kelso J, Prüfer K, Pääbo S (2016) Nuclear DNA sequences from the Middle Pleistocene Sima de los Huesos hominins. Nature 531:504
361. Keller A, Graefen A, Ball M, Matzas M, Boisguerin V, Maixner F, Leidinger P, Backes C, Khairat R, Forster M, Stade B, Franke A, Mayer J, Spangler J, McLaughlin S, Shah M, Lee C, Harkins TT, Sartori A, Moreno-Estrada A, Henn B, Sikora M, Semino O, Chiaroni J, Rootsi S, Myres NM, Cabrera VM, Underhill PA, Bustamante CD, Vigl EE, Samadelli M, Cipollini G, Haas J, Katus H, O'Connor BD, Carlson MRJ, Meder B, Blin N, Meese E, Pusch CM, Zink A (2012) New insights into the Tyrolean Iceman's origin and phenotype as inferred by whole-genome sequencing. Nat Commun 3:698
362. Oskam CL, Bunce M (2012) DNA extraction from fossil eggshell. Methods Mol Biol 840:65
363. Palkopoulou E, Mallick S, Skoglund P, Enk J, Rohland N, Li H, Omrak A, Vartanyan S, Poinar H, Götherström A, Reich D, Dalén L (2015) Complete genomes reveal signatures of demographic and genetic declines in the wooly mammoth. Curr Biol 25:1395
364. Budzikiewicz H (2015) Mass spectrometry in natural product structure elucidation. Prog Chem Org Nat Prod 100:77
365. Seifert WK, Moldowan JM, Demaison GJ (1984) Source correlation of biodegraded oils. Org Geochem 6:633
366. Reynolds WF, Mazzola EP (2015) Nuclear magnetic resonance in the structural elucidation of natural products. Prog Chem Org Nat Prod 100:223
367. Marshall AO, Wehrbein RL, Lieberman BS, Marshall CP (2012) Raman spectroscopic investigations of Burgess shale-type preservation: a new way forward. Palaios 27:288
368. Marshak S (2015) Essentials of geology, 5th edn. WW Norton, New York
369. Horsfield B, Rullkötter J (1994) Diagenesis, catagenesis, and metagenesis of organic matter. In: Magoon L, Dow WG (eds) The petroleum system—from source to trap. Am Assoc Petrol Geol Spec M60:189
370. Dahl JEP, Moldowan JM, Peters KE, Claypool GE, Rooney MA, Michael GE, Mello MR, Kohnen ML (1999) Diamondoid hydrocarbons as indicators of natural oil cracking. Nature 399:54
371. Dahl JEP, Moldowan JM, Peakman TM, Clardy JC, Lobkovsky E, Olmstead MM, May PW, Davis TJ, Steeds JW, Peters KE, Pepper A, Ekuan A, Carlson RMK (2003) Isolation and structural proof of the large diamond molecule, cyclohexamantane ($C_{26}H_{30}$). Angew Chem Int Ed 42:2040
372. Melezhik VA, Filippov MM, Romashkin AE (2004) A giant palaeoproterozoic deposit of shungite in NW Russia: genesis and practical applications. Ore Geol Rev 24:135
373. Buseck PR (2002) Geological fullerenes: review and analysis. Earth Planet Sci Lett 203:781

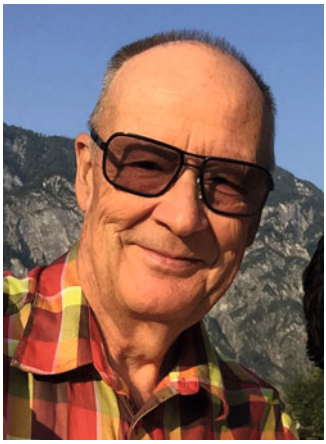

Heinz Falk has been Professor Emeritus at the Institute of Organic Chemistry of the Johannes Kepler University, Linz, Austria since 2007. He studied chemistry at the University of Vienna starting in 1959 and completed his dissertation in organometallic chemistry in 1966. In 1971, he spent a postdoctoral year at ETH Zürich in the laboratory of Albert Eschenmoser. Upon his return to Vienna in 1972 he attained the Habilitation in Organic Chemistry at the University of Vienna. Starting in 1966 he served as an assistant at the Institute of Organic Chemistry at the University of Vienna before being promoted to Associate Professor of Physical Organic Chemistry in 1975. In 1979, he became Full Professor of Organic Chemistry at the Johannes Kepler University of Linz, where he founded the Institute of Organic Chemistry, serving in this chair position for 28 years. From 1989 through 1991, he was Dean of the Faculty of Engineering and Natural Sciences.

Falk's main research area is the structural analysis, synthesis, stereochemistry, and photochemistry of plant and animal photosensitizing and photosensory pigments. Besides fundamental studies of the chemistry of bile pigments, the main group of compounds covered in his work are pigments derived from the fundamental phenanthro[1,10,9,8-*opqra*]perylene-7,14-dione chromophore inclusive of natural pigments like hypericin. Furthermore, he has pursued research on applied problems of industrial relevance, including oxidation, ozonization, non-natural amino acids, and catalysis. During the course of his career, he has supervised nearly one hundred doctoral students and several postdoctoral students. He has published two books: (1978) Ausgewählte Übungsbeispiele. Zur Nomenklatur Organischer Verbindungen. Springer-Verlag, Wien New York; ISBN 3211814795, and (1989) The Chemistry of Linear Oligopyrroles and Bile Pigments. Springer-Verlag, Wien New York; ISBN 3211821120. He has published about 300 papers and has several patents.

Dr. Falk has served as Editor-in-Chief of Monatshefte für Chemie/Chemical Monthly for a decade and as series Editor of Progress in the Chemistry of Organic Natural Products since 1998. He is, in addition to his memberships in the American, Austrian, and German Chemical Societies and the New York Academy of Sciences, an elected member of the Austrian Academy of Sciences and the European Academy of Sciences.

Klaus Wolkenstein is a postdoctoral researcher at the Max Planck Institute for Biophysical Chemistry in Göttingen. He studied geology/paleontology at the University of Heidelberg and completed his dissertation on phenanthroperylene quinone pigments in fossil crinoids in 2005. After a postdoctoral stay (2007–2010) at the Johannes Kepler University Linz in the laboratory of Wolfgang Buchberger, he worked at the State Museum of Natural History Stuttgart followed by a postdoctoral stay (2012–2015) at the Geoscience Centre of the University of Göttingen.

Dr. Wolkenstein's main research area is the structural analysis of natural products of both fossil and extant organisms. Current research focuses on the occurrence of polyphenolic pigments in the fossil record. His scientific achievements include the discoveries of the proisocrinins and the borolithochromes. In 2006, he received the Tilly Edinger award of the German Paleontological Society.

Phthalides: Distribution in Nature, Chemical Reactivity, Synthesis, and Biological Activity

Alejandra León, Mayela Del-Ángel, José Luis Ávila, and Guillermo Delgado

Contents

A. León • M. Del-Ángel • J.L. Ávila • G. Delgado (✉)
Department of Natural Products, Institute of Chemistry, Universidad Nacional Autónoma de México, Circuito Exterior, Ciudad Universitaria, Coyoacán, 04510 Mexico City, Mexico
e-mail: aleleon@unam.mx; mayela.delangelm@comunidad.unam.mx; jluisga_89@comunidad.unam.mx; delgado@unam.mx

A.D. Kinghorn, H. Falk, S. Gibbons, J. Kobayashi (eds.), *Progress in the Chemistry of Organic Natural Products, Vol. 104*, DOI 10.1007/978-3-319-45618-8_2

1 Introduction

Phthalides are a relatively small group of natural compounds found in several higher and lower plant and fungal genera. Classifiable by structure, the monomeric and dimeric phthalides are known principally as the bioactive constituents in several plants used in traditional medicine in Asia, Europe, and North America. Phthalides are also isolated from several species of fungi.

Although the ancient historical record is fragmentary, there is evidence of the exchange of medicinal herbs between Asia and Europe along the Silk Road trading

routes established by Alexander the Great (356–326 BC), and several old Chinese texts mention medicinal plants that contain phthalides that were included in these routes. In northern Mexico and the southern United States, the medicinal use of the phthalide-containing rootstock of *Ligusticum porteri* has been recorded since the eighteenth century. Relatively few reviews have addressed the phthalides [1–3]. This contribution aims to provide a broad treatment of the topic, with an overview of phthalide chemical structures, natural sources, research methodologies, selected chemical syntheses and reactions, and the main reported bioactivities of phthalides.

1.1 Traditional Uses of Plants that Contain Phthalides

Compiled in ca. 200 AD from ancient oral traditions (ca. 2800 BC), the "Shen Nong Bencaojing" is one of the oldest Chinese texts on agriculture and plants used traditionally to include a description of the use of "Danggui" (*Angelica sinensis* (Oliv.) Diels roots, family Umbelliferae, a plant that contains phthalides) "for enriching the blood" [4]. This plant is included in the Pharmacopoeia of the People's Republic of China, together with other two phthalide-containing plants, *Ligusticum sinense* Oliv. ("Rhizoma Ligustici", "Chinese Lovage", "Gaoben", used to relieve pain) and *Ligusticum chuanxiong* S.H. Qiu, Y.Q. Zeng, K.Y. Pan, Y.C. Tang & J.M. Xu ("Rhizoma Chuanxiong" or "Szechwan Lovage Rhizome", used to promote the flow of blood) [5]. The traditional uses, as well as the chemical constituents and bioactivities of the latter species have been reviewed [6, 7], including bioactivities with other plants [8].

A tea prepared with the rootstock of the North American phthalide-containing species, *Ligusticum porteri* J.M. Coult. & Rose, is commonly used to alleviate stomachache and colic [9], ulcers and diarrhea as well as to treat diabetes and circulatory problems [10, 11]. Infusions of this plant also play a role in the ritual-curing ceremonies in northern Mexico and the southern United States, for which this medicinal plant is highly regarded, mainly by the native Raramuri ethnic group [12]. Some illustrations of this plant material in different stages are shown in Fig. 1.

Not confined in the human sphere of activity, Kodiak bears have been reported to chew the roots of this plant, and to rub the root-saliva mixture into their fur [13].

1.2 Early Chemical Studies (1897–1977) of Phthalides in the Family Umbelliferae

Several of the first reports on the chemistry of phthalides appeared at the end of the nineteenth century, where they were identified as the odor constituents of celery (*Apium graveolens* L.) by the Italian researchers Ciamician and Silber in 1897. The provision of essential oil from celery seed (by the Schimmel Company, Leipzig, Germany) allowed Ciamician and Silber (working in Bologna, Italy) to isolate what

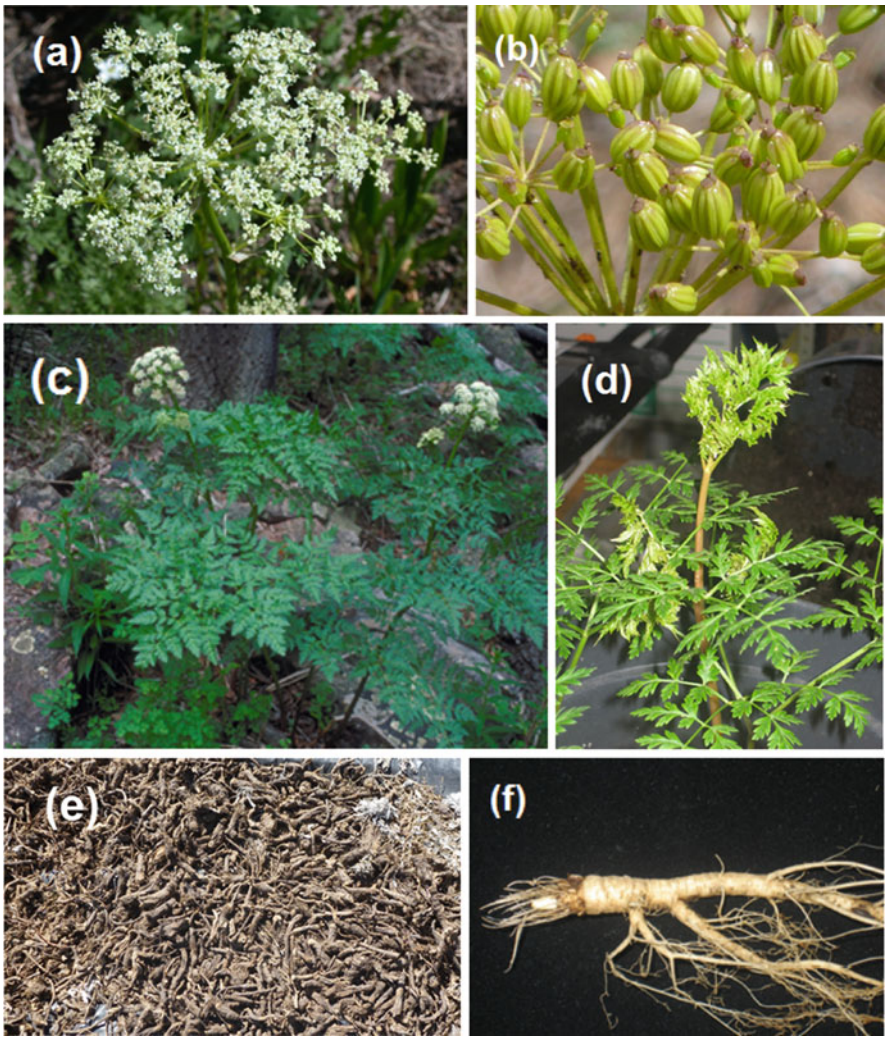

Fig. 1 *Ligusticum porteri* J. M. Coult. & Rose (Umbelliferae). (**a**) Flowers of *L. porteri*, photo: M. E. Harte, Bugwood.org; (**b**) Immature flowers of *L. porteri*, photo: R. Bye and E. Linares, Instituto de Biología, Universidad Nacional Autónoma de México; (**c**) Wild plant, *L. porteri* (Colorado, USA), photo: D. Powell, USDA Forest Service, Bugwood.org; (**d**) Cultivated plant, *L. porteri* (Mexico City), photo: G. Delgado; (**e**) Rootstocks of mature plants of *L. porteri*, photo: R. Bye and E. Linares, Instituto de Biología, Universidad Nacional Autónoma de México; (**f**) Young rootstock of cultivated *L. porteri*, photo: G. Delgado

they called sedanolide and sedanonic anhydride [14]; "sedane" is the Italian translation of celery. These substances could be structurally characterized as a result of their transformation to sedanonic acid [15], for which structure **1** was proposed and later, following the analyses of derivatives [16] and intermediates [16, 17], proven to be correct. The published account on these experiments [18] was, according to Barton, "one of the early classics of natural products chemistry"

[19]. A decade later, in 1910, Swenholt obtained the volatile fraction from celery seeds provided by the John A. Salzer Seed Company (La Crosse, Wisconsin, USA). This fraction was saponified and from the organic residue sedanonic acid (**1**) was characterized [20]. Fourteen years later, Berlingozzi established that the odorant properties of celery correlated with the nature of the side chain of phthalides [21–25], a finding subsequently confirmed by other authors [26, 27].

In 1921, Murayama, when leading a chemical investigation of the highly regarded Japanese drug "Sen-Kyu", isolated "cnidium lactone", a compound that had been named previously by Sakai in 1916. This compound was also obtained from the roots of *Cnidium officinale* Makino, which has a long history in traditional Asian medicine, and is named "Hsiung-Ch'uang" in mainland China [28]. Following re-isolation from a second population of the same species [26], it was concluded that "cnidium lactone" was similar in structure to sedanolide, isolated by Ciamician and Silber. However, the instability and the practical difficulties of isolating phthalides hampered any further characterization or identification of these substances.

In 1934, Noguchi reisolated "cnidium lactone" and noting its close structural relationship with sedanolide, proposed that stereoisomeric characteristics may underlie any structural differences [27].

From the saponified extract of the fruits of another species in the Umbelliferae, *Ligusticum acutilobum* Siebold & Zucc., Kariyone and Kotani [29], isolated an acid, which could be transformed to a lactone; and these two compounds were later characterized as valerophenone *o*-benzoic acid (**2**) and (*Z*)-butylidenephthalide (**3**) [30, 31]. Although the structures of sedanolide and "cnidium lactone" remained unclear [32], a study of the essential oil of lovage by Naves [33], resulted in the characterization of (*Z*)-butylidenephthalide (**3**), butylphthalide (**4**) and what Ciamician and Silber had named sedanonic anhydride (sedanonic acid lactone), which was found to be (*Z*)-6,7-dihydro-ligustilide (**5**). Compound **2** was obtained as a saponification product of the essential oil of the crude drug named "Toki" (*Angelica acutiloba* (Siebold & Zucc.) Kitag.) [34].

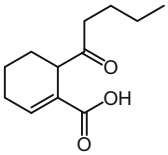

1 (sedanonic acid)

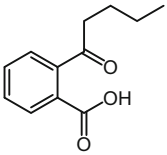

2 (valerophenone *o*-benzoic acid)

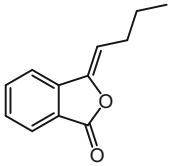

3 ((*Z*)-butylidenephthalide)

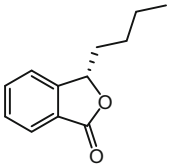

4 ((*S*)-3-butylphthalide)

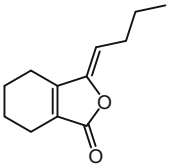

5 ((*Z*)-6,7-dihydroligustilide, sedanonic anhydride)

Barton and de Vries [19] then determined the chemical formulas of sedanolide **6** (by $NaBH_4$-mediated reduction of sedanonic acid (**1**)), and cnidium lactone (**7**, cnidilide), although without assigning the configurations of the chiral carbons.

(*Z*)-Ligustilide (**8**) was characterized from the roots of *Ligusticum acutilobum* (common name in Japanese: "Hokkai-Toki") and from *Cnidium officinale* by Mitsuhashi and Nagai [35]. The 6,7-dihydro derivative **5** was found to generate sedanonic acid (**1**) following its saponification. The structures of neocnidilide (**6**) and cnidilide (**7**), determined following extraction from the roots of *C. officinale*, indicated that sedanolide (represented by formula **6**, leaving aside the configurational assignments), actually comprised a mixture of neocnidilide (**6**) and butylphthalide (**4**) [36]. The configurations at C-3, C-3a, and C-7a for cnidilide (cnidium lactone) and at C-3 of isocnidilide (*trans*-sedanolide) were determined as shown in formulas **7** and **9**, respectively, by using chiroptical methods [37, 38]. The synthesis of butyltetra- and hexahydrophthalides was used to establish the identity of neocnidilide and *trans*-sedanenolide with the configurational assignments showed in formula **6**, and also confirmed structures **7** and **9** for cnidilide and isocnidilide, respectively [39].

At the same time, phthalides **3**, **4**, and **8** were characterized from *Meum athamanticum* Jacq. [40] and some experimental improvements for the separation and characterization of phthalides were reported [41].

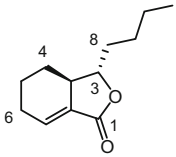

6 (neocninilide, (*trans*)-sedanolide)

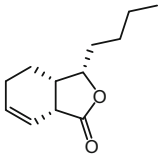

7 (cnidilide, cnidium lactone)

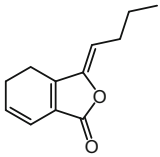

8 ((*Z*)-ligustilide)

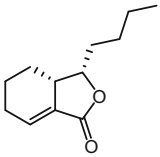

9 (isocnidilide, (*cis*)-sedanolide)

Phthalides **10**–**13** were isolated from celery, indicating that they are responsible for its characteristic odor [42], since these substances were structurally similar to those reported by Berlingozzi and associates more than three decades earlier [21–25]. Butylphthalide (**4**), sedanolide (**6**), 3-*n*-butylhexahydrophthalide (**14**) [43], as well as senkyunolide A (formerly named sedanenolide) (**15**) were also isolated from celery [44].

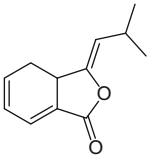

10 ((*Z*)-isobutylidene-3a,4-dihydrophthalide)

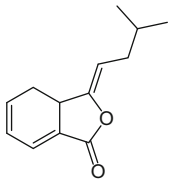

11 ((*Z*)-isovalidene-3a,4-dihydrophthalide)

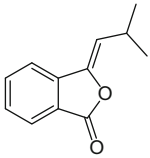

12 ((*Z*)-isobutylidene-phthalide)

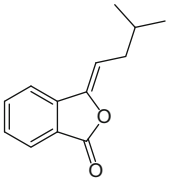

13 ((*Z*)-isovalidene-phthalide)

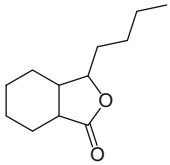

14 (3-butyl-hexahydrophthalide)

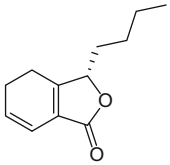

15 (sedanenolide, senkyunolide A)

3-Butylphthalide (**4**) and cnidilide (**7**) were characterized from the essential oil of the Chinese medicinal plant "Gaoben" (*Ligusticum sinense*) [45]. Reinvestigation of *Cnidium officinale* subsequently allowed the characterization of compounds **3**–**5**, **8** and **15** (permitting the (3*S*)-configuration for **15** to be defined), and a mass spectrometric fragmentation pattern for these compounds was proposed [46].

A 1979 review of the phthalides in the family Umbelliferae included their chemotaxonomic aspects, biosynthesis, and stereochemical assignments [47]. It is interesting to note that, at that time, no dimeric phthalides had yet been isolated.

2 Distribution of Phthalides in Nature

2.1 Phthalides in the Umbelliferae (syn. Apiaceae)

A number of studies on phthalides from Umbelliferae family members have been conducted to verify the presence of phthalides, with investigations on the volatile odor constituents of celery (*Apium graveolens*). These studies permitted the characterization of compounds **3**, **4**, **8**, and **10** [48], and **3**, **6**, **8**, and **16** [49]. Additionally, the monomeric phthalides **3**, **4**, **6**, **7**, **8**, and **15** were identified from *Cnidium officinale* [50].

The first dimeric phthalide reported in the literature was angeolide (**17**), which was isolated from *Angelica glauca* Edgew. (a species distributed in the Western Himalayas). The chemical structure of angeolide was confirmed to be a Diels–Alder adduct of (*E*)-ligustilide (**18**), which acts as diene and dienophile. Both (*E*)-**17** and (*Z*)-ligustilide (**8**) were isolated and characterized from this plant species [51]. The direct nomenclature used to name the ligustilide dimers incorporates: (a) the numbers of the connected atoms (describing the adduct derived from the reaction diene + dienophile); (b) the stereochemical descriptors *endo*- and *exo*-, and (c) the name of the monomers. Therefore, angeolide (**17**) could be named as *endo*-[3.3′a,8.6′]-(*E*,*E*′)-diligustilide.

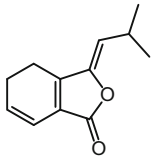

16 ((*Z*)-isobutylidene-4,5-dihydrophthalide)

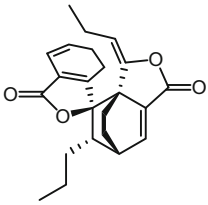

17 (angeolide)

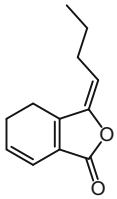

18 ((*E*)-ligustilide)

The monomeric phthalides **4**, **6**, **8**, and **18** were identified from the roots of *Cenolophium denudatum* (Fisch. ex Hornem.) Tutin and *Coriandrum sativum* L. (coriander) [52]; compounds **3**, **8**, **15**, **18**, and **19–21** were found as constituents of the essential oil from the roots of *Levisticum officinale* W.D.J. Koch [53], and from the roots of *Silaum silaus* (L.) Schinz & Thell. and *Anethum sowa* Roxb. ex Fleming, **5**, **6**, **8**, and **15** were characterized [54]. Neocnidilide (**6**), (*Z*)-ligustilide (**8**), and senkyunolide A (**15**) were present in *Anethum graveolens* L. (dill); phthalide **8** was characterized from *Todaroa montana* Webb ex Christ [55] and compounds **3**, **4**, **8**, and **15** were identified from the roots of *Opopanax chironium* Koch.

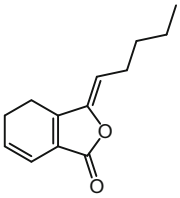

19 ((*Z*)-validene-4,5-dihydrophthalide)

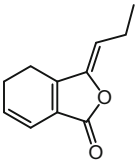

20 ((*Z*)-propylidene-phthalide)

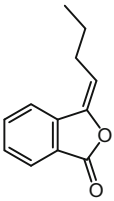

21 ((*E*)-butylidene-phthalide)

From *Ligusticum wallichii* Franch. were isolated a *trans*-diol named (*Z*)-ligustidiol (**22**) [56] (later renamed as senkyunolide I, see below), and the Diels–Alder adduct of (*Z*)-ligustilide, termed (*Z*,*Z*′)-diligustilide (**23**) [57] (later renamed by Höfle as levistolide A, see below). This last compound could be named *endo*-[3a.7′,6.6′]-(*Z*,*Z*′)-diligustilide, following the nomenclature that indicates the connections between the monomers. The [π2s + π2s] dimer, [6.8′,7.3′]-(*Z*,*Z*′)-diligustilide **24**, named riligustilide, was characterized from *Ligusticum acutilobum* [58].

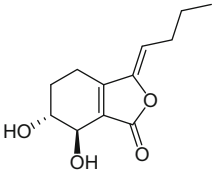

22 (6,7-*trans*-ligustidiol, senkyunolide I)

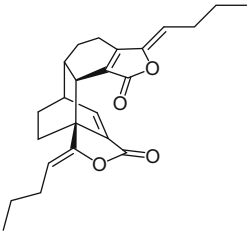

23 ((*Z*,*Z*′)-diligustilide, levistolide A)

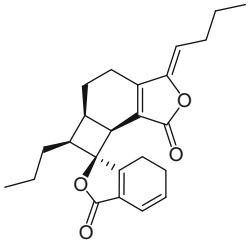

24 (riligustilide)

Compounds **25** ((*Z*)-3-butylidene-7-hydroxy-phthalide, later renamed senkyunolide B), **26** (*cis*-6,7-dihydroxy-ligustilide, later renamed senkyunolide H), and **22** (senkyunolide I) were isolated from *Ligusticum wallichii*, together with a dimer named wallichilide **27** [59]. It is interesting to note that methyl ester **27** could be an artifact derived from the ring opening of diligustilide (levistolide A, **23**) and esterification, given its isolation from a hot water extract, followed by HPLC purification using MeOH–H_2O–HOAc.

A series of hydroxyphthalide derivatives were isolated from the rhizomes of *Cnidium officinale* by Mitsuhashi and associates; these were senkyunolides A (**15**), B (initially **25**, but later corrected to **37**, see below), C (**28**), D (**29**), E (**30**), F (**31**), G (**32**), H (**26**), I (**22**), and J (**33**). With the exception of senkyunolide J, all were optically inactive [60].

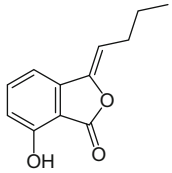

25 (3-butylidene-7-hydroxyphthalide)

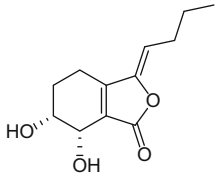

26 (6,7-*cis*-ligustidiol, senkyunolide H)

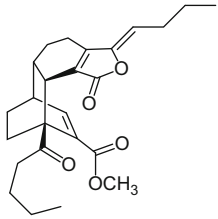

27 (wallichilide)

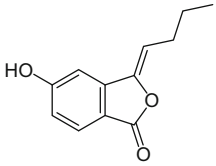

28 (senkyunolide C)

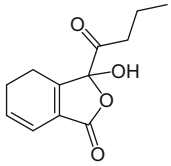

29 (senkyunolide D)

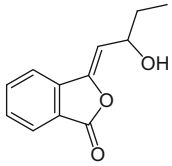

30 (senkyunolide E)

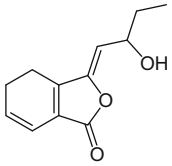

31 (senkyunolide F)

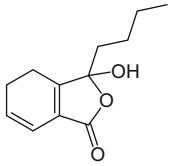

32 (senkyunolide G)

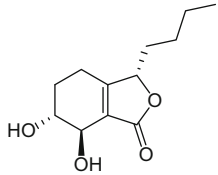

33 (senkyunolide J)

(*Z*)-Ligustilide (**8**) was found in the roots of *Capnophyllum peregrinum* Lange, while compounds **7**, **8**, and **15**, were identified from the roots of *Peucedanum ostruthium* (L.) W.D.J. Koch [61]. (*Z*)-5-Hydroxy-butylidene-phthalide ((**28**) senkyunolide C) and the dihydroxyphthalide **34**, were characterized from the rhizomes of *Ligusticum wallichii* [62].

(*Z*)- and (*E*)-Butylidenephthalides ((**3**) and (**21**)), butylphthalide (**4**), (*Z*)-ligustilide (**8**), senkyunolide A (**15**), angeolide (**17**), (*Z*,*Z*′)-diligustilide ((**23**), renamed by Höfle as levistolide A), and levistolide B (**35**), were all identified from the underground parts of *Levisticum officinale* ("Radix Levici") [63]. This last compound could be also named *endo*-[3a.7′,6.6′]-(*E*,*Z*′)-diligustilide.

The [π2s + π2s]-cyclodimer derived from ligustilide, termed angelicolide (**36**), was found as an additional constituent from *Angelica glauca*, and its structure was confirmed by X-ray analysis as a derivative of (*E*)-ligustilide (**18**) [64].

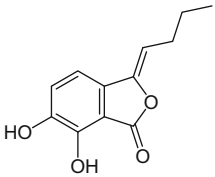

34 ((*Z*)-4,5-dihydroxy-3-butylidenephthalide)

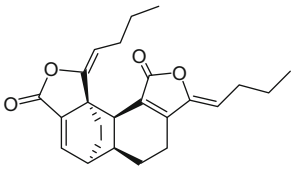

35 (levistolide B)

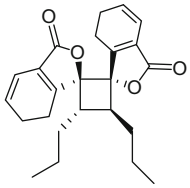

36 (angelicolide, [8,8'.3,3']-(*E*,*E*')-diligustilide)

Three phthalide derivatives, **15**, **22**, and **23**, were isolated from the rhizomes of *Meum athamanticum* [65]. Additional compounds including senkyunolides I (**22**), H (**26**), C (**28**), E (**30**), and F (**31**) were also identified. The structure of senkyunolide B was corrected from 7-hydroxy- (**25**) to 4-hydroxy-butylidenephthalide (**37**) by comparison of spectroscopic properties, which was possible by their occurrence in this natural source [66].

From the roots of *Apium graveolens* were identified phthalides **4**, **6**, **7**, **8**, and **15**, and from *A. graveolens* var. *rapaceum* (Mill.) DC., compounds **3**, **4**, **6**, **8**, **15**, and **18** were characterized. *Petroselinum crispum* (Mill.) Fuss. var. *tuberosum* (Bernh. ex Richb.) Soó (parsley) was used to isolate **8** and **15**, while from *Bifora testiculata* (L.) Roth, compounds **6**, **8**, and **15** were found [67]. A study of Angelicae Radix ("Chinese Tang-kuei") allowed the characterization of (*Z*)-butylidenephthalide (**3**), butylphthalide (**4**), and (*Z*)-ligustilide (**8**) [68].

Diligustilide (levistolide A (**23**)), riligustilide (**24**), (*Z*)-6,7-epoxy-ligustilide (**38**), and an additional dimer, 3,8-dihydro-[6.6′,7.3a′]-(*Z*′)-diligustilide (**39**), were all identified from the rhizomes of *Ligusticum wallichii* [69]. The structure of this last dimer was corrected to structure **40** [70], which was then reisolated from *Ligusticum chuanxiong* and later renamed senkyunolide P [71].

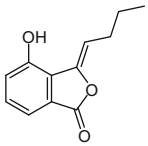

37 (4-hydroxy-butylidenephthalide)

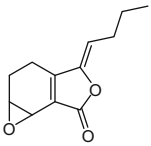

38 ((*Z*)-6,7-epoxy-ligustilide)

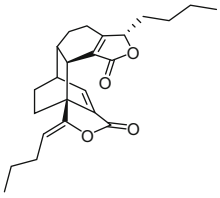

39 ((*Z*')-3,8-dihydro-6.6',7.3'a-diligustilide)

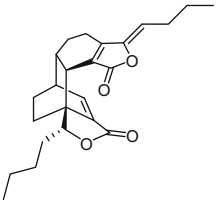

40 (senkyunolide P)

The known senkyunolides I (**22**), H (**26**), E (**30**), F (**31**), as well as levistolide A (**23**), were found as constituents of *Angelica acutiloba*, along with 11-angeloyl-senkyunolide F (**41**), tokinolide A (**42**), and tokinolide B (**43**) [72]. A series of known monomeric phthalides, together with senkyunolides K (**44**), L (**45**), and M (**46**), was characterized from *Ligusticum wallichii* [73]. (*Z*)-Ligustilide (**8**), (*Z*,*Z*′)-diligustilide ((**23**) levistolide A) and riligustilide (**24**) were found as constituents of *Ligusticum porteri* [70], and senkyunolides O (**47**) and P (**40**) were identified from *Ligusticum chuanxiong* [71]. The ^{1}H and ^{13}C NMR spectroscopic data of some monomeric phthalides have been reported in the literature [74].

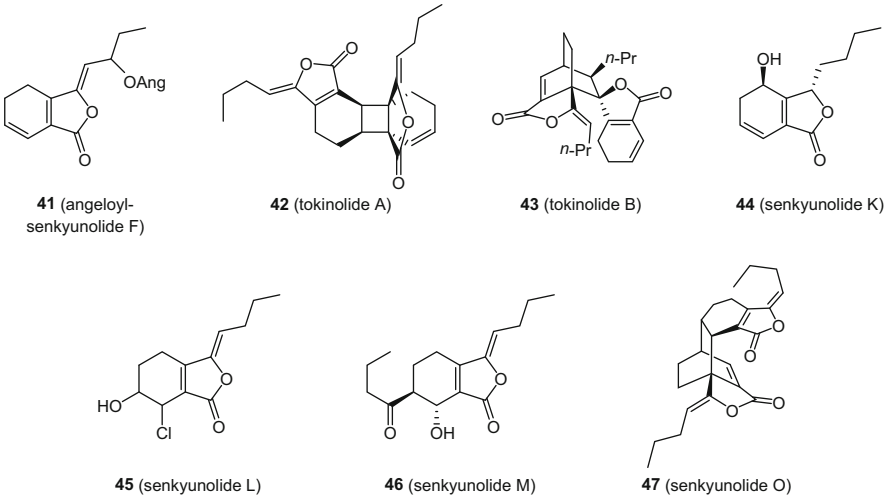

41 (angeloyl-senkyunolide F) **42** (tokinolide A) **43** (tokinolide B) **44** (senkyunolide K)

45 (senkyunolide L) **46** (senkyunolide M) **47** (senkyunolide O)

(*Z*)-Ligustilide (**8**) has been proposed as a benchmarking constituent for preparations of *Ligusticum officinale* [75], and its relative abundance in the essential oil of this species has been studied [76]. Both (*Z*)-butylidenephthalide (**3**), and (*Z*)-ligustilide (**8**) have been found in *Pituranthos tortuosus* (Desf.) Benth. & Hook. f. ex Asch. & Schweinf. [77], and these compounds together with (*E*)-ligustilide and monoterpenes were found as constituents of the rootstock of *Ligusticum porteri* [78].

The volatile aroma constituents of celery and related species have been the subject of several investigations [79, 80], and despite a wide variation in the chemical constituents reported [81, 82], these studies confirmed early observations that monomeric phthalides were responsible for the characteristic aroma of celery. Volatile components isolated from celery plants grown with different fertilizers have also been analyzed [83]. Compound NG-072 (**48**), purported as being useful for the treatment of Alzheimer's disease, was characterized from celery, although without assigning the configuration of the chiral centers [84]. Phthalides **3**, **4**, **6**, **9**, **15**, and **21**, as well as the unstable compound **49**, were characterized from parsley (*Petroselinum crispum*) [85]. The Diels–Alder adduct **50**, derived from (*Z*)-ligustilide (**8**) (diene) and (*E*)-ligustilide (**18**) (dienophile), were isolated from *Angelica sinensis* and named E-232 [86]. An additional series of phthalides was isolated from *Ligusticum chuanxiong*, including (*E*)-senkyunolide E (**51**),

senkyunolide N (**52**), and senkyunolide J (**33**) [44]. The absolute configurations of these last two compounds were established as depicted in their structural formulas [87]. From this source were isolated senkyunolide Q (**53**) and methyl 2-(1-oxo-pentyl)-benzoate (**54**) [88], which is the methyl ester of compound **2** characterized by Noguchi in earlier investigations of *Ligusticum* species [30, 31].

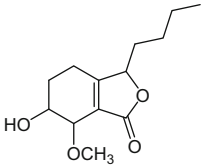

48 (NG-072)

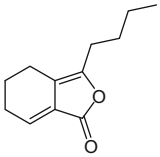

49 (3-butyl-5,6-dihydro-4*H*-isobenzofuran-1-one)

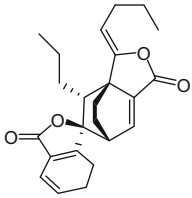

50 (E-232)

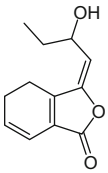

51((*E*)-senkyunolide E)

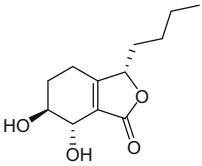

52 (senkyunolide N)

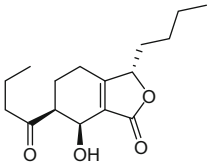

53 (senkyunolide Q)

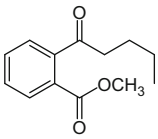

54 (methyl 2-(1-oxo-pentyl)-benzoate)

The preparation of derivatives of the monomeric and dimeric phthalides has been limited to structural studies. The reactivity of (*Z*)-ligustilide (**8**) acting as a biological electrophile, has been explored by Beck and Stermitz [89], and their interesting results obtained are described in Sect. 5.1.4.

(*Z*)-Ligustilide (**8**) was characterized from *Ligusticum mutellina* (L.) Crantz [90] and *Angelica sinensis* [91] and the monomeric phthalides **3**, **8**, **21**, and **22** were found in *Angelica glauca* roots [92]. Both senkyunolide R (**55**) and senkyunolide S (**56**) were characterized as constituents of *Ligusticum chuanxiong* [93].

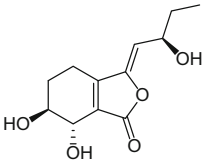

55 (senkyunolide R)

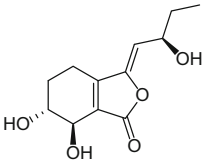

56 (senkyunolide S)

The separation of 3-butylphthalide enantiomers ((*S*)-enantiomer: structure **4**) and their odor thresholds have now been established [94]. Enantioselective analyses of the flavor-imparting compounds (3-butylphthalide derivatives) in celery, celeriac, and fennel have also been investigated [95] with seasonal variations in the composition of volatile components (including phthalides) from different parts of the lovage plant reported [96]; compound **8** was found in the essential oils of

Lomatium torreyi J.M. Coult. & Rose [97], *Meum athamanticum* [98] and *Trachyspermum roxburghianum* H. Wolff [99]. (*Z*)-Ligustilide (**8**) was also found as a constituent of non-polar extracts of the roots from *Ligusticum porteri*, *L. filicinum*, and *L. tenuifolium* [100].

From elicitor-treated parsley cell suspension cultures were isolated four phthalides, namely, 3-butylidene-7-hydroxy-phthalide (**25**), and 3-butylidene-5-hydroxy-phthalide (senkyunolide C (**28**)) and its 7-*O*-*β*-D-glucopyranoside (**57**) and 7-*O*-(6′-malonyl)-*β*-D-glucopyranoside (**58**) derivatives [101]. An analysis of the water-soluble fraction of the methanol extract of celery seed afforded three more phthalide glycosides, named celephthalide A (**59**), celephthalide B (**60**) (with an unresolved configuration at C-3), and celephthalide C (**61**) [102]. As noted in Beck and Chou's review on phthalides [2], the structure of celephthalide C (**61**) was found to be similar to that of neocnidilide (**6**).

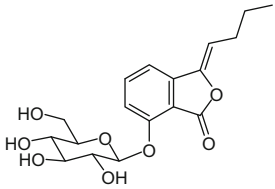

57 (7-hydroxy-butylidenephthalide 7-*O*-*β*-D-glucopyranoside)

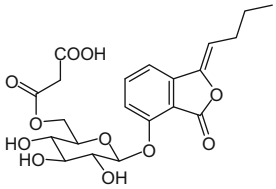

58 (7-hydroxy-butylidenephthalide 7-*O*-(6'malonyl)-*β*-D-glucopyranoside)

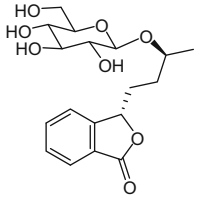

59 (celephthalide A)

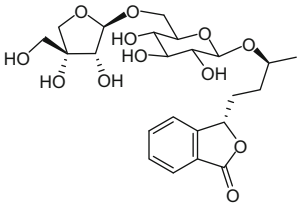

60 (celephthalide B)

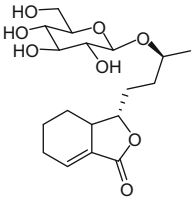

61 (celephthalide C)

The accumulation of some secondary metabolites of *Ligusticum chuanxiong* (including phthalides) has been correlated with the developmental stages of the plant [103], with (*Z*)-butylidenephthalide (**3**) and (*Z*)-ligustilide (**8**) found as volatiles of *Angelica tenuissima* Nakai [104] and *Meum athamanticum* [105].

Several dimeric phthalides were isolated from *Ligusticum chuanxiong*, and characterized as levistolide A (**23**), riligustilide (**24**), tokinolide B (**43**), 4,5-dehydrotokinolide B (**62**), and 3,8-dihydrolevistolide A (**63**) [106]. This last compound had been previously prepared by catalytic reduction of [6.6′,7,3a′]-(*Z*,*Z*′)-diligustilide A (syn: levistolide A (**23**)) and its structure was firmly established [70]; therefore, the compound isolated from *L. chuanxiong* requires structural revision. A series of phthalides, including butylphthalide (**4**), cnidilide (**7**), (*Z*)-ligustilide (**8**), senkyunolide I (**22**), levistolide A (**23**), riligustilide (**24**), (*Z*)-7-hydroxy-butylidenephthalide (**25**), senkyunolide H (**26**), tokinolide B (**43**), the triol **64** [107], (*S*)-4-hydroxy-butylphthalide (**65**) [108] and the dimeric

phthalides chuanxiognolides A (**66**) and B (**67**), were also reported as constituents of *L. chuanxiong* [103].

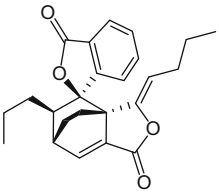

62 (4,5-dehydro-tokinolide B)

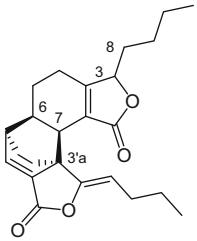

63 (3,8-dihydro-levistolide A)

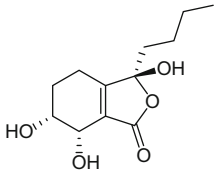

64

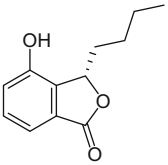

65

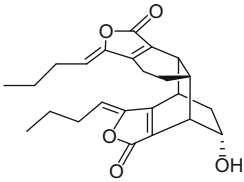

66 (chuangxiognolide A)

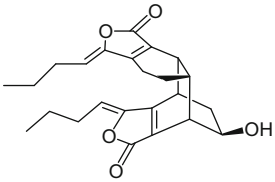

67 (chuangxiognolide B)

The dimeric phthalides riligustilide (**24**) and gelispirolide (**68**) were isolated from *Angelica sinensis* [109], with three new phthalides (**69–71**) purified from the same plant [110]. (*Z*)-Butylidenephthalide (**3**), (*Z*)-ligustilide (**8**), levistolide A (**23**), riligustilide (**24**), and compounds **72** and **73** were also isolated from a population of *A. sinensis* [111]. From an aqueous extract of *Ligusticum chuanxiong* was isolated a lactone derivative (**74**) considered as a phthalide analog [112].

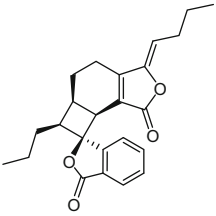

68 (gelispirolide)

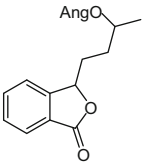

69 (10-angeloyloxi-butylphthalide)

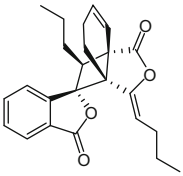

70 (sinaspirolide)

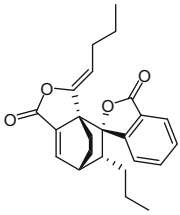

71 (ansaspirolide)

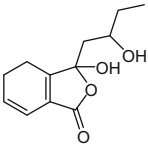

72

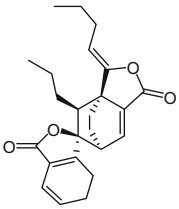

73 ((3Z,3a*R*,6*S*,3'*R*,8'*S*)-3a.8',6.3'-diligustilide)

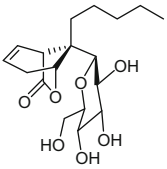

74 (ligusticoside)

Ligusticum chuanxiong is recognized widely as an effective medicinal plant. Of more than 200 compounds that have been isolated from this species, the phthalides are considered to be the characteristic metabolites. Recent reviews compiling the chemical profile of *L. chuanxiong* [113] and its pharmacological properties [114] have been published.

Four not previously reported phthalides (**75**–**78**), together with compounds **4**, **7**, **8**, **22**, **23**, **27**, and **43**, have also been isolated from *Ligusticum chuanxiong* [115].

Sedanonic acid (**1**) and phthalides **6**, **22**, **26**, **52**, and **79**–**85**, were isolated from *Ligusticum sinense* Oliv. cv. *chaxiong*, with some compounds displaying activity against neuronal injury [116]. From the roots of the same species were isolated (*Z*)-ligustilide (**8**), and the dimeric phthalides chaxiongnolide A (**86**) and chaxiongnolide B (**87**) [117]. This last-mentioned compound had been previously characterized as a semisynthetic substance that was obtained by the differentiated cyclization of the ketoacid derived from tokinolide B (**43**) [118]. 7-Acetyl-senkyunolide H (**88**) was isolated from the roots of *Angelica sinensis* [119], and (*Z*)-ligustilide (**8**) has been found in good yields in different plant parts of *Kelussia odoratissima* Mozaff [120].

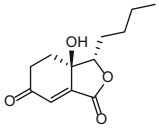

75 (chuanxiongnolide R1)

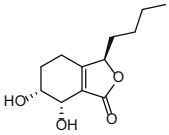

76 (chuanxiongnolide R2)

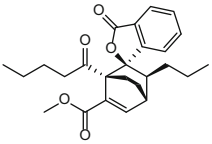

77 (chuanxiongdiolide R1)

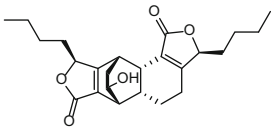

78 (chuanxiongdiolide R2)

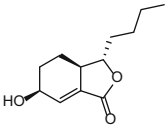

79 ((3*S*,3a*R*,6*S*)-6-hydroxysedanolide)

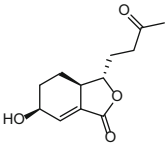

80 (6-hydroxy-sedanolide-10-one)

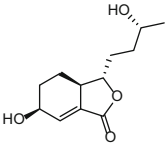

81 (10-hydroxysedanolide)

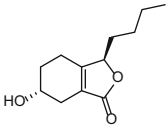

82

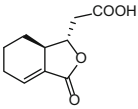

83 ((3*S*,3a*R*)-3-(2-carbonyl)-ethyl-3a,4,5,6-tetrahydrophthalide)

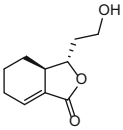

84

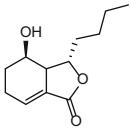

85 ((3*S*,3a*R*,4*R*)-4-hydroxy-sedanolide)

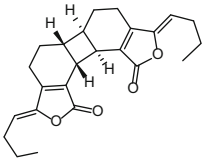

86 (chaxiongnolide A)

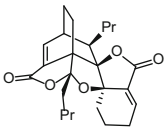

87 (chaxiongnolide B, cyclization product of the ketoacid derived from tokinolide B)

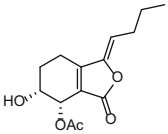

88 (7-acetyl-senkyunolide H)

2.2 Phthalides in Other Plant Families

This section refers to the presence of phthalides that have been found in several plant families, other than the Umbelliferae (Apiaceae).

2.2.1 Bignoniaceae

From a methanol extract of the wood of *Catalpa ovata* G. Don, used traditionally as a diuretic in Japan, was isolated catalpalactone (**89**) [121]. Inouye and co-workers confirmed its structure, by preparing several derivatives. Compound **89** was obtained from the same plant several years later [122, 123].

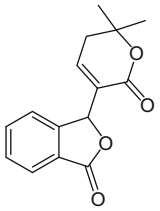

89 (catalpalactone)

2.2.2 Cactaceae

Compounds from the leaves, flowers and fruits of *Opuntia leindheimeiri* var. *linguiformis* (Griffiths) L.D. Benson, the leaves and flowers of *O. macrorhiza* Engelm., and the leaves of *O. microdasys* (Lehm.) Pfeiff. were extracted by steam distillation, and (*E*)-butylidenephthalide (**21**) was identified by GC-MS [124].

2.2.3 Compositae (syn. Asteraceae)

Several species of the genus *Helichrysum* have yielded phthalides. 5,7-Dihydroxyphthalide (**90**) and 5-methoxy-7-hydroxy-phthalide (**91**) were isolated from *H. italicum* (Roth) G. Don [125, 126]. Both phthalides and arenophthalide A (**92**) were contained in the organic extracts of *H. arenarium* (L.) Moench [127, 128]. On the other hand, *H. platypterum* DC. yielded platyphterophthalide (**93**) [129]. Venditti and co-workers carried out a chemical

analysis of a chromatographic fraction of *H. microphyllum* (Willd.) Benth. & Hook. f. ex Kirk of medium polarity, and characterized phthalides **94** and **95** [130].

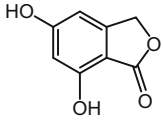

90 (5,7-dihydroxyphthalide)

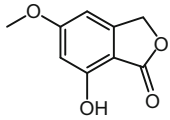

91 (7-hydroxy-5-methoxyphthalide)

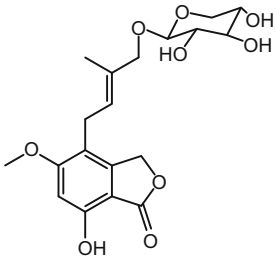

92

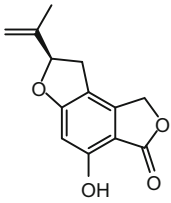

93 (platyphterophthalide)

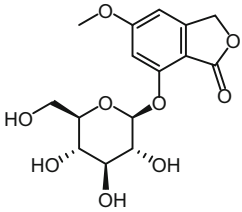

94

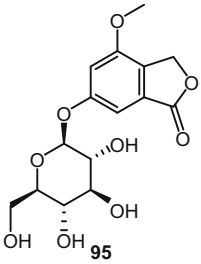

95

Talapatra and co-workers [131] analyzed the petroleum ether, chloroform, and alcoholic extracts of *Anaphalis contorta* (D. Don) Hook. f., and from these were isolated 5,7-dihydroxyphthalide (**90**), 5-methoxy-7-hydroxyphthalide (**91**), and 5-hydroxy-7-*O*-(3′-methyl-but-2′-enyl)phthalide (anaphatol, **96**). Phthalidochromene (**97**), araneophthalide (**98**) and aranochromanophthalide (**99**) were later obtained from the aerial parts of *Anaphalis araneosa* DC. [129].

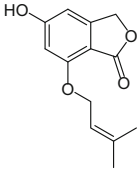

96 (anaphatol)

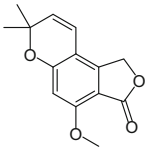

97 (phthalidochromene)

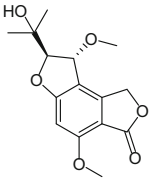

98 (araneophthalide)

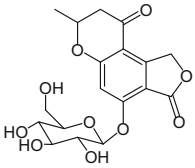

99 (arachromanophthalide)

A 3-substituted phthalide with thiophene, which was called chrycolide (**100**), was isolated from an extract of *Chrysanthemum coronarium* L. [132].

Stuppner's research group analyzed *Scorzonera tomentosa* L., a plant that has been used traditionally for the treatment of infertility and as an analgesic, anthelmintic, and antirheumatic in Turkey. From the methanol extract were isolated three phthalides as racemic mixtures, namely, (±)-scorzophthalide (**101**), (±)-hydramacrophyllol A (**102**), and (±)-hydromacrophyllol B (**103**) [133].

From the aerial parts of *Gnaphalium adnatum* DC. (Wall.) ex Thwaites [134] were isolated compounds **90** and **104–108**.

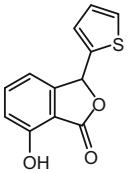

100 (chrycolide)

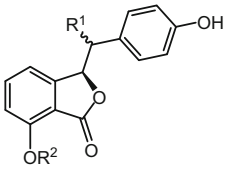

(±)-**101** (scorzophthalide) $R^1 = \alpha$-H, $R^2 = Me_2$
(±)-**102** (hydramacrophyllol A) $R^1 = \alpha$-OH, R^2 = H
(±)-**103** (hydramacrophyllol B) $R^1 = \beta$-OH, R^2 = H

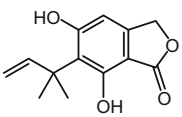

104 (gnaphalide A)

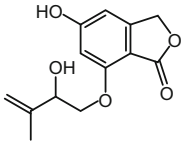

105 (gnaphalide B)

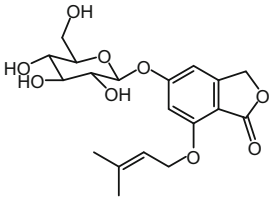

106 (gnaphalide C)

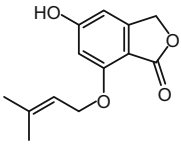

107

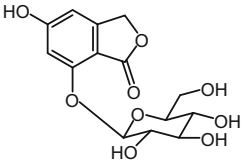

108

2.2.4 Fumaraceae

In a search for spirobenzyl-isoquinolines from *Fumaria parviflora* Lam., four phthalideisoquinolines were found, namely, (+)-adlumidine (**109**), (–)-corlumine (**110**), (+)-bicuculline (**111**), and (+)-α-hydrastine (**112**) [135].

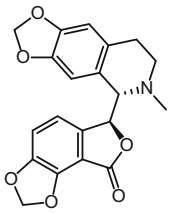

109 ((+)-adlumidine)

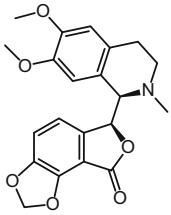

110 ((–)-corlumine)

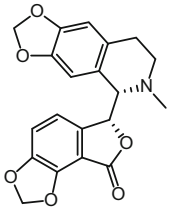

111 ((+)-bicuculline)

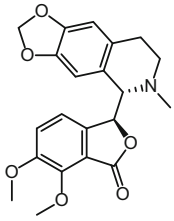

112 ((+)-α-hydrastine)

2.2.5 Gentianaceae

From the leaves of *Gentiana pedicellata* (Wall. ex D. Don) Griseb., pedicelloside (**113**) [136] and pedirutinoside (**114**) were isolated by Chulia and co-workers [137]. Garcia and associates analyzed the aerial parts of *Gentiana pyrenaica* L. and obtained 3-(3-*O*-*β*-D-glucosylpropyl)phthalide, which was named pediglucoside (**115**), and 3-[3-(6-vanilloyloxy-*O*-*β*-D-glucosyl)propyl]phthalide, or 6′-vanilloylpediglucoside (**116**) [138].

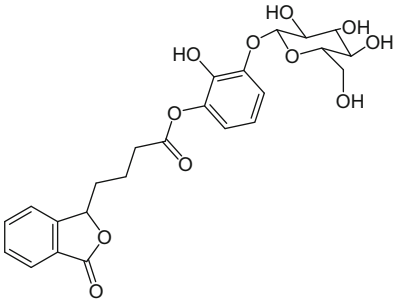

113 (pedicelloside)

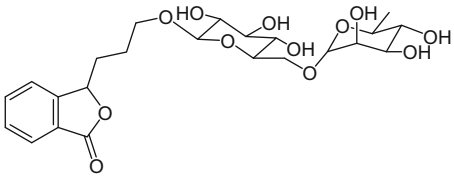

114 (pedirutinoside)

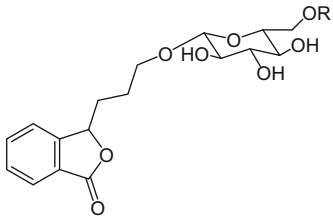

115 (pediglucoside) R = H
116 (6'-vanilloylpediglucoside) R = vanilloyl

2.2.6 Lamiaceae

Scutellaria baicalensis Georgi has been used in Chinese traditional medicine for the treatment of diarrhea and inflammatory diseases. Its phytochemical investigation has yielded butylidenephthalide (**3**), (*S*)-butylphthalide (**4**), neocnidilide (**6**), cnidilide (**7**), (*Z*)-ligustilide (**8**), and senkyunolide A (**15**) [139].

2.2.7 Leguminosae (syn. Fabaceae)

Malan and Roux performed the isolation of 5,6-dihydroxyphthalide (**117**), identified as meconine (**118**) after methylation with diazomethane, in the chemical analysis of *Peltogyne pubescens* Benth. and *Peltogyne venosa* (Vahl) Benth. [140]. 4,6-Dimethoxyphthalide (**119**) was isolated from a methanolic extract of *Albizzia julibrissin* Durazz. [141].

2.2.8 Loganiaceae

Preparations from the stem bark of *Anthocleista djalonensis* A. Chev. have been used traditionally for curing fever, as a purgative, and for stomachache, and from the organic extract of this species, 4-carbomethoxy-5,7-dimethoxy-6-methylphthalide (**120**) (djalonensin) was obtained [142].

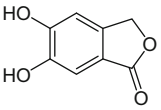

117

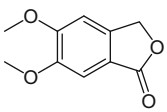

118

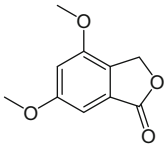

119

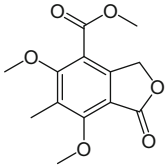

120 (djalonensin)

2.2.9 Oleaceae

From the essential oil of the stem bark of *Forsythia japonica* Makino, Kameoka and co-workers isolated and characterized 3-ethyl-7-hydroxyphthalide (**121**) [143].

2.2.10 Onocleaceae

(±)-Matteucen C (**122**) and (±)-matteucen D (**123**) were isolated as racemic products, along with some isocoumarins, from the rhizomes of *Matteuccia orientalis* (Hook.) Trevis. [144].

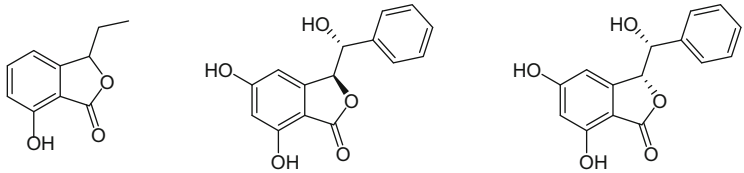

121 **122** ((±)-matteucen C) **123** ((±)-matteucen D)

2.2.11 Orchidaceae

Shihunine (**124**) is a secondary metabolite of *Dendrobium lohohense* Tang & F.T. Wang. It was found as a racemic mixture, as deduced by the lack of optical properties [145, 146]. Pierardine (**126**) was isolated from the methanol extract of *Dendrobium pierardii* Roxb. ex Hook. as an optically active compound [147]. Later, it was synthesized and its absolute configuration (*S*) was assigned by comparison of its physical characteristics with those previously reported for (3*S*)-butylphthalide (**4**) [148]. Shihunine (**124**) was also reported as a metabolite of *D. pierardii*, as well as betaine (**125**), which exists in polar solvents.

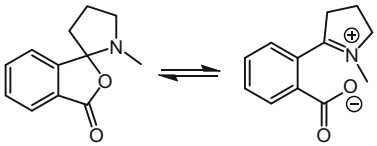

124 (shihunine) **125** (betaine)

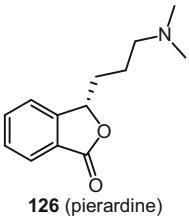

126 (pierardine)

2.2.12 Papaveraceae

Setigerumine I (**127**) was isolated from *Papaver setigerum* DC., which also yielded the well known α-noscapine (**128**). The relative configuration of the new phthalide was determined through NMR spectroscopic experiments, and it was isolated as a racemic mixture [149].

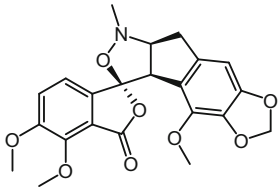

127 (setigerumine I)

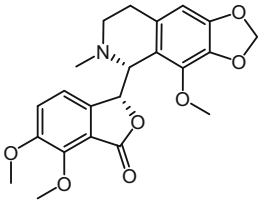

128 (α-noscapine)

2.2.13 Pittosporaceae

From the Chinese and Taiwanese *Pittosporum illicioides* Makino var. *illicioides*, were isolated six hitherto unknown phthalides, **129–134**. According to the method described, enantiomers **129** and **132** eluted differentially by column chromatography over silica gel [150]; since this is not possible, a compound configurational error in this report seems probable [150]. The absolute configurations of the compounds were determined by comparison of their specific rotations with known 3-alkylphthalides [151].

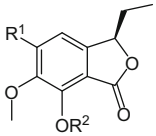

129 $R^1 = R^2 = H$
130 $R^1 = OMe$, $R^2 = H$
131 $R^1 = OMe$, $R^2 = Me$

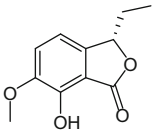

132

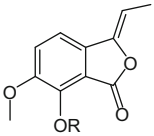

133 R = H
134 R = Me

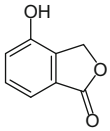

135 (4-hydroxyphthalide)

2.2.14 Poaceae (syn. Gramineae)

4-Hydroxyphthalide (**135**) was isolated from an acetone extract of crushed oat grain (both *Avena fatua* L. and *Avena sativa* L.). Considering that 4-oxygen-substituted phthalides are seldom found in Nature, the author suggested that it cannot be ruled out that 4-oxy-phthalides have another biosynthetic origin than that through the more common 3-alkyl and 3,5- and/or 7-oxygen substituted phthalides [152].

2.2.15 Polygonaceae

From the methanol extract of the root tubers of *Polygonum multiflorum* Thunb., a medicinal plant used traditionally for the treatment of hyperlipidemia, were obtained *trans*- and *cis*-(*E*)-3-butylidene-4,5,6,7-tetrahydro-6,7-dihydroxy-3*H*-isobenzofuranone **136** and **137**. The absolute configurations of these compounds were not determined [153].

2.2.16 Saxifragaceae

Thunberginol F (**138**) is a phthalide isolated from the methanol extract of "Hydrangeae Dulcis Folium", i.e. the fermented and dried leaves of *Hydrangea macrophylla* (Thunb.) Ser. var. *thunbergii* Makino. The double bond configuration was established by NOE experiments of its trimethyl derivative [154, 155]. From the ethyl acetate-soluble part of the same extract, were found hydramacrophyllols A (**102**) and B (**103**), the former with low optical purity and the last as a racemic mixture, suggesting that **103** is an artifact. The absolute configuration of **102** was not determined [155–157].

2.2.17 Typhaceae

The phytochemical investigation of the rhizomes of *Typha capensis* (Rohrb.) N.E. Br. yielded typhaphthalide (**139**) and radulanolide (**140**) [158].

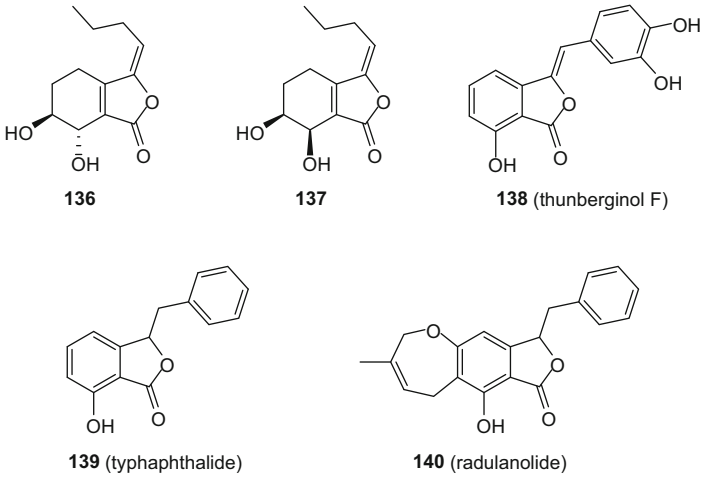

2.3 Phthalides in Fungi

In 1913, Alsberg and Black reported the isolation of an acid of molecular formula $C_{17}H_{20}O_6$, which they called mycophenolic acid (MPA (**141**)), from *Penicillium stonoliferum* Thom [159]. Its structure was not correctly determined until the late 1940s and early 1950s as **141** [160–162]. This phthalide was also found in cultures of fifteen strains of *Penicillium brevicompactum* Dierckx and *Penicillium biourgeianum* K.M. Zalessky [163], as well as *Penicillium brunneostoloniferum* S. Abe [164], *Penicillium echinulatum* Raper & Thom ex Fassat. [165], *Penicillium roqueforti* Thom [166], *Penicillum verrucosum* Dierckx [167], and *Phomopsis longicolla* Hobbs [168]. San Martin and co-workers reported that *P. brevicompactum* produces not only mycophenolic acid, but also its methyl ester **142** [169]. From *Penicillium crustosum* Thom was also isolated 5-hydroxy-7-methoxy-4-methylphthalide (**143**) [170].

Structurally similar compounds to **141** have been isolated from different sources. Euparvic acid (**144**) and the phthalides **145**–**147** were isolated from *Eupenicillium parvum* Raper et Fennell [171], and compound **147** and penicacids A–C (**148**–**150**) were found to be metabolites from *Penicillium* sp. SOF07 [172]. Phthalides **151** [173], **152**, and **153** [174] were obtained from *Penicillium brevicompactum*, but their configurations were not established. In all these cases, MPA (**141**) was isolated along with the aforementioned compounds.

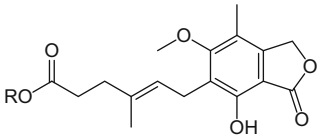

141 (mycophenolic acid) R = H
142 R = Me

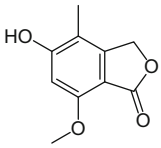

143 (5-hydroxy-7-methoxy-4-methylphthalide)

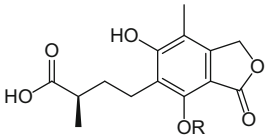

144 (euparvic acid) R = H
145 R = Me

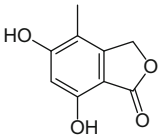

146

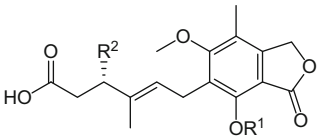

147 R^1 = H; R^2 = OH
148 (penicacid A) R^1 = CH_3; R^2 = OH
149 (penicacid B) R^1 = H; R^2 = OGlc

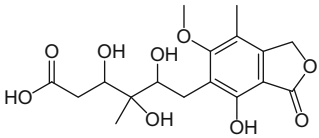

150 (penicacid C)

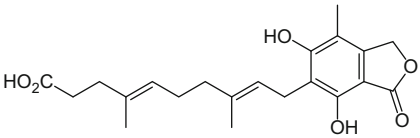

151

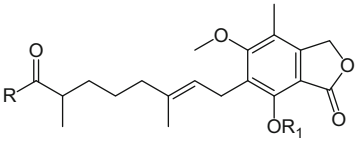

152 R = OH
153 R = Me

Birkingshaw and co-workers [175] isolated cyclopaldic acid (**154**) from cultures of two strains of *Penicillium cyclopium* Westling. This compound has also been found to be a secondary metabolite of *Aspergillus duricaulis* Raper et Fennell [176], *Seiridium cupressi* (Guba) Boessew. [177], *Penicillium commune* Thom, and *Penicillium mononematosum* (Frisvad, Filt. & Wicklow) Frisvad [178]. Compound **154** was found in some *Penicillium* spp. along with the related metabolite deoxycyclopaldic acid (**155**) [179], which was also isolated from *Microsphaeropsis arundinis* PSU-G18 [180]. *Aspergillus duricaulis* also yielded chromanols **156–159** as additional terpenoidal phthalides [181].

Two sesquiterpene-cyclopaldic acid hybrid derivatives were found to be metabolites from *Pestalotiopsis* sp., an endophytic fungus isolated from the leaves of the mangrove *Rhizophora mucronata* Lam. These phthalides were named pestaliotiopens A (**160**) and B (**161**), and their configurations were determined through spectroscopic methods and theoretical calculations. The sesquiterpene moiety is derived from altiloxin B, which preserves its absolute configuration in the hybrid compounds. The authors suggested that the formation of each individual scaffold (mycophenolic acid and altiloxin B) occurs previously and then both moieties join to form these compounds [182].

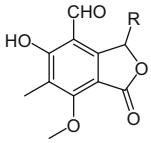

154 (cyclopaldic acid) R = OH
155 (deoxycyclopaldic acid) R = H

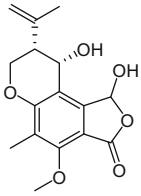

156

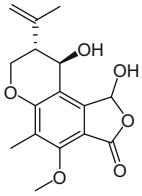

157

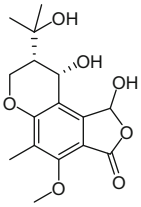

158

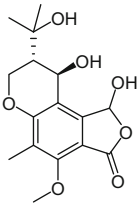

159

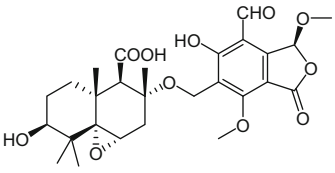

160 (pestalotiopen A)

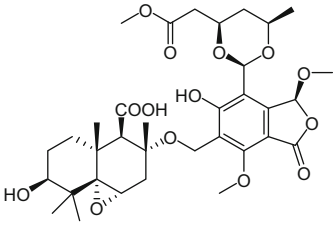

161 (pestalotiopen B)

McGowan and coworkers isolated gladiolic acid (**162**) from a culture of *Penicillium gladioli* L. McCullogh & Thom. This compound was found to display antibacterial and fungistatic activities [183]. Grove established its structure, suggesting that should there be a tautomeric equilibrium between the

hydroxylactone **162** and the aldehydic acid **163**, as occurs with mycophenolic acid (**141**) [184, 185].

Other studies have shown that gladiolic acid (**162**) and dihydrogladiolic acid (**164**) (which also exists in an equilibrium with aldehydic acid **165**) are constituents of the culture of *Penicillium gladioli* [186–188]. A modification of the experimental procedure originally employed for the isolation, allowed the characterization of compound **166**, which was considered an artifact [189]. From the endophytic fungal strain *Phomopsis* sp. A123 was isolated dihydrogladiolic acid (**164**) as an optically active compound, along with its 3-ethoxy derivative, **167**, named phomotone [190].

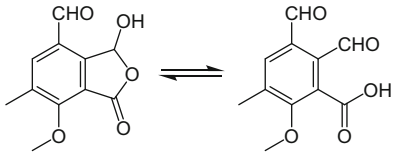

162 (gladiolic acid) **163**

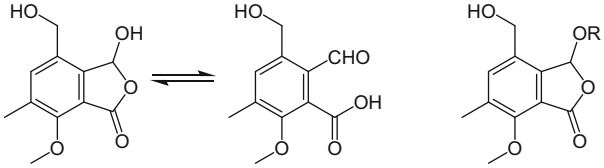

164 (dihydrogladiolic acid) **165** **166** R = Me
167 R = Et (phomotone)

Alternaria kikuchiana S. Tanaka is a well-known parasite, which causes black spot disease in Japanese pears. Chemical investigation of the culture filtrates of the broth yielded *iso*-ochracinic acid (**168**) [191], and this compound has also been characterized from a fungicolous hyphomycete resembling *Cladosporium* [192].

Herbaric acid (**169**), an analog of *iso*-ochracinic acid, is produced by *Cladosporium herbarium* (Pers.) Link, a fungus associated with the Indonesian sponge *Callyspongia aerizusa*. It is interesting to note that other strains of this fungus, isolated from *Aplysina aerophoba*, collected in the Mediterranean Sea, did not produce this phthalide [193]. A closely related phthalide to herbaric acid is acetophthalidin (**170**), which was isolated from the fungal strain BM923 [194].

Phthalide **171** and its *β*-D-glucopyranoside **172** were isolated from a mycophilic *Hansfordia* species, along with other natural products [195].

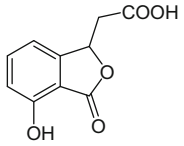

168 (*iso*-ochracinic acid)

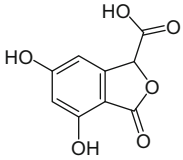

169 (herbaric acid)

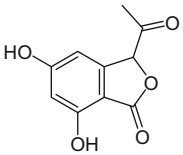

170 (acetophthalidin)

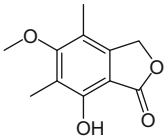

171

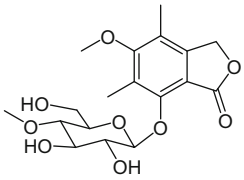

172

Several anti-*Helicobacter pylori* phthalides (**173–179**) were isolated from the basidiomycete *Phanerochaete velutina* CL6387, but these phthalides did not display antibacterial activities against other microorganisms against which they were evaluated. The stereochemical assignments of some of these compounds were not completed [196].

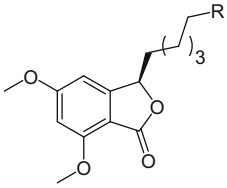

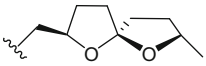

173 (CJ-12,954)

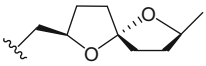

174 (CJ-13,014)

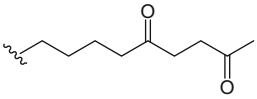

175 (CJ-13,015)

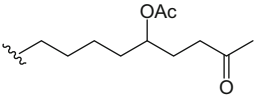

176 (CJ-13,102)

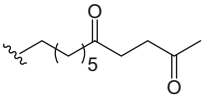

177 (CJ-13,103)

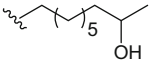

178 (CJ-13,104)

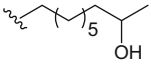

179 (CJ-13,108)

From the culture broth of *Penicillium vulpinum* (Cooke & Massee) Seifert & Samson were isolated several natural products including 3-butyl-7-hydroxyphthalide (**180**), which did not display cytotoxic activity [197].

The phthalide **181**, as well as its derivative **182**, were isolated by Sobolevskaya and co-workers from the mycelial fungus *Penicillium claviforme* Bainter, as found on the surface of the seagrass, *Zostera marina* L. They determined the absolute configuration of **181** by comparison of its specific rotation with previously reported data [198]. The absolute configuration at the carbinolic carbon of **182** was determined through the modified Mosher method as (*R*) (the corrected drawing is depicted in the present contribution since in the original paper the (*S*)-enantiomer appeared).

Chemical analysis of the culture filtrate of *Aspergillus silvaticus* Fennell and Raper IFO8173 yielded silvaticol (**183**), *O*-methylsilvaticol (**184**), and nidulol (**185**) [199].

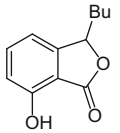

180 (3-butyl-7-hydroxy-phthalide)

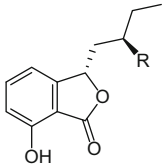

181 R = H
182 R = OH

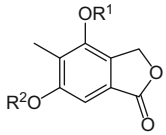

183 (silvaticol) R^1 = Me; R^2 = H
184 (*O*-methylsilvaticol) R^1 = R^2 = Me

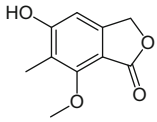

185 (nidulol)

From *Sporotrichum laxum* CBS 578.63 were isolated two long-chain phthalides named spirolaxine (**186**) and sporotricale (**187**) [200].

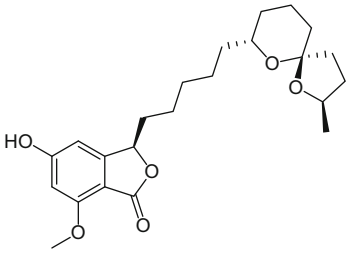

186 (spirolaxine)

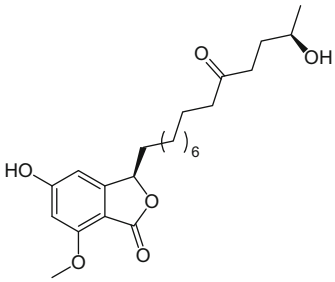

187 (sporotricale)

The fungus *Phomopsis convolvulus* Ormeno-Nuñez, Reedeler, & A.K. Waston is a pathogen of the perennial plant *Convolvulus arvensis* L. (Convolvulaceae), and has been studied for the potential biological control of this plant. A chemical investigation of this fungus afforded the phthalides convolvulanic acid A (**188**), convolvulanic acid B (**189**), and convolvulol (**190**) [201].

Compounds **189–191** and xylariphthalide A (**192**) were also isolated from the fungus *Everniastrum cirhatum* (Fr.) Hale ex Sipman (Xylariaceae) [202]. The authors reported that compound **192** displayed a low specific rotation value, presumably due to tautomerism of the hemiacetal group.

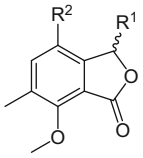

	R^1	R^2
188 (convolvulanic acid A)	OH	COOH
189 (convolvulanic acid B)	H	COOH
190 (convolvulol)	H	CH_2OH
191	H	Me
192 (xylariphthalide A)	OH	CH_2OAc

Isopestacin (**193**) is a 3-phenylsubstituted phthalide found as a racemic mixture in a culture of *Pestalotiopsis microspore* (Speg.) But. & Peres, an endophyte from *Terminalia morobensis* Coode [203]. A similar phthalide is cryphonectric acid (**194**), an optically active abundant metabolite of *Cryphonectria parasitica* (Murrill) M.E. Barr [204].

An antioxidant phthalide, 4,5,6-trihydroxy-7-methylphthalide, named epicoccone (**195**), was isolated from the fungus *Epicoccum* sp. [205]. Phthalides **195** and **196** were purified and characterized from a culture of the fungus *Cephalosporium* sp. AL031 [206].

From the antibacterial active culture broth of *Cytospora* sp. and *Diaporthe* sp. collected in Costa Rica, several octaketides were obtained, including the bioactive phthalide cytosporone E (**197**) [207].

During a screening protocol to discover compounds that bind to the cancer target Akt1, it was found that the fungal culture of *Oidiodendron* sp. displayed activity. From this sample, a new phthalide was isolated and characterized as 3-methyl-4,5,6-trihydroxy-phthalide (**198**) [208].

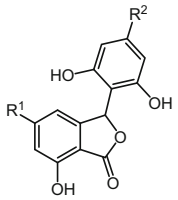

193 (isopestacin) R^1 = Me, R^2 = H
194 (cryphonectric acid) R^1 = OH, R^2 = COOH

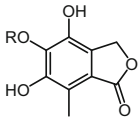

195 (epicoccone) R = H
196 R = Me

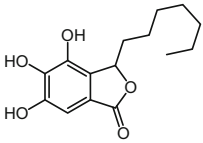

197 (cytosporone E)

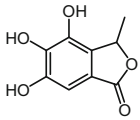

198 (3-methyl-4,5,6-tri-hydroxyphthalide)

The fungus *Alternaria porri* (Ellis) Cif. is a pathogen of onion, from a culture broth of which 5-(3′,3′-dimethylallyloxy)-7-methoxy-6-methylphthalide (**199**) was characterized [209], along with **200** [210]. Phthalide **199** was also isolated from a liquid culture of endophytic *Pestalotiopsis photiniae* (Thüm) Y.X. Chen, obtained from the plant *Podocarpus macrophyllus* D. Don [211, 212].

The O-prenylated phthalides **201** and **202** were isolated from an unidentified fungus named "Sterile Dark". Both of these displayed modest antifungal activity against

Cladosporium herbarium, but only phthalide **201** was active against *Gaeumannomyces gramini* var. *tritici* J. Walker, which causes the "take-all" disease in plants [213].

Silvaticol (**185**) and marilones A–C (**203–205**) were obtained from the culture medium of the fungus *Stachylidium* sp., which was isolated from the sponge *Callispongia* sp. Compound **203** displayed antiplasmodial activity, and **205** showed antagonistic activity towards the 5-HT_{2B} serotonin receptor [214].

Compounds **199**, **200**, and **206–208** were characterized from *Pestalotiopsis photiniae* as antifungal constituents against *Fusarium graminearum*, *Botrytis cinerea* and *Phytophtora nicotianae*, which are considered plant pathogens [211]. Yoganathan and co-workers [215] isolated fuscinarin (**209**) from the soil fungus *Oidiodendron griseum* Robak.

Salfredin B_{11} (**210**) is a prenylated phthalide isolated from *Crucibilum* sp. (strain RF-3817), which displayed aldose reductase inhibitory activity [216].

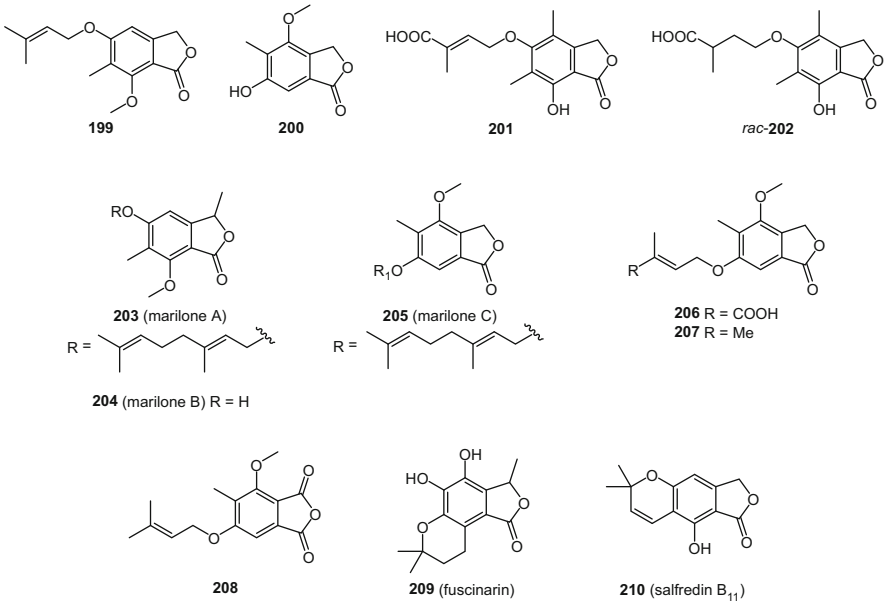

From a marine fungus of the order Pleosporales were isolated (3*S*,3′*R*)-3-(3′-hydroxybutyl)-7-methoxy-phthalide (**211**) and the deoxy derivative **212**. This last compound displayed weak cytotoxic activity against selected cancer cell lines [217]. The absolute configuration of **211** was determined through the Mosher ester method, and the absolute configuration of **212** was determined by comparison of the specific rotations of both these compounds.

The organic extract of the fermentation culture of the endophytic fungus *Pestalotiopsis foedan* exhibited activity against *Candida albicans*, *Geotrichum candidum*, and *Aspergillus fumigatus*. From this extract were isolated pestaphthalides A (**213**) and B (**214**), and compounds **215–217**. Phthalides **213** and **214** exhibited modest activity toward the above-mentioned fungi [218].

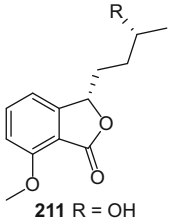

211 R = OH
212 R = H

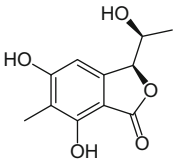

213 (pestaphthalide A)

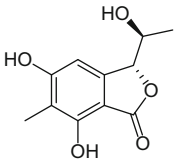

214 (pestaphthalide B)

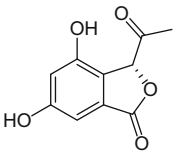

215

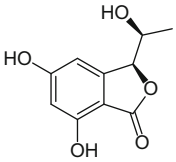

216

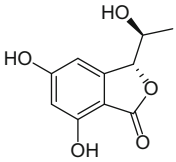

217

From the edible and cultivable mushroom *Sparassis crispa* (Japanese common name: "Hanabiratake"), were purified the phthalides **218**–**223**, in addition to other constituents [219]. Compounds **218**–**220** were named hanabiratakelides A–C, respectively [219]. Phthalides **221**–**223** were previously found from other sources [131, 220]. These compounds displayed discernible antioxidant, antiinflammatory, and cytotoxic activities.

The fungus *Pestalotiopsis heterocornis* (Guba) Y.X. Chen was isolated from the stems of *Bruguiera gymnorhiza* (L.) Lam. (Rhizophoraceae), and phthalides **171**, **224**, and **227** were isolated a fermentation broth [221].

Several radical scavenging and cytotoxic isocoumarins along with the antioxidant phthalide **226** were isolated from the endophytic fungus *Colletotrichum* sp. [222].

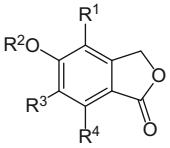

	R^1	R^2	R^3	R^4
218 (hanabiratakelide A)	OH	H	OMe	H
219 (hanabiratakelide B)	H	H	OMe	OH
220 (hanabiratakelide C)	OH	H	OH	OMe
221	H	Me	H	OMe
222	H	Me	OH	OMe
223	OH	Me	H	OMe

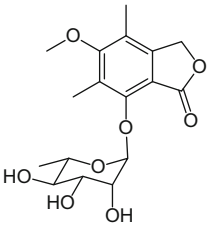

224

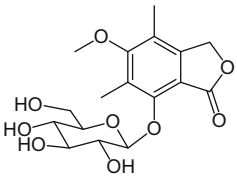

225

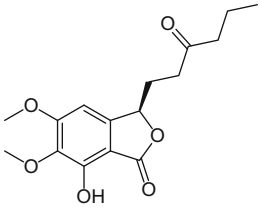

226 (colletotrialide)

Microsphaeropsis arundinis PSU-G18 is a source of a wide range of phthalides. From its broth and mycelial ethyl acetate extract were characterized deoxycyclopaldic acid (**155**), microsphaerophthalides A–G (**227–233**), and another four highly substituted phthalides **234–237**. Microsphaerophthalides C–G (**229–233**) belong to the less common 3-oxygenated phthalides. The absolute configurations of these compounds were determined by comparison of their specific rotations [180].

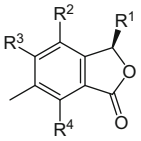

	R^1	R^2	R^3	R^4
227 (microsphaerophthalide A)	H	CH_2OEt	OH	OMe
228 (microsphaerophthalide B)	H	CHO	OMe	OH
229 (microsphaerophthalide C)	OEt	CHO	OMe	OH
230 (microsphaerophthalide D)	OEt	CH_2OMe	OH	OMe
231 (microsphaerophthalide E)	OEt	CH_2OEt	OH	OMe
232 (microsphaerophthalide F)	OMe	OMe	OH	OMe
234	H	Me	OH	OH
235	H	CH_2OMe	OH	OMe
236	H	Me	OH	OMe
237	Me	Me	Me	OMe

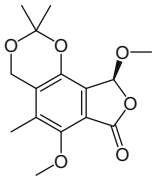

233 (microsphaerophthalide G)

A crude extract obtained from the culture broth of the fungus *Acremonium* sp., an endophyte from the mangrove plant *Rhizophora apiculata* Blume (Rhizophoraceae), displayed antibiotic activity towards *Candida albicans* and *Cryptococcus neoformans*. Several isocoumarin derivatives and a phthalide named acremonide (**238**) were obtained from this endophytic fungus, and these compounds displayed activity toward both microorganisms [223].

The fungus *Bipolaris* sp. was isolated from the seagrass *Halophila ovalis* (R. Br.) Hook. f., and from this fungus were purified and characterized several chromanones, anthraquinones, and phenolic compounds, including the phthalide bipolaride (**239**) [224].

The absolute configuration of sporotricale (**187**) was determined using the Mosher ester method, and 6-hydroxysporotricale (**240**) was characterized from *Sporotrichum laxum* (syn: *Phanerochaete pruinosum*) CBS 578.63 [225]. This fungus was recently reinvestigated and the anti-*Helicobacter pylori* phthalides spirolaxine (**186**) and sporotricale (**187**) were reisolated [226].

Pseudaboydins A (**241**) and B (**242**) were obtained from the fungus *Pseudallescheria boydii* associated with the starfish *Acanthaster planci*. The

configuration of both phthalides was established using their CD spectra, using previously developed empirical rules [227]. A *Penicillium* sp. (strain ZH58) was found to produce phthalide **243** [228]. Phthalide **244** was isolated from the fermentation broth of the fungus *Pezicula* sp., occurring in the twigs of *Forsythia viridissima* Lindl. (Oleaceae) [229].

Paecilocin A (**245**) was isolated from *Paecilomyces variotii*, a fungus obtained from the jellyfish *Nepolinema nomurai*. The absolute configuration of paecilocin A (**245**) was assigned by comparison of its specific rotation with that of (3*S*)-butylphthalide (**4**) [230]. 5,7-Dihydroxy-4-methylphthalide (**148**) was characterized from a culture filtrate of *Aspergillus flavus* [231]. Xylaral (**246**) was isolated from *Xylaria polymorphus* (Pers.) Grev., the well-known "dead man's fingers" fungus [232].

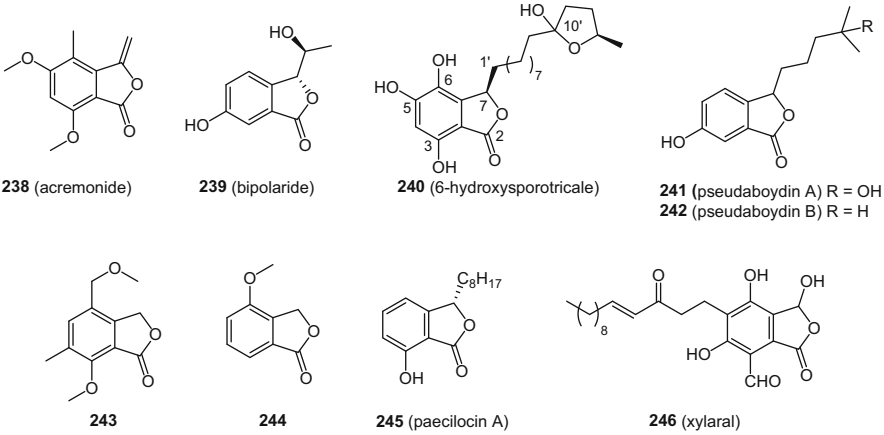

7-Hydroxy-4,6-dimethylphthalide (**247**) was isolated from *Penicillium megasporum* NHL2977 [233]. It was also found in a culture of *Diaporthe phaseolorum* (Cooke & Ellis) Sacc. [234]. Compounds **248**, **249**, and **250** were characterized from *Phomopsis* sp. A123 [235]. Phthalide **250** has been previously isolated from the marine fungus *Diaporthe* sp. [236].

Excelsione, also named phomopsidone (**251**), was almost simultaneously isolated from an unidentified fungus growing in the inner stem of the tree *Knightia excelsa* R. Br. [237], and from *Phomopsis* strain E02091 [238]. Phomopsidone A (**252**), a phthalide that includes an oxetane ring in its structure, was found also in this last-named fungus [235].

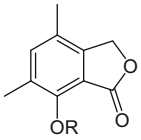

247 R = H
248 R = Me

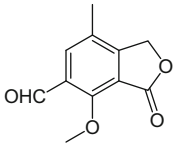

249

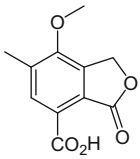

250

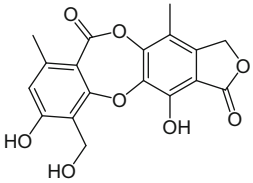

251 (excelsione, phomopsidone)

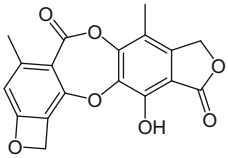

252 (phomopsidone A)

As a result of an investigation of *Penicillium vermiculatum* Dang., a cytotoxic compound was isolated and named vermistatin [239–241]. Its structure was later elucidated as **253**, and its absolute configuration was assigned by analysis of the CD spectrum [241]. Compound **253** has also been found in *Penicillium verruculosum* [242], and *Talaromyces flavus* FKI-0076 and IFM52668 [243, 244]. This compound was named fijiensin when it was isolated from *Mycosphaerella fijiensis* Morelet in 1990 [245].

From *Mycosphaerella fijiensis*, **253** was isolated with its dihydro- (**254**), acetoxydihydro- (**255**), and hydroxydihydro- (**256**) derivatives, as well as penisimplicissin (**257**). The absolute configurations of **254** and **255** were determined through the Mosher ester method [246]. Compounds **253** and **257** were also isolated from a culture of *Talaromyces thailandiasis* T. Douthop, L. Manoch, A. Kijjoa, M. Pinto, L. Gales, A. Damas, A.M.S. Silva, G. Eaton & W. Herz, together with **256** [247], and from *Penicillium rubrum* Stoll together with **254** [248].

The absolute configuration of **253** was confirmed through X-ray analysis, when it was isolated from the fungus *Guignardia* sp. no. 4382, along with two new derivatives, **258** and **259**, for which the absolute configurations were in turn assigned by comparison of their CD spectra with that of **253**. Compounds **253** and **258** were characterized from the fungus *Eurotium rubrum* [249].

The fungus *Penicillium* sp. HN29-2B1 was found to be a source of several derivatives. From its mycelium and culture medium were characterized **253**, **258**–**259**, 6-demethylvermistatin (**260**), 6-demethylpenicimplissinin (**261**), 5′-hydroxypenisimplicissin (**262**), and 2″-*epi*-hydroxydihydrovermistatin (**263**). The absolute configurations of **260** and **261** were determined by analysis of their CD data, while that of **263** was assigned as (3*R*,2″*S*) by means of single-crystal X-ray diffraction [250]. Phthalide **260** has been previously isolated from *Guignardia* sp. no. 4832 [251]. Compounds **257**, **258**, **260**, and neosarphenol A (**264**) were isolated from an ethanol extract of the culture of *Neosartorya glabra* CGMCC32286 by Liu and co-workers [252].

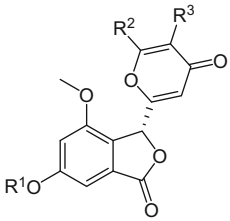

	R^1	R^2	R^3
253 (vermistatin)	Me		H
254 (dihydrovermistatin)	Me		H
255 (acetoxydihydrovermistatin)	Me		H
256 (hydroxydihydrovermistatin)	Me		H
257 (penisimplicissin)	Me	Me	H
258 (methoxyvermistatin)	Me		OMe
259 (hydroxyvermistatin)	Me		OH
260 (6-demethylvermistatin)	H		OH
261 (6-demethylpenisimplicissin)	H	Me	H
262 (5'-hydroxypenisimplicissin)	Me	Me	OH
263 (2"-epihydroxydihydrovermistatin)	Me		H
264 (neosarphenol)	H		OMe

Two anthraquinone phthalides, namely, rubellins C and D (**265** and **266**, respectively), were found in extracts from a strain of *Mycosphaerella rubella* (Niessl & J. Schröt.) Magnus [253]. Rubiginone H (**267**) was isolated from the methanol extract of the mycelium of *Streptomyces* sp. (strain Go N1/5) [254].

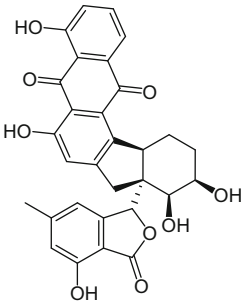

265 (rubellin C)

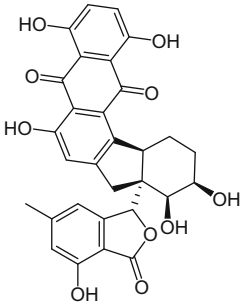

266 (rubellin D)

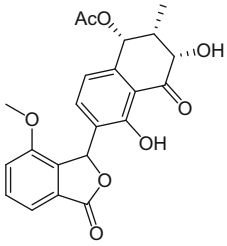

267 (rubiginone H)

An extract from the culture broth of *Penicillium rubrum* Stoll yielded rubralides A–C (**268**–**270**) [255]. The absolute configurations of **268** and **270** were established by comparison of their CD spectra with that of vermistatin (**253**), while the absolute configuration of **269** was not determined. Compound

269 and talaromycolides A–C (**271**–**273**) were isolated from *Talaromyces pinophilus* AF-02 [256].

From a methanol extract of the culture of *Penicillium* sp. IFB-E022, an endophytic fungal strain residing in the stems of *Quercus variabilis* Blume (Fagaceae), were isolated penicidones A (**274**) and B (**275**) by Tan and co-workers [257]. The absolute configuration at C-8 for both compounds was established as (8*R*) by comparison of the specific rotation with those of vermistatin (**253**), dihydrovermistatin (**254**), and penisimplicissin (**257**).

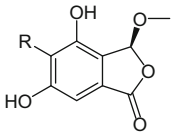

268 (rubralide A) R = Me
269 (rubralide C) R = CHO

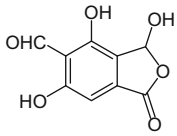

270 (rubralide B)

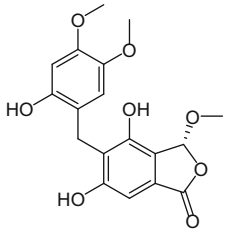

271 (talaromycolide A)

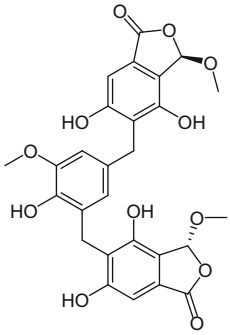

272 (talaromycolide B)

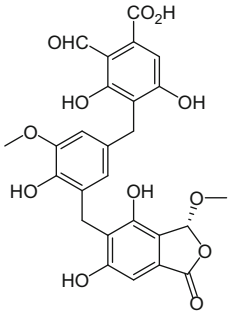

273 (talaromycolide C)

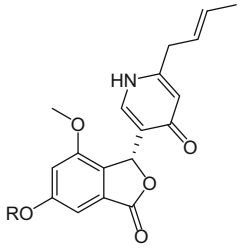

274 (penicidone A) R = Me
275 (penicidone B) R = H

Phthalides bearing two substituents at C-3 are not found frequently as natural products. One example is compound **276**, which was isolated from an ethyl acetate extract of the culture broth of *Halloroselinia oceanica* BCC 5149 [258]. This phthalide was also found in broth cultures of *Leptosphaeria* sp. KTC 727 [259] and *Paraphoma radicina* (McAlpine) Morgan-Jones & J.F. White [260]. Hashimoto and coworkers characterized compounds **276** and **277** from *Leptosphaeria* sp. KTC 727 [259]. Another example of this class of phthalides is compound **278**, isolated from an extract of the culture of *Emericella unguis* Malloch & Cain [261]. Corollosporine (**279**) is a compound from *Corollospora maritima* Werderm., which was characterized as a racemic mixture. It displayed antibacterial activity against *S. aureus* and other bacteria [262].

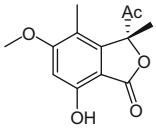

276

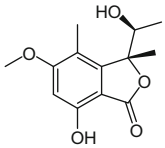

277

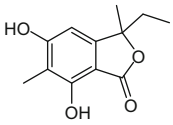

278 (3-ethyl-5,7-dihydroxy-3,6-dimethylphthalide)

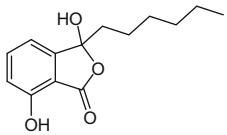

279 (corollosporine)

2.4 Phthalides in Lichens

Takenaka and co-workers isolated 3,5-dihydroxyphthalic acid and the phthalides **280–282** from the polyspore-derived mycobionts of *Graphis proserpens* Vain. [263].

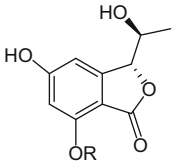

280 R = Me
281 R = H

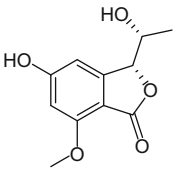

282

2.5 Phthalides in Liverworts

Asakawa and co-workers reported that radulanolide (**140**) was isolated from an organic extract from *Radula complanata* (L.) Dumont, a liverwort which causes allergic contact dermatitis [264]. The methanol extract of *Balantiopsis rosea* Berggr. yielded balantiolide (**283**), for which the structure was established by analysis of its spectroscopic data and by the preparation of its acetyl derivative (**284**) [265].

Asakawa's group [266] obtained 3-(4′-methoxy-benzyl)-5,6-dimethoxy-phthalide (**285**) from the ether extract of the liverwort *Frullania falciloba* Taylor ex Lehm. This structure was similar to 3-substituted phthalides previously isolated from *Radula complanata* [264] and *Balantiopsis rosea* [265]. The same group reported the phthalide **286** [267]).

Kraut and co-workers [268] analyzed the constituents of the liverwort *Frullania muscicola* Steph., and from a crude extract was purified the previously isolated balantiolide (**283**) [265] as well as 3-(3′,4′-dimethoxybenzyl)-5,7-dimethoxyphthalide (**287**) and 3-(4′-hydroxy-3′-methoxybenzyl)-5,7-dimethoxyphthalide (**288**). From an organic extract of *Plagiochila killarniensis* Pears., Rycroft and co-workers characterized killarniesolide (**289**). Acetylation of compound **289** afforded **290**, establishing the substitution of the benzylic ring [269].

Chemical investigation of *Plagiochila buchtiniana* Steph. provided 3-(4′-methoxybenzyl)-7-hydroxyphthalide (**291**), whereas work-up of *P. diversifolia* Lindenb. & Gottsche yielded 3-(4′-methoxybenzyl)-7-methoxyphthalide (**292**), 3-(3′,4′-dimethoxybenzyl)-7-methoxyphthalide (**293**), and 3-(3′,4′,5′-trimethoxybenzyl)-7-methoxyphthalide (**294**) [270].

Chemical analysis of the organic extracts of *Frullania falciloba* afforded 3-(4′-methoxybenzyl)-5,7-dimethoxyphthalide (**295**) [271], for which the structure was drawn in an erroneous manner in reference [266].

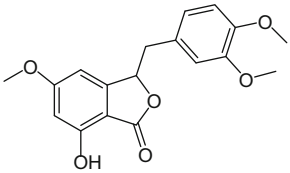

283 (balantiolide)

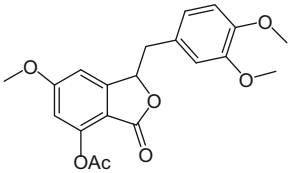

284

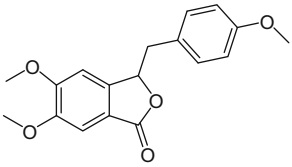

285

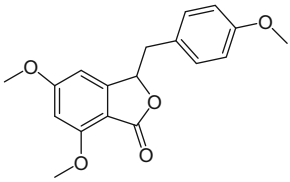

286

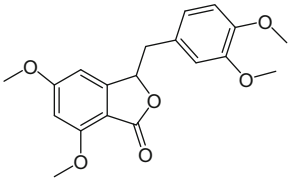

287

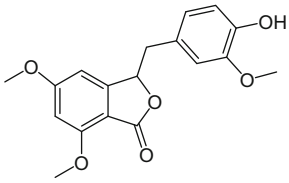

288

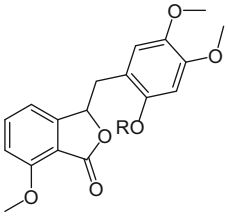

289 R = H (killarniesolide)
290 R = Ac

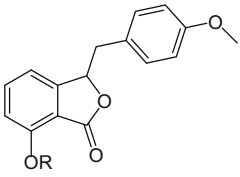

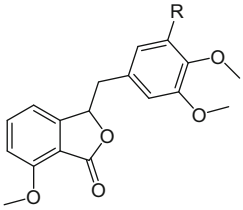

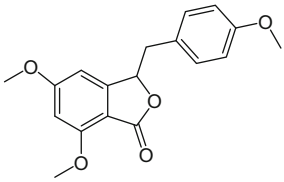

291 R = H
292 R = Me

293 R = H
294 R = OMe

295

3 Analytical Aspects

This section summarizes some methods employed for the extraction, isolation, chemical characterization, dereplication, and to achieve quality control of phthalides.

3.1 Extraction, Isolation, and Chemical Characterization

Historically, the extraction techniques for obtaining phthalides have focused on the use of non-polar solvents such as petroleum ether [127, 140, 272], hexane [36, 78, 142], and pentane [50]. Steam distillation has been employed for the extraction of several phthalides, such as sedanenolide ((**15**) senkyunolide A), (*Z*)- (**8**) and (*E*)-lingustilide (**18**), (*Z*)- (**3**) and (*E*)-butylidenephthalide (**21**), and butylphthalide (**4**) [42, 44, 273–275]. For obtaining polar compounds such as the diols, senkyunolide I (**22**) and senkyunolide H (**26**), in older work the plant rhizomes were defatted with non-polar solvents and then extracted with more polar solvents such as chloroform [65], or with water, followed by partition with an organic solvent [59], or extracted with acetone and methanol [60, 101, 276]. Several conventional procedures such as decoction [277, 278], percolation [279], sonication [279, 280], and reflux [281] have been used. Other techniques employed include supercritical fluid extraction (SFE) [274, 282–284], solid-phase microextraction (SPME) [285], microwave-assisted extraction [113, 286], and the use of biomembranes [287]. Pressurized liquid extraction (PLE) is an option that allows the quantification of phthalides [288–290]. A recently developed high-pressure ultrasonic-assisted extracted technology method has been applied for the purification of this type of phytochemicals [291, 292].

Regarding phthalide isolation, in earlier work, crude organic extracts were subjected to basic aqueous partitioning to remove acid and phenolic compounds [42, 293]. The organic layer obtained was then subjected to distillation for obtaining several fractions, yielding phthalides [19, 293]. A frequently used method for the isolation of phthalides is column chromatography (CC) over adsorbents or solid supports such as silica gel [103, 116], alumina [51], polyamide (CC6) [69], Sephadex LH-20 [66], and reversed-phase (C_{18}) silica gel [153]. Other reported methods are preparative thin-layer chromatography (PTLC) [294], vacuum-liquid chromatography (VLC) [294, 295], medium-pressure liquid chromatography (MPLC) [294], high-vacuum distillation [80, 106], centrifugal circular thin-layer chromatography (CCTLC) [69], high-speed countercurrent chromatography (HSCCC) [106, 296–298], and droplet-countercurrent chromatography (DCCC) [110]. Normal- [299], reversed-phase [110, 295], and high-performance liquid chromatography (HPLC) are common methods used for the isolation of phthalides.

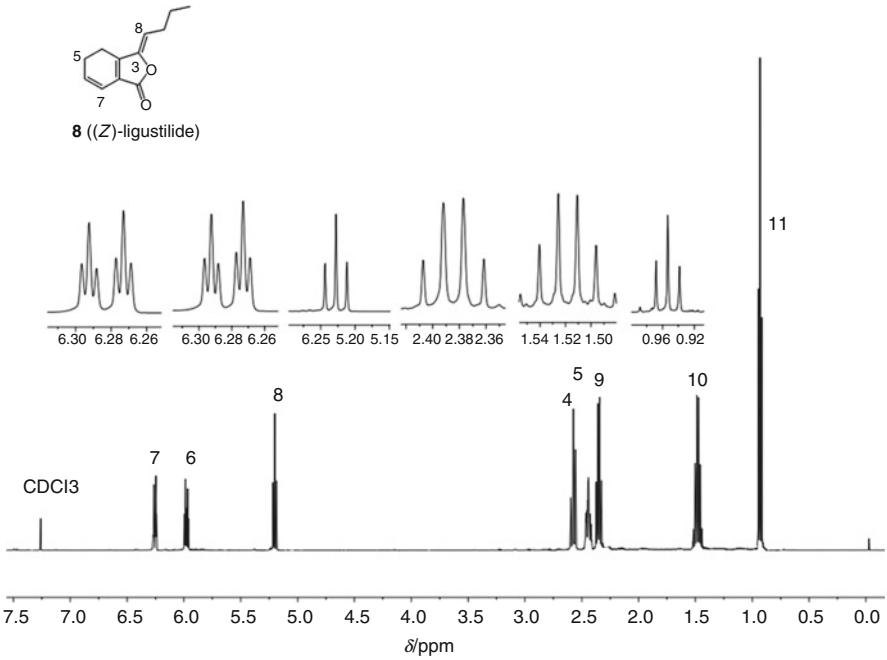

Fig. 2 ^{1}H NMR spectrum (500 MHz, $CDCl_3$) of (*Z*)-ligustilide (**8**)

The chemical characterization of phthalides has involved the determination of melting points [293], boiling points [36, 42], and chemical transformations such as saponification [293], hydrolysis [293], hydrogenation [35], ozonolysis [36], and oxidation [36], among others. Later on, these procedures were complemented with methods including infrared spectrometry [41, 44], ultraviolet spectroscopy [42, 44, 293], refractive indices [19, 293], optical rotations [293], gas chromatography (GC) [42], mass spectrometry (MS) [42], and NMR spectroscopy [36, 41]. Later, GC coupled to selective mass detectors and high resolution mass spectrometry (GC-MS) [44, 48] were included. The use of NMR spectroscopy [41, 51] and X-ray diffraction analysis has increased [51, 103], and a combination of both has been applied [93, 103, 300].

Figures 2, 3, and 4 show the ^{1}H NMR spectra for compounds **8**, **23**, and **43**, which are natural constituents of *Ligusticum porteri* [70].

3.2 Dereplication and Quality Control (HPLC, MS, NMR)

Dereplication is a process that facilitates the determination of the composition of a mixture of substances or of an extract [301]. It is focused on the rapid analysis of

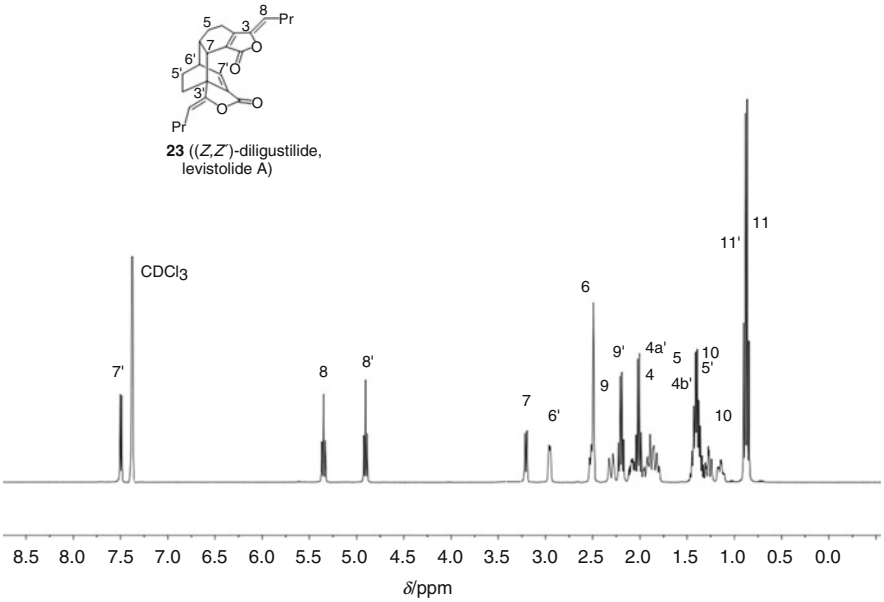

Fig. 3 ^{1}H NMR spectrum (500 MHz, $CDCl_3$) of diligustilide (**23**)

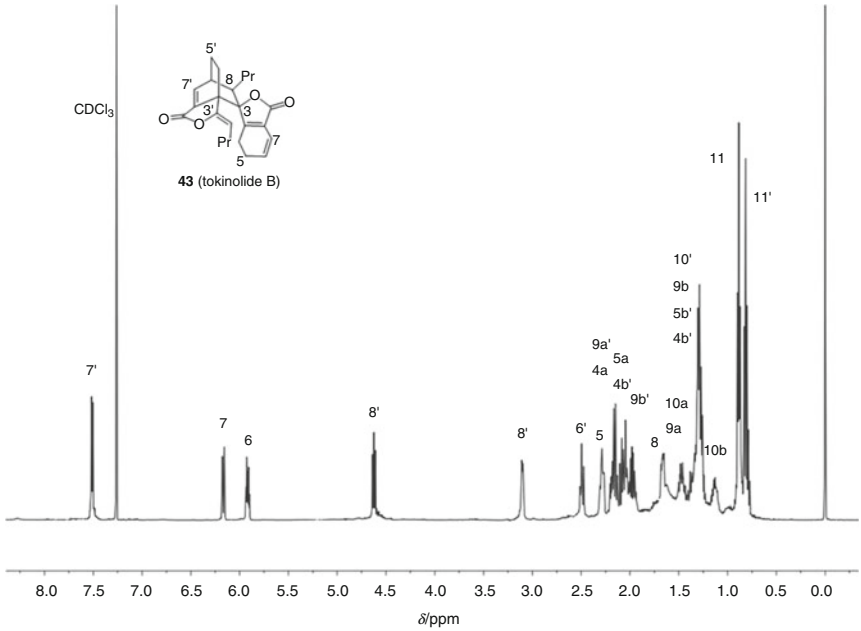

Fig. 4 ^{1}H NMR spectrum (500 MHz, $CDCl_3$) of tokinolide B (**43**)

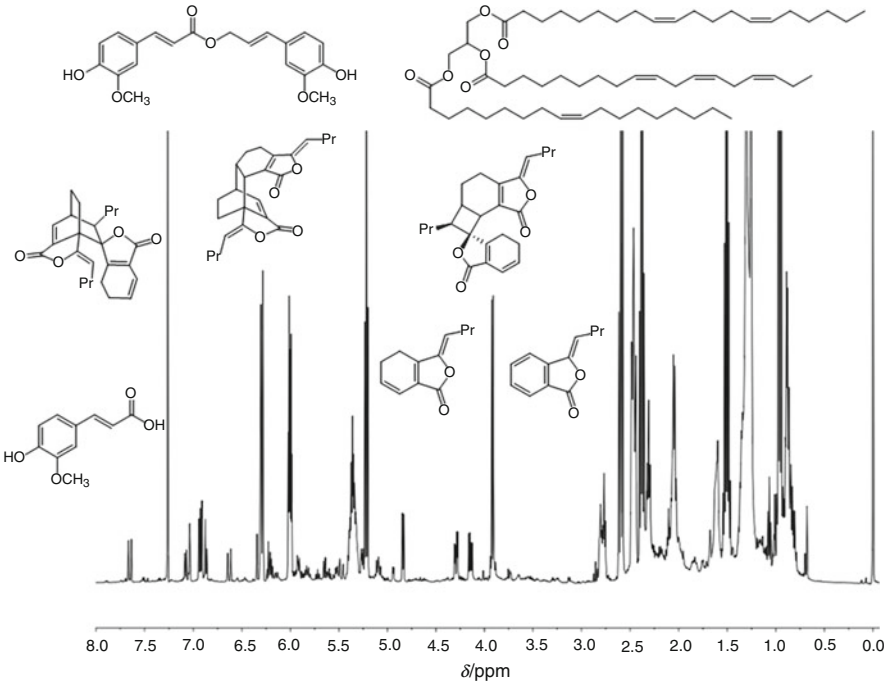

Fig. 5 Analysis of the components of *Ligusticum porteri* acetone extract by ^{1}H NMR spectroscopy (500 MHz, $CDCl_3$) [300]

known components present in crude plant material or medicinal herbal products without the isolation of compounds, and is based on the use of TLC, HPLC, and HPLC-coupled spectroscopic techniques, for instance, LC-MS and LCMS/MS [302, 303], and GC-MS [304]. Access to 1D ^{1}H NMR data at the initial steps of dereplication of crude extracts can accelerate substantially the whole process, e.g. the identification of the constituents in a crude acetone extract from rhizomes of *Ligusticum porteri* [300] (Fig. 5).

Quality control aims to ensure the consistency, efficacy, and safety of preparations from plants used in traditional medicine. A chemical fingerprint indicates the presence of multiple chemical markers within a sample. It has been used for determining the presence of phthalides in several Asian medicinal plants and herbal remedies [277, 305]. Among the phthalides present, (*Z*)-ligustilide (**8**) typically has been selected as a marker compound to perform the quality control of the roots of *Angelica sinensis* or *Ligusticum chuanxiong*, and HPLC and GC-MS are the main analytical methods for its quantification [281, 288, 305–308].

The identification and quantification of two major phthalides from *Ligusticum porteri* were established using a HPLC-diode array (DAD) method for quality

control purposes [309]. The secondary metabolite profiles of plants may be affected by many factors, including seasonal changes, harvesting time, cultivation sites, post-harvesting processing, adulterants or substitutes of raw materials, and procedures of extraction and preparation [60, 310, 311]. A practical tool for determining the variation of the constituents of plants (in the form of crude fresh extracts) is NMR spectroscopy. A qualitative chemical analytical procedure of an acetone extract of the rhizomes of *Ligusticum porteri* using ^{1}H NMR spectroscopy has been reported to establish the presence of the individual components (Fig. 5). This analysis verified that the dimeric phthalides diligustilide (**23**), riligustilide (**24**), and tokinolide B (**43**) occur as natural products in fresh *L. porteri* rhizomes. A protocol involving NMR spectroscopy has been developed for quantifying some of the constituents from this natural source [300].

Qin and co-workers reported the use of NMR spectroscopy to analyze *Ligusticum chuanxiong* rhizomes of several commercial types, collected from different regions in mainland China. The ^{1}H NMR spectra and HPLC profiles allowed comparison of the characteristics of the major constituents [311].

3.3 DOSY Experiments of Extracts of Ligusticum porteri

NMR spectroscopy is a powerful analytical technique for the examination of mixtures of organic compounds, which includes a specific procedure called Pulsed Gradient Spin Echo (PGSE) NMR, or the so-called Diffusion Ordered SpectroscopY (DOSY). This experimental technique is a tool for analyzing complex mixtures based on different translation diffusion coefficients, D, which depend on the molecular weight, size and shape of each compound. DOSY spectra show the diffusion coefficients on the vertical axis and the ^{1}H NMR chemical shifts on the horizontal axis [312, 313].

DOSY analysis [300] allowed the determination of the presence of (*Z*)-butylidenephthalide (**3**), (*Z*)-ligustilide (**8**), tokinolide B (**43**), diligustilide (**23**), ferulic acid (**296**), and coniferyl ferulate (**297**) in an acetone extract of the dried rhizomes of *Ligusticum porteri*. The NMR spectrum revealed four main diffusion rate levels: A, B, C, and D (Figs. 6 and 7). Looking at the δ 7.00–4.3 ppm region, the signals that appeared with a diffusion coefficient of 1.75×10^{-10} m^2/s (highlighted as level A), corresponding to a mixture of ferulic acid (**296**) and coniferyl ferulate (**297**). At levels B and C (diffusion coefficient range 2.20–2.45 $\times 10^{-10}$ m^2/s), the most representative signals were found for diligustilide (**23**) (H-7′ at δ 7.50, H-8 at δ 5.35 and H-8′ at δ 4.90 ppm) and tokinolide B (**43**) (H-7′ at δ 7.64 and H-8′ at δ 4.45 ppm). This analysis confirmed the occurrence of dimeric phthalides. The monomer (*Z*)-ligustilide (**8**) displayed a diffusion coefficient of 3.65×10^{-10} m^2/s (level D). DOSY NMR is a useful tool for detection of adulterants in plant extracts,

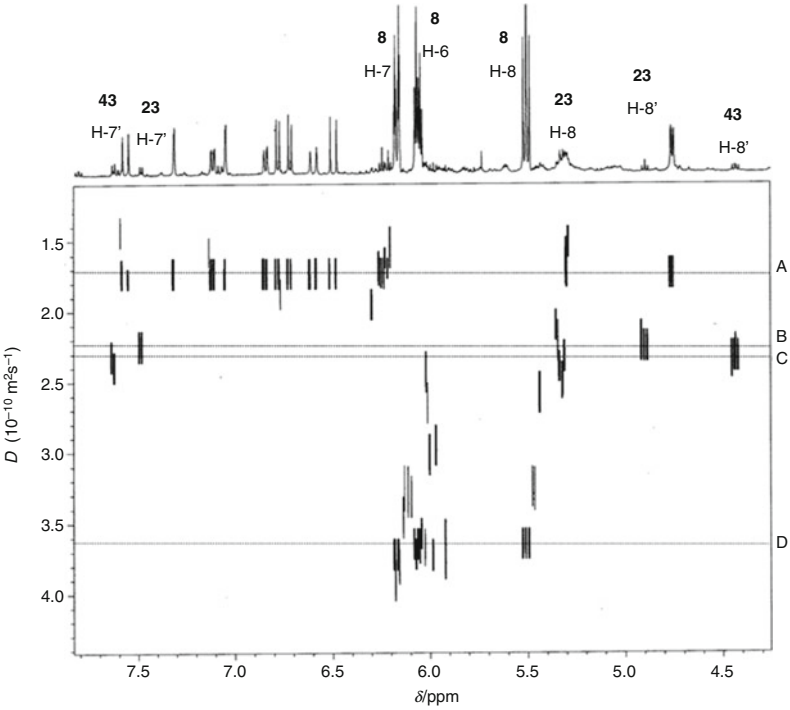

Fig. 6 DOSY spectrum of the acetone extract of *Ligustium porteri*. The ^{1}H NMR spectrum of the acetone extract is shown at the top. The assignments of some signals for (*Z*)-ligustilide (**8**), diligustilide (**23**), and tokinolide B (**43**) are displayed

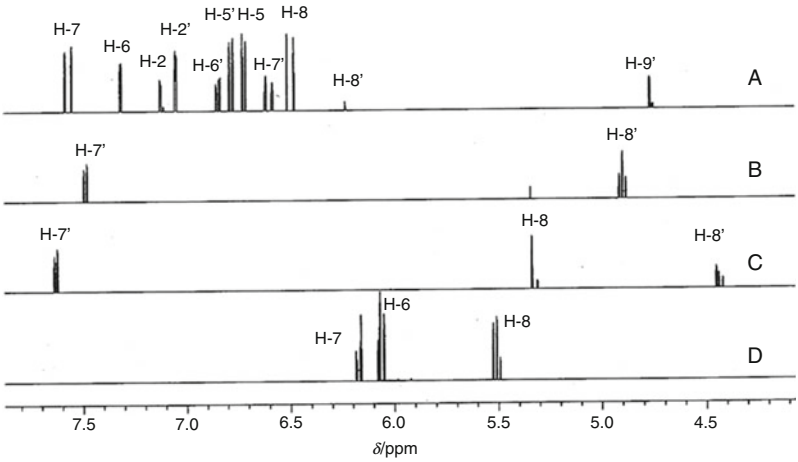

Fig. 7 DOSY slice spectrum with different diffusion coefficients: level A, mixture of ferulic acid (**296**) and coniferyl ferulate (**297**); levels B and C, diligustilide (**23**) and tokinolide B (**43**), respectively, and level D, (*Z*)-ligustilide (**8**)

or for fast and complete analysis of the phytochemical content of extracts and herbal medicines.

4 Biosynthesis of Phthalides

The study of the biosynthesis of phthalides began with the structural determination of mycophenolic acid (**141**), which is constituted by a phthalide fragment (derived from the polyketide pathway) and a terpene fragment (derived from the isoprenoid pathway). Birch and co-workers reported labeling studies with [1-^{14}C], identifying the polyketide and terpenoid pathways [314]. Afterwards, the presence of methoxy and methyl groups in the benzene ring of mycophenolic acid was demonstrated by the same group of investigators, using feeding experiments incorporating [$^{14}CH_3$]-methionine in cultures of *Penicillium brevicompactum* [315].

In 1966, the biosynthesis of phthalides was investigated also by Mitsuhashi and Nomura [272]. They studied the biogenetic origin of butylphthalides by conducting feeding experiments to explain the formation of ligustilide (**8**) in *Levisticum officinale*, and determined that the alkylphthalides have polyketide precursors.

In further work of this type, Canonica and co-workers [316] demonstrated by labeling experiments that the methyl group at C-4 in mycophenolic acid is incorporated at the tetraketide step, and that the formation of the benzene ring was carried out followed by subsequent transformations, yielding 5,7-dihydroxy-4-methylphthalide. Bedford et al. [317] studied the nature of the polyketide intermediates in the biosynthetic pathway from basic units, as acetate and mevalonate. Their study was performed with comparative incorporation experiments using [1′-^{14}C]-orsellinic acid and [1′-^{14}C]-4,6-dihydroxy-2,3-dimethylbenzoic acid, showing that the latter compound is a precursor of mycophenolic acid (**141**). A detailed review including the biosynthesis of mycophenolic acid (**141**) was published by Bentley [318].

The production of MPA (**141**) and analogs has been proposed using metabolic engineering as shown in Chart 1. Regueira et al. carried out experiments on the discovery of the involved enzymes (polyketide synthases, starter unit acyl carrier protein transacylase, β-ketoacylsynthase, acyltransferase, and methyltransferase, as well as the product template and acyl carrier protein responsible for the backbone synthesis of **141**) by means of the production of mpaC (which assembled the phthalide fragment of **141**) in a "gene cluster" in *Penicillium brevicompactum* [319].

Recently, Su and co-workers reported that phthalides could be biosynthesized through the acetate-malonate pathway. (*Z*)-Ligustilide (**8**), sedanolide (**6**), and some other derivatives are the result of reductions, oxidations, decarboxylation, cyclization, and dehydration [116].

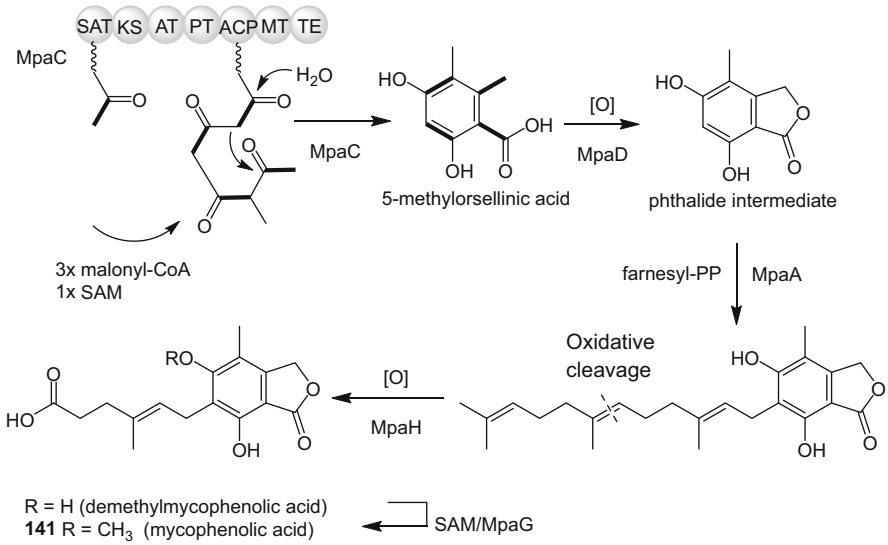

Chart 1 Biosynthesis route for mycophenolic acid ((**141**) MPA) (adapted from [319])

5 Reactions of Phthalides

Phthalides have been studied widely by some investigators, in attempts to understand the reactivity of this class of natural products, as well as aiming to establish structure-activity relationships (SAR) of biologically active natural phthalides, or determining their structures.

5.1 Derivatives of Monomeric Phthalides

5.1.1 Diels–Alder Adducts from (*Z*)-Ligustilide

One remarkable feature of the apparently simple structure of (*Z*)-ligustilide (**8**) is the conjugated cyclohexadiene moiety, which makes it able to undergo Diels–Alder reactions, both as diene and dienophile. Several natural dimeric phthalides, such as diligustilide (**23**) and tokinolide B (**43**), are Diels–Alder adducts of (*Z*)-ligustilide (**8**), and have been partially synthesized from this compound [320, 321] (see Sect. 6.2.1).

Some semisynthetic derivatives have been prepared from (*Z*)-ligustilide (**8**) and several dienophiles through Diels–Alder reactions. Thus, in the early 1960s, Mitsuhashi and co-workers [35] carried out the reaction of this phthalide with maleic anhydride, obtaining both *endo*-**298** and *exo*-**298** isomers. A 3:1 ratio for the products was reported more recently (see Fig. 8) [322]. The reaction with ethyl acrylate afforded *exo*- and *endo*-**299**, with this last compound being the major product. Theoretical calculations agreed with the experimental results, since the transition state involved in the formation of the major isomer was lower in energy.

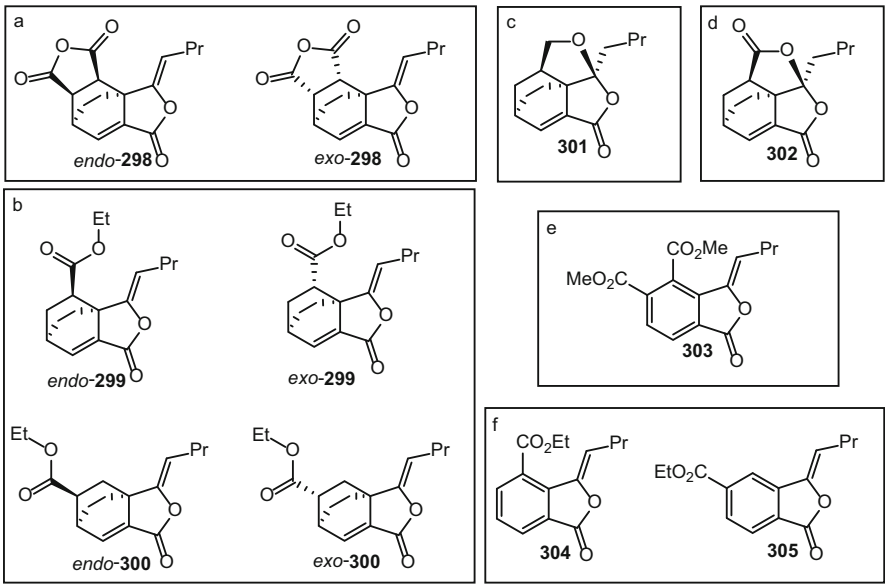

Fig. 8 Diels–Alder adducts of (*Z*)-ligustilide (**8**) with: (**a**) maleic anhydride; (**b**) ethyl acrylate, (**c**) acrylic acid, and (**d**) allyl alcohol. Alder–Rickert reaction products of (*Z*)-ligustilide (**8**) with (**e**) DMAD and (**f**) ethyl propiolate

When (*Z*)-ligustilide (**8**) was reacted with allyl alcohol in the presence of *p*-TsOH, or with acrylic acid **301** and **302** were obtained. The regio- and stereoselectivity of both reactions is noteworthy, since only one product was observed in each case. In the same study, Alder–Rickert reactions of (*Z*)-ligustilide (**8**) with ethyl propiolate or dimethyl acetylenedicarboxylate (DMAD) were carried out, yielding butylidenephthalide-type derivatives **303–305** [322].

5.1.2 Preparation of Linear Dimers from (*Z*)-Ligustilide

In an attempt to explore the [π4s + π2s] cycloadditions of (*Z*)-ligustilide (**8**) catalyzed by Lewis acids, the formation of the linear dimers **306–309** was reported, rather than of Diels–Alder adducts [323].

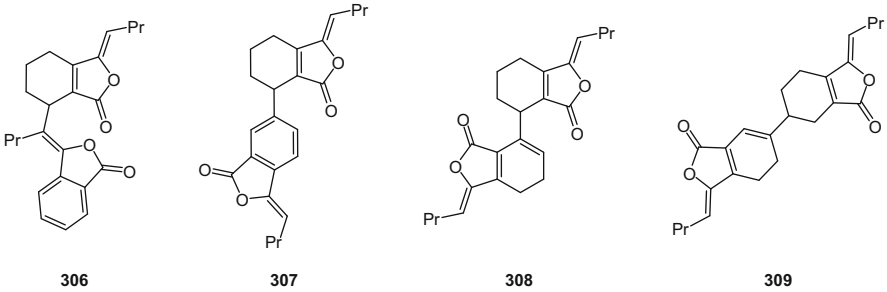

The authors suggested that complexation of Lewis acids with carbonyl oxygen or olefinic carbons, promoted cationic mechanisms. Thus, as depicted in Chart 2, it was proposed that the formation of the major product proceeded by a nucleophilic attack from C-6–C-7 double bond electrons towards C-8, in a 1,6-addition, facilitated by the complexation of Lewis acid with oxygen. Subsequent isomerizations through proton transfer reactions led to a cyclohexadiene that was dehydrogenated to yield the observed product **306** [323] (Chart 2).

Similarly, the presence of Lewis acid promoted 1,2 addition of one olefin moiety of (*Z*)-ligustilide (**8**) to the C-6–C-7 double bond of another (*Z*)-ligustilide (**8**) molecule through other carbocations (Chart 3). It is interesting to note that the second major product corresponds to the formation of an allyl cation at C-7, which is more stable than that formed when the cation is formed at C-6 [323].

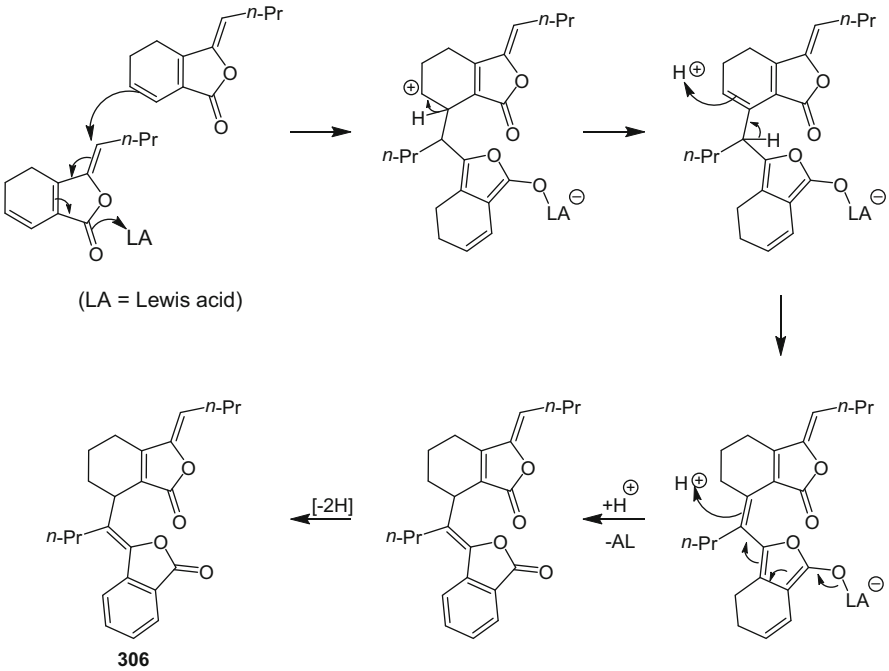

Chart 2 Formation of the major linear dimer **306**

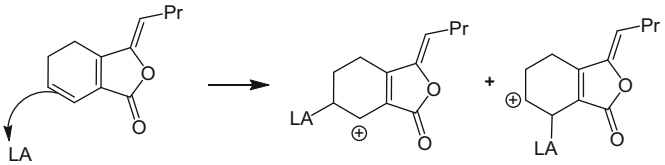

Chart 3 Other carbocations in linear dimer formation

Then, nucleophilic attack of one molecule of **8** to one of the cationic intermediates produces the carbon–carbon bonds necessary to yield dimers **307–309**, for which the formation takes place after acid–base equilibration steps, and dehydrogenation (in the case of **307**) [323].

5.1.3 Instability of (*Z*)-Ligustilide

Pauli and co-workers evaluated the purity and relative stability of isolates of (*Z*)-ligustilide (**8**) through quantitative NMR spectroscopy and GC-MS, and found that this compound decomposed rapidly when stored in $CDCl_3$ solution, or without solvent, even at −30°C. It was observed that the degradation process was slower when (*Z*)-ligustilide (**8**) was stored in hexane, methanol, DMSO, or in a mixture of hexane, ethyl acetate, methanol, and water (9:1:9:1). The degradation pathway was characterized by combining NMR and GC-MS techniques, leading to the determination of an epoxide, 4,5-dihydro-3-hydroxy-8-oxo-butylphthalide (**310**), butyraldehyde, and phthalic anhydride as degradation products [324].

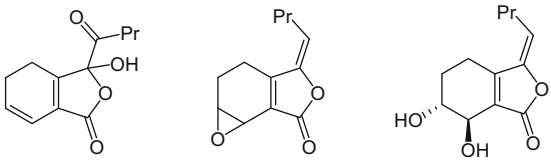

310 **311** **312**

Lin and co-workers detected that (*Z*)-ligustilide (**8**) spontaneously produced minor amounts of the dimeric phthalides diligustilide (levistolide A, **23**), riligustilide (**24**), and a mixture of *cis*- and *trans*-ligustidiol (**22** and **26**), suggesting that these phthalides could be artifacts [310]. However, various attempts to transform (*Z*)-ligustilide (**8**) into its Diels–Alder adducts on a preparative scale, did not proceed in good yields [35, 320, 321]. In addition, dimeric phthalides have been found in freshly prepared extracts of *L. porteri* [300], confirming their existence as natural products.

Hu and co-workers established that decomposition of (*Z*)-ligustilide (**8**) is influenced by temperature, light, and oxygen, and that the addition of vitamin C delays its transformation [325].

Additional evidence of the facile transformation of (*Z*)-ligustilide (**8**) were provided by Lau and co-workers. They analyzed the chemical composition of crude extracts of *Angelica sinensis* roots and *Ligusticum chuangxiong* rhizomes by gas chromatography-triple quadrupole mass spectrometry, and comparison of the extracts of the same plants before and after treatment with wine. (*S*)-Butylphthalide (**4**), (*Z*)-butylidenephthalide (**3**), senkyunolide A (**15**),

(*Z*)-ligustilide (**8**), and ferulic acid (**296**) were used as chemical markers. It was concluded that there were variations of the relative content of these compounds after wine treatment, indicating that the stability of phthalides depends on the presence of other compounds [326].

More recently, it was observed that (*Z*)-ligustilide (**8**), when exposed to sunlight at room temperature, was transformed into (*Z*)-6,7-epoxyligustilide (**38**), senkyunolide I (**22**), senkyunolide H (**26**), **311**, and **312**, as racemic mixtures, confirming the main degradation products of (*Z*)-ligustilide (**8**) [327].

5.1.4 Functional Group Transformations

Many reactions of phthalides have been carried out to determine the reactivity of this group of compounds, to establish structure–activity relationships, or as a tool for their structure elucidation.

Mitsuhashi and Kobayashi reported the epoxidation of (*Z*)-ligustilide (**8**) followed by hydrolysis, yielding senkyunolides H (**26**) and G (**22**), while senkyunolide A (**15**) gave senkyunolide J (**33**) [328]. When the hydrolysis of epoxyligustilide was conducted with hydrochloric acid, senkyunolide L (**45**), a chlorohydrin, was formed [73]. The same group also obtained reduced derivatives of ligustilide (**8**) [35], and, in an attempt to prepare the Diels–Alder adducts (tokinolide B (**43**) or diligustilide (**23**)), they subjected (*Z*)-ligustilide (**8**) to pyrolysis. The dimers were not observed, but instead small amounts of a dialdehyde, a product of oxidation of the C-6–C-7 double bond, was observed [72].

Beck and Stermitz submitted (*Z*)-ligustilide (**8**) to nitrogen and sulfur nucleophiles, obtaining a 1,2-addition product from the former nucleophile (**313**). It was found that the sulfur nucleophile gave a 1,6-addition to the α,β,γ,δ–unsaturated carbonyl fragment (**314**), and another addition–elimination product (**315**), and a disubstitution product (**316**). The results were in agreement with hard and soft acid and base theory [89].

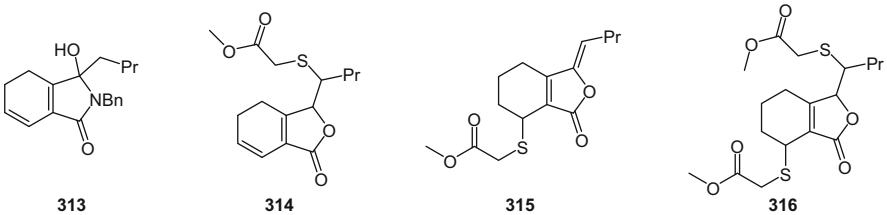

Cyclopaldic acid (**154**) exhibited insect-biting deterrent and larvicidal activities. Thus, in order to establish a structure–activity relationship (SAR) profile, Cimmino and co-workers [329] synthesized isocyclopaldic acid (**317**) and prepared other

cyclopaldic acid derivatives: this compound was mono- and tetraacetylated to afford **318** and **319**. The aldehyde reacted with 2,4-dinitrophenylhydrazine to give the corresponding hydrazone (**320**). Treatment of cyclopaldic acid with dansyl hydrazine yielded products **321** and **322**. The natural phthalide was also treated with 5-azidopentanoic acid and *N*,*N*′-dicyclohexylcarbodiimide, giving **323**. Finally, when the natural phthalide was treated with $NaBH_4$, the products **324** and **325** were obtained (see Chart 4) [329].

Wu and co-workers [330] prepared derivatives of mycophenolic acid (**141**). Its protected derivative was subjected to aminolysis, yielding the amidophenol **326**. The phenolic group was then transformed to thioacetate **327**, azide **328** and mesylate **329**. Furthermore, the mesyl derivative was used for the preparation of three new heterocyclic compounds, the corresponding 2,3-dihydroisoindolone (**330**), 2,3-dihydro-*N*-methylisoindolone (**331**), and benzothiophenone (**332**).

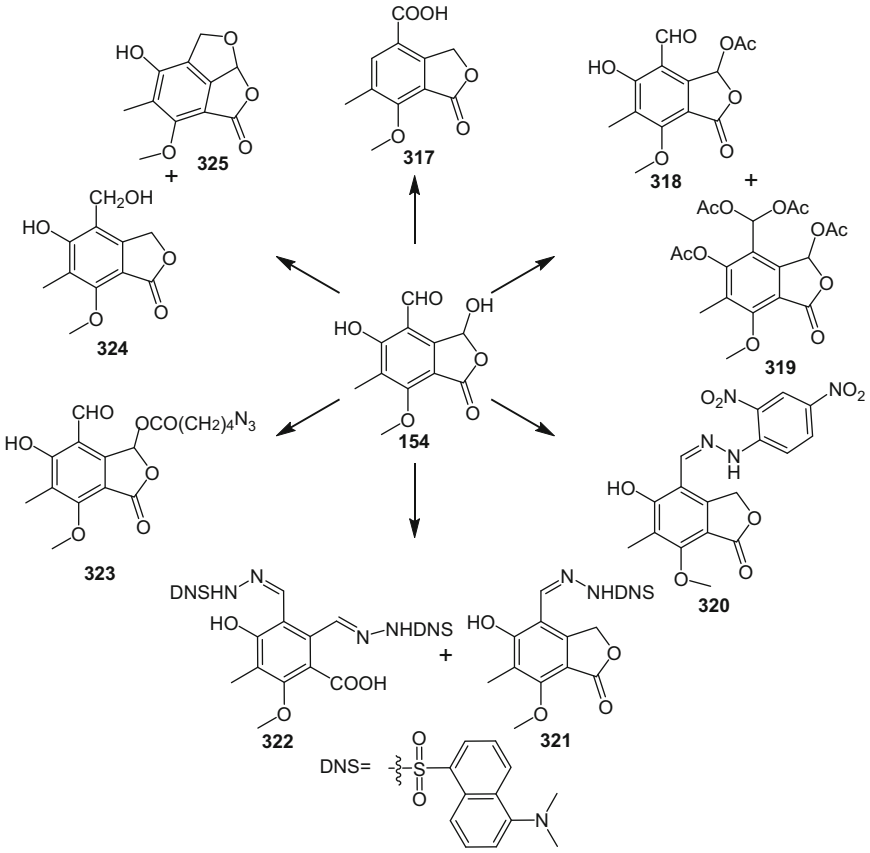

Chart 4 Cyclopaldic acid derivatives

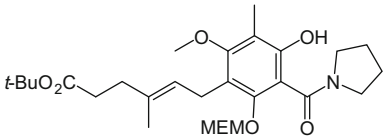

326

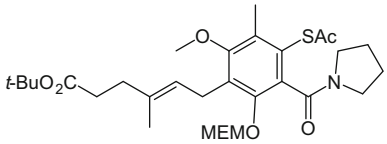

327

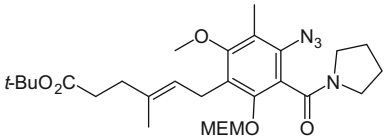

328

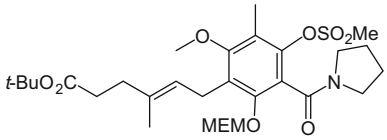

329

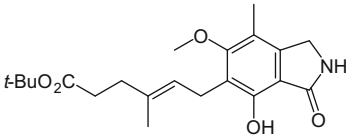

330

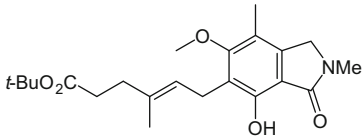

331

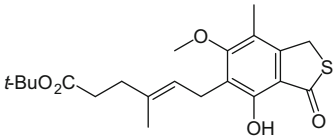

332

5.2 *Derivatives of Dimeric Phthalides*

The natural dimeric phthalides are obtained basically as [π4s + π2s] and [π2s + π2s] cycloadducts from two units of monomeric phthalides such as (*Z*)-ligustilide (**8**) and from (*Z*)-butylidenephthalide (**3**). They display interesting reactivities due to their topological characteristics and the presence of several reactive sites.

One of the first reports concerning the reactivity of dimers led to the correction of a structure obtained from *Ligusticum wallichii* by means of the catalytic hydrogenation of diligustilide (**23**), which yielded a mixture of 3,8,7′,7a′-tetrahydrodiligustilide (**333**) and (*Z*′)-3,8-dihydro-[6.6′,7.3a′]-diligustilide (**39**). This last compound had been previously reported as a natural compound, but spectroscopic data analysis permitted a structural correction to **40** (Chart 5) [70].

5.2.1 Intramolecular Condensations of Dimeric Phthalides

Alkaline treatment of diligustilide (**23**) under different conditions yielded the intramolecular condensation products **339**, **340** and **343**. The mechanism was

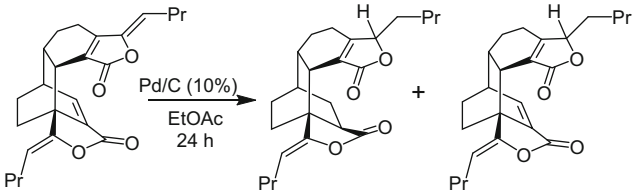

Chart 5 Hydrogenation of diligustilide (**23**)

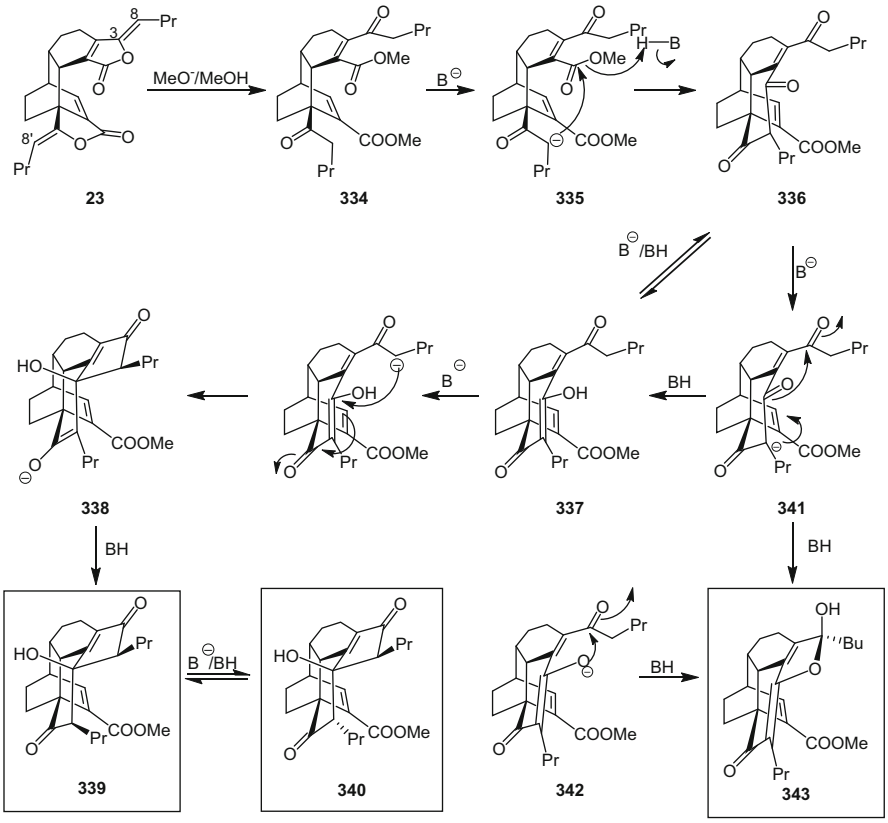

Chart 6 Base-catalyzed intramolecular condensation of diligustilide (**23**)

proposed as follows: the diketo diester **334** (obtained from the methanolysis of diligustilide (**23**)) underwent intramolecular reaction through deprotonation of the methylene at C-8′ (intermediate **335**), and subsequent addition to the carbonyl group-generated intermediates **336** and **337**. The carbanion of this last compound reacted intramolecularly to yield intermediate **338**, which equilibrated yielding **339** and **340** (Chart 6). O-Alkylation of tautomers **341** and **342** afforded **343** [331].

Treatment of diligustilide (**23**) with Na_2CO_3 in $Me_2CO/MeOH/H_2O$ afforded **340**, **339**, **343**, **344** (demethylwallichilide), and **345** (Chart 7).

Attempts to find better conditions to obtain products **339** and **343** and the hydrolysis products **344** and **345** from diligustilide (**23**) were made [332].

Treatment of tokinolide B (**43**) under basic conditions (NaOH in THF) yielded cyclotokinolide B (**346**) derived from an intramolecular condensation procedure. Its formation began with a chemoselective nucleophilic attack of the hydroxide ion to the carbonyl group at C-1, to produce an enolate (intermediate **A**), followed by Michael addition of the carbanion to the enone, by means of 5-*exo*-trigonal cyclization, yielding intermediate **B**, which produced cyclotokinolide B (**346**) (Chart 8). The results showed that intramolecular cyclizations are a general feature for these dimeric phthalides [333].

Treatment of tokinolide B (**43**) with base in acetone under reflux afforded ketoacid **347** by chemoselective lactone ring opening.

The reaction of ketoacid **347** with the chiral amines ((–)-(*S*)-α-methylbenzylamine and (+)-(*R*)-α-methylbenzylamine) under pressure afforded product **87**, tokinolide B (**43**), and the starting material (Chart 9).

The ketoacid of tokinolide B (**347**) displayed chemoselectivity under basic conditions. Strong alkaline conditions afforded **346** via C-alkylation, while mild alkaline conditions produced compound **87** (via O-alkylation) [118] (Chart 10).

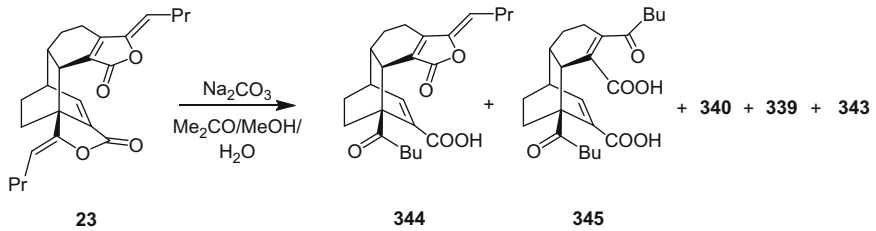

Chart 7 Products derived from basic hydrolysis of diligustilide (**23**)

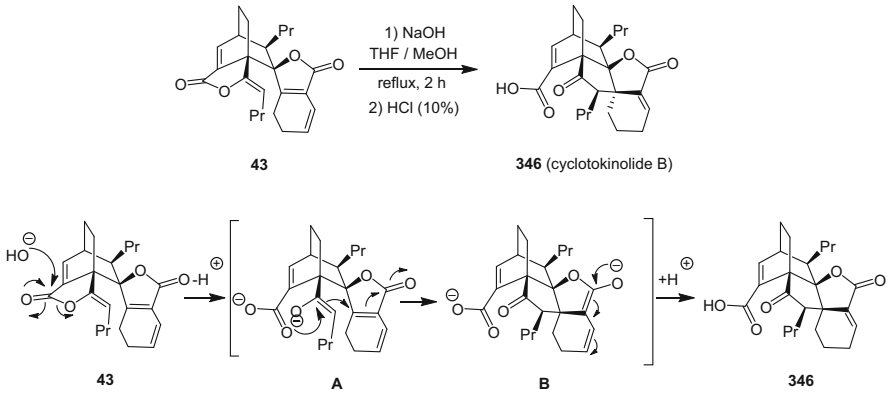

Chart 8 Formation of cyclotokinolide B (**346**)

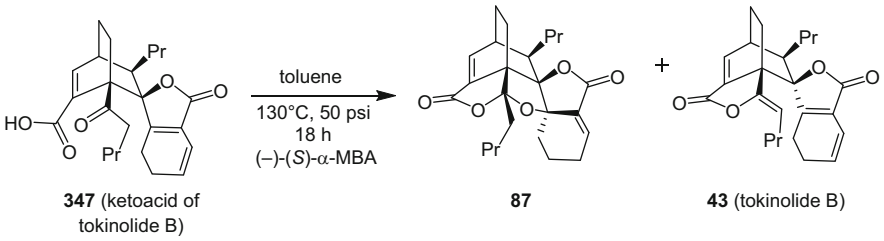

Chart 9 Derivatives obtained from the ketoacid of tokinolide B (**347**)

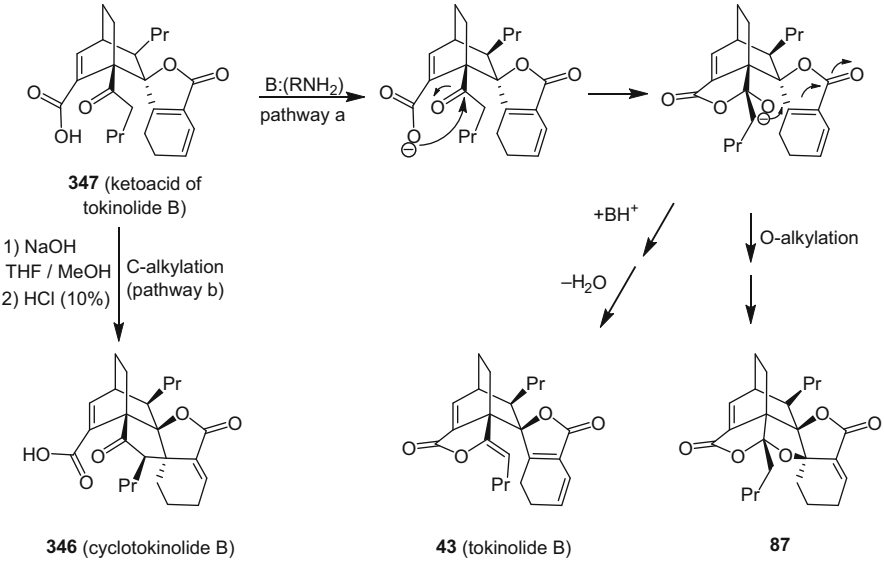

Chart 10 Proposed mechanism for the formation of **87** and **347**

This last compound was later characterized as a natural product from *Ligusticum sinense* cv. *chaxiong* and named chaxiongnolide B (**87**) [117] (see Chart 10).

Comparison of calculated energies for compounds **87**, **346**, and **347** indicated that **87** had a lower energy, followed by **346**, and this outcome may be correlated with the number of rings and conformational constraints of the structures (Fig. 9) [118].

The results on derivatives of intramolecular condensation provided evidence of the particular chemical reactivity of the natural dimeric phthalides.

5.2.2 Synthesis and Stereochemical Assignments of Enantiopure Derivatives

Taking in consideration that natural dimeric phthalides are found as racemic mixtures [70], enantiomeric derivatives of tokinolide B (**43**) and diligustilide

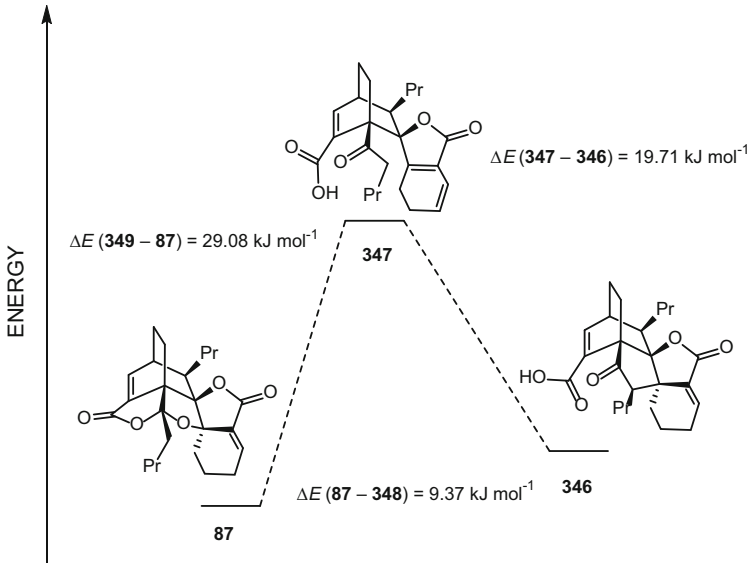

Fig. 9 Representation of total energies of **87**, **346**, and **347**. (Molecular computations were done at the B3LYP/6-311G level of theory)

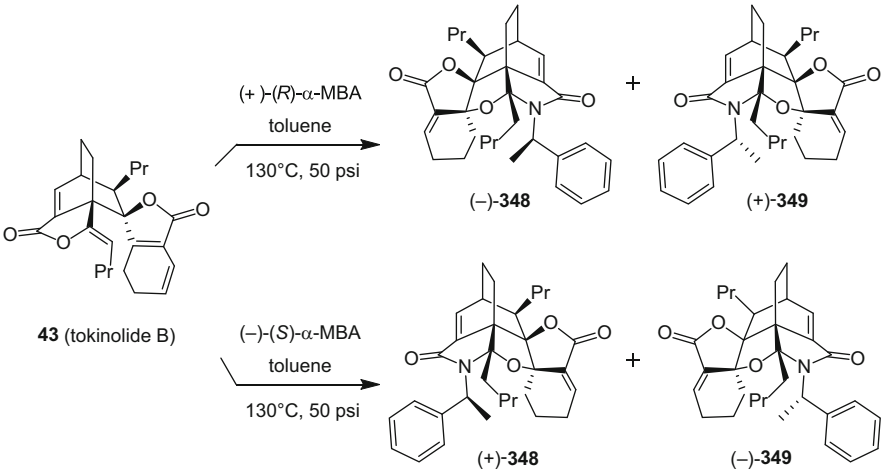

Chart 11 Diastereomeric mixtures of enantiomerically pure derivatives of tokinolide B (**43**)

(**23**) were prepared and evaluated as cytotoxic agents. Treatment of **43** with (+)-(*R*)-α-methylbenzylamine ((*R*)-MBA) and (–)-(*S*)-α-methylbenzylamine ((*S*)-MBA) afforded pairs of diastereomeric products, namely, (−)-**348** + (+)-**349** and (+)-**348** + (−)-**349** (Chart 11) [334].

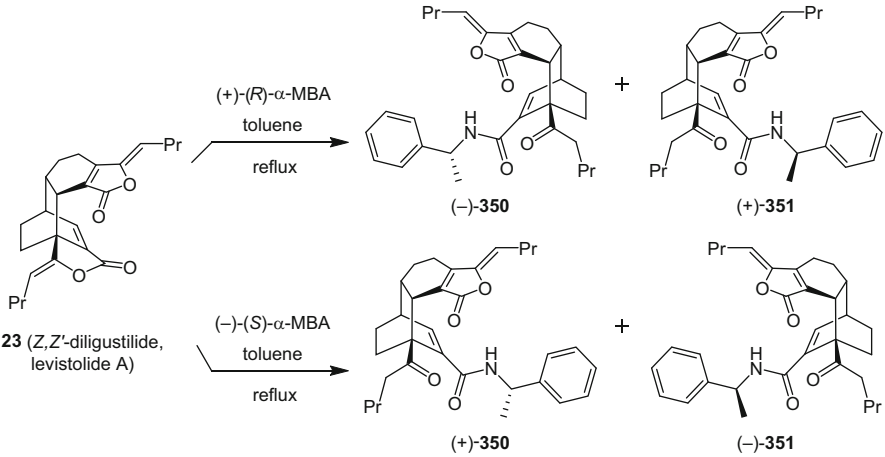

Chart 12 Diastereomeric mixtures of enantiomerically pure derivatives obtained from diligustilide (**23**)

The absolute configurations of (−)-**348**, (+)-**349**, (+)-**348**, and (−)-**349** were determined by analyzing their ECD curves, using the exciton chirality method and defining the direction of the transition dipole moments of the chromophores.

In a complementary manner, the enantiopure derivatives (−)-**350** + (+)-**351**, and (+)-**350** + (−)-**351**, were obtained, in turn, by treatment of diligustilide (**23**) with (*R*)- and (*S*)-α-MBA (Chart 12) [335].

The absolute configurations of the amides were determined by the interpretation of the electronic circular dichroism curves (ECD), as previously described for the derivatives of tokinolide B (**43**) [334, 335].

5.3 Biotransformations

Mycophenolic acid (**141**) and **143** were isolated from a culture of *Penicillium crustosum*, when mixtures of either ferulic (**296**) and quinic acids (**352**) or 3-methoxy-4-hydroxycinnamic acid (**353**) and 3,4-methylenedioxycinnamic (**354**) acids were added to the medium [170].

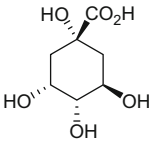

352 (quinic acid)

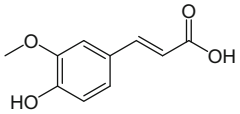

353 (3-methoxy-4-hydroxy cinnamic acid)

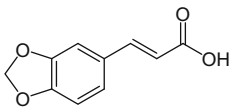

354 (3,4-methylenedioxycinnamic acid)

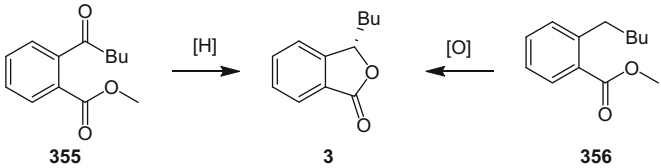

Chart 13 Microbial preparation of (*S*)-butylphthalide (**3**)

(*S*)-Butylidenephthalide (**3**) was prepared in 99% enantiomeric excess through microbial reduction of methyl 2-butyrylbenzoate (**355**) or microbial oxidation of methyl 2-pentylbenzoate (**356**) [336] (Chart 13).

Other derivatizations have been carried out for the resolution of racemic mixtures of phthalides. For example, the enzymatic resolution of racemic 3-butylidenephthalide (**3**) was achieved with Novozyme 435, which catalyzed the reaction between (*S*)-butylidenephthalide (**3**) and acetic anhydride to afford 2-((1*S*)-acetoxypentyl)-benzoic acid (**357**) in 98% *ee*, with up to 50.9% of unreacted 3-butylidenephthalide (**3**) remaining in 95.7% *ee* of the (*R*)-enantiomer [337–340] (Chart 14).

Several derivatives (**358–365**) of mycophenolic acid (**141**) were obtained by treatment with *Streptomyces* sp. [341, 342].

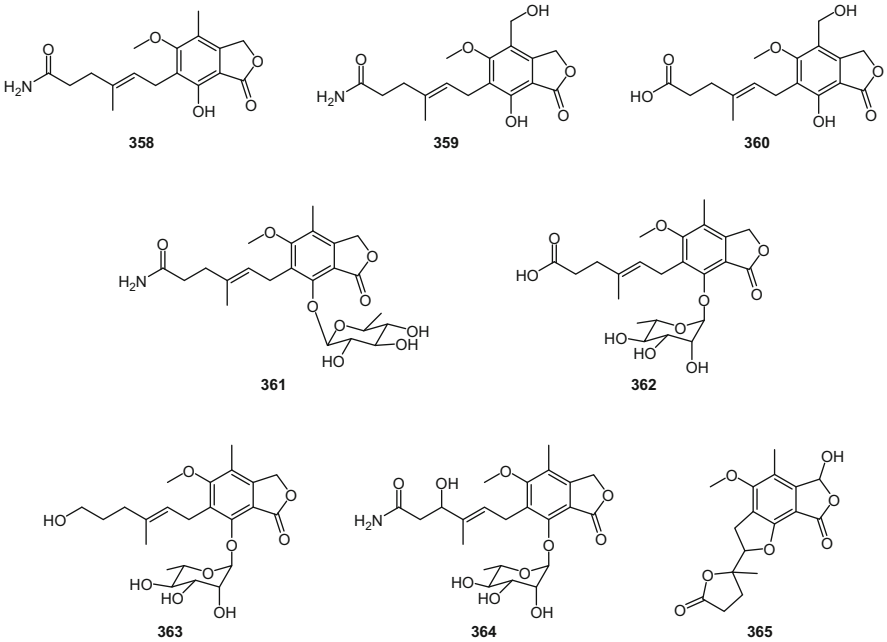

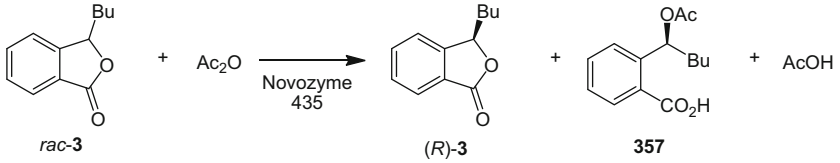

Chart 14 Enzymatic resolution of *rac*-**3**

Other modifications of **141** have been carried out by subjecting this phthalide to microbial transformation by 21 different species of bacteria, fungi and algae, furnishing phthalides **360** and **366–382**. The most common and abundant transformation products were the hydroxylactone **367**, resulting from oxidation at C-3, and **360**, by benzylic oxidation of the methyl group. Compound **372** was also obtained in relatively good yield. It is noteworthy that several *Penicillium* spp. were able transform mycophenolic acid (**141**) [343].

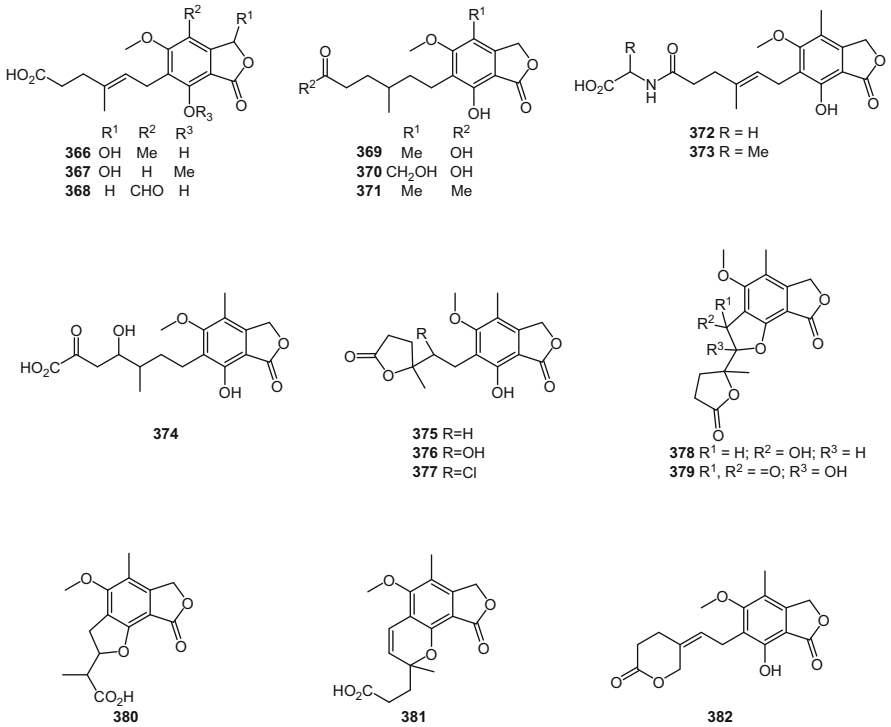

When *Polyporus brumalis* (Pers.) Fr. was supplemented with the phthalideisoquinoline derivative, (–)-β-hydrastine (**383**), this compound was hydroxylated with retention of configuration, yielding **384**, probably due to the action of a cytochrome-P450-dependent monooxygenase [344] (Chart 15).

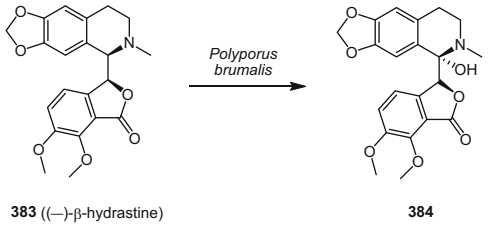

Chart 15 Hydroxylation of (–)-β-hydrastine (**383**)

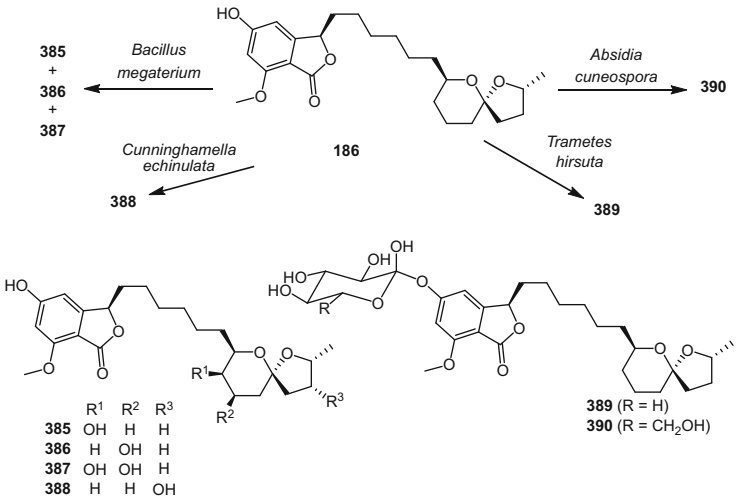

Chart 16 Microbial transformation of spirolaxine (**186**)

Spirolaxine (**186**) has been biotransformed by several microorganisms. *Bacillus megaterium* yielded phthalides **385–387** and *Cunninghamella echinulata* yielded **388** [345]. *Trametes hirsuta* transformed **186** into **389**, while *Absidia cuneospora* produced **390** [346] (Chart 16).

6 Synthesis of Phthalides

In view of the relevant biological properties of phthalides and, in particular, their chemical reactivity, many investigations have been devoted to the synthesis of these compounds. Research on this topic has resulted in a number of specific and interesting methodological procedures. In this section, selected approaches concerned with this topic are described. As a prior consideration, it is important to mention that Mal and co-workers [3] recently published a review covering part of this topic; nonetheless, in the present chapter the specific syntheses of naturally occurring phthalides are featured.

6.1 Synthesis of Monomeric Phthalides

The most direct approach for the synthesis of natural phthalides is to start from other natural phthalides. For example, Cimmino and co-workers prepared isocyclopaldic acid through a Canizzaro reaction, by treatment of cyclopaldic acid with base, reducing C-3 and oxidizing the formaldehyde at C-5 [329]. Other examples of this approach are the semisynthesis of senkyunolides H-J (**26**, **22**, and **33**) and L (**45**) [73, 328] (see above).

Salfredin B_{11} (**210**) was synthesized by Babu and Mali [347] from **90** and 3-chloro-3-methylbutyne, and subsequent thermal cyclization with dimethylphenylamine (Chart 17).

The terpenoid phthalide **151** was proved to be involved in the biosynthesis of mycophenolic acid (**141**), and was prepared by semi- and total synthesis [173] (Chart 18). Mycophenolic acid (**141**) was reduced to the corresponding aldehyde

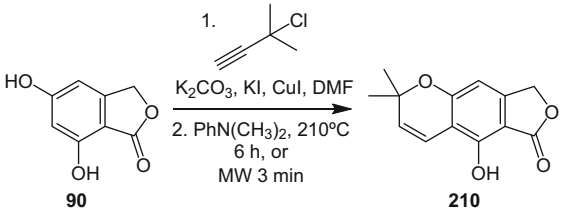

Chart 17 Synthesis of salfredin B_{11} (**210**)

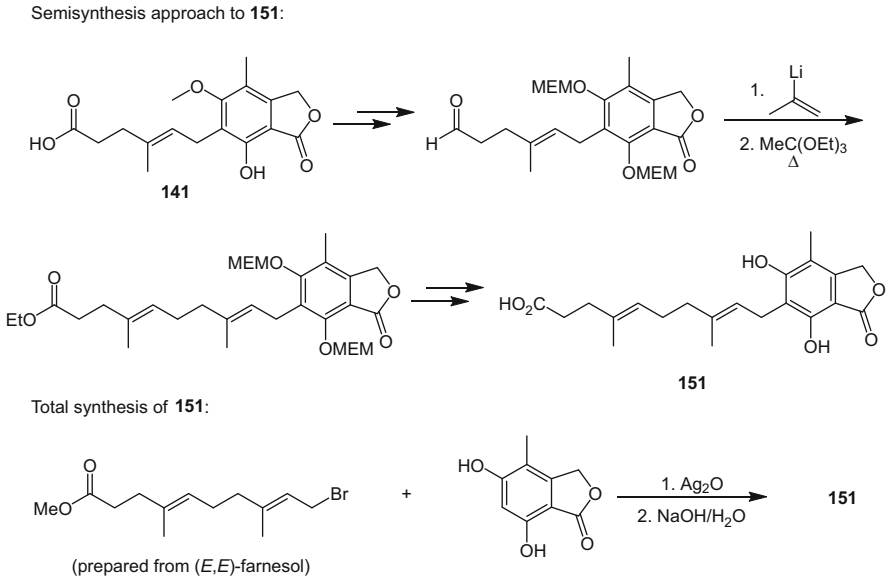

Chart 18 Semisynthesis and total synthesis of phthalide **151**

and coupled with propenyl lithium. The resulting compound yielded the natural product **151** after a Claisen-type rearrangement and hydrolysis. On the other hand, the total synthesis consisted basically of transforming (*E*,*E*)-farnesol into 10-bromo-4,8-dimethyl-deca-4,8-dienoic acid, and conducting the alkylation of 5,7-dihydroxy-3-methylphthalide with the former compound, in the presence of Ag_2O.

A number of more complex total syntheses of natural phthalides have been developed and some selected examples are described below.

6.1.1 Formation of the Cyclohexane Ring: The Alder–Rickert Reaction

The Diels–Alder reaction between cyclohexadienes and acetylenes, followed by retrocycloaddition, yields substituted benzenes and ethylene. This transformation is called the Alder–Rickert reaction and has been employed widely for the synthesis of phthalides substituted at C-4, C-5, C-6, and/or C-7 [348].

One of the first reports using the Alder–Rickert reaction was Birch and Wright's total synthesis of mycophenolic acid (**141**) [315], devoted to the formation of the benzene ring needed for the phthalide moiety, as depicted in Chart 19. The synthesis started from resorcinyl dimethyl ether, which was subjected twice to sequential Vilsmeier–Haack formylation/Wolff–Kishner reduction steps, followed by Birch's reduction and isomerization of the product. The resulting cyclohexadiene was subjected to an Alder–Rickert reaction with dimethyl acetylene dicarboxylate (DMAD), yielding a substituted dimethyl phthalic ester. It was then demethylated and converted into the corresponding phthalic anhydride, which was in turn

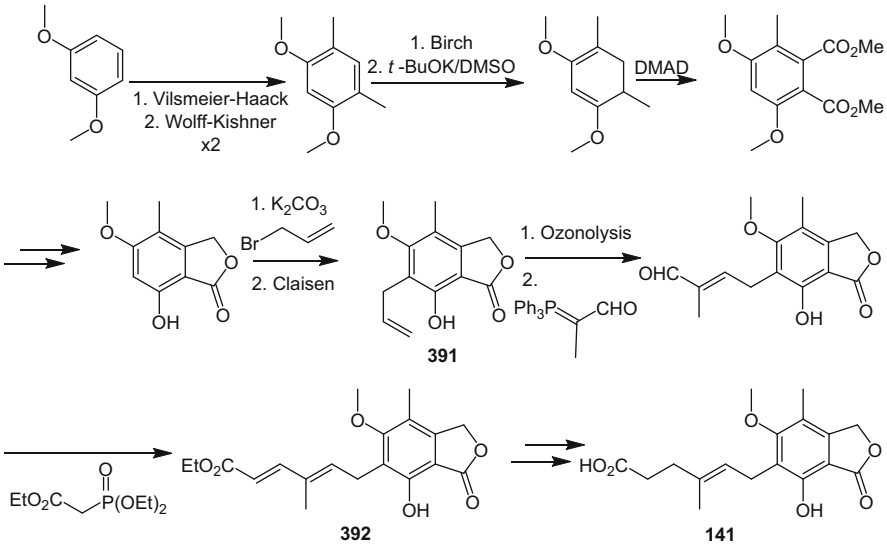

Chart 19 Birch's synthesis of mycophenolic acid (**141**)

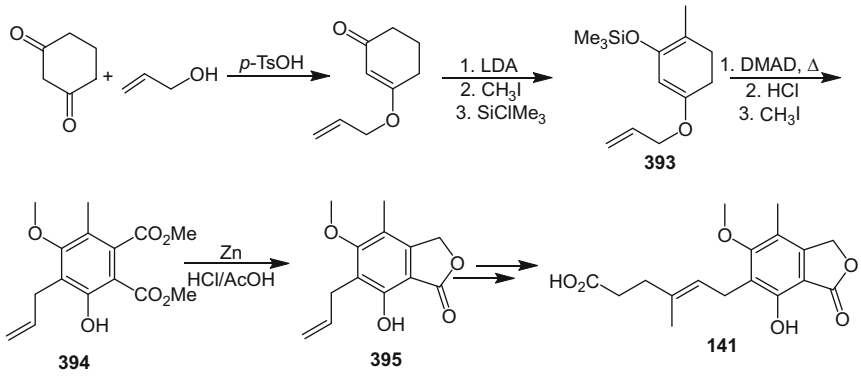

Chart 20 Patterson's synthesis of mycophenolic acid (**141**)

selectively reduced with Zn/HCl. Alkylation of the hydroxy group followed by Claisen rearrangement furnished **391**. This last compound was subjected to ozonolysis, then to a Wittig reaction, and next to the Horner–Wadsworth–Emmons reaction, yielding the ethyl ester of dehydromycophenolic acid **392**. Finally, this compound was hydrolyzed and reduced with diimide to yield MPA (**141**) (see Chart 19).

Patterson also reported a synthesis of **141** involving the Alder–Rickert reaction between trimethylsilyloxy enol **393** and DMAD, as shown in Chart 20 [349]. The product was then isomerized through a Claisen rearrangement. The resulting dimethyl *o*-dicarboxylbenzoate **394** was reduced with Zn to yield phthalide **395**, which was subjected to ozonolysis. This aldehyde was reacted with 2-propenyl magnesium bromide, and the thermolysis of the resulting alcohol with triethyl orthoacetate in the presence of propionic acid yielded MPA (**141**). More recently, Barrett and co-workers [350] reported an additional total synthesis of MPA (**141**) in 12 steps, which included a biomimetic cyclization–aromatization step starting from a polyketide-like compound.

The fungal phthalides 5-(3′,3′-dimethylallyloxy)-7-methoxy-6-methylphthalide (**199**), 6-(3′,3′-dimethylallyloxy)-4-methoxy-5-methylphthalide (**207**), and silvaticol (**183**) were prepared by Hariprakasha and co-workers [351] using the Alder–Rickert reaction between diene **396** and DMAD to furnish a polysubstituted benzene ring that was then *O*-prenylated and hydrolyzed to furnish **397** (see Chart 21).

Acid-catalyzed dehydration of diacid **397** yielded the corresponding phthalic anhydride, which was reduced with $NaBH_4$ and hydrolyzed with K_2CO_3, yielding silvaticol (**183**) (Chart 22).

A mixture of prenylated phthalides **199** and **207** was obtained, accomplishing the cyclization of phthalic acid **397** with DCC, and then reducing with $NaBH_4$. An alternative approach to these phthalides is to reduce the dimethyl phthalic ester **398** with DIBAL, followed by oxidative cyclization of the diol with PCC. It is interesting to note that the use of each procedure produces a switch in regioselectivity. Thus, the former methodology forms phthalides **199** and **207** in a 1:4 ratio; on the other hand, the ratio using the second methodology was 3:1 (see Chart 23) [351].

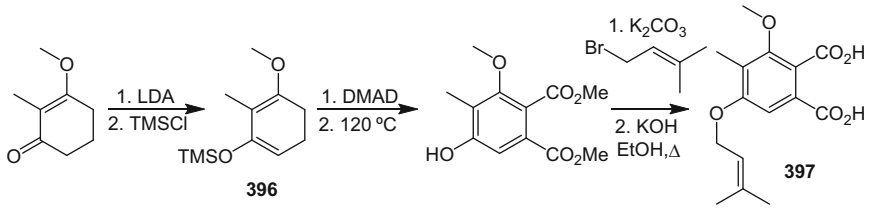

Chart 21 Synthesis of silvaticol (**183**) (Part 1)

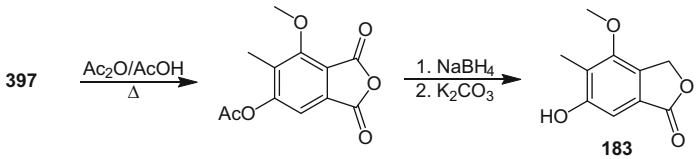

Chart 22 Synthesis of silvaticol (**183**) (Part 2)

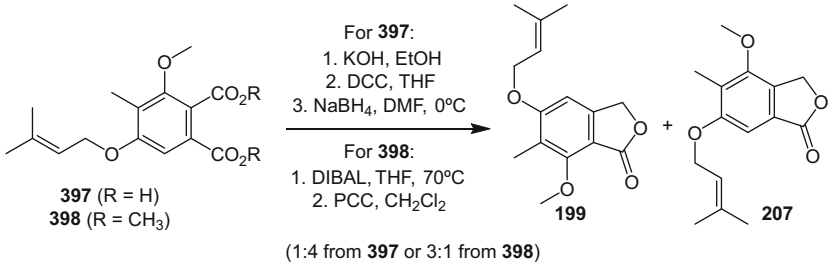

Chart 23 Synthesis of phthalides **199** and **207**

Kuwahara and co-workers [352] prepared both enantiomers of the fungal phthalide **202** starting from the protected dienol **399**, which underwent an Alder–Rickert reaction and then deprotection to yield 4-hydroxy-6-methoxy-3,5-dimethyl-1,2-benzene-dicarboxylate (**400**). Alkaline hydrolysis and reduction with Zn in aqueous HCl furnished phthalide **401**. After O-alkylation with the appropriate bromoester, deprotection, and oxidation, both enantiomers of **202** were obtained. The preparation of both enantiomers allowed identification of (*S*)-**202** as the natural product (see Chart 24).

6.1.2 Preformed Cyclohexane Ring and Formation of the Lactone Ring

The syntheses of less substituted phthalides, and mainly 3-substituted phthalides, have been investigated widely. In these cases, the use of accessible preformed benzene rings is a common feature, and there are several procedures for obtaining the lactone ring. A procedure for the preparation of 3-(2,6-dihydroxyphenyl)

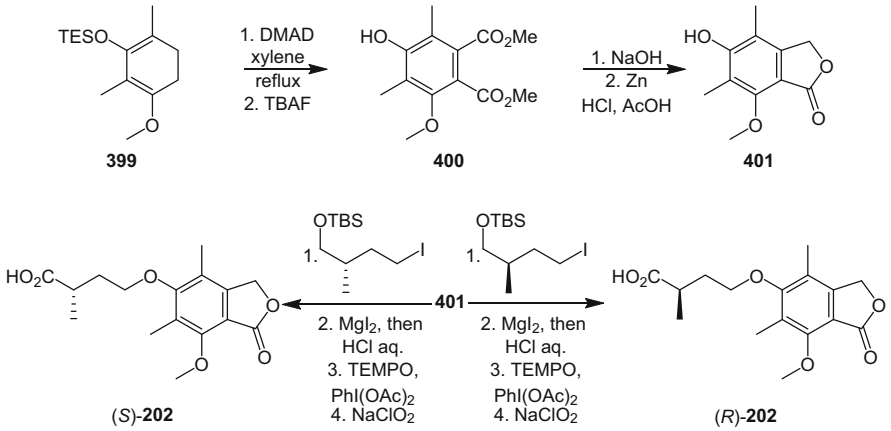

Chart 24 Total synthesis of **202**

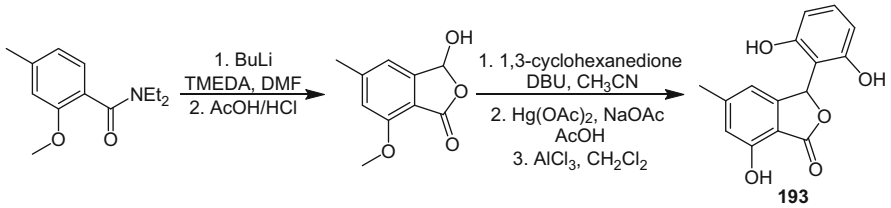

Chart 25 Preparation of isopestacin (**193**)

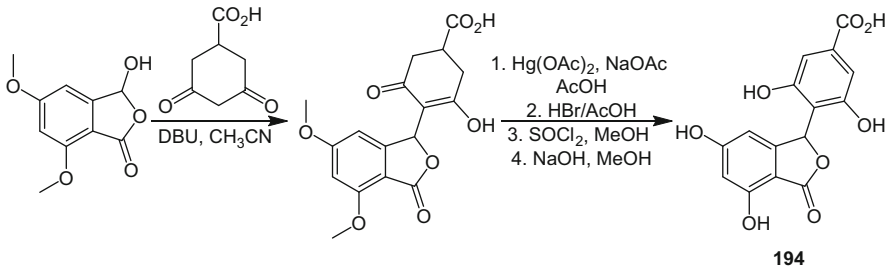

Chart 26 Preparation of cryphonectric acid (**194**)

phthalides was developed by Mal and co-workers. It is based on the reaction of phthalaldehydic acids with enamines of 1,3-cyclohexanediones and subsequent aromatization, and it was used for the preparation of isopestacin (**193**) and cryphonectric acid (**194**). This latter compound was esterified and hydrolyzed for its characterization. Attempts to prepare these natural products in an enantioselective manner were futile (see Charts 25 and 26) [353].

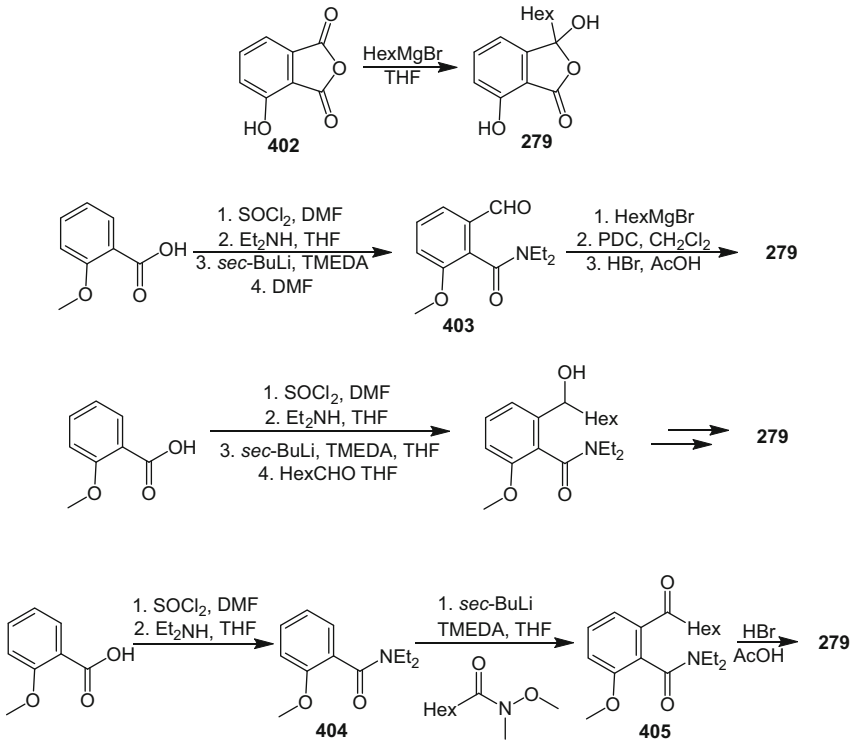

Chart 27 Synthesis methodologies for corollosporine (**281**)

Ohzeki and Mori carried out four approaches to obtain corollosporine (**279**), which are shown in Chart 27. The first of these consisted of a one-step reaction of 3-hydroxyphthalic anhydride (**402**) with hexylmagnesium bromide, which was the most direct route (36% yield), although it lacked effectiveness because of difficulties in purification. The second method involved the preparation of *N*,*N*-diethylacetamide of *o*-methoxybenzoic acid, followed by the *ortho*-metalation of Snieckus conducted with *sec*-butyllithium in the presence of tetramethylethylenediamine (TMEDA), and then *N*,*N*-dimethylformamide (DMF), furnishing **403**. This product was first converted into a secondary alcohol through a Grignard reaction with hexylmagnesium bromide, then oxidized to the ketone, and finally hydrolyzed and demethylated with hydrobromic acid to yield **279**. Another synthetic route avoided the Grignard reaction of **403** by treatment of an *ortho*-metallated anion with heptanal and following the above-described steps (oxidation, hydrolysis, and demethylation), afforded the desired compound. The last strategy consisted of a reaction of *N*,*N*-diethylacetamide **404** with the appropriate Weinreb amide and hydrolysis and demethylation of the furnished ketone **405** to yield **279** [354].

In the procedure described by Ranade and co-workers, ethyl 3,5-dimethoxybenzoate (**406**) was reduced, acetylated, and formylated (by means of the Vilsmeier–Haack reaction) to produce **407**. An oxidative cyclization of this last compound led

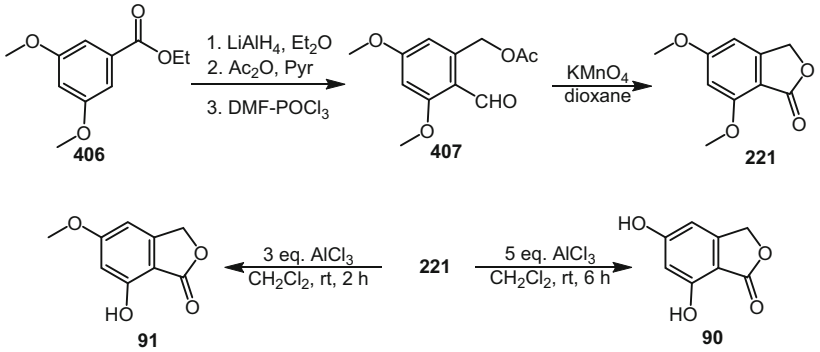

Chart 28 Synthesis of **90**, **91** and **221**

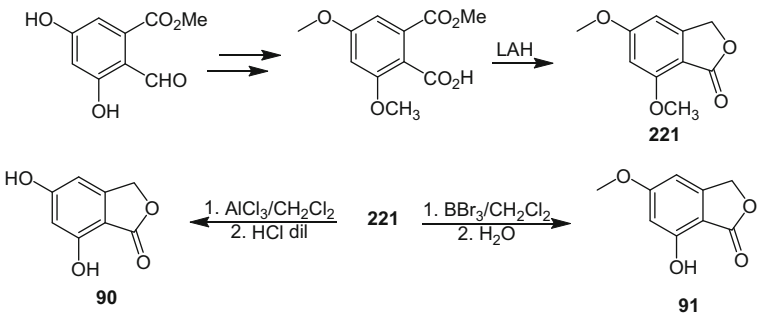

Chart 29 Alternative synthesis of **90**, **91** and **221**

to naturally occurring 5,7-dimethoxyphthalide (**221**), which was mono- or bidemethylated with $AlCl_3$ to yield the corresponding natural phthalides **90** and **91** (see Chart 28) [355].

Similarly, Talapatra and Talapatra synthesized these three natural phthalides starting from methyl 2-formyl-3,5-hydroxybenzoate, with protection and selective reduction with LAH, yielding one of the natural phthalides (**221**). Compounds **90** and **91** were obtained through partial or total demethylation, almost in the same conditions reported previously (see Chart 29) [356].

The synthesis of 3-substituted phthalides, among them senkyunolides B (**37**) and C (**28**), was achieved starting from appropriate 3-hydroxybenzoates (**408** or **409**) that were converted into nonaflates, to effect cross coupling of the resulting products with alkynes through a palladium-catalyzed Negishi type reaction. Hydrolysis of the resulting 2-alkynylbenzoates (**410** or **411**) and selective 5-*exo-dig* cyclization catalyzed by silver powder gave these phthalides in good yield. It is worth mentioning that when $AgNO_3$ was used as the catalyst instead of Ag powder, the resulting products were the analogous isocoumarins. In addition, senkyunolide E (**30**) was synthesized by saponification of methyl 2-(3-hydroxypentynyl)benzoate [357]. This procedure is shown in Chart 30.

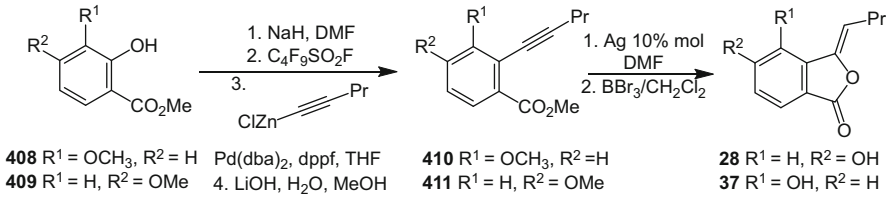

Chart 30 Synthesis of 3-alkenylphthalides from alkynyl benzoates

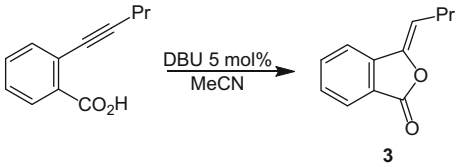

Chart 31 Synthesis of (*Z*)-butylidenephthalide (**3**)

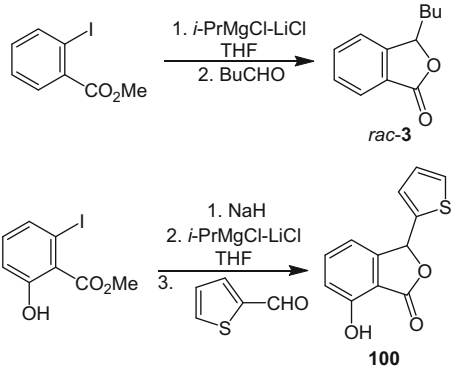

Chart 32 Synthesis of 3-substituted phthalides through Barbier reactions

In a similar manner, Kanazawa and Terada synthesized (*Z*)-butylidenephthalide (**3**) from *o*-pentynylbenzoic acid by means of a nucleophilic intramolecular addition, catalyzed by DBU (see Chart 31) [358].

Kuethe and Maloney employed a method essentially based on halogen–metal exchange of methyl *o*-iodoesters via a Barbier-type reaction with *i*-PrMgCl-LiCl, followed by quenching with carbonyl compounds, yielding racemic mixtures of the natural phthalides 3-butylidenephthalide (*rac*-**3**) and chrycolide (**100**) [359] (Chart 32).

Mondal and Argade reported regioselective procedures starting from 5,7-dihydroxyphthalide (**90**) and an α,β-unsaturated aldehyde, through which it proved possible to obtain selectively two kinds of skeletons, representing an adequate synthetic procedure for salfredin B_{11} (**210**) and phthalidochromene (**97**). When

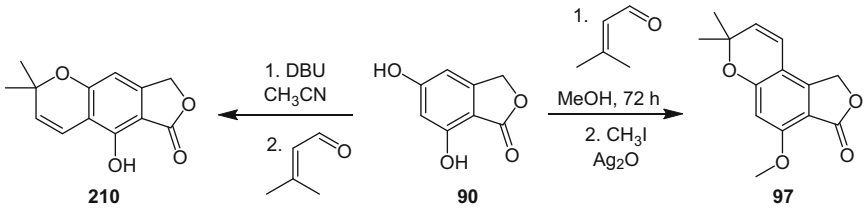

Chart 33 Synthesis of tricyclic terpenoid phthalides

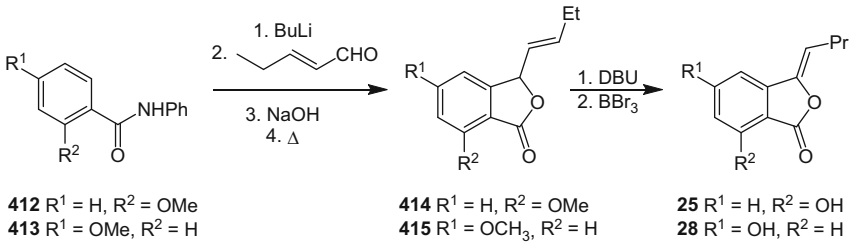

Chart 34 Wakamatsu's synthesis approach to 3-alkenylhydroxyphthalides

the starting phthalide was treated with DBU or other diaza-bases, a dianion was formed, and the more reactive C-6 anion underwent a nucleophilic attack (1,2-addition) at the carbonyl carbon from 3-methyl-3-butenal. The subsequent attack from oxygen at the remaining vinylic system, followed by dehydration, furnished the linear structure of salfredin B_{11}-like products. However, if 5,7-dihydroxyphthalide (**90**) was refluxed in methanol, with subsequent additions of the aldehyde, the "angular" tricycle was obtained exclusively, after methylation in the presence of Ag_2O, leading to the natural product **97** (see Chart 33) [360].

Wakamatsu and co-workers developed a synthetic pathway consisting of the lithiation of 2-methoxy-*N*-phenylbenzamide **412** (prepared from the corresponding carboxylic acid) with butyllithium in the presence of TMEDA, followed by nucleophilic attack on (*trans*)-2-pentenal, hydrolysis, and thermal cyclization, affording phthalide **414**, which was further isomerized and demethylated to yield the natural compound (*Z*)-3-butylidene-7-hydroxyphthalide (**25**). Similarly, (*Z*)-3-butylidene-5-hydroxyphthalide (**28**) was obtained starting from benzamide **413** and phthalide **415** as the intermediate (see Chart 34) [361].

Li's group synthesized (*Z*)-ligustilide (**8**) starting from *o*-formylbenzoic acid, which was converted into a 1:1 (*E*)/(*Z*) mixture of 2-butylidenebenzoic acid through a Wittig reaction, then oxidized with H_2O_2. The resulting *threo*/*erythro* mixture of 8-hydroxy-3-butylphthalide was reduced under Birch conditions, and the hydroxyphthalide obtained was dehydrated, affording **8** (see Chart 35) [362].

Beck and Stermitz reported an improved methodology for synthesizing phthalide **8** in three steps, starting from phthalide, which was treated with lithium diisopropyl amide (LDA) and then butyraldehyde, followed by Birch reduction and dehydration with MsCl (see Chart 36) [89].

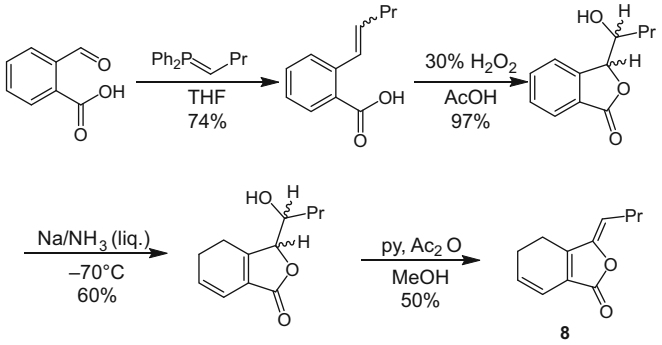

Chart 35 Li's synthesis of (*Z*)-ligustilide (**8**)

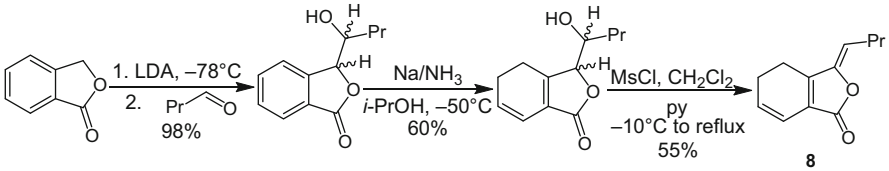

Chart 36 Beck's synthesis of (*Z*)-ligustilide (**8**)

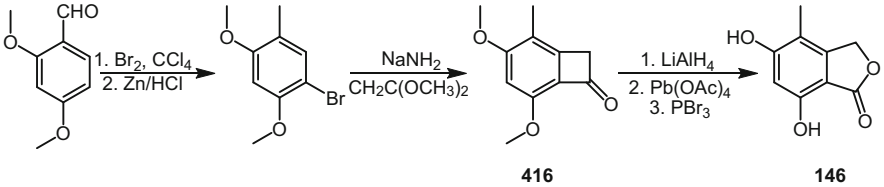

Chart 37 Synthesis of phthalide **146**

Kobayashi and co-workers developed a procedure in which 5,7-dihydroxy-4-methylisobenzofuran-1-(3*H*)-one (**146**) was synthesized from benzocyclobutenone **416** (prepared from 2,4-dimethoxybenzaldehyde, which was brominated and then reduced through a Clemmensen reaction to afford 1-bromo-2,4-dimethoxy-5-methylbenzene, and then treated with 1,1-dimethoxyethylene under Birch conditions. This compound (**416**) was transformed into the natural phthalide through reduction ($LiAlH_4$) and subsequent oxidation (with $Pb(OAc)_4$) [363]. Phthalide **146** can be used for the synthesis of MPA (**141**), so it constitutes a formal synthesis of the last-mentioned compound (see Chart 37).

The synthesis of naturally occurring 7-hydroxy-4,6-dimethylphthalide (**247**) was achieved by Takei and co-workers by means of the silylation of butenolide **417** with trialkylsilyl chloride, furnishing a furan-type diene **418**. The key step in this synthetic procedure was the Diels–Alder reaction between the former compound and maleic anhydride, for which the product, under hydrolysis, yielded the substituted phthalic anhydride **419**. This product was selectively reduced with

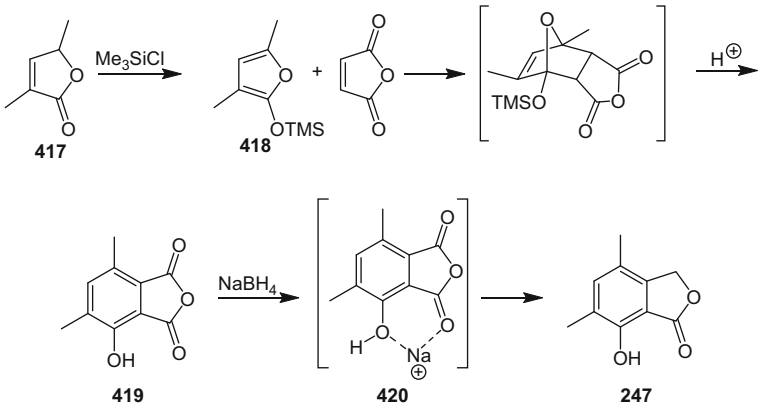

Chart 38 Synthesis of compound **247**

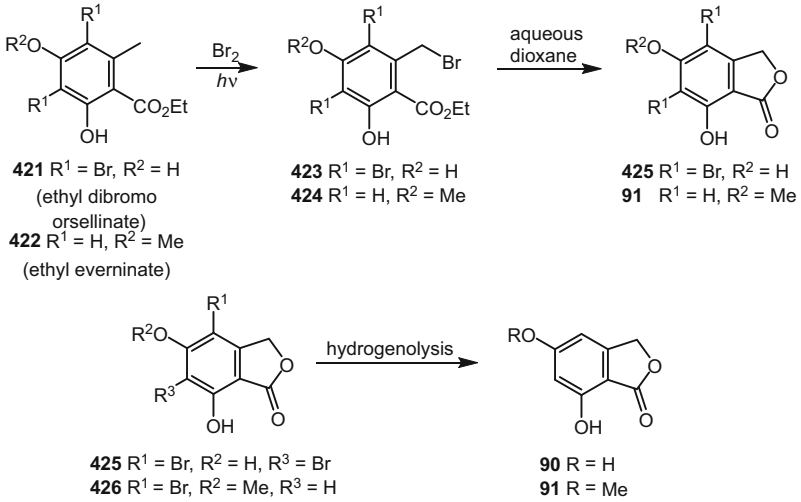

Chart 39 Synthesis of **90** and **91**

$NaBH_4$ (as a result of chelation of sodium cation with the hydroxy and carbonyl groups; intermediate **420**), yielding **247** (see Chart 38) [364].

Allison and Newbold accomplished the synthesis of naturally occurring 5,7-dihydroxyphthalide (**90**) and 7-hydroxy-5-methoxyphthalide (**91**) by benzylic bromination of ethyl dibromo orsellinate (**421**) or ethyl everninate (**422**) (producing **423** and **424**, respectively), followed by treatment with aqueous dioxane, which furnished **91**. To obtain **90**, a further step of hydrogenolysis of **425** was necessary. An alternative method to obtain **91**, also using the hydrolysis/cyclization process as an essential feature, took advantage of the by-product of the bromination reaction, i.e. the dibromo derivative of ethyl everninate, which, after hydrolysis, furnished phthalide **426**. Through a hydrogenolysis of the resulting product, the bromine atom attached to C-4 was replaced by hydrogen, yielding **91** [365] (Chart 39).

Canonica and co-workers carried out the preparation of the phthalide framework necessary for the synthesis of MPA (**141**), via Michael addition of sodium diethylmalonate to 3-methyl-3-penten-2-one and subsequent Dieckmann condensation. The resulting product was aromatized and then methylated; the corresponding acid was obtained under hydrolysis, and its chloride was prepared and reacted with ammonia, producing an amide, which was N-chlorinated. The product was photolytically converted and demethylated to produce **146**, which after alkylation and other functional group transformations, yielded **141** (see Chart 40) [366].

Mali and Patil reported a synthesis procedure in which a Wittig reaction between **427** and *n*-butylidenetriphenylphosphorane provided the corresponding vinyl benzoic acid, which was iodinated and cyclized with I_2/KI aqueous solution. After treatment with NaOAc in EtOH, HI was eliminated. Finally, the oxygen at C-7 was demethylated with $AlCl_3$ in CH_2Cl_2 to yield (*Z*)-3-butylidene-7-hydroxyphthalide (**25**), a natural compound isolated from *Ligusticum wallichii* (see Chart 41) [367].

Thibonnet's group synthesized natural phthalides **432** and **433**, using as a key step a Sonogashira coupling-oxacyclization, between *o*-iodobenzoic acid **428** and acetylenes **429** or **430**. It is noteworthy that due to the presence of methoxy substituents on benzene, the only observed products are phthalides **431** and **432**, from a 5-*endo-dig* oxacyclization, and not the coumarin, which would be formed through a 6-*exo-dig* attack (see Chart 42) [368].

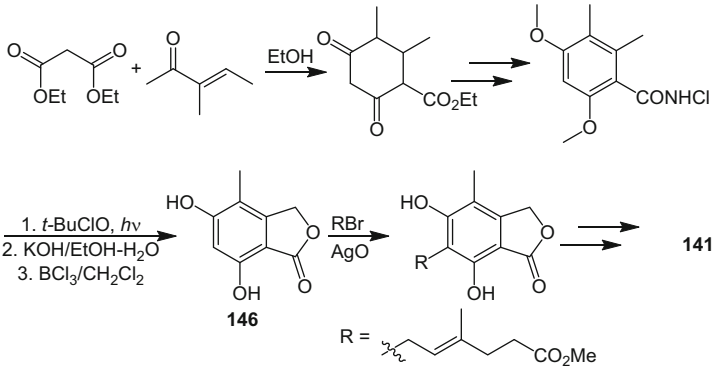

Chart 40 Canonica's synthesis of compound **141**

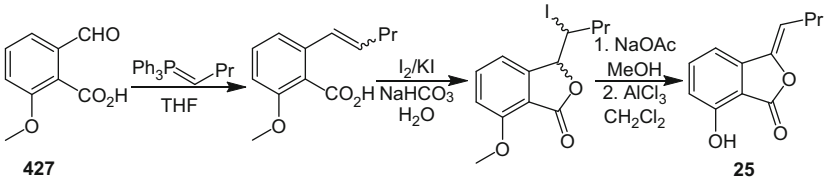

Chart 41 Synthesis of phthalide **25**

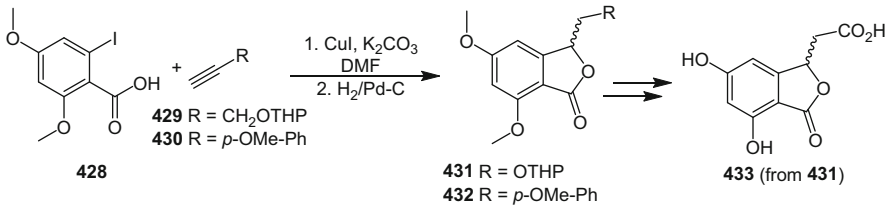

Chart 42 Synthesis of compounds **432** and **433**

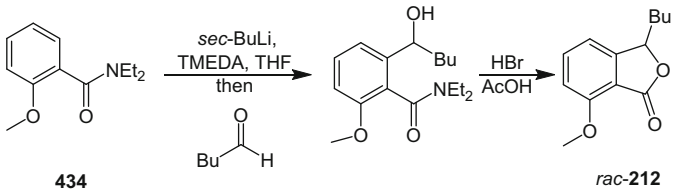

Chart 43 Synthesis of *rac*-**212**

Ohzeki and Mori used a simple two-step procedure consisting of *ortho*-lithiation of *N*,*N*-diethyl-*o*-methoxybenzamide (**434**) followed by nucleophilic attack on pentanal and lactonization to obtain a racemic mixture of 3-butyl-7-hydroxyphthalide (*rac*-**212**) (see Chart 43) [369].

6.1.3 Lactone Ring Formed Prior to Benzene Ring

Maldonado and co-workers reported an original synthesis of demethyl nidulol (**435**), a natural phthalide from *Aspergillus nidulans* (Eidam) G. Winter and *A. duricaulis*, where the formation of the lactone preceded the formation of the benzene ring. The procedure consisted of the preparation of compounds **436** and **437**, which were able to undergo an intramolecular Michael addition from the anion of the diactivated methylene moiety to the α,β-unsaturated propargyl or iodovinyl carbonyl fragments to afford the lactone ring. A subsequent Dieckmann condensation led to **435** (see Chart 44) [370].

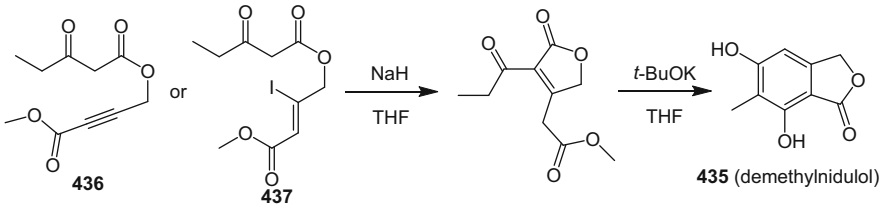

Chart 44 Preparation of demethyl nidulol (**435**)

6.1.4 Stereoselective Syntheses of Phthalides

Butylphthalide (**4**), (+)-matteucen C ((+)-**122**), (−)-matteucen C ((−)-**122**), and demethyl pestaphthalide (**216**), were synthesized by Santhosh and co-workers, as shown in Chart 45, via oxidative cyclization of the corresponding *o*-cyanostyrenes (**437**, **438**, and **439**), achieved with chiral oxo osmium complexes AD-mix (α- or β-). The mechanism of cyclization was investigated through indirect experiments, and was suggested to consist of oxidation of the carbon–carbon double bond with two of the oxygen atoms bonded to osmium, followed by nucleophilic attacks of the benzylic oxygen to nitrile carbon and of nitrile nitrogen to osmium. Subsequent hydrolysis yielded the desired phthalide. It is worth mentioning that the synthesis of both (+)- and (−)-matteucen C (**122**) confirmed the *syn* relationship of the substituents at C-3 and C-8 (See Chart 45) [371].

Koert and co-workers prepared (+)-pestaphthalide A (**213**) and (−)-pestaphthalide B (**214**), as depicted in Chart 46, by a stereodivergent synthesis from 2,6-dimethoxytoluene, which was selectively *meta* borylated. The resulting arylboronate was submitted to Suzuki-Miyaura coupling with (*Z*)-1-bromopropene, delivering a (*Z*)-alkene, which was epoxidized asymmetrically under Katsuki–Jacobsen conditions, and subsequently hydrolyzed either with aqueous perchloric acid in the presence of manganese III catalyst, or with aqueous 10-camphorsulphonic acid, leading to 4:1 and 1:3 mixtures of *cis*/*trans* diols,

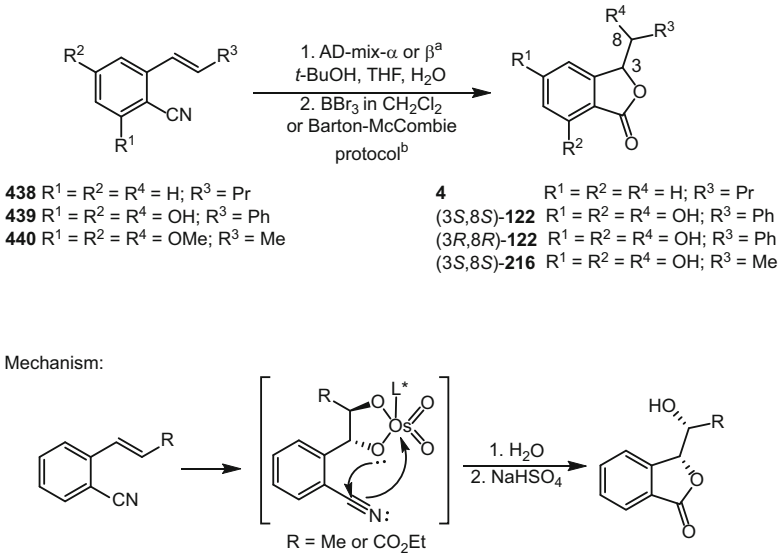

Chart 45 Enantioselective synthesis of matteucen C (**122**), demethylpestephthalide (**216**) and butylphthalide (**4**), and the underlying stereoselective determining step. (**a**) AD-mix-β was used for (−)-matteucen C (**122**); (**b**) Barton–McCombie protocol was used for synthesizing butylphthalide (**4**)

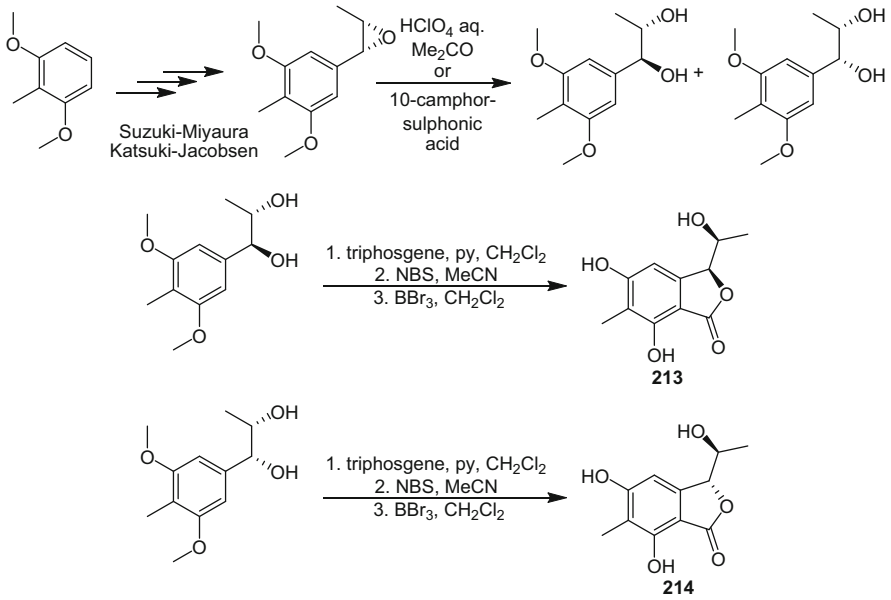

Chart 46 Syntheses of pestaphthalides A (**213**) and B (**214**)

respectively. The former was converted into cyclic carbonates with triphosgene. The convenient carbonate was subjected to bromination (with NBS), and then bromine–lithium exchange yielded an intermediate that rearranged to the corresponding phthalide, when heated to 20°C (see Chart 46) [372].

Watanabe and co-workers prepared a mixture of enantiomerically pure (−)-(*S*)-sedanenolide (senkyunolide A, **15**) and (−)-(3*S*)-butylphthalide (**4**) and a mixture of their enantiomers. This was achieved by esterification of 2,4-pentadienoic acid with the appropriate enantiomer of 1-heptyn-3-ol. The resulting ester was cyclized through a Diels–Alder reaction to give the corresponding mixture of (–)-(*S*)-sedanenolide (**15**) and (−)-(3*S*)-butylphthalide (**4**) or their enantiomers (see Chart 47) [373].

In another approach, summarized in Chart 48, (*R*)-butylphthalide ((*R*)-**4**) and other phthalides were prepared enantioselectively via Grignard-type reactions with *o*-oxazynyl-substituted benzaldehydes as electrophiles, yielding the appropriate alcohol in a diastereoselective manner, according to the Felkin–Ahn model. Hydrolysis of the oxazine moiety led to the corresponding ethylacetal, which, after oxidation with MCPBA and $BF_3{\cdot}OEt_2$, afforded phthalide (*R*)-**4** [374].

A reverse Wacker oxidation, aided by the presence of lactone oxygen, was used by Brimble and co-workers to prepare (−)-herbaric acid ((−)-**169**), in the following manner. An enantiomerically pure benzylic alcohol (accessible by enzymatic resolution), was reacted with carbonyl diimidazole (CDI) and diethylamine, yielding a carbamate, which was lactonized by bromine–lithium exchange. The desired product ((−)-**169**) was obtained from the 5,7-dimethoxy-3-vinyl-phthalide, by

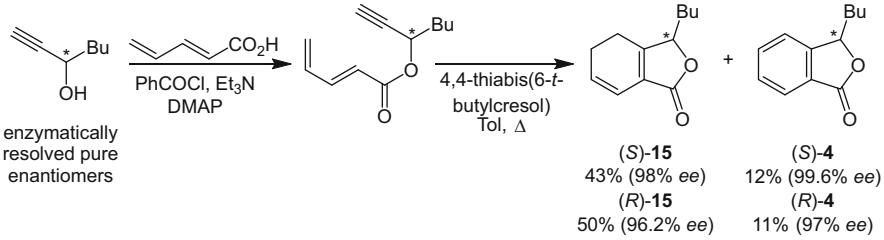

Chart 47 Syntheses of sedanenolide (**15**) and butylphthalide (**4**)

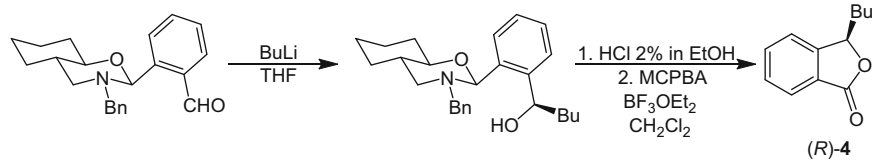

Chart 48 Enantioselective synthesis of (*R*)-butylphthalide ((*R*)-**4**)

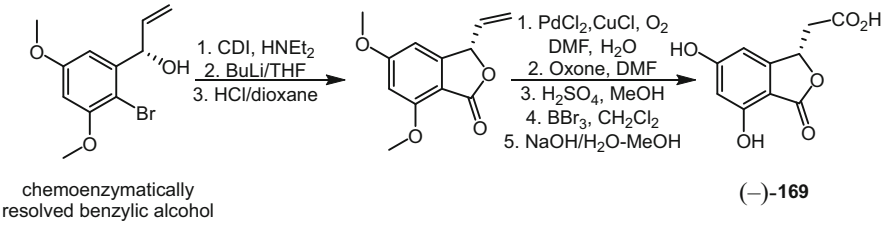

Chart 49 Synthesis of (−)-herbaric acid ((−)**169**)

reverse Wacker oxidation ($PdCl_2$, CuCl, O_2, DMF), oxidation of the resulting aldehyde (oxone, DMF), esterification, demethylation, and hydrolysis. This procedure is depicted in Chart 49 [375].

The syntheses of both enantiomers of acetophthalidin (*S*)-(**170**) and (*R*)-(**170**) were accomplished by Kitahara and co-workers, through stereoselective Sharpless dihydroxylation of 5-(1-propenyl)-bisbenzyl-resorcinol with either AD-mix-α or AD-mix-β, yielding (*S*,*S*)- and (*R*,*R*)- hydroxyphthalides, respectively. Oxidation of the alcohol to the ketone with Dess–Martin periodinane, followed by hydrogenolysis, yielded the enantioenriched (*S*)-(**170**) and (*R*)-(**170**) (see Chart 50) [376].

In order to confirm the configuration of (−)-3-butyl-4-hydroxyphthalide (**65**), Mitsuhashi's research group developed an asymmetric synthesis for this compound, as shown in Chart 51. Thus, the chiral aminal of *m*-methoxybenzaldehyde (**441**) was *ortho*-alkylated stereoselectively with *n*-pentanal, and, after acidulation, a diastereomeric mixture of lactols was obtained. This mixture was oxidized to the

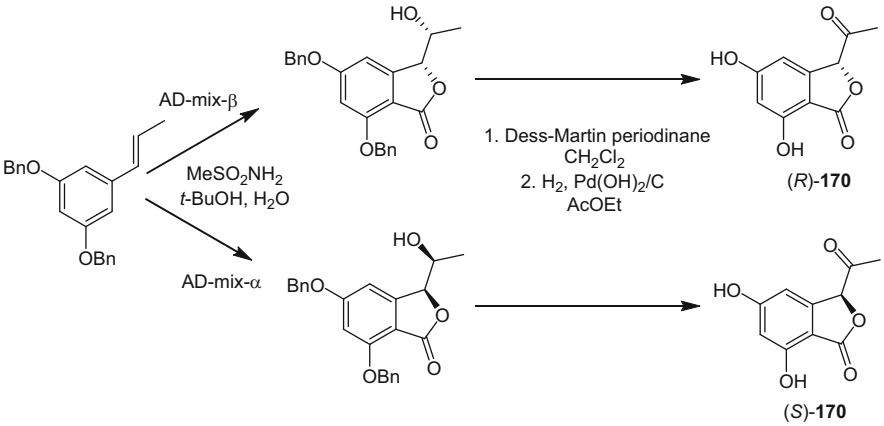

Chart 50 Synthesis of both enantiomers of acetophthalidin ((*S*)-**170**) and (*R*)-(**170**))

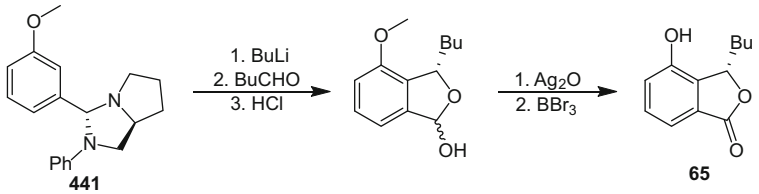

Chart 51 Synthesis of (−)-3-butyl-4-hydroxyphthalide (**65**)

corresponding lactone and the methyl ether was deprotected with BBr_3, affording phthalide **65** [108].

Another approach for the syntheses of chiral 3-substituted alkylphthalides with high enantiomeric excesses, was the use of *o*-phthalaldehyde. This, after reaction with an appropriate enantiomerically pure *N*-alkylvalinol, yielded oxazolidinyl benzaldehyde **442**, which was reacted with alkylmetallic reagents. The resulting product was further transformed to give enantioenriched 3-substituted natural phthalides (**4**, **443**, **444**). The stereoselective alkylation step was strongly influenced by the solvent, achieving enantiomeric excesses up to 90% of the (*R*)-enantiomer in a mixture of THF and dioxane, and 33% of the (*S*)-enantiomer in diethyl ether (see Chart 52) [151].

Both enantiomers of 3-butyl-7-hydroxyphthalide (**212**) were synthesized by Ohzeki and Mori, starting from methyl 2,6-dihydroxybenzoate, which was alkylated through a Suzuki–Miyaura coupling. The resulting olefin was dihydroxylated with either AD-mix-α or AD-mix-β to obtain enantiomerically pure diols. Further transformations gave both (*R*)- and (*S*)-enantiomers of the phthalide. The well-known stereochemistry of the Sharpless' epoxidation was used to confirm the configuration of the natural product as (*S*) (see Chart 53) [369].

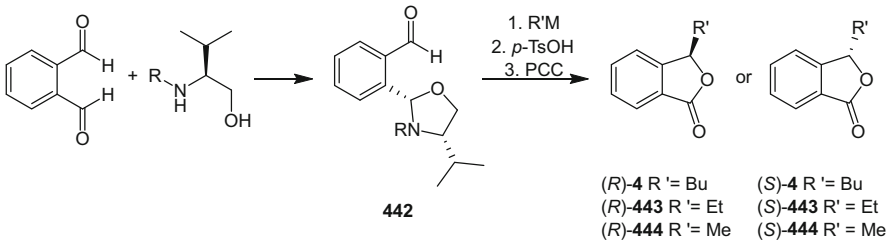

Chart 52 Syntheses of enantiomerically pure 3-alkylphthalides

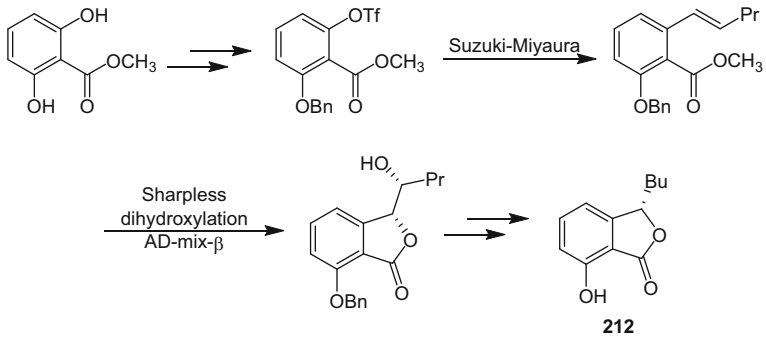

Chart 53 Synthesis of (*S*)-**212**. The enantiomer ((*R*)-**212**) was obtained using AD-mix α

6.2 *Synthesis of Dimeric Phthalides*

The synthesis of dimeric phthalides has been studied, mainly using (*Z*)-ligustilide (**8**) as starting material. It is interesting to note that dimeric phthalides have been isolated as racemic mixtures from members of the Apiaceae (Umbelliferae) plant family, and have displayed several biological activities (see Sect. 7). Diligustilide (levistolide A, **23**) and tokinolide B (**43**) have been derivatized to enantiomerically pure compounds, as described in Sect. 5.2.2.

6.2.1 [π4s + π2s] Cycloadditions

Wakamatsu and co-workers [320] described the preparation of diligustilide (levistolide A, **23**) and tokinolide B (**43**) from (*Z*)-ligustilide (**8**), by a Diels–Alder process. It was observed that tokinolide B (**43**) was transformed partially to levistolide A (**23**) under the reaction conditions (Chart 54). Calculations of HOMO and LUMO of (*Z*)-ligustilide (**8**) were also carried out to explain the regioselectivity of the dimers formed. A similar thermal reaction in a sealed tube of (*Z*)-ligustilide (**8**) allowed its conversion to diligustilide (**23**), confirming the regio- and stereoselectivity of the reaction [321] (see Chart 54).

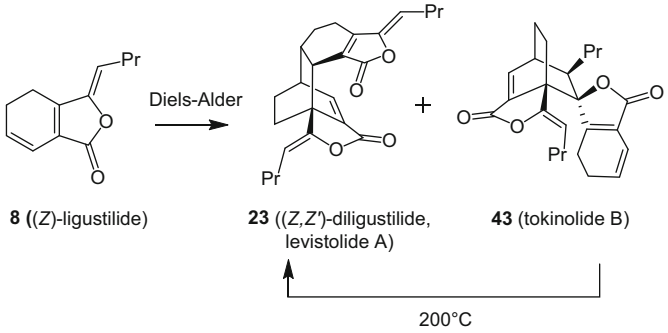

Chart 54 Diels–Alder reaction of (*Z*)-ligustilide (**8**)

6.2.2 [π2s + π2s] Cycloadditions

Although the majority of natural dimeric phthalides are formed by [π4s + π2s] reactions, several dimeric phthalides such as riligustilide (**24**), tokinolide A (**42**), and *endo*-(*Z*,*Z*′)-[3.3′,8.8′]-diligustilide (**445**) are biosynthesized through [π2s + π2s] cycloadditions [72, 304, 377, 378].

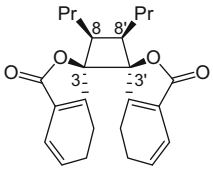

445 (*endo*-(*Z*,*Z'*)-[3.3',8.8']-diligustilide)

The situ-, regio- and stereochemical possibilities of the three olefins of (*Z*)-ligustilide (**8**) have been considered in the formation of [π2s + π2s] photocyclodimers, but there are no direct guidelines available to predict the structure of the products. (*Z*)-Ligustilide (**8**) was exposed to photochemical conditions, affording the natural product riligustilide (**24**), *endo*-(*Z*,*Z*′)-[3.8′,8.3′]-diligustilide (**446**), *endo*-(*Z*,*Z*′)-[3a.7a′,7a.3a′]-diligustilide (**447**) and *exo*-(*Z*,*Z*′)-[3a.7a′,7a.3a′]-diligustilide (**448**) (Chart 55). It was found that in the triplet state the carbon atoms of the side chain of **8** were quasi-coplanar with the lactone ring, bringing down the steric hindrance for the transition states, and also that the regioselectivity was determined by orbital coefficients and energies. Frontier molecular orbitals and Mülliken charge calculations agreed with the experimental yields obtained for the reaction products [378].

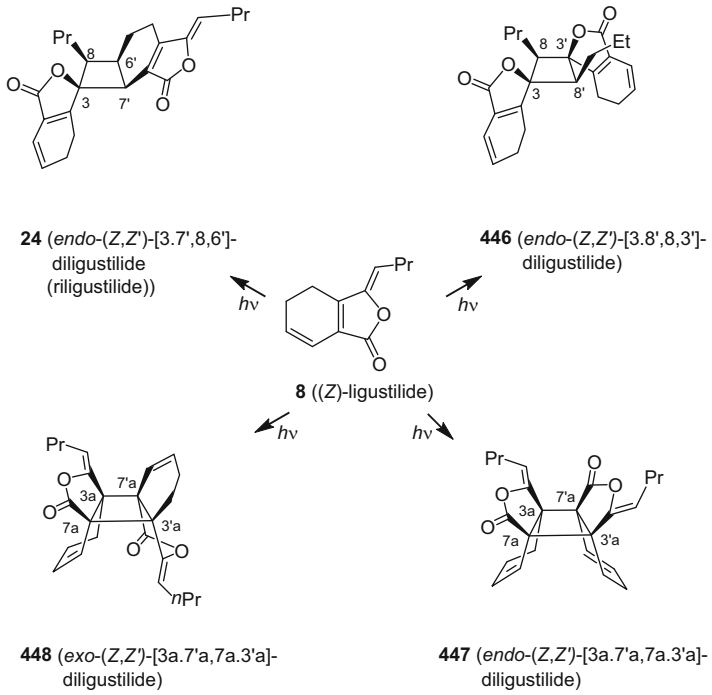

Chart 55 Photocyclodimerization of (*Z*)-ligustilide (**8**)

7 Biological Activity

The evaluation of biological activity has been a prominent aspect of phthalide research. While a number of biological activities have been attributed to natural product extracts containing phthalides, these data have been complicated by the presence of more than one active constituent (i.e. the biologically active constituents are not exclusively phthalides). With this in mind, the present contribution reviews mainly the bioactivities of natural and semisynthetic phthalides as pure compounds.

Several reviews on related topics have been published [1, 114, 379–382], with some of them focusing exclusively on one compound, such as mycophenolic acid (**141**) [318] or noscapine (**128**) [383–386]. The current review is neither intended to be a comprehensive treatment of the biological activity of natural phthalides as whole, nor on the individual compounds mentioned. Instead, an integrated overview is presented of the most relevant biological activities of this type of compounds is presented here.

7.1 Antioxidant Effects

Several human diseases are associated with oxidative damage. The overproduction of reactive oxygen species (ROS) damages the cell [387], and eukaryotic cells have developed defensive enzymatic systems. (*Z*)-Butylidenephthalide (**3**), (*Z*)-ligustilide (**8**), senkyunolide I (**22**), sinaspirolide (**70**), and ansaspirolide (**71**), were screened for their antioxidant activity at 100 μ*M*. All these compounds showed activity in scavenging 2,2-diphenyl-1-picrylhydrazyl (DPPH) radicals. Also, ansaspirolide (**71**) was the most active in inducing the activity of NAD(P)H-quinone oxidoreductase 1 (NQO1), but was also cytotoxic for the host hepatoma cells (Hepa1c1c7). (*Z*)-Butylidenephthalide (**3**) and (*Z*)-ligustilide (**8**) also successfully induced NQO1. The transcription of several antioxidant enzymes is regulated by antioxidant response elements (ARE) in promoter units. (*Z*)-Ligustilide (**8**) induced ARE reporter activity in a dose-dependent manner (5–20 μ*M*) [388]. Senkyunolides I (**22**) and H (**26**) both induced heme oxygenase-1 (HO-1), with senkyunolide H showing the most potent effect, and the induction was related to the activation of Nrf2 (nuclear factor E2-related factor-2)/ARE pathway. Both compounds were inhibitors of ROS formation and lipid peroxidation in human liver hepatocellular carcinoma cells (HepG2) [389]. Colletotrialide (**226**) demonstrated a low antioxidant activity, scavenging DPPH with an IC_{50} value of >324 μ*M*. It also inhibited weakly superoxide anion radical formation (by xanthine/xanthine oxidase) ($IC_{50} > 648$ μ*M*); superoxide anion radical generation (in differentiated human promyelocytic leukemia cells (HL-60)) ($IC_{50} > 130$ μ*M*); xanthine oxidase ($IC_{50} > 648$ μ*M*), and aromatase ($IC_{50} > 16.2$ μ*M*) [222].

The antioxidant properties of (*Z*)-ligustilide (**8**) and *cis*-(*Z*,*Z*′)-3a.7a′,7a.3a′-diligustilide (**447**) have been assessed using human umbilical vein endothelial cells (HUVECs), evaluating the oxidative damage caused by hydrogen peroxide (H_2O_2). Treatment with **447** protected HUVECs ($IC_{50} = 15.14$ μ*M*), with (*Z*)-ligustilide (**8**) displaying an IC_{50} of 0.55 μ*M*. Lactate dehydrogenase (LDH) leakage provoked by H_2O_2 was also reduced by **447** at concentrations of 25, 50, and 100 μ*M*. The application of **447** also increased superoxide dismutase (SOD) activity and decreased malondialdehyde (MDA) levels, confirming its antioxidant properties [387].

Epicoccone (**195**) prevented lipid peroxidation (62%) when used at 37 μg/cm^3 [205], while isopestacin (**193**) was found to scavenge hydroxyl radicals at a concentration of 0.22 m*M* and the superoxide radicals at 0.185 m*M* [203].

7.2 Analgesic Effects

(*Z*)-Ligustilide (**8**) has analgesic effects, since administration to mice at doses of 2.5, 5, and 10 mg/kg (p.o.), caused a dose-dependent reduction in the both the

writhing response induced by acetic acid and formalin-induced licking time [390]. Compound **8** has also been evaluated at the higher dosages of 20, 60, and 100 mg/kg, with the same results: a delayed licking time and reduced writhing response both occurred [391]. In a similar study, (*Z*)-butylidenephthalide (**3**), (*Z*)-ligustilide (**8**), and diligustilide (**23**), suppressed the irritation induced by acetic acid, with diligustilide (**23**) showing the greatest effect. (*Z*)-Butylidenephthalide (**3**) and (*Z*)-ligustilide (**8**) also demonstrated an antinociceptive effect when using a hot-plate assay [392].

7.3 Antihyperglycemic Effects

Type 2 diabetes mellitus is a chronic condition associated with abnormal levels of blood glucose. Both (*Z*)-butylidenephthalide (**3**) and (*Z*)-ligustilide (**8**) decreased the postprandial blood glucose peak in mice treated with streptozotocin [393]. (*Z*)-Butylidenephthalide (**3**) also inhibited the activity of yeast α-glucosidase in vitro in a concentration-dependent manner ($IC_{50} = 2.35$ m*M*). Docking analysis (using the (*E*)-isomer (**21**)) showed that this compound binds close to the catalytic site [393].

In screens for competitive binding to PPAR-γ, paecilocin A (**245**) used at 100 μ*M* demonstrated comparable activities to rosiglitazone, a PPAR-γ agonist used for the treatment of type 2 diabetes mellitus. Compounds **449** and **450** also showed comparable binding properties to rosiglitazone, whereas **451**–**454**, which contain benzyl or methyl groups, were less effective. The introduction of additional substituents failed to enhance activity, as shown for compounds **452**–**454** and **457**–**460**. Phthalides **455** and **456** showed no enhanced activity, with compound **455** slightly more active than **456** [394].

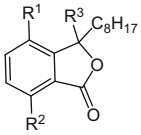

	R^1	R^1	R^3
449	OH	H	H
450	H	OH	H
451	H	OMe	H
455	H	H	H
459	OH	H	OH
460	H	OH	OH

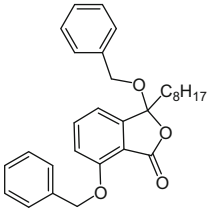

452

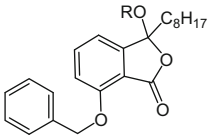

453 R = H
454 R = Me

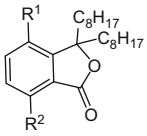

	R^1	R^2
456	H	H
457	OH	H
458	H	OH

7.4 Antithrombotic and Antiplatelet Effects

Thrombosis is the main cause of the thromboembolic complications of ischemic disorders. One pharmacological strategy has been to re-establish the blood flow to the ischemic site by dissolving the clot. Another strategy is to prevent clot formation. To this end, the search for new antithrombotic agents has continued [395]. (*Z*)-Ligustilide (**8**), administered for three days at doses of 10 or 40 mg/kg (p.o.), demonstrated both antithrombotic and antiplatelet activities [395]. (*Z*)-Butylidenephthalide (**3**) showed antiplatelet activity, and inhibited the aggregation of washed rabbit-derived platelets, induced by collagen, arachidonic acid, platelet activating factor, and adenosine diphosphate (ADP). (*Z*)-Butylidenephthalide (**3**) also inhibited the release of adenosine triphosphate (ATP) from these platelets [396]. (*R*)-Butylphthalide (*ent*-**4**) and (*S*)-butylphthalide (**4**) inhibited also platelet aggregation [397], with blood viscosity reduced by *rac*-butylphthalide (*rac*-**4**), cnidilide (**7**), senkyunolide A (**15**), senkyunolide P (**40**), and tokinolide B (**43**) [398].

7.5 Neurological Effects

7.5.1 Stroke

Stroke is a leading cause of disability in adults and is the third most prevalent cause of mortality in the world [399, 400]. Treatment options are currently limited. Intraperitoneal administration of (*Z*)-ligustilide (**8**) to mice undergoing transient forebrain cerebral ischemia/reperfusion (I/R), at dosages of 5 and 20 mg/kg, reduced infarct volume in a dose-dependent manner. The administration of **8** also decreased MDA content, restored the activities of glutathione peroxidase (GSH-PX) and SOD in ischemic brain tissues, and regulated pro- and antiapoptotic effector proteins [401]. Oral administration of (*Z*)-ligustilide (**8**) at doses of 20 or 80 mg/kg to rats with middle cerebral artery occlusion (MCAO) also showed, after 24 h of obstruction, a marked reduction in infarct volume and brain edema. (*Z*)-Ligustilide also ameliorated neurobehavioral impairment and improved survival rate [400]. In terms of the immune response, microglia are activated during ischemia. Both (*Z*)-ligustilide (**8**) and senkyunolide A (**15**) inhibited neuroinflammation, blocked the production of TNF-α and nitrites in murine microglial cells (BV-2), and reduced TNF-α production from peripheral blood monocyte-derived macrophages (PBMac) [399].

Oral administration of (*Z*)-ligustilide (**8**) at doses of 20, 40 or 80 mg/kg, 3 and 0.5 h before the MCAO procedure, reduced the neurological deficit score, and the infarct volume in a dose-dependent manner. The expression of erythropoietin (EPO, an endogenous protective factor) was also enhanced and the level of the stress-induced protein RTP801 (an endogenous detrimental factor) was reduced.

The cytoprotection conferred by EPO could be mediated by the phosphorylation of ERK promoted by **8**. (*Z*)-Ligustilide (**8**) also increased cell viability and decreased the leakage of LDH, although concentrations above of 5 μ*M* were cytotoxic to neurons maintained in cell culture. Transfection of human neuroblastoma cells (SH-SY5Y) with the pcDNA3.1-RTP801 plasmid DNA increased LDH leakage and RTP801 expression, both of which were inhibited by (*Z*)-ligustilide (**8**) [402]. Compound **8** protected PC12 cells from apoptosis induced by oxygen-glucose deprivation (OGD), induced tolerance to oxidative stress, induced HO-1 expression, and promoted translocation of Nrf2 [403] to the nucleus (an inducible transcription factor that regulates multiple cellular antioxidant systems during stroke) [404]. (*Z*)-Ligustilide (**8**) also regulated the homeostasis of glutathione (GSH) [403].

Zhu et al. evaluated the effect of (*Z*)-ligustilide (**8**) on the Nrf2/HO-1 pathway, and it was found that this compound provoked a significant decrease of infarct volume, improved neurological function, and attenuated neuronal loss (at 16 and 32 mg/kg, i.v.) in transient MCAO-induced damage [404]. The results concerning the Nrf2 and HO-1 proteins were similar to those obtained by Rong et al. [403]. (*Z*)-Ligustilide (**8**) activates the Nrf2 pathway, with its protective action possibly mediated by the Nrf2/HO-1 pathway [404]. Noscapine (**128**) improved clinical prognosis in ischemic stroke patients [405].

Subarachnoid hemorrhage (SAH) is a stroke subtype that can lead to cerebral vasospasm. The treatment of rats with (*Z*)-ligustilide (**8**) at a dose of 20 mg/kg improved neurobehavioral scores, reduced edema, improved the permeability of the blood brain barrier, and with vasospasms diminished. (*Z*)-Ligustilide (**8**) may ameliorate tissue damage caused by SAH by mechanisms that involve apoptosis [406].

Permanent bilateral ligation of the common carotid artery is an experimental model for cerebral hypoperfusion (used for the study of dementia), which impairs memory and learning. Administration of (*Z*)-ligustilide (**8**) prevented the structural and functional abnormalities in the brain of rats subjected to this procedure. (*Z*)-Ligustilide also protected the hippocampus from damage, ameliorated cognitive deficits, decreased MDA and acetylcholinesterase (AChE) levels, and increased the activity of the SOD and choline acetyltransferase (ChAT) [407].

7.5.2 Alzheimer's Disease and Cognitive Impairment

Alzheimer's disease is a progressive neurodegenerative disease characterized by damage to the regions of the brain that regulate cognitive function in the elderly [408]. The cytotoxicity induced by the amyloid β-peptide (Aβ) in Alzheimer's disease, together the effects of (*Z*)-ligustilide (**8**) and 11-angeloylsenkyunolide F (**41**), have been evaluated. Cell viabilities following exposure to $A\beta_{1–40}$ were 61.6 and 69.4%, respectively, at 10 and 50 μg/cm^3 for (*Z*)-ligustilide (**8**). The same concentrations of 11-angeloylsenkyunolide F (**41**) produced viabilities of 59.5 and

67.1%. The toxicities of these compounds were also analyzed, with 50 μg/cm^3 (*Z*)-ligustilide (**8**) shown to be toxic (53.0% of cell viability) [408].

A second group of investigators reported cytotoxicity data using Aβ_{25-35} and oral administration of **8** (40 mg/kg) for 15 days (from the 6th to 20th day). (*Z*)-Ligustilide (**8**) prevented cognitive dysfunction and attenuated the morphologic changes and neuronal loss induced by injection of Aβ_{25-35}. The injection of Aβ_{25-35} increased the expression of Aβ, amyloid precursor protein, and Tau protein, with (*Z*)-ligustilide (**8**) preventing all of these effects [409].

Some studies have suggested that the widespread loss of ACh-containing neurons, and the reduction in activity of ChAT, are early biological signs of Alzheimer's disease. (*Z*)-Ligustilide (**8**) (at 10 or 40 mg/kg daily for 26 days) was tested on an model of Alzheimer's disease using scopolamine, which increases AChE activity and decreases ChAT activity. Phthalide **8** improved spatial long-term memory, prevented spatial short-term memory deficits, inhibited AChE activity ($IC_{50} = 6.48$ mg/kg), and increased ChAT activity ($ED_{50} = 7.66$ mg/kg) [410]. (*Z*)-Ligustilide (**8**) has also demonstrated a cytoprotective effect, and protected against the cognitive impairment and neurotoxicity induced by D-galactose (at a dose of 80 mg/kg/8 weeks) in aged mice brains, by improving spatial learning and memory. MDA levels and the expression of cleaved caspase-3 were both diminished on the administration of **8**. The decline in activity of Na^+–K^+-ATPase provoked by D-galactose was also prevented by (*Z*)-ligustilide (**8**), with a diminution of astrocytic activation [411].

Phthalide NG-072 (**48**) has been reported to be effective in the potential treatment of Alzheimer's disease, by enhancing axon growth [84].

7.5.3 Parkinson's Disease

Parkinson's disease is a neurodegenerative pathology characterized by a progressive loss of dopaminergic nigrostriatal neurons. Current therapies for Parkinson's disease depend mainly on dopamine replacement using levodopa (L-dopa) and antioxidants; however, there is certain evidence of the toxicity of dopamine and its metabolites. Dopamine at concentrations ranging from 200 to 800 μ*M* affected the viability of PC12 cells in a concentration-dependent manner. (*Z*)-Ligustilide (**8**) used at 50 μ*M* decreased cell viability by 9.6%, but the combination of **8** (50 μ*M*) and dopamine (500 μ*M*) was even more cytotoxic to PC12 rat dopaminergic cells, reducing viability by almost 90%. The same treatment as for PC12 on the SH-SY5Y (human neuroblastoma), HepG2 (human hepatoma), MCF-7 (human breast adenocarcinoma), HeLa (human epithelial carcinoma), and PC3 (human prostate cancer) cell lines, revealed that only the dopaminergic cell lines were adversely affected. Cells treated with dopamine or (*Z*)-ligustilide (**8**) died via apoptosis and necrosis, with a mixture of these compounds increasing levels of cell death to 56.8%, and decreasing GSH levels to 28.8% [412].

7.5.4 GABAergic and Sedative Effects

The $GABA_A$ receptor is a target for drugs that modulate sedative, anxiolytic, anticonvulsant, muscle relaxant, and amnesic activities. Binding to the $GABA_A$ receptor using [^{3}H] flunitrazepam and diazepam as positive controls, demonstrated that both gelispirolide (**68**) and riligustilide (**24**) inhibited [^{3}H]diazepam binding to $GABA_A$ receptors (the IC_{50} values were 29 and 24 μ*M*) [109].

(*Z*)-Ligustilide (**8**) at 5–20 mg/kg, and (*Z*)-butylidenephthalide (**3**) at 10–30 mg/kg (i.p.) reversed pentobarbital-induced sleep shortened by social isolation stress. Both phthalides (at 20 mg/kg) attenuated the effects of methoxamine and yohimbine, which decreased the time of the pentobarbital sleep period. (*Z*)-Ligustilide (**8**) potentiated the effects of diazepam in pentobarbital-induced sleep in mice, suggesting noradrenergic suppression. Both phthalides also attenuated the effect of a benzodiazepine receptor inverse agonist. Taken together, the $GABA_A$ receptor may be implicated in the activity of these compounds [413].

The hypnotic time induced by sodium pentobarbital in mice increased significantly by pretreatment with 50 mg/kg of (*Z*)-ligustilide (**8**), diligustilide (**23**), tokinolide B (**43**), senkyunolide F (**31**) and several semi-synthetic products, including the diketo diacid of diligustilide (**345**), demethylwallichilide (**344**), *rel*-(3′*S*)-3′,8′-dihydrodemethylwallichilide (**461**), and *rel*-(3′*R*)-3′,8′-dihydrotokinolide B (**462**). The increases in hypnosis, expressed as percentages, were 46.3, 24.6, 70.8, 34.6, 66.0, 52.3, 36.2, and 100%, respectively. Compounds **43** and **462** demonstrated the highest activities [276]. In the same model, compounds **15** and **4** displayed similar effects [414]. Phthalideisoquinolines, (+)-bicuculline (**111**) [415, 416], (+)-hydrastine (**112**), and corlumine (**110**) were found to be antagonists of the $GABA_A$ receptor, with the most potent antagonist proving to be **112**, with **111** more potent than **110**; all three phthalides are convulsive agents [417].

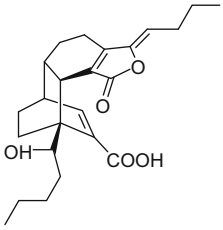

461 (*rel*-(3′*S*)-3′,8′-dihydro demethylwallichilide)

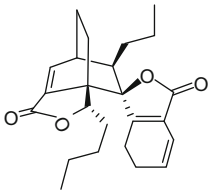

462 (*rel*-(3′*R*)-3′,8′-dihydrotokinolide B)

7.5.5 Anticonvulsive Effects

Epilepsy is a disorder characterized by abnormal neuronal electrical activity [418] with periodic and unpredictable seizures [419]. *rac*-Butylphthalide (*rac*-**4**) and senkyunolide A (**15**) were shown to be anticonvulsive agents against metrazole, electroshock-, and audio-induced seizures [420]. Yang et al. confirmed the

anticonvulsive effects of both phthalides [421]. *rac*-Butylphthalide protected against chronic epilepsy induced by coriaria lactone [422], and at 700 mg/kg prevented abnormalities in the hippocampus [423]. Both enantiomers of butylphthalide (**4**) protected from the seizures induced by electro-shock [424].

7.6 Progestogenic Effects

The hormone progesterone is necessary for menstrual and reproductive health. During menopause, hormone replacement therapy is an effective treatment against hormonal disorders. Some phthalides have shown progesterone-like activity. For example, 3,8-dihydrodiligustilide (**63**) ($EC_{50} = 91$ nM) was shown to be a potent and specific activator of the progesterone receptor, with riligustilide (**24**) ($EC_{50} = 81$ μM) displaying weaker activity. Levistolide A ((**23**) (Z,Z')-diligustilide) was inactive, which demonstrates the importance of minor structural variations in this type of molecule for biological activity [106].

7.7 Cytotoxic Effects

The current lack of specificity for multiple antitumor therapies has led to a search for novel, more targeted agents [219]. 3-Methyl-4,5,6-trihydroxyphthalide (**198**) is an agent that has been tested for activity against the serine/threonine-protein kinase Akt1, which regulates metabolism, proliferation, and cell survival, and showed an IC_{50} value of 19.7 μM. The IC_{50} for the functional inhibition of Bad phosphorylation by Akt1 was 30.4 μM [208]. Cytotoxicities for **198** against several cancer cell lines are listed in Table 1.

In the treatment of liver fibrosis, suppression of the growth of liver stellate cells (HSC) with the induction of apoptosis has been suggested to be a plausible therapeutic approach. (Z,Z')-[6.8′,7.3′]-Diligustilide (**24**) and levistolide A (**23**)

Table 1 IC_{50} values for 3-methyl-4,5,6-trihydroxyphthalide (**198**) against several human cancer cell lines [208]

Cell line	IC_{50}/μM
T cell lymphoblast (Jurkat)	20
Myeloma cells derived from peripheral blood lymphocytes (RPMI-8226)	67
Central nervous system cancer (SNB-75)	60
Melanoma (SK-MEL-28)	37
Ovarian cancer (OVCAR-5)	74
Breast cancer (BT-549)	24
Lymphoma (U937)	60

((*Z*,*Z*′)-diligustilide) were found to reduce the cell proliferation stimulated by platelet-derived growth factor (PDGF-BB) in immortalized liver stellate cells (HSC-T6) and in immortalized human stellate cells (LI-90), with **23** showing a higher potency than **24**. Both compounds induced apoptosis in HSC stimulated by PDGF-BB, without significant toxicity to primary hepatocytes, when used at 5–40 μ*M* for **24**, and 1–20 μ*M* for **23** [425].

Noscapine (**128**) has been in Phase I/II clinical trials for non-Hodgkin's lymphoma or chronic lymphocytic leukemia refractory to chemotherapy [426]. In addition, noscapine also displayed activity against HT-29, colon carcinoma (SW480), and the human colon adenocarcinoma (LoVo) cell lines, with selectivity against the latter cell line ($IC_{50} = 75$ μ*M*) [427]. There have been several studies of the bioactivity of noscapine (**128**), which concluded that its mechanism of action is related to microtubule assembly [428–430].

Topoisomerases are enzymes that are involved in the progression of the cell cycle and their inhibition can be used as targets for cancer chemotherapy. Senkyunolides N (**52**) and J (**33**), and sedanolide (**6**) exhibited inhibitory effects against topoisomerases I and II, with **6** completely inhibiting both enzymes at 100 μg/cm^3 [431]. The cytotoxic and antiproliferative effects of senkyunolide A (**15**), (*Z*)-ligustilide (**8**), and (*Z*)-butylidenephthalide (**3**) were evaluated using the human colon cancer cell line (HT-29) and the normal human colon fibroblast cell line (CCD-18Co). The phthalides decreased cell viability for tumor-derived cell lines (IC_{50} values ranging from 8.6 to 51.2 μ*M*), without any significant effect on the viability of normal cells. Of these agents, senkyunolide A (**15**) was the most selective [432].

(*Z*)-Butylidenephthalide (**3**) prevented cell cycle entry in glioblastoma multiforme brain tumor cells, when used at 75 μg/cm^3. This compound also induced apoptosis and prolonged the survival of mice after malignant brain tumor cell implantation [433].

(*S*)-3-Butyl-7-methoxyphthalide (**212**) is a natural product that has been previously synthesized; its IC_{50} values against several cell lines are shown in Table 2 [217].

Compound **199** displayed activity against HeLa and KB cells (IC_{50} 36.0 and 14.0 μg/cm^3) [210, 212]. Porriolide (**200**) also displayed activity against KB cells

Table 2 IC_{50} values for (*S*)-3-butyl-7-methoxyphthalide (**212**) against several cancer cell lines

Cell line	IC_{50}/μg cm^{-3}
Human lung carcinoma (A549)	44.0
Human epidermoid carcinoma of the mouth (KB)	32.0
HeLa	31.0
Human mammary adenocarcinoma (T47 D)	30.0
Murine leukemia cell line (P388)	25.8

($IC_{50} = 59.0$ μg/cm^3) [209]. Phthalide **199** induced apoptosis, with the authors suggesting that proliferation was inhibited by a G1 phase arrest in HeLa cells [212].

Hanabiratakelides A ((**218**) HA), B ((**219**) HB), and C ((**220**) HC) were found to display cytotoxic activities against colon cancer cells (Caco-2 and colon-26 cells). The respective IC_{50} values for HA (**218**) and HC (**220**) were 342 and 535 μ*M* in Caco-2 cells. In turn, the IC_{50} values for colon-26 cells were 96 μ*M* for HA (**218**), 18 μ*M* for HB (**219**), and 49 μ*M* for HC (**220**). These compounds also showed superoxide dismutase (SOD)-like activity, with IC_{50} values of 15.7, 49.0, and 3.2 μ*M* for HA (**218**), HB (**219**), and HC (**220**), respectively [219].

Marilones A (**203**), and C (**205**) also showed weak cytotoxic activities against three cell lines: NCI-H460 (lung), MCF7 (breast), and SF268 (central nervous system). Cytotoxicities were comparable for **203** ($LC_{50} > 100$ μ*M*) and **205** ($LC_{50} = 99.6$ μ*M*) against NCI-H460 and MCF7 [214].

Colletotrialide (**226**) has been tested against several cell lines with IC_{50} values of 162.1 μ*M* for HuCCA-1, HepG2, and the A549 cell lines, and slightly less, at 147.8 μ*M*, for the acute lymphoblastic leukemia line (MOLT-3) [222].

Several additional natural and semi-synthetic phthalides have been assayed for their bioactivities against three cancer cell lines. The enantiomers (–)-**348**, (+)-**349**, (+)-**348**, (–)-**349**, (–)-**350**, (+)-**350**, (+)-**351**, (–)-**351**, were more active (see Table 3), with helenalin used as a positive control [118, 334, 335].

Table 3 IC_{50} values of several natural and semi-synthetic phthalides against three human cancer cell lines

	IC_{50}/μ*M*		
	Cell line		
Compound	Leukemia (K562)	Colon (HCT-15)	Lung (SK-LU-1)
Dilustilide (**23**)	26.6	10.5	7.1
Rilugustilide (**24**)	46.1	44.8	13.2
Tokinolide B (**43**)	26.6	10.5	7.1
Chaxiongnolide B (**87**)	30.6	23.1	37.4
Demethylwallichilide (**344**)	47.2	>100	>100
Diketo diacid of dilustilide (**345**)	19.9	71.6	42.6
Cyclotokinolide (**346**)	21.9	28.4	22.9
Ketoacid of tokinolide B (**347**)	>100	>100	>100
(–)-**348**	5.7	5.4	4.1
(+)-**348**	13.9	7.5	4.9
(–)-**349**	5.2	5.2	4.3
(+)-**349**	21.7	8.5	5.9
(–)-**350**	13.8	36.7	27.0
(+)-**350**	4.4	12.2	7.3
(–)-**351**	17.1	9.6	7.1
(+)-**351**	10.4	32.5	26.9

5-(3′,3′-Dimethylallyloxy)-7-hydroxy-6-methylphthalide (**463**) exhibited moderate activity against the myeloid liver carcinoma (SMMC-7721) and MCF-7 cell lines, with IC_{50} values of 1.8 and 29.0 μ*M* [434].

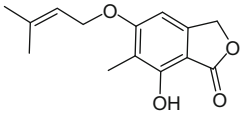

463

Multi-drug resistance (MDR) is an obstacle for many current cancer therapies. One of the mechanisms involved in MDR is the elimination of compounds by conjugating them by phase II enzymes, including glutathione *S*-transferase (GST). 11-Angeloylsenkyunolide F (**41**) and tokinolide B (**43**) inhibited GST enzyme (IC_{50} 16.8 and 7.3 μ*M*, respectively), in a reversible and noncompetitive process, docking analysis showed that both compounds interacted with the active site. Compounds **41** and **43** showed low cytotoxicity against the A549 and MDA-MB-231 cell lines, with both reversing MDR in these cell lines [435].

7.8 Inhibition of the Abnormal Proliferation of Vascular Smooth Muscle Cells

Another biological activity that has been investigated for natural occurring phthalide derivatives is the proliferation of vascular smooth muscle cells. Abnormal proliferation is seen in atherosclerosis and in atherosclerotic plaques [436, 437]. Some phthalides have been reported to inhibit this proliferation in a concentration-dependent manner. Senkyunolide H (**26**) was the most active ($IC_{50} = 0.1$ μg/cm^3) of the following compounds: (*Z*)-butylidenephthalide (**3**) ($IC_{50} = 3.25$ μg/cm^3), (*Z*)-ligustilide (**8**) ($IC_{50} = 1.68$ μg/cm^3), senkyunolide A (**15**) ($IC_{50} = 1.52$ μg/cm^3), and neocnidilide (**6**) ($IC_{50} = 6.22$ μg/cm^3). 3-Butylphthalide (**4**), cnidilide (**7**), and senkyunolide I (**22**) also demonstrated weak effects [436].

Kobayashi et al. also investigated the effect of various phthalides on the competence and progression of the cell cycle proliferation. The most active phthalide was senkyunolide L (**45**), followed by senkyunolide H (**26**), senkyunolide J (**33**), senkyunolide I (**22**), (*Z*)-ligustilide (**8**), senkyunolide A (**15**), and (*Z*)-butylidenephthalide (**3**) [437].

The effect of phthalide **8** on the abnormal proliferation of vascular smooth muscle cells was related to its inhibition of ROS production [438]. (*Z*)-Butylidenephthalide (**3**) and (*Z*)-ligustilide (**8**) both inhibited the proliferation of vascular smooth muscle cells stimulated with basic fibroblast growth factor [439]. Compound **8** also displayed positive effects in a rat model of atherosclerosis [440].

7.9 Insecticidal Effects

The larvicidal activities of (*Z*)-butylidenephthalide (**3**) and (*Z*)-ligustilide (**8**) were evaluated against *Drosophila melanogaster*. Compound **3** was found to be more active than **8** ($LC_{50} = 0.94$ μmol/cm^3 and $LC_{50} = 2.54$ μmol/cm^3), although both were less effective than rotenone. Acute adulticidal activity, resulting in 100% mortality, was seen when compound **3** was used at a dose of 5.0 μg/adult ($LD_{50} = 0.84$ μg/adult), and was more potent than the value obtained for rotenone [441].

(*Z*)-Ligustilide (**8**) deterred the biting of both *Aedes aegypti* and *Anopheles stephensi* at 25 nmol/cm^2 more effectively than *N*,*N*-diethyl-3-methylbenzamide, which is considered to be one of the most effective mosquito repellents [442]. Sedanolide (**6**) showed 100% of mortality at 50 μg/cm^3 against *A. aegypti* [294].

Bemisia tabaci is one of the most important insect pests and participates in the transmission of numerous plant-pathogenic viruses. The most pathogenic biotypes of *B. tabaci* are the B- and Q-biotypes. The residual contact toxicities of (*Z*)-ligustilide (**8**) ($LC_{50} = 268.4$ ppm), and (*Z*)-butylidenephthalide (**3**) ($LC_{50} = 254.2$ ppm) were comparable to cypermethrin, but lower than other insecticides; **3** was more toxic than (*S*)-butylphthalide (**4**) ($LC_{50} = 338.9$ ppm) against the B-biotype females. The toxicity of these compounds against the Q-biotype females was also tested. (*Z*)-Ligustilide (**8**) and (*Z*)-butylidenephthalide (**3**) showed more pronounced toxicity against the B-biotype females than the Q-biotype. (*Z*)-Butylidenephthalide (**3**) also demonstrated acaricidal activity against two dust mite species, *Dermatophagoides farina* and *D. pteronyssinus* [443].

7.10 Bactericidal, Antifungal, Antiviral, Immunosuppressant, and Antiparasitic Effects

Mycophenolic acid (**141**) is an antibiotic agent with activity against a broad range of microorganisms including *Cryptococcus neoformans*, *Candida albicans*, *C. stellatoidean*, *C. tropicalis*, *C. parakrusei*, and *Trichophyton* species, and showed moderate inhibition of *Staphylococcus aureus* [444], which has developed some resistance to this antibiotic [445]. Mycophenolic acid (**141**; MPA) was effective in suppressing psoriasis [446], and its morpholine ester was useful in reducing episodes of allograft rejection [447]. The pharmacokinetics and pharmacodynamics of MPA analogs have been reviewed recently [448, 449].

The increasing prevalence of multidrug resistant organisms has led to the search for new, more effective, and nontoxic agents. (*Z*)-Ligustilide (**8**) showed a moderate potentiation of norfloxacin activity against a norfloxacin-resistant strain of *S. aureus*. It also reduced the minimum inhibitory concentration of norfloxacin ($MIC_{\text{norfloxacin}} = 16$ μg/cm^3) at 50 μg/cm^3 [450].

Sedanolide (**6**) displayed 100% mortality against *Panagrellus redivivus* at 25 μg/cm^3, and also against *Caenorhabditis elegans* at 50 μg/cm^3. Senkyunolides N (**52**) and J (**33**) also showed nematicidal effects against *P. redivivus* at 100 μg/cm^3 [294].

(*Z*)-Ligustilide (**8**) and the semi-synthetic product [7-(methyl thioglycolyl)-(6,7-dihydro)]-(*Z*)-ligustilide (**315**) showed weak activities against *Bacillus subtilis*, *Staphylococcus aureus*, *Candida albicans*, *Sacharomyces cerevisiae*, and *Klebsiella pneumoniae*. Phthalide **8** also displayed weak antiviral activity. (*Z*)-Ligustilide has a number of electrophilic sites and can accept nucleophiles, which might explain some of the mechanisms related to these bioactivities [89].

Cytosporone E (**197**) showed activity against *Staphylococcus aureus*, *Enterococcus faecalis*, *Escherichia coli*, and *Candida albicans* [207], while corollosporine (**279**) was active against *S. aureus* [262]. The antibacterial activity of some synthetic analogs was determined. Data for *MIC* values and the minimum bactericidal concentrations (*MBC*) after 24 h against the *Helicobacter pylori* strain 11637 are listed in Table 4.

Epimers **173** and **178** containing a 5,5-spiroacetal functionality were found to be potent anti-*Helicobacter pylori* derivatives. The (2″*R*) diastereomer **464** showed less potent bioactivity than the (2″*S*) isomer **465** [451].

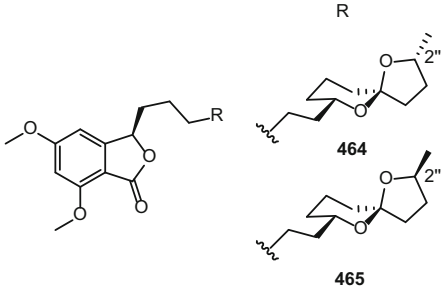

Spirolaxine (**186**) and sporotricale (**187**) showed specific activity against *Helicobacter pylori*. Awaad et al. also found that (–)-β-hydrastine (**383**), inhibited the growth of *H. pylori* (*MIC* 100 μg/cm^3) [452]. Marilone A (**203**) exhibited

Table 4 Efficacy of some phthalides against *Helicobacter pylori*

Compound	*MIC*/μg cm^{-3}	*MBC*/μg cm^{-3}
CJ-13,102 (**176**)	1.25	2.5
CJ-13,104 (**178**)	12.5	50
CJ-13,108 (**179**)	10	10–20
CJ-13,015 (**175**)	2.5	5
CJ-12,954 (**173**)	0.02	0.02
CJ-13,014 (**174**)	0.02	0.02
Spirolaxine (**186**)	0.2	>2
464	0.5	1
465	0.125	0.125

antiplasmodial activity (against *Plasmodium berghei*) in a dose-dependent manner ($IC_{50} = 12.1$ μ*M*) [214].

Microsphaerophthalide B (**228**) and microsphaerophthalide F (**232**) both displayed activity against *Microsporum gypseum* SH-MU-4 and *Cryptococcus neoformans*, respectively, both with a *MIC* value of 64 μg/cm^3. Compound **232** showed weak activity against *M. gypseum* (*MIC* = 200 μg/cm^3) [180].

(*Z*)-Butylidenephthalide (**3**), (*S*)-butylphthalide (**4**), (*Z*)-ligustilide (**8**), and (*E*)-butylidenephthalide (**21**), were evaluated against *Mycobacterium tuberculosis* $H_{37}Rv$, and *M. bovis* BCG. All had comparable IC_{50} values, ranging from 200 to 250 mg/dm^3 [453]. (±)-Concentricolide (**466**) inhibited the cytopathic effect ($EC_{50} = 0.31$ μg/cm^3) induced by HIV-1 in C8166 cells [454].

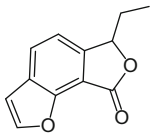

466 ((±)-concentricolide)

7.11 Herbicidal and Antifungal Effects on Plant Pathogens

The search for agents with phytotoxic and antifungal activities is relevant to the control of weeds in agricultural crops. Convolvulanic acid B (**189**) was found to be a potent phytotoxic substance, inhibiting growth (100%) and chlorosis of *Lemna paucicostata* plants at concentrations of 5.9×10^{-4} and 3.5×10^{-4} *M*, respectively. Convolvulanic acid A (**188**) and convolvulol (**190**) also inhibited the growth of *L. paucicostata*, in turn, by 80% and 50% [201]. Phthalide **201** showed antifungal activity against *Gaeumannomyces graminis* var. *tritici* and *Cladosporium herbarum*. Compound **202** also displayed activity against *Cladosporium herbarum* [352].

Phthalides **199**, **206**, **208**, and porriolide (**200**) were evaluated for their activity against *Fusarium graminearum*, *Botrytis cinerea*, and *Phytophthora nicotianae* (see Table 5). Porriolide (**200**) was found to be the most active phthalide, with *MIC* values comparable to ketoconazole, which was used as a reference compound [211].

Table 5 Activities of phthalides against some fungal plant pathogens

Compound	*MIC*/μg cm^{-3}		
	F. graminearum	*B. cinerea*	*P. nicotianae*
206	6.3	6.3	6.3
208	6.3	12.5	6.3
199	3.1	25	6.3
200	3.1	6.3	6.3

Some phthalides alter the development of plants and fungi. Thus, rubralides A (**268**) and B (**269**) inhibited the root growth of *Lactuca sativa* at 100 mg/dm^3 [255], cryphonectric acid (**194**) influenced the formation of tomato seedlings at 100 μ*M* [204], basidifferquinones A (**467**), B (**468**), and C (**469**) induced fruiting-body formation of *Favolus arcularius* [455, 456], and isopestacin (**193**) had an inhibitory effect against *Pythium ultimum*, a plant pathogenic oomycete [203].

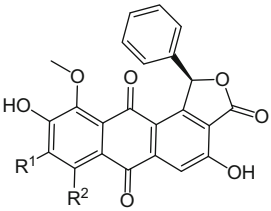

	R^1	R^2
467 (basidifferquinone A)	Me	OH
468 (basidifferquinone B)	H	OH
469 (basidifferquinone C)	H	H

7.12 Bioavailability and Routes of Administration

The majority of previous studies have analyzed the effects of (*Z*)-butylidenephthalide (**3**) and (*Z*)-ligustilide (**8**), with reports of the low bioavailability of these compounds.

The absorption, distribution, metabolism and excretion of isotopically labeled (*Z*)-butylidenephthalide (**3**) after hot or cold dermal administration have been evaluated. Compound **3** was subsequently detected in the liver, bile, and kidney at 0 h, and in the intestinal contents at 4 h. Radioactivity was maximal at 0 h in the skin and plasma (and then decreased, $t_{1/2}$ 0.5–1 h), and was sustained in the liver, bile, and kidney until 1 h, and thereafter accumulated in the small and large intestines, cecum and its contents, reaching maximal values 1–2 h later. Altogether, 70% of the unaltered or metabolized (*Z*)-butylidenephthalide (**3**) was captured from the urine at 8 h, increasing to 80% within 24 h; only 5% was excreted into the feces within 24 h. The cysteine conjugate **470** was detected in both the urine and feces. It was demonstrated that (*Z*)-butylidenephthalide (**3**) immediately permeated through the skin into the circulatory system [457].

Multiple types of pharmacokinetic studies on (*Z*)-ligustilide (**8**) have been conducted. After intravenous (i.v.) administration, compound **8** (15.6 mg/kg) exhibited extensive distribution through the body (V_d 3.76 L/kg), with rapid elimination from the plasma ($t_{1/2}$ 0.31 h). When (*Z*)-ligustilide (**8**) was administered intraperitoneally (i.p.) at a low dose (26 mg/kg), it was rapidly absorbed (T_{max} 0.05 h) and eliminated ($t_{1/2}$ 0.36 h), with i.p. bioavailability estimated to be 52%, which indicated an extensive hepatic first-pass metabolism. At a higher dose (52 mg/kg), the bioavailability was 98%, suggesting nonlinear and dose-dependent pharmacokinetics. In the case of oral administration, pharmacokinetic parameters could only be obtained at a concentration of 500 mg/kg. Compound **8** was found to be rapidly absorbed (C_{max} 0.66 μg/cm^3), with oral bioavailability established at

2.6%. Eight metabolites were identified, among them (*Z*)-butylidenephthalide (**3**), senkyunolides I (**22**) and H (**26**), and 3-hydroxybutylphthalide (**471**), as well as 11-hydroxyligustilide (**472**), **473**, and **474**. All metabolites were generated by NADPH-dependent monooxygenases [458]. Ding et al. also evaluated metabolite production after the oral administration of compound **8** (200 mg/kg), and obtained similar results to those obtained by Yan et al. [458], in addition to characterizing the metabolites **28**, **475**, and **476** [459].

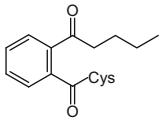

470 (cysteine conjugate)

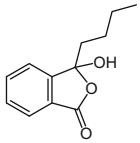

471 (3-hydroxybutylphthalide)

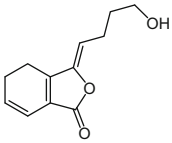

472 (11-hydroxyligustilide)

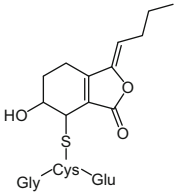

473 (isomer of hydroxyligustilide glutathione conjugate)

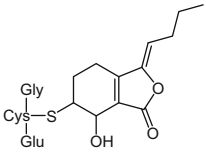

474 (isomer of hydroxyligustilide glutathione conjugate)

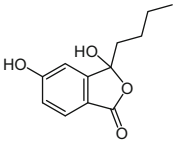

475 (3,5-dihydroxy-3-butylphthalide)

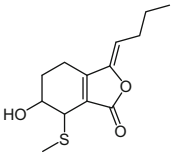

476 (6,7-dihydro-6-hydroxy-7-sulfomethylligustilide)

Compound **8** has a neuroprotective effect (see above) with a rapid onset of action following direct transport from the nasal cavity to the central nervous system (CNS). Phthalide **8** was administered to each rat nostril at 45 mg/kg, and brain tissues were collected at sequential periods of time (5–240 min) after administration. HPLC analyses of the brain tissue homogenates, together with a pharmacokinetic study, showed that **8** could be detected 5 min after administration. It was concluded that intranasal administration of (*Z*)-ligustilide (**8**) could have a rapid effect and might be more effective in the treatment of acute CNS diseases [460].

The use of nano-emulsions as a strategy to increase bioavailability is under active consideration. For instance, the anti-inflammatory effects (endotoxin-induced uveitis in rats) of orally administered (*Z*)-ligustilide (**8**) versus a nano-emulsion of ligustilide (LIGNE) were evaluated. The emulsion improved absorption given that (*Z*)-ligustilide (**8**) (20 mg/kg) was not detectable in plasma, while LIGNE remained detectable for up to 1.5 h. The nano-emulsion also improved the anti-inflammatory effect of **8** [461].

A complex of (*Z*)-ligustilide (**8**) and hydroxypropyl-β-cyclodextrin (LIG/HP-β-CD) was also prepared and quantified in rat plasma; its absolute bioavailability was found to be higher than that for (*Z*)-ligustilide (**8**) alone [462].

The pharmacokinetics of noscapine (**128**) were evaluated in male and female mice following oral (75, 150, and 300 mg/kg) and i.v. (10 mg/kg) administration. Noscapine (**128**) was easily absorbed (C_{max} 13.37, 24.48 and 49.47 μg/cm^3 in male mice, and 12.18, 22.00, and 44.00 μg/cm^3 in female mice). The AUC_{last} at 75 and 150 mg/kg were similar, but at 300 mg/kg were threefold higher, which suggested a nonlinear or saturable behavior. The $t_{1/2}$ values were similar at 75 and 300 mg/kg, but were lower at 150 mg/kg for both male and female mice. After i.v. administration, **128** was almost undetectable after 3–4 h of infusion; the $t_{1/2}$ values were 0.39 and 1.05 for males and females, respectively. It was shown that noscapine (**128**) was absorbed rapidly, and widely distributed at all doses [426].

8 Concluding Remarks

Studies on the occurrence of phthalides in Nature suggest that they are mainly confined to several higher plant families, fungi, lichens, and liverworts, with some sections of the Apiaceae plant family providing the major natural sources of these compounds. Structural analogues of (*Z*)-ligustilide and their dimers, together with mycophenolic acid analogues, could be considered as chemical markers for plant and fungal phthalides, respectively.

Chemical derivatization studies on monomeric and dimeric phthalides have demonstrated that their distinct chemical reactivities could be explained in terms of specific stereoelectronic characteristics and relative instabilities.

In the future, new analytical techniques will accelerate the structural characterization of additional minor compounds from different natural sources, establishing their interactions with macromolecular receptors and their metabolism as xenobiotic agents.

Synthesis strategies for phthalides have evolved from linear preparations to convergent ones that include efficient enantiodifferentiated reactions using new catalysts. It is foreseeable that progress in the chemistry of phthalides will focus on the exploration of their chemical and biological spaces by means of greener methodologies, including more efficient syntheses and bioassays.

Phthalides have been extensively evaluated in terms of their bioactivity, with a considerable recent literature being available on this topic. For instance, mycophenolic acid analogues are commercially available immunosupressants prescribed for autoimmune diseases, with other applications under study. Many natural phthalides display a variety of biological activities, and, in the case of compounds from the Apiaceae, most agree with the traditional medicinal uses of their natural plant sources. It has been stated that "phthalides are responsible for numerous bioactivities; however their exact mode of action is not yet realized..." [2]. One would envisage that future efforts to investigate the biological activities of phthalides, particularly in terms of neurological diseases, might show considerable promise.

References

1. Lin G, Chan SS-K, Chung H-S, Li S-L (2005) Chemistry and biological activities of naturally occurring phthalides. Stud Nat Prod Chem 32:611
2. Beck JJ, Chou S-C (2007) The structural diversity of phthalides from the Apiaceae. J Nat Prod 70:891
3. Karmakar R, Pahari P, Mal D (2014) Phthalides and phthalans: synthetic methodologies and their applications in the total synthesis. Chem Rev 114:6213
4. Yang SZ (2007) The divine farmer's Materia Medica. A translation of the Shen Nong Ben Cao Jing. Blue Poppy Press, Boulder, CO
5. Yao D, Zhang J, Chu L, Bao X, Shun Q, Qi P (1995) A colored atlas of the Chinese Materia Medica specified in pharmacopoeia of the People's Republic of China. Guangdong Science and Technology Press, Guangzhou
6. Chan SS-K, Yan R, Lin G (2013) Chuanxiong (*Ligusticum cuanxiong*). In: Li SP, Wang YT (eds) Pharmacological activity-based quality control of Chinese herbs. Nova Science, New York, p 273
7. Li W, Tang Y, Chen Y, Duan J (2012) The advance in chemical isolation and analysis of Chuanxiong. Molecules 17:10614
8. Wang L, Zhang J, Hong Y, Feng Y, Chen M, Wang Y (2013) Phytochemical and pharmacological review of Da Chanxiong formula: a famous herb pair composed of Chuanxiong Rhizoma and Gastrodiae Rhizoma for headache. Evid Based Complement Altern Med Article ID 425369
9. Seiz de Lira BJ (1777) Descripción geográfica de Guazápares. Vol II. Relaciones topográficas de los pueblos de México. Biblioteca Nacional, Madrid, MS 2450
10. Appelt GD (1985) Pharmacological aspects of selected herbs employed in Hispanic folk medicine in the San Luis Valley of Colorado, USA: I. *Ligusticum porteri* (Osha) and *Matricaria chamomilla* (Manzanilla). J Ethnopharmacol 13:51
11. Bye RA, Linares E (1986) Ethnobotanical notes from the Valley of San Luis, Colorado (USA). J Ethnobiol 6:289
12. Linares E, Bye RA (1987) A study of four medicinal plant complexes of Mexico and adjacent United States. J Ethnopharmacol 19:153
13. Newton P (1992) Can animals teach us medicine? Over the counter and into the forest. Br Med J 305:1517
14. Ciamician G, Silber P (1897) Ueber die hochsiedenden Bestandtheile des Sellerieöls. Ber Dtsch Pharm 30:492
15. Cichy M, Höfle G (1897) Ueber die Spaltungs-producte der Sedanonsäure. Ber Dtsch Pharm 30:501
16. Ciamician G, Silber P (1897) Ueber die Sedanolsäure. Ber Dtsch Pharm 30:1424
17. Ciamician G, Silber P (1897) Ueber die Sedanolsäure und das Sedanolid. Ber Dtsch Pharm 30:1427
18. Ciamician G, Silber P (1898) Studi sui principii dell'essenza di sedano. Gazz Chim Ital 1:438
19. Barton DHR, DeVries JX (1963) The constitution of sedanolide. J Chem Soc C:1916
20. Swenholt J (1910) Oil of celery seed. Midl Drug Pharm Rev 44:220
21. Berlingozzi S, Mazza FP (1926) Sulle idroftalidi. I. Azione dei magnesio-iodo-alchili sull'anidride-D-tetraidroftalica. Gazz Chim Ital 56:88
22. Berlingozzi S, Cione L (1927) Sulle idroftalidi. II. Azione de l'amalgama di sodio sule monoalchiliden-ftalidi. Gazz Chim Ital 57:243
23. Berlingozzi S (1927) Sulle idroftalidi. III. Derivati della D-diidroftalidi. Gazz Chim Ital 57:248
24. Berlingozzi S, Lupo G (1927) Sulle idroftalidi. IV. Sul derivato *n*-butilico della tetraidroftalide. Gazz Chim Ital 57:255
25. Berlingozzi S (1927) Sulle idroftalidi. V. Contributo allo studio dei rapporti fra costituzione e odore. Gazz Chim Ital 57:264

26. Murayama Y, Itakagi T (1923) Chemical constituents of a Chinese drug “Hsiung- Ch’uang”. II. J Pharm Soc Jpn 43:143
27. Noguchi T (1934) Beitrage zur Kenntnis der chemischen Bestandteile von Sen-Kyu. J Pharm Soc Jpn 54:913
28. Murayama IY (1921) Chemical constituents of a Chinese drug “Hsiung-Ch’uang”. J Pharm Soc Jpn 41:951
29. Kariyone T, Kotani M (1937) Constituents of the fruits of *Ligusticum acutilobum*. III. J Pharm Soc Jpn 57:183
30. Noguchi T, Fujita S, Kawanami M (1937) Über die Bestandteile der Wurzel von *Ligusticum actilobum*. I. J Pharm Soc Jpn 57:769
31. Noguchi T, Kawanami M (1937) Über die Bestandteile der Wurzel von *Ligusticum actilobum* II, IV. Mitteil. Zur Kenntnis der chemischen Bestandteile der Umbelliferae. J Pharm Soc Jpn 57:783
32. Noguchi T, Kawanami M (1937) Über die Dehydrierungsprodukte des Sedanolid, Cnidiumlacton und Sedanonsäure. J Pharm Soc Jpn 57:778
33. Naves YR (1943) Études sur les matières vegetales volatiles XXIV. Composition de l’huile essentiele et du résinoïde de livéche (*Levisticum officinale* Koch). Helv Chim Acta 26:1281
34. Takahashi S, Hikino H, Sasaki Y (1958) Pharmacognostical components of Umbelliferous plants IX. Toki 9. Components of the roots of *Angelica acutiloba* and *A. acutiloba* var. *sugiyamae*. J Pharm Soc Jpn 79:1156
35. Mitsuhashi H, Nagai U (1963) Studies on the constituents of Umbelliferae. VII. Structure of ligustilide. Tetrahedron 19:1277
36. Mitsuhashi H, Muramatsu T (1964) Studies on the constituents of Umbelliferae plants. IX: Structure of cnidilide and neocnidilide. Tetrahedron 20:1971
37. Nagai U, Mitsuhashi H (1965) Constituents of Umbelliferae plants. X. Stereochemistry of 3-butylhydrophthalides. Tetrahedron 21:1433
38. Nagai U, Shishido T, Chiba R, Mitsuhashi H (1965) Constituents of Umbelliferae plants. XI. Stereochemistry of 3-butylhydrophthalides. Tetrahedron 21:1701
39. Cocker W, McMurry TBH, Sainsbury DM (1966) Synthesis of certain *n*-butyltetra- and hexa-hydrophthalides. J Chem Soc C:1152
40. Stahl E, Bohrmann H (1966) Phthalide als Hauptbestandteile des Ätherischen Öls der Früchte von *Meum athamanticum*. Naturwissenschaften 110:118
41. Bohrmann H, Stahl E, Mitsuhashi H (1967) Studies of the constituents of Umbelliferae plants. XIII. Chromatographic studies on the constituents of *Cnidium officinale* Makino. Chem Pharm Bull 15:1606
42. Gold J, Wilson CW (1963) Alkylidene phthalides and dihydrophthalides from celery. J Org Chem 28:985
43. Wilson CW (1970) Relative recovery and identification of carbonyl compounds from celery essential oil. J Food Sci 35:766
44. Bjeldanes LF, Kim IS (1977) Phthalide components of celery essential oil. J Org Chem 42:2333
45. Saiki Y, Okamoto (née Suzuki) M, Ueno A, Uchida M, Fukushima S (1970) Gas chromatographical studies on natural volatile oils. VIII. On the essential oils of Chinese Medicine “Gaoben.” J Pharm Soc Jpn 90:344
46. Yamagishi T, Kaneshima H (1977) Constituents of *Cnidium officinale* Makino. Structure of senkyunolide and gas chromatography-mass spectrometry of the related phthalides. J Pharm Soc Jpn 97:237
47. Gijbels MJM, Scheffer JJC, Baerheim Svendsen A (1979) Phthalides in Umbelliferae. Riv Ital EPPOS 61:335
48. Fehr D (1979) Study on the aroma substances of celery (*Apium graveolens* L.). Part I. Pharmazie 34:658
49. Fehr D (1981) Study on the aroma substances of celery (*Apium graveolens* L.). Part 2. Pharmazie 36:374

50. Gijbels MJM, Scheffer JJC, Baerheim Svendsen A (1981) Analysis of phthalides from Umbelliferae by combined liquid-solid and gas-liquid chromatography. Chromatographia 14:452
51. Banerjee SK, Gupta BD, Sheldrick WS, Höfle G (1982) Angeolide, a novel lactone from *Angelica glauca*. Liebigs Ann Chem:699
52. Gijbels MJM, Scheffer JJC, Svendsen Baerheim A (1982) Phthalides in roots of *Cenolophium denudatum* and in roots, herb and fruits of *Coriandrum sativum*. Fitoterapia 53:17
53. Gijbels MJM, Scheffer JJC, Baerheim Svendsen A (1982) Phthalides in the essential oil from roots of *Levisticum officinale*. Planta Med 44:207
54. Gijbels MJM, Scheffer JJC, Baerheim Svendsen A (1982) Phthalides in roots of *Silaum silaus* (L.) Schinz et Thell. Sci Pharm 50:158
55. Gijbels MJM, Fischer FC, Scheffer JJC, Baerheim Svendsen A (1983) Phthalides in roots of *Anethum graveolens* and *Todaroa montana*. Sci Pharm 51:414
56. Kaouadji M, Puech-Baronnat M, Mariot A-M (1983) (*Z*)-Ligustidiol, nouveau phthalide hydroxyle isole de *Ligusticum wallichii* Franch. Tetrahedron Lett 24:4675
57. Kaouadji M, Reutenauer H, Chulia AJ, Marsura A (1983) (*Z,Z′*)-Diligustilide, noveau phthalide dimere isole de *Ligusticum wallichii* Franch. Tetrahedron Lett 24:4677
58. Meng Y, Wang Q, Zhang H, Chen Y, Fab Y, Wang F (1984) Molecular structure of riligustilide. Lanzhou Daxue Xuebao, Ziram Kexueban 19:76 (Chem Abstr 100:135781j)
59. Wang P, Guo X, Wang Y, Fukuyama Y, Miura I, Sugawara M (1984) Phthalides from the rhizome of *Ligusticum wallichii*. Phytochemistry 23:2033
60. Kobayashi M, Fujita M, Mitsuhashi H (1984) Components of *Cnidium officinale* Makino: occurrence of pregnenolone, coniferyl ferulate, and hydroxyphthalides. Chem Pharm Bull 32:3770
61. Gijbels MJ, Fischer FC, Scheffer JJ, Baerheim Svendsen A (1984) Phthalides in roots of *Capnophyllum peregrinum* and *Peucedanum ostruthium*. Planta Med 50:110
62. Puech-Baronnat M, Kaouadji M, Mariotte AM (1984) (Z)-5-Hydroxy- and (Z)-4,5-dihydroxybutylidene-3-phthalides, new compounds isolated from *Ligusticum wallichii*. Planta Med 50:105
63. Cichy M, Wray V, Höfle G (1984) Neue Inhaltsstoffe von *Levisticum officinale* Koch Liebstöckel. Liebigs Ann Chem:397
64. Banerjee SK, Gupta BD, Sheldrick WS, Höfle G (1984) Lactonic constituents of *Angelica glauca*. Liebigs Ann Chem:888
65. Kaouadji M, Mariotte AM, Reutenauer H (1984) Phthalide derivatives from *Meum athamanticum* Jacq. Z Naturforsch C 39C:872
66. Kaouadji M, Pouget C, Kaouadji M (1986) Additional phthalide derivatives from *Meum athamanticum*. J Nat Prod 49:184
67. Gijbels MJM, Fischer FC, Scheffer JJC, Baerheim Svendsen A (1985) Phthalides in roots of *Apium graveolens*, *A. graveolens* var. *rapaceum*, *Bifora testiculata* and *Petroselinum crispum* var. *tuberosum*. Fitoterapia 56:17
68. Sheu SJ, Ho YS, Chen YP, Hsu HY (1987) Analysis and processing of Chinese herbal drugs: VI. The study of Angelicae Radix. Planta Med 53:377
69. Kaouadji M, De Pachtere F, Pouget C, Chulia A, Lavaitte S (1986) Three additional phthalide derivatives, an epoxymonomer and two dimers from *Ligusticum wallichii* rhizomes. J Nat Prod 49:872
70. Delgado G, Reza-Garduño RG, Toscano RA, Bye R, Linares E (1988) Secondary metabolites from the roots of *Ligusticum porteri* (Umbelliferae). X-ray structure of *Z*-6.6′,7,3′a-diligustilide. Heterocycles 27:1305
71. Naito T, Katsuhara T, Niitsu K, Ikeya Y, Okada M, Mitsuhashi H (1991) Phthalide dimers from *Ligusticum chuangxiong* Hort. Heterocycles 32:2433
72. Tsuchida T, Kobayashi M, Kaneko K, Mitsuhashi H (1987) Studies on the constituents of Umbelliferae plants. XVI. Isolation and structures of three new ligustilide derivatives from *Angelica acutiloba*. Chem Pharm Bull 35:4460

73. Kobayashi M, Mitsuhashi H (1987) Studies on the constituents of Umbelliferae plants XVII. Structures of three new ligustilide derivatives from *Ligusticum wallichii*. Chem Pharm Bull 35:4789
74. Fischer FC, Gijbels MJM (1987) *cis*- and *trans*-Neocnidilide; ^{1}H- and ^{13}C-NMR data of some phthalides. Planta Med 53:77
75. Segebrecht S, Schilcher H (1989) Ligustilide: guiding component for preparations of *Levisticum officinale* roots. Planta Med 55:572
76. Szebeni-Galambosi Z, Galambosi B, Holm Y (1992) Growth, yield and essential oil of lovage grown in Finland. J Essent Oil Res 4:375
77. Abdel-Mogib M, Ayyad SN, Metwally MA, Dawidar AM (1992) Lactones from *Pituranthos tortusus* (Apiaceae). Pak J Sci Ind Res 35:93
78. Delgado G, Reza-Garduño RG, Ríos MY, del Río F (1992) Phthalides and monoterpenes of the hexane of the roots of *Ligusticum porteri*. Planta Med 58:570
79. MacLeod AJ, Macleod G, Snyder CH (1988) Volatile aroma constituents of celery. Phytochemistry 27:373
80. MacLeod G, Ames JM (1989) Volatile components of celery and celeriac. Phytochemistry 28:1817
81. Van Wassenhove F, Dirinck P, Ghent B, Vulsteke G (1990) Aromatic volatile composition of celery and celeriac cultivars. HortScience 25:556
82. Tang J, Station AE, Brunswick N (1990) Free and glycosidically bound volatile compounds in fresh celery. J Agric Food Chem 38:1937
83. Van Wassenhove FA, Dirinck PJ, Schamp NM, Vulstekel GA (1990) Effect of nitrogen fertilizers on celery volatiles. J Agric Food Chem 38:220
84. Maruhashi M, Hanada K, Misogami K, Nagakura A (1992) Novel phthalide derivative as NGF enhancer from *Apium graveolens*. Jpn Kokai Tokkyo Koho JP 04334378 A 19921120 (Chem Abstr 118:240924)
85. Nitz S, Spraul MH, Drawert F (1992) 3-Butyl-5,6-dihydro-4*H*-isobenzofuranone, a sensorial active phthalide in parsley roots. J Agric Food Chem 40:1038
86. Hon P, Lee C, Choang F, Chui K, Wong HNC (1990) A ligustilide dimer from *Angelica sinensis*. Phytochemistry 29:1189
87. Naito T, Katsuhara T, Niitsu K, Ikeya Y, Okada M, Mitsuhashi H (1992) Two phthalides from *Ligusticum chuanxiong*. Phytochemistry 31:639
88. Naito T, Niitsu K, Ikeya Y, Okada M, Mitsuhashi H (1992) A phthalide and 2-farnesyl-6-methyl benzoquinone from *Ligusticum chuanxiong*. Phytochemistry 31:1787
89. Beck JJ, Stermitz FR (1995) Addition of methyl thioglycolate and benzylamine to (*Z*)-ligustilide, a bioactive unsaturated lactone constituent of several herbal medicines. An improved synthesis of (*Z*)-ligustilide. J Nat Prod 58:1047
90. Brandt JJ, Schultze W (1995) Composition of the essential oils of *Ligusticum mutellina* (L.) Crantz (Apiaceae). J Essent Oil Res 7:231
91. Dung NX, Cu LD, Moi LD, Leclerck PA (1996) Composition of the leaf and flower oils from *Angelica sinensis* (Oliv.) Diels cultivated in Vietnam. J Essent Oil Res 8:503
92. Kaul PN, Mallavarapu GR, Chamoli RP (1996) The essential oil composition of *Angelica glauca* roots. Planta Med 62:80
93. Naito T, Ikeya Y, Okada M, Mistuhashi H, Maruno M (1996) Two phthalides from *Ligusticum chuangxiong*. Phytochemistry 41:233
94. Bartschat D, Maas B, Smietana S, Mosandl A, Lebensmittelchemie I, Frankfurt JWG (1996) Stereoisomeric flavour compounds LXXIII: 3-butylphthalide: chirospecific analysis, structure and properties of the enantiomers. Phytochem Anal 7:131
95. Bartschat D, Beck T, Mosandl A (1997) Stereoisomeric flavor compounds. 79. Simultaneous enantioselective analysis of 3-butylphthalide and 3-butylhexahydrophthalide stereoisomers in celery, celeriac, and fennel. J Agric Food Chem 45:4554

96. Bylaité E, Venskutonis RP, Roozen JP (1998) Influence of harvesting time on the composition of volatile components in different anatomical parts of lovage (*Levisticum officinale* Koch.). J Agric Food Chem 46:3735
97. Bedrossian A, Beauchamp PE, Dev V, Kwan S, Munevar-Mendoza E, Okoreeh E (1998) Composition of the essential oil of *Lomatium torreyi*. J Essent Oil Res 10:473
98. Tirillini B, Pellegrino R, Menghini A, Tomaselli B (1999) Essential oil components in the epigeous and hypogeous parts of *Meum athamanticum* Jacq. J Essent Oil Res 11:251
99. Choudhury S, Rajkhowa A, Dutta S, Kanjilal PB, Sharma RK, Leclercq PA (2000) Volatile seed oils of *Trachyspermum roxburghianum* Benth. ex Kurz. from India. J Essent Oil Res 12:731
100. Gillespie SG, Duszynski J (1998) Phthalides and monoterpenes of the hexane extracts of the roots of *Ligusticum porteri*, *L. filicinum* and *L. tenuifolium*. Planta Med 64:1998
101. Hagemeier J, Batz O, Schmidt J, Wray V, Hahlbrock K, Strack D (1999) Accumulation of phthalides in elicitor-treated cell suspension cultures of *Petroselinum crispum*. Phytochemistry 51:629
102. Kitajima J, Ishikawa T, Satoh M (2003) Polar constituents of celery seed. Phytochemistry 64:1003
103. Li Y, Peng S, Zhou Y, Yu K-B, Ding L-S (2006) Two new phthalides from *Ligusticum chuanxiong*. Planta Med 72:652
104. Ka MH, Choi EH, Chun HS, Li KG (2005) Antioxidant activity of volatile extracts isolated from *Angelica tenuissimae* roots, peppermint leaves, pine needles, and sweet flag leaves. J Agric Food Chem 53:4124
105. Palá-Paúl J, Garc R (2004) Essential oil composition of the leaves and stems of *Meum athamanticum* Jacq., from Spain. J Chromatogr 1036:245
106. Lim LS, Shen P, Gong YH, Yong EL (2006) Dimeric progestins from rhizomes of *Ligusticum chuanxiong*. Phytochemistry 67:728
107. Wen Y, He S, Xue K, Cao F (1986) Chemical components of *Ligusticum chuanxiong*. Zhongcaoyao 17:122
108. Ogawa Y, Hosaka K, Chin M, Mitsuhashi H (1989) Synthesis of (-)-3-butyl-4-hydroxyphthalide. Heterocycles 29:865
109. Deng S, Chen SN, Lu J, Wang ZJ, Nikolic D, van Breemen RB, Santarsiero BD, Mesecar A, Fong HHS, Farnsworth NR, Pauli GF (2006) GABAergic phthalide dimers from *Angelica sinensis* (Oliv.) Diels. Phytochem Anal 17:398
110. Deng S, Chen SN, Yao P, Nikolic D, van Breemen RB, Bolton JL, Fong HHS, Farnsworth NR, Pauli GF (2006) Serotonergic activity-guided phytochemical investigation of the roots of *Angelica sinensis*. J Nat Prod 69:536
111. Lü J-L, Duan J-A, Tang Y-P, Yang N-Y, Zhang L-B (2009) Phthalide mono- and dimers from the radix of *Angelica sinensis*. Biochem Syst Ecol 37:405
112. Chang X-L, Jiang Z-Y, Ma Y-B, Zhang X-M, Tsim KWK, Chen J-J (2009) Two new compounds from the roots of *Ligusticum chuanxiong*. J Asian Nat Prod Res 11:805
113. Li W, Tang Y, Chen Y, Duan J-A (2012) Advances in the chemical analysis and biological activities of Chuanxiong. Molecules 17:10614
114. Ran X, Ma L, Peng C, Zhang H, Qin L-P (2011) *Ligusticum chuanxiong* Hort.: a review of chemistry and pharmacology. Pharm Biol 49:1180
115. Huang J, Lu XQ, Zhang C, Lu J, Li GY, Lin RC, Wang JH (2013) Anti-inflammatory ligustilides from *Ligusticum chuanxiong* Hort. Fitoterapia 91:21
116. Wei Q, Yang J, Ren J, Wang A, Ji T, Su Y (2014) Bioactive phthalides from *Ligusticum sinense* Oliv. cv. *chaxiong*. Fitoterapia 93:226
117. Yang J-B, Wang A-G, Wei Q, Ren J, Ma S-C, Su Y-L (2014) New dimeric phthalides from *Ligusticum sinense* Oliv. cv. *chaxiong*. J Asian Nat Prod Res 16:747
118. León A, Toscano RA, Cogordán JA, Delgado G (2010) Differentiated cyclization of the ketoacid derived from tokinolide B. Heterocycles 82:1567

119. Niu Y, Wang S (2014) A new phthalide from *Angelica sinensis* radix. China J Chin Mater Med 39:80
120. Raeisi S, Mirjalili MH, Nadjafi F, Hadian J (2015) Variability in the essential oil content and composition in different plant organs of *Kelussia odoratissima* Mozaff. (Apiaceae) growing wild in Iran. J Essent Oil Res 27:283
121. Inouye H, Okuda T, Hirata Y, Nagakura N, Yoshizaki M (1967) Structure of catalpalactone, a new phthalide from catalpa wood. Chem Pharm Bull 15:786
122. Inouye H, Okuda T, Hayashi T (1975) Quinones and related compounds in higher plants. II. On the naphthoquinones and related compounds from catalpa wood. Chem Pharm Bull 23:384
123. Fujiwara A, Mori T, Iida A, Ueda S, Hano Y, Nomura T, Tokuda H, Nishino H (1998) Antitumor-promoting naphthoquinones from *Catalpa ovata*. J Nat Prod 61:629
124. Bregaoui A, Boughallleb N, Ben Jannet H, Harzallah-Shiric F, El Mahjoub M, Mighri Z (2007) Chemical composition and antifungal activity of volatiles from three *Opuntia* species growing in Tunisia. Pak J Biol Sci 10:2485
125. Opitz L, Hansel R (1971) Phthalide aus *Helichrysum italicum*. Arch Pharm 304:228
126. Zapesochnaya GG, Dzyadevich TV, Karasartov BS (1990) Phenolic compounds of *Helichrysum italicum*. Chem Nat Compd 26:342
127. Vrkoč J, Ubik K, Sedmera P, Vrkoč J, Ubik K, Sedmera P (1973) Phenolic extractives from the achenes of *Helichrysum arenarium*. Phytochemistry 12:2062
128. Vrkoč J, Buděšínský M, Dolejš L, Vašíčková S (1975) Arenophthalide A: a new phthalide glycoside from *Helichrysum arenarium* roots. Phytochemistry 14:1845
129. Jakupovic J, Schuster A, Sun H, Bohlmann F, Bhakuni DS (1987) Prenylated phthalides from *Anaphalis araneosa* and *Helichrysum platypterum*. Phytochemistry 26:580
130. Venditti A, Lattanzi C, Ornano L, Maggi F, Sanna C, Ballero M, Alvino A, Serafini M, Bianco A (2016) A new glucosidic phthalide from *Helichrysum microphyllum* subsp. *tyrrhenicum* from La Maddalena Island (Sardinia, Italy). Nat Prod Res 30:789
131. Talapatra B, Roy MK, Talapatra SK (1980) Structures of two new phthalides from *Anaphalis contorta* Hook f. Indian J Chem B 19B:927
132. Tada M, Chiba K (1984) Novel plant growth inhibitors and an insect antifeedant from *Chrysanthemum coronarium* (Japanese name: Shungiku). Agric Biol Chem 48:1367
133. Sari A, Zidorn C, Ellmerer EP, Özgökçe F, Ongania KH, Stuppner H (2007) Phenolic compounds from *Scorzonera tomentosa* L. Helv Chim Acta 90:311
134. Zheng X-P, Cui Q-F, Zhao J-F, Yang L-J, Zhang H-B, Yang X-D, Li L (2014) Three new phthalides from *Gnaphalium adnatum*. Helv Chim Acta 97:1638
135. Blaskó G, Hussain SF, Shamma M (1981) (–)-Corlunmine, a new phthalideisoquinoline alkaloid from *Fumaria parviflora*. J Nat Prod 44:475
136. Chulia AJ, Kaouadji M, Mariotte A-M (1989) Pedicelloside, nouveau phtalide isole de *Gentiana pedicellata Wall*. Tetrahedron Lett 25:5039
137. Chulia AJ, Garcia J, Mariotte A-M (1986) New phthalide glycoside from *Gentiana pedicellata*. J Nat Prod 49:514
138. Garcia J, Mpondo Mpondo E, Chulia AJ, Kaouadji M, Cartier G (1989) Two phthalide glucosides from *Gentiana pyrenaica*. Phytochemistry 28:1759
139. Fukuhara K, Fujimori T, Shigematsu H, Ohnishi A (1987) Essential oil of *Scutellaria baicalensis* G. Agric Biol Chem 51:1449
140. Malan E, Roux DG (1974) (+)-2,3-*trans*-Pubeschin, the first catechin analogue of peltogynoids from *Peltogyne pubescens* and *P. venosa*. Phytochemistry 13:1575
141. Nakano Y, Takasima T (1975) Extractives of *Albizzia julibrissin* heartwood. Mokuzai Gakkaishi 21:577
142. Okorie DA (1976) A new phthalide and xanthones from *Anthochleista djalonensis* and *Anthochleista vogelli*. Phytochemistry 15:1799
143. Kameoka H, Miyazawwa M, Haze K (1975) 3-Ethyl-7-hydroxyphthalide from *Forsythia japonica*. Phytochemistry 14:1676

144. Shao P, Zhang X, Li B, Jiao W, Wu L, Yao X-S (2010) New isocoumarin and phthalide derivatives from the rhizomes of *Matteuccia orientalis*. Chem Pharm Bull 58:1650
145. Inubushi Y, Tsuda Y, Konita T, Matsumoto S (1964) Shihuhine: a new phthalide-pyrrolidine alkaloid. Chem Pharm Bull 12:749
146. Inubushi Y, Tsuda Y, Konita T, Matsumoto S (1968) The structure of shihunine, a new phthalide-pyrrolidine alkaloid. Chem Pharm Bull 16:1014
147. Elander M, Leander K, Lüning B (1969) Studies on Orchidaceae alkaloids XIV. A phthalide alkaloid from *Dendrobium pierardii* Roxb. Acta Chem Scand 23:2177
148. Elander M, Gawell L, Leander K (1971) Studies on Orchidaceae alkaloids XXII. Synthesis and absolute configuration of pierardine, lactone-betaine isomerization of shihunine. Acta Chem Scand 25:721
149. Lee C, Choe S, Lee JW, Jin Q, Lee MK, Hwang BY (2013) Alkaloids from *Papaver setigerum*. Bull Kor Chem Soc 34:1290
150. Chou TH, Chen IS, Hwang TL, Wang TC, Lee TH, Cheng LY, Chang YC, Cho JY, Chen JJ (2008) Phthalides from *Pittosporum illicioides* var. *illicioides* with inhibitory selectivity on superoxide generation and elastase release by neutrophils. J Nat Prod 71:1692
151. Takahashi H, Tsubuki T, Higashiyama K (1991) Highly diastereoselective reaction of chiral *o*-[2-(1,3-oxazolidinyl)]benzaldehydes with alkylmetallic reagents: synthesis of chiral 3-substituted phthalides. Chem Pharm Bull 39:3136
152. Knights BA (1966) Isolation of 4-hydroxyphthalide from oat grain. Nature 210:1261
153. Grech JN, Li Q, Roufogalis BD, Duke CC (1994) Novel Ca^{2+}-ATPase inhibitors from the dried root tubers of *Polygonum multiflorum*. J Nat Prod 57:1682
154. Yoshikawa M, Uchida E, Chatani N, Murakami N, Yamahara J (1992) Thunberginols A, B, and F, new antiallergic and antimicrobial principles from Hydrangeae Dulcis Folium. Chem Pharm Bull 40:3121
155. Yoshikawa M, Shimada H, Yagi N, Murakami N, Shimoda H, Yamahara J, Matsuda H (1996) Development of bioactive functions in Hydrangeae Dulcis Folium. VI. Syntheses of thunberginols A and F and their 3′-deoxy-derivatives using regiospecific lactonization of stilbene carboxylic acid: structures and inhibitory activity on histamine release of hydramacraphyllols A and B. Chem Pharm Bull 44:1890
156. Yoshikawa M, Harada E, Naitoh Y, Inoue K, Matsuda H, Shimoda H, Yamahara J, Murakami N (1994) Development of bioactive functions in Hydrangeae Dulcis Folium. III. On the antiallergic and antimicrobial principles of Hydrangeae Dulcis Folium. (1). Thunberginols A, B, and F. Chem Pharm Bull 42:2225
157. Yoshikawa M, Harada E, Yagi N, Okuno Y, Muraoka O, Aoyama H, Murakami N (1994) Chemical transformation from dihydroisocoumarin into benzylidenephthalide by use of regiospecific oxidative lactonization mediated by copper chloride(II). Syntheses of thunberginol F and hydramacrophyllols A and B. Chem Pharm Bull 42:721
158. Shode FO, Mahomed AS, Rogers CB (2002) Typhaphthalide and typharin, two phenolic compounds from *Typha capensis*. Phytochemistry 61:955
159. Alsberg CL, Black OF (1913) Contributions to the study of maize deterioration. Biochemical and toxicological investigations of *Penicillium puberulum* and *Penicillium stoloniferum*. U S Dep Agric Bur Plant Ind 270:7
160. Clutterbuck PW, Raistrick H (1933) Studies in the biochemistry of micro-organisms. XXXI. The molecular constitution of the metabolic products of *Penicillium brevi-compactum* Dierckx and related species. II. Mycophenolic acid. Biochem J 27:654
161. Birkinshaw JH, Bracken A, Morgan EN, Raistrick H (1948) Studies in the biochemistry of micro-organisms. 78. The molecular constitution of mycophenolic acid, a metabolic product of *Penicillium brevi-compactum* Dierckx. Part 2. Possible structural formulae for mycophenolic acid. Biochem J 43:216
162. Birkinshaw JH, Raistrick H, Ross DJ (1952) Studies in the biochemistry of micro-organisms. 86. The molecular constitution of mycophenolic acid, a metabolic product of *Penicillium*

brevi-compactum Dierckx. Part 3. Further observations on the structural formula for mycophenolic acid. Biochem J 50:630
163. Clutterbuck WP, Oxford AE, Raistrick H, Smith G (1932) Studies in the biochemistry of micro-organisms. XXIV: The metabolic products of *Penicillium brevi-compactum* series. Biochem J 26:1441
164. Nakajima S, Nozawa K (1979) Isolation in high yield of citrinin from *Penicillium odoratum* and of mycophenolic acid from *Penicillium brunneo-stoloniferum*. J Nat Prod 42:423
165. Anderson HA, Bracewell JM, Fraser AR, Jones D, Robertson GW, Russell JD (1988) 5-Hydroxymaltol and mycophenolic acid, secondary metabolites from *Penicillium echinulatum*. Trans Br Mycol Soc 91:649
166. Sumarah MW, Miller JD, Blackwell BA (2005) Isolation and metabolite production by *Penicillium roqueforti*, *P. paneum* and *P. crustosum* isolated in Canada. Mycopathologia 159:571
167. Torrenegra RD, Baquero JE, Calderón JS (2005) Actividad antimicrobiana y asignación completa de RMN ^{1}H y ^{13}C del ácido micofenólico aislado de *Penicillium verrucosum*. Rev Latinoam Quím 33:76
168. Erbert C, Lopes AA, Yokoya NS, Furtado NAJC, Conti R, Pupo MT, Lopes JLC, Debonsi HM (2012) Antibacterial compound from the endophytic fungus *Phomopsis longicolla* isolated from the tropical red seaweed *Bostrychia radicans*. Bot Mar 55:435
169. Rovirosa J, Diaz-Marrero A, Darias J, Painemal K, San Martin A (2006) Secondary metabolites from marine *Penicillium brevicompactum*. J Chil Chem Soc 51:775
170. Valente AMMP, Ferreira AG, Daolio C, Filho ER, Boffo EF, Souza AQL, Sebastianes FLS, Melo IS (2013) Production of 5-hydroxy-7-methoxy-4-methylphthalide in a culture of *Penicillium crustosum*. An Acad Bras Cienc 85:487
171. Habib E, León F, Bauer JD, Hill RA, Carvalho P, Cutler HG, Cutler SJ (2008) Mycophenolic derivatives from *Eupenicillium parvum*. J Nat Prod 71:1915
172. Chen Z, Zheng Z, Huang H, Song Y, Zhang X, Ma J, Wang B, Zhang C, Ju J (2012) Penicacids A-C, three new mycophenolic acid derivatives and immunosuppressive activities from the marine-derived fungus *Penicillium* sp. SOF07. Bioorg Med Chem Lett 22:3332
173. Colombo L, Gennari C, Potenza D, Scolastico C, Aragozzini F (1979) (*E*,*E*)-10-(1,3-Dihydro-4,6-dihydroxy-7-methyl-3-oxoisobenzofuran-5-yl)-4,8-dimethyldeca-4,8-dienoic acid: total synthesis and role in mycophenolic acid biosynthesis. J Chem Soc Chem Commun:1021
174. Lu X, Zheng Z, Zhang H, Huo C, Dong Y, Ma Y, Ren X, Ke A, He J, Gu Y, Shi Q (2009) Two new members of mycophenolic acid family from *Penicillium brevicompactum* Dierckx. J Antibiot 62:527
175. Birkinshaw JH, Raistrik H, Ross DJ, Stickings CE (1952) Studies in the biochemistry of micro-organisms. 85. Cyclopolic and cyclopaldic acids, metabolic products of *Penicillium cyclopium* Westling. Biochem J 50:610
176. Brillinger GU, Heberle W, Weber B, Achenbach H (1978) Metabolic products of microorganisms 167. Cyclopaldic acid from *Aspergillus duricaulis*. 1. Production, isolation and biological properties. Arch Microbiol 116:245
177. Evidente A, Motta A, Sparapano L (1993) Seiricardines B and C, phytotoxic sesquiterpenes from three species of *Seiridium* pathogenic for cypress. Phytochemistry 33:69
178. Frisvad JC, Filtenborg O (1989) *Terverticillate penicillia*: chemotaxonomy and mycotoxin production. Mycologia 81:837
179. Shimada A, Nakaya K, Takeuchi S, Kimura Y (2001) Deoxycyclopaldic acid and cyclopaldic acid, plant regulators, produced by *Penicillium* sp. Z Naturforsch B 449
180. Sommart U, Rukachaisirikul V, Tadpetch K, Sukpondma Y, Phongpaichit S, Hutadilok-Towatana N, Sakayaroj J (2012) Modiolin and phthalide derivatives from the endophytic fungus *Microsphaeropsis arundinis* PSU-G18. Tetrahedron 68:10005
181. Achenbach H, Mühlenfeld A, Weber B, Brillinger GU (1982) Highly substituted chromanols from cultures of *Aspergillus duricaulis*. Tetrahedron Lett 23:4659

182. Hemberger Y, Xu J, Wray V, Proksch P, Wu J, Bringmann G (2013) Pestalotiopens A and B: stereochemically challenging flexible sesquiterpene-cyclopaldic acid hybrids from *Pestalotiopsis* sp. Chem Eur J 19:15556
183. Brian PW, Curtis PJ, Grove JF, Hemming HG, McGowan JC (1946) Gladiolic acid: an antifungal and antibacterial metabolic product of *Penicillium gladioli* McCull. and Thom. Nature 157:697
184. Grove JF (1952) Gladiolic acid, a metabolic product of *Penicillium gladioli*. I. Structure. Biochem J 50:648
185. Grove JF (1953) Gladiolic acid, a metabolic product of *Penicillium gladioli*. 2. Structure and fungistatic activity. Biochem J 54:664
186. Raistrick H, Ross DJ (1952) Studies in the biochemistry of micro-organisms. 87. Dihydrogladiolic acid, a metabolic product of *Penicillium gladioli* Machacek. Biochem J 50:635
187. Duncanson LA, Grove JF, Zealley J (1953) Gladiolic acid. Part III. The structures of norisogladiolic acid, dihydrogladiolic acid, and cyclopolic acid. J Chem Soc:3637
188. Brown JJ, Newbold GT (1953) Phthalaldehydes and related compounds. Part III. Synthesis of deoxygladiolic acid and experiments relating to structure of dihydrogladiolic acid. J Chem Soc:3648
189. Starratt AN (1970) Structure of an artifact formed during isolation of *Penicillium gladioli* metabolites. Can J Chem 48:2940
190. Li Y-Y, Wang M-Z, Huang Y-J, Shen Y-M (2010) Secondary metabolites from *Phomopsis* sp. A123. Mycology 1:254
191. Kameda K, Namiki M (1974) A new phthalide from a fungus, *Alternaria kikuchiana*. Chem Lett 1491
192. Höller U, Gloer JB, Wicklow DT (2002) Biologically active polyketide metabolites from an undetermined fungicolous hyphomycete resembling *Cladosporium*. J Nat Prod 65:876
193. Jadulco R, Brauers G, Edrada RA, Ebel R, Wray V, Sudarsono, Proksch P (2002) New metabolites from sponge-derived fungi *Curvularia lunata* and *Cladosporium herbarum*. J Nat Prod 65:730
194. Cui C-B, Ubukata M, Kakeya H, Onose R, Okada G, Takahashi I, Isono K, Osada H (1996) Acetophthalidin, a novel inhibitor of mammalian cell cycle, produced by a fungus isolated from a sea sediment. J Antibiot 49:216
195. Schneider G, Anke H, Sterner O (1997) New secondary metabolites from a mycophilic *Hansfordia* species. Nat Prod Lett 10:133
196. Dekker KA, Inagaki T, Gootz TD, Kaneda K, Nomura E, Sakakibara T, Sakemi S, Sugie Y, Yamauchi Y, Yoshikawa N, Kojima N (1997) CJ-12,954 and tts congeners, new anti-*Helicobacter pylori* compounds produced by *Phanerochaete velutina*: fermentation, isolation, structural elucidation and biological activities. J Antibiot 50:833
197. Makino M, Endoh T, Ogawa Y, Watanabe K, Fujimoto Y (1998) Studies on the metabolites of *Penicillium vulpinum*. Heterocycles 48:1931
198. Afiyatullov SS, Leshchenko EV, Sobolevskaya MP, Gerasimenko AV, Khudyakova YV, Kirichuk NN, Mikhailov VV (2015) New 3-[2′(*R*)-hydroxybutyl]-7-hydroxyphthalide from marine isolate of the fungus *Penicillium claviforme*. Chem Nat Compd 51:111
199. Fujita M, Yamada M, Nakajima S, Kawai K, Nagai M (1984) *O*-Methylation effect on the carbon-13 nuclear magnetic resonance signals of *ortho*-disubstituted phenols and its application to structure determination of new phthalides from *Aspergillus silvaticus*. Chem Pharm Bull 32:2622
200. Arnone A, Assante G, Nasini G, De Pava OV (1990) Spirolaxine and sporotricale: two long-chain phthalides produced by *Sporotrichum laxum*. Phytochemistry 29:613
201. Tsantrizos Y, Ogilvie K, Watson A (1992) Phytotoxic metabolites of *Phomopsis convolvulus*, a host-specific pathogen of field bindweed. Can J Chem 70:2276
202. Zou J, Li J, Wu Z-Y, Zhao Q, Wang G-Q, Zhao H, Chen G-D, Sun X, Guo L-D, Gao H (2015) New α-pyrone and phthalide from the Xylariaceae fungus. J Asian Nat Prod Res 17:705

203. Strobel G, Ford E, Worapong J, Harper JK, Arif AM, Grant DM, Fung PCW, Chau RMW (2002) Isopestacin, an isobenzofuranone from *Pestalotiopsis microspora*, possessing anti-fungal and antioxidant activities. Phytochemistry 60:179
204. Arnone A, Assante G, Nasini G, Strada S, Vercesi A (2002) Cryphonectric acid and other minor metabolites from a hypovirulent strain of *Cryphonectria parasitica*. J Nat Prod 65:48
205. Abdel-Lateff A, Fisch KM, Wright AD, König GM (2003) A new antioxidant isobenzofuranone derivative from the algicolous marine fungus *Epicoccum* sp. Planta Med 69:831
206. Huang XZ, Zhu Y, Guan XL, Tian K, Guo JM, Wang H Bin, Fu GM (2012) A novel antioxidant isobenzofuranone derivative from fungus *Cephalosporium* sp. AL031. Molecules 17:4219
207. Brady SF, Wagenaar MM, Singh MP, Janso JE, Clardy J (2000) The cytosporones, new octaketide antibiotics isolated from an endophytic fungus. Org Lett 2:4043
208. Mullady EL, Millett WP, Yoo HD, Weiskopf AS, Chen J, DiTullio D, Knight-Connoni V, Hughes DE, Pierceall WE (2004) A phthalide with in vitro growth inhibitory activity from an *Oidiodendron* strain. J Nat Prod 67:2086
209. Suemitsu R, Ohnishi K, Morikawa Y, Nagatomo S (1995) Zinnimidine and 5-(3′,3′-dimethylallyloxy)-7-methoxy-6-methylphthalide from *Alternaria porri*. Phytochemistry 38:495
210. Phuwapraisirisan P, Rangsan J, Siripong P, Tip-Pyang S (2009) New antitumour fungal metabolites from *Alternaria porri*. Nat Prod Res 23:1063
211. Yang X-L, Zhang S, Hu Q-B, Luo D-Q, Zhang Y (2011) Phthalide derivatives with antifungal activities against the plant pathogens isolated from the liquid culture of *Pestalotiopsis photiniae*. J Antibiot 64:723
212. Chen C, Yang RL (2013) A phthalide derivative isolated from endophytic fungi *Pestalotiopsis photiniae* induces G1 cell cycle arrest and apoptosis in human HeLa cells. Braz J Med Biol Res 46:643
213. Takahashi K, Koshino H, Narita Y, Yoshihara T (2005) Novel antifungal compounds produced by sterile dark, an unidentified wheat rhizosphere fungus. Biosci Biotechnol Biochem 69:1018
214. Almeida C, Kehraus S, Prudêncio M, König GM (2011) Marilones A-C, phthalides from the sponge-derived fungus *Stachylidium* sp. Beilstein J Org Chem 7:1636
215. Yoganathan K, Rossant C, Ng S, Huang Y, Butler MS, Buss AD (2003) 10-Methoxydihydrofuscin, fuscinarin, and fuscin, novel antagonists of the human CCR5 receptor from *Oidiodendron griseum*. J Nat Prod 66:1116
216. Matsumoto K, Nagashima K, Kamigauchi T, Kawamura Y, Yasuda Y, Ishii K, Uotani N, Sato T, Nakai H, Terui Y, Kikuchi J, Ikenisi Y, Yoshida T, Kato T, Itazaki H (1995) Salfredins, new aldose reductase inhibitors produced by *Crucibulum* sp. RF-3817 I. Fermentation, isolation and structures of salfredins. J Antibiot 48:439
217. Prachyawarakorn V, Mahidol C, Sureram S, Sangpetsiripan S, Wiyakrutta S, Ruchirawat S, Kittakoop P (2008) Diketopiperazines and phthalides from a marine derived fungus of the order Pleosporales. Planta Med 74:69
218. Ding G, Liu S, Guo L, Zhou Y, Che Y (2008) Antifungal metabolites from the plant endophytic fungus *Pestalotiopsis foedan*. J Nat Prod 71:615
219. Yoshikawa K, Kokudo N, Hashimoto T, Yamamoto K, Inose T, Kimura T (2010) Novel phthalide compounds from *Sparassis crispa* (Hanabiratake), Hanabiratakelide A-C, exhibiting anti-cancer related activity. Biol Pharm Bull 33:1355
220. Rana NM, Sargent MV, Elix JA (1975) Structure of the lichen depsidone variolaric acid. J Chem Soc Perkin Trans 1:1992
221. Xing J-G, Deng H-Y, Luo D-Q (2011) Two new compounds from an endophytic fungus *Pestalotiopsis heterocornis*. J Asian Nat Prod Res 13:1069

222. Tianpanich K, Prachya S, Wiyakrutta S, Mahidol C, Ruchirawat S, Kittakoop P (2011) Radical scavenging and antioxidant activities of isocoumarins and a phthalide from the endophytic fungus *Colletotrichum* sp. J Nat Prod 74:79
223. Rukachaisirikul V, Rodglin A, Sukpondma Y, Phongpaichit S, Buatong J, Sakayaroj J (2012) Phthalide and isocoumarin derivatives produced by an *Acremonium* sp. isolated from a mangrove *Rhizophora apiculata*. J Nat Prod 75:853
224. Arunpanichlert J, Rukachaisirikul V, Tadpetch K, Phongpaichit S, Hutadilok-Towatana N, Supaphon O, Sakayaroj J (2012) A dimeric chromanone and a phthalide: metabolites from the seagrass-derived fungus *Bipolaris* sp. PSU-ES64. Phytochem Lett 5:604
225. Bava A, Dallavalle S, Fronza G, Nasini G, Vajna de Pava O (2006) Absolute configuration of sporotricale and structure of 6-hydroxysporotricale. J Nat Prod 69:1793
226. Wang S, Zhang S, Zhou T, Zhan J (2013) Three new resorcylic acid derivatives from *Sporotrichum laxum*. Bioorg Med Chem Lett 23:5806
227. Lan W-J, Liu W, Liang W-L, Xu Z, Le X, Xu J, Lam C-K, Yang D-P, Li H-J, Wang L-Y (2014) Pseudaboydins A and B: novel isobenzofuranone derivatives from marine fungus *Pseudallescheria boydii* associated with starfish *Acanthaster planci*. Mar Drugs 12:4188
228. Yang J, Huang R, Qiu SX, She Z, Lin Y (2013) A new isobenzofuranone from the mangrove endophytic fungus *Penicillium* sp. (ZH58). Nat Prod Res 27:1902
229. Wang J, Wang G, Zhang Y, Zheng B, Zhang C, Wang L (2014) Isolation and identification of an endophytic fungus *Pezicula* sp. in *Forsythia viridissima* and its secondary metabolites. World J Microbiol Biotechnol 30:2639
230. Liu J, Li F, La Kim E, Li JL, Hong J, Bae KS, Chung HY, Kim HS, Jung JH (2011) Antibacterial polyketides from the jellyfish-derived fungus *Paecilomyces variotii*. J Nat Prod 74:1826
231. Grove JF (1972) New metabolic products of *Aspergillus flavus*. Part II. Asperflavin, anhydroasperflavin, and 5,7-dihydroxy-4-methylphthalide. J Chem Soc Perkin Trans 1:2406
232. Gunawan S, Steffan B, Steglich W (1990) Xylaral, ein Hydroxyphthalid-Derivat aus Fruchtkörpern von *Xylaria polymorpha* (Ascomycetes). Liebigs Ann Chem:825
233. Nozawa K, Udagawa S, Nakahima S, Kawai K (1989) A dioxopiperazine derivative from *Penicillium megasporum*. Phytochemistry 28:929
234. Wang R-Y, Fang M-J, Huang Y-J, Zheng Z-H, Shen Y-M (2006) 7-Hydroxy-4,6-dimethyl-3*H*-isobenzofuran-1-one. Acta Chrystallogr E E62:O4172
235. Zhang W, Xu L, Yang L, Huang Y, Li S, Shen Y (2014) Phomopsidone A, a novel depsidone metabolite from the mangrove endophytic fungus *Phomopsis* sp. A123. Fitoterapia 96:146
236. Lin X, Huang Y, Fang M, Wang J, Zheng Z, Su W (2005) Cytotoxic and antimicrobial metabolites from marine lignicolous fungi, *Diaporthe* sp. FEMS Microbiol Lett 251:53
237. Lang G, Cole ALJ, Blunt JW, Robinson WT, Munro MHG (2007) Excelsione, a depsidone from an endophytic fungus isolated from the New Zealand endemic tree *Knightia excelsa*. J Nat Prod 70:310
238. Meister J, Weber D, Martino V, Sterner O, Anke T (2007) Phomopsidone, a novel depsidone from an endophyte of the medicinal plant *Eupatorium arnottianum*. Z Naturforsch C 62:11
239. Fuska J, Fusková A, Nemec P (1979) Vermistatin, an antibiotic with cytotoxic effects, produced from *Penicillium vermiculatum*. Biologia 34:735
240. Proksa B, Liptaj T, Prónayová N, Fuska J (1994) (−)-Mitorubrinic acid, a new metabolite of *Penicillium vermiculatum* Dang. F-852. Chem Pap 48:429
241. Fuska J, Uhrin D, Proksa B, Voticky Z, Ruppeldt J (1986) The structure of vermistatin, a new metabolite from *Penicillium vermiculatum*. J Antibiot 39:1605
242. Murtaza N, Husain SA, Sarfaraz TB, Sultana N, Faizi S (1997) Isolation and identification of vermistatin, ergosterol, stearic acid and mannitol, metabolic products of *Penicillium verruculosum*. Planta Med 63:191
243. Arai M, Tomoda H, Okuda T, Wang H, Tabata N, Masuma R, Yamaguchi Y, Omura S (2002) Funicone-related compounds, potentiators of antifungal miconazole activity, produced by *Talaromyces flavus* FKI-0076. J Antibiot 55:172

244. Komai S, Hosoe T, Itabashi T, Nozawa K, Okada K, de Galba Maria CT, Chikamori M, Yaguchi T, Fukushima K, Miyaji M, Kawai K (2004) A new funicone derivative isolated from *Talaromyces flavus* IFM52668. Mycotoxins 54:15
245. Upadhyay RK, Strobel GA, Coval SJ, Clardy J (1990) Fijiensin, the first phytotoxin from *Mycosphaerella fijiensis*, the causative agent of black sigatoka disease. Experientia 46:982
246. Komai S, Hosoe T, Itabashi T, Nozawa K, Yaguchi T, Fukushima K, Kawai K (2005) New vermistatin derivatives isolated from *Penicillium simplicissimum*. Heterocycles 65:2771
247. Dethoup T, Manoch L, Kijjoa A, Pinto M, Gales L, Damas AM, Silva AMS, Eaton G, Herz W (2007) Merodrimanes and other constituents from *Talaromyces thailandiasis*. J Nat Prod 70:1200
248. Stierle AA, Stierle DB, Girtsman T (2012) Caspase-1 inhibitors from an extremophilic fungus that target specific leukemia cell lines. J Nat Prod 75:344
249. Xia XK, Huang HR, She ZG, Cai JW, Lan L, Zhang JY, Fu LW, Vrijmoed LLP, Lin YC (2007) Structural and biological properties of vermistatin and two new vermistatin derivatives isolated from the marine-mangrove endophytic fungus *Guignardia* sp. No. 4382. Helv Chim Acta 90:1925
250. Liu Y, Xia G, Ma L, Ding B, Lu Y, He L, Xia X, She Z (2014) Vermistatin derivatives with α-glucosidase inhibitory activity from the mangrove endophytic fungus *Penicillium* sp. HN29-3B1. Planta Med 80:912
251. Xia X-K, Liu F, She Z-G, Yang L-G, Li M-F, Vrijmoed LLP, Lin Y-C (2008) ^{1}H and ^{13}C NMR assignments for 6-demethylvermistatin and two penicillide derivatives from the mangrove fungus *Guignardia* sp. (no. 4382) from the South China Sea. Magn Reson Chem 46:693
252. Liu W, Zhao H, Li R, Zheng H, Yu Q (2015) Polyketides and meroterpenoids from *Neosartorya glabra*. Helv Chim Acta 98:515
253. Arnone A, Nasini G (1989) Secondary mould metabolites. XXV. The structures of rubellins C and D, two novel anthraquinone metabolites from *Mycosphaerella rubella*. Gazz Chim Ital 119:35
254. Puder C, Zeeck A (2000) New biologically active rubiginones from *Streptomyces* sp. J Antibiot 53:329
255. Imura YK, Oshinari TY, Oshino HK, Ujioka SF, Kada KO, Himada AS (2007) Rubralactone, rubralides A, B and C, and rubramin produced by *Penicillium rubrum*. Biosci Biotechnol Biochem 71:1896
256. Zhai M-M, Niu H-T, Li J, Xiao H, Shi Y-P, Di D-L, Crews P, Wu Q-X (2015) Talaromycolides A–C, novel phenyl-substituted phthalides isolated from the green Chinese onion-derived fungus *Talaromyces pinophilus* AF-02. J Agric Food Chem 63:9558
257. Ge HM, Shen Y, Zhu CH, Tan SH, Ding H, Song YC, Tan RX (2008) Penicidones A-C, three cytotoxic alkaloidal metabolites of an endophytic *Penicillium* sp. Phytochemistry 69:571
258. Chinworrungsee M, Kittakoop P, Isaka M, Chanphen R, Tanticharoen M, Thebtaranonth Y (2002) Halorosellins A and B, unique isocoumarin glucosides from the marine fungus *Halorosellinia oceanica*. J Chem Soc Perkin Trans 1:2473
259. Tayone WC, Honma M, Kanamaru S, Noguchi S, Tanaka K, Nehira T, Hashimoto M (2011) Stereochemical investigations of isochromenones and isobenzofuranones isolated from *Leptosphaeria* sp. KTC 727. J Nat Prod 74:425
260. El-Elimat T, Raja HA, Figueroa M, Falkinham III JO, Oberlies NH (2014) Isochromenones, isobenzofuranone, and tetrahydronaphthalenes produced by *Paraphoma radicina*, a fungus isolated from a freshwater habitat. Phytochemistry 104:114
261. Kawahara N, Nakajima S, Satoh Y, Yamakazi M, Kawai K-I (1988) Studies on fungal products XVIII. Isolation and structures of a new fungal depsidone related to nidulin and new phthalide from *Emericella unguis*. Chem Pharm Bull 36:1970
262. Liberra K, Jansen R, Lindequist U (1998) Corollosporine, a new phthalide derivative from the marine fungus *Corollospora maritima* Werderm. 1069. Pharmazie 53:578

263. Takenaka Y, Morimoto N, Hamada N, Tanahashi T (2011) Phenolic compounds from the cultured mycobionts of *Graphis proserpens*. Phytochemistry 72:1431
264. Asakawa Y, Takikawa K, Toyota M, Takemoto T (1982) Novel bibenzyl derivatives and *ent*-cuparene-type sesquiterpenoids from *Radula* species. Phytochemistry 21:2481
265. Asakawa Y, Takikawa K, Tori M, Campbell EO (1986) Isotachin C and balantiolide, two aromatic compounds from the New Zealand liverwort *Ballantiopsis rosea*. Phytochemistry 25:2543
266. Asakawa Y, Takikawa K, Tori M (1987) Bibenzyl derivatives from the Australian liverwort *Frullania falciloba*. Phytochemistry 26:1023
267. Asakawa Y, Ludwiczuk A, Nagashima F (2013) Chemical constituents of Bryophytes. Bio- and chemical diversity, biological activity, and chemosystematics. In: Kinghorn AD, Falk H, Kobayashi J (eds) Progress in the chemistry of organic natural products, vol 95. Springer, Vienna, 796 p
268. Kraut L, Mues R, Simsim M (1994) Sesquiterpene lactones and 3-benzylphthalides from *Frullania muscicola*. Phytochemistry 37:1337
269. Rycroft DS, Cole WJ, Aslam N, Lamont YM, Gabriel R (1999) Killarniensolide, methyl orsellinates and 9,10-dihydrophenanthrenes from the liverwort *Plagiochila killarniensis* from Scotland and the Azores. Phytochemistry 50:1167
270. Heinrichs J, Anton H, Gradstein SR, Mues R, Heirichs J, Anton H, Gradstein SR, Mues R (2000) Systematics of *Plagiochila* sect. *Glaucescentes* Carl (Hepaticae) from tropical America: a morphological and chemotaxonomical approach. Plant Syst Evol 220:115
271. Nagashima F, Toyota M, Asakawa Y (2006) Bazzanane sesquiterpenoids from the New Zealand liverwort *Frullania falciloba*. Chem Pharm Bull 54:1347
272. Mitsuhashi H, Nomura M (1966) Studies on the constituents of Umbelliferae plants. XII. Biogenesis of 3-butylphthalide. Chem Pharm Bull 14:777
273. Kim MR, El-Aty AMA, Kim IS, Shim JH (2006) Determination of volatile flavor components in Danggui cultivars by solvent free injection and hydrodistillation followed by gas chromatographic-mass spectrometric analysis. J Chromatogr A 1116:259
274. Kim MR, El-Aty AMA, Choi J-H, Lee KB, Shim JH (2006) Identification of volatile components in *Angelica* species using supercritical-CO_2 fluid extraction and solid phase microextraction coupled to gas chromatography-mass spectroscopy. Biomed Chromatogr 20:1267
275. Dong L, Deng C, Wang B, Shen X (2007) Fast determination of *Z*-ligustilide in plasma by gas chromatography/mass spectrometry following headspace single-drop microextraction. J Sep Sci 30:1318
276. León A, Toscano RA, Tortoriello J, Delgado G (2011) Phthalides and other constituents from *Ligusticum porteri*: sedative and spasmolytic activities of some natural products and derivatives. Nat Prod Res 25:1234
277. Su S, Cui W, Zhou W, Duan J, Shang E, Tang Y (2013) Chemical fingerprinting and quantitative constituent analysis of siwu decoction categorized formulae by UPLC-QTOF/MS/MS and HPLC-DAD. Chin Med 8:1
278. Song ZH, Ji ZN, Lo CK, Dong TTX, Zhao KJ, Ll OTW, Haines CJ, Kung SD, Tsim KWK (2004) Chemical and biological assessment of a traditional Chinese herbal decoction prepared from Radix Astragali and Radix *Angelica sinensis*: orthogonal array design to optimize the extraction of chemical constituents. Planta Med 70:1222
279. Yang X, Wu X, Guo H (2012) Effect of different solvents on extraction of effective components from *Ligusticum chuanxiong*. China J Chin Mater Medica 37:1942
280. Yi T, Leung KS-Y, Lu G-H, Chan K, Zhang H (2006) Simultaneous qualitative and quantitative analyses of the major constituents in the rhizome of *Ligusticum chuanxiong* using HPLC-DAD-MS. Chem Pharm Bull 54:255
281. Tang Y, Zhu M, Yu S, Hua Y, Duan JA, Su S, Zhang X, Lu Y, Ding A (2010) Identification and comparative quantification of bio-active phthalides in essential oils from Si-Wu-Tang, Fo-Shou-San, Radix Angelica and Rhizoma Chuanxiong. Molecules 15:341

282. Dauksas E, Venskutonis PR, Sivik B (1999) Supercritical CO_2 extraction of the main constituents of lovage (*Levisticum officinale* Koch.) essential oil in model systems and overground botanical parts of the plant. J Supercrit Fluids 15:51
283. Dauksas E, Venskutonis PR, Sivik B, Nillson T (2002) Effect of fast CO_2 pressure changes on the yield of lovage (*Levisticum officinale* Koch.) and celery (*Apium graveolens* L.) extracts. J Supercrit Fluids 22:201
284. Teng J, Chen H, Li D, Luo A (2006) Identification and characterization of supercritical fluid extracts of Rhizoma Chuanxiong by high performance liquid chromatography ion trap mass spectrometry. Front Chem China 4:454
285. Zhang C, Qi M, Shao Q, Zhou S, Fu R (2007) Analysis of the volatile compounds in *Ligusticum chuanxiong* Hort. using HS-SPME-GC-MS. J Pharm Biomed Anal 44:464
286. Yansheng C, Zhida Z, Changping L, Qingshan L, Peifang Y, Welz-Biermann U (2011) Microwave-assisted extraction of lactones from *Ligusticum chuanxiong* Hort. using protic ionic liquids. Green Chem 13:666
287. Dong ZB, Li SP, Hong M, Zhu Q (2005) Hypothesis of potential active components in *Angelica sinensis* by using biomembrane extraction and high performance liquid chromatography. J Pharm Biomed Anal 38:664
288. Lao SC, Li SP, Kan KKW, Li P, Wan JB, Wang YT, Dong TTX, Tsim KWK (2004) Identification and quantification of 13 components in *Angelica sinensis* (Danggui) by gas chromatography-mass spectrometry coupled with pressurized liquid extraction. Anal Chim Acta 526:131
289. Li P, Li SP, Lao SC, Fu CM, Kan KKW, Wang YT (2006) Optimization of pressurized liquid extraction for *Z*-ligustilide, *Z*-butylidenephthalide and ferulic acid in *Angelica sinensis*. J Pharm Biomed Anal 40:1073
290. Xie J-J, Lu J, Qian Z-M, Yu Y, Duan J-A, Li S-P (2009) Optimization and comparison of five methods for extraction of coniferyl ferulate from *Angelica sinensis*. Molecules 14:555
291. Liu J-L, Zheng S-L, Fan Q-J, Yuan J-C, Yang S-M, Kong F-L (2014) Optimization of high-pressure ultrasonic-assisted simultaneous extraction of six major constituents from *Ligusticum chuanxiong* rhizome using response surface methodology. Molecules 19:1887
292. Zhang Y, Liu C, Qi Y, Li Y, Li S (2015) Development of circulating ultrasonic-assisted online extraction coupled to countercurrent chromatography and centrifugal partition chromatography for simultaneous extraction and isolation of phytochemicals: application to *Ligusticum chuanxiong* Hort. Ind Eng Chem Res 54:3009
293. Mitsuhashi H, Nagai U, Muramatsu T, Tashiro H (1960) Studies on the constituents of Umbelliferae plants. II. Isolation of the active principles of *Ligusticum* root. Chem Pharm Bull 8:243
294. Momin RA, Nair MG (2001) Mosquitocidal, nematicidal, and antifungal compounds from *Apium graveolens* L. seeds. J Agric Food Chem 49:142
295. Chou S-C, Everngam MC, Sturtz G, Beck JJ (2006) Antibacterial activity of components from *Lomatium californicum*. Phytother Res 20:153
296. Zhang DL, Teng HL, Li GS, Liu K, Su ZG (2006) Separation and purification of *Z*-ligustilide and senkyunolide A from *Ligusticum chuanxiong* Hort. with supercritical fluid extraction and high-speed counter-current chromatography. Sep Sci Technol 41:3397
297. Wang X, Shi X, Li F, Liu J, Cheng C (2008) Application of analytical and preparative high-speed counter-current chromatography for separation of *Z*-ligustilide from crude extract of *Angelica sinensis*. Phytochem Anal 19:193
298. Wei Y, Huang W, Gu Y (2013) Online isolation and purification of four phthalide compounds from Chuanxiong Rhizoma using high-speed counter-current chromatography coupled with semi-preparative liquid chromatography. J Chromatogr A 1284:53
299. Kwon JH, Ahn YJ (2002) Acaricidal activity of butylidenephthalide identified in *Cnidium officinale* rhizome against *Dermatophagoides farinae* and *Dermatophagoides pteronyssinus* (Acari: Pyroglyphidae). J Agric Food Chem 50:4479

300. León A, Chávez MI, Delgado G (2011) ^{1}H and DOSY NMR spectroscopy analysis of *Ligusticum porteri* rhizome extracts. Magn Reson Chem 49:469
301. Lang G, Mayhudin NA, Mitova MI, Sun L, Van Der Sar S, Blunt JW, Cole ALJ, Ellis G, Laatsch H, Munro MHG (2008) Evolving trends in the dereplication of natural product extracts: new methodology for rapid, small-scale investigation of natural product extracts. J Nat Prod 71:1595
302. Zschocke S, Liu JH (1998) Comparative study of roots of *Angelica sinensis* and related Umbelliferous drugs by thin layer chromatography, high-performance liquid chromatography, and liquid chromatography-mass spectrometry. Phytochem Anal 9:283
303. Zschocke S, Klaiber I, Bauer R, Vogler B (2005) HPLC-coupled spectroscopic techniques (UV, MS, NMR) for the structure elucidation of phthalides in *Ligusticum chuanxiong*. Mol Divers 9:33
304. Beauchamp PS, Bottini AT, Dev V, Melkani AB, Timbrook J (1993) Analysis of the essential oil from *Lomatium californicum* (Nutt.) Math. and Const. Dev Food Sci 32:605
305. Lu G-H, Chan K, Liang Y-Z, Leung K, Chan C-L, Jiang Z-H, Zhao Z-Z (2005) Development of high-performance liquid chromatographic fingerprints for distinguishing Chinese Angelica from related Umbelliferae herbs. J Chromatogr A 1073:383
306. Lu GH, Chan K, Chan CL, Leung K, Jiang ZH, Zhao ZZ (2004) Quantification of ligustilides in the roots of *Angelica sinensis* and related umbelliferous medicinal plants by high-performance liquid chromatography and liquid chromatography-mass spectrometry. J Chromatogr A 1046:101
307. Yang B, Chen J, Lee FS-C, Wang X (2008) GC-MS fingerprints for discrimination of *Ligusticum chuanxiong* from *Angelica*. J Sep Sci 31:3231
308. Yi T, Leung KS-Y, Lu G-H, Zhang H, Chan K (2005) Identification and comparative determination of senkyunolide A in traditional Chinese medicinal plants *Ligusticum chuanxiong* and *Angelica sinensis* by HPLC coupled with DAD and ESI-MS. Chem Pharm Bull 53:1480
309. Rivero I, Juárez K, Zuluaga M (2012) Quantitative HPLC method for determining two of the major active phthalides from *Ligusticum porteri* roots. J AOAC Int 95:84
310. Li S-L, Yan R, Tam Y-K, Lin G (2007) Post-harvest alteration of the main chemical ingredients in *Ligusticum chuanxiong* Hort. (Rhizoma Chuanxiong). Chem. Pharm Bull 55:140
311. Qin HL, Deng AJ, Du GH, Wang P, Zhang JL, Li ZH (2009) Fingerprinting analysis of Rhizoma Chuanxiong of commercial types using H-1 nuclear magnetic resonance spectroscopy and high performance liquid chromatography method. J Integr Plant Biol 51:537
312. Morris KF, Johnson CS (1992) Diffusion-ordered two-dimensional nuclear magnetic resonance spectroscopy. J Am Chem Soc 114:3139
313. Morris KF, Johnson CS (1993) Resolution of discrete and continuous molecular size distributions by means of diffusion-ordered 2D NMR spectroscopy. J Am Chem Soc 115:4291
314. Birch AJ, English RJ, Massy-Westropp RA, Slaytor M, Smith H (1958) Studies in relation to biosynthesis. Part XIV. The origin of nuclear methyl groups in mycophenolic acid. J Chem Soc 365
315. Birch AJ, Wright JJ (1969) A total synthesis of mycophenolic acid. Aust J Chem 22:2635
316. Canonica L, Kroszczynski W, Ranzi BM, Rindone B, Santaniello E, Scolastico C (1972) Biosynthesis of mycophenolic acid. J Chem Soc Perkin Trans 1:2639
317. Bedford CT, Knitell P, Money T, Phillips GT, Salisbury P (1973) Biosynthesis of mycophenolic acid. Can J Chem 51:694
318. Bentley R (2000) Mycophenolic acid: a one hundred year odyssey from antibiotic to immunosuppressant. Chem Rev 100:3801
319. Regueira TB, Kildegaard KR, Hansen BG, Mortensen UH, Hertweck C, Nielsen J (2011) Molecular basis for mycophenolic acid biosynthesis in *Penicillium brevicompactum*. Appl Environ Microbiol 77:3035

320. Ogawa Y, Mori Y, Maruno M, Wakamatsu T (1997) Diels-Alder reaction of ligustilide giving levistolide A and tokinolide B. Heterocycles 45:1869
321. Rios MY, Delgado G, Toscano RA (1998) Chemical reactivity of phthalides. Relay synthesis of diligustilide, *rel*-(3′*R*)-3′,8′-dihydrodiligustilide and wallichilide. Tetrahedron 54:3355
322. Lager E, Sundin A, Toscano RA, Delgado G, Sterner O (2007) Diels-Alder adducts derived from the natural phthalide *Z*-ligustilide. Tetrahedron Lett 48:4215
323. Rios MY, Delgado G (1999) Lewis acid catalyzed transformations of *Z*-ligustilide. J Mex Chem Soc 43:127
324. Schinkovitz A, Pro SM, Main M, Chen SN, Jaki BU, Lankin DC, Pauli GF (2008) Dynamic nature of the ligustilide complex. J Nat Prod 71:1604
325. Cui F, Feng L, Hu J (2006) Factors affecting stability of *Z*-ligustilide in the volatile oil of Radix *Angelica sinensis* and *Ligusticum chuanxiong* and its stability prediction. Drug Dev Ind Pharm 32:747
326. Zhan JY-X, Zhang WL, Zheng KY-Z, Zhu KY, Chen J-P, Chan P-H, Dong TT-X, Choi RC-Y, Lam H, Tsim KW-K, Lau DT-W (2013) Chemical changes of *Angelica sinensis* Radix and Chuanxiong Rhizoma by wine treatment: chemical profiling and marker selection by gas chromatography coupled with triple quadrupole mass spectrometry. Chin Med 8:12
327. Zuo A-H, Cheng M-C, Zhuo R-J, Wang L, Xiao H-B (2013) Structure elucidation of degradation products of *Z*-ligustilide by UPLC-QTOF-MS and NMR spectroscopy. Acta Pharm Sin 48:911
328. Kobayashi M, Fujita M, Mitsuhashi H (1987) Studies on the constituents of Umbelliferae plants. XV. Constituents of *Cnidium officinale*: occurrence of pregnenolone, coniferyl ferulate and hydroxyphthalides. Chem Pharm Bull 35:1427
329. Cimmino A, Andolfi A, Avolio F, Ali A, Tabanca N, Khan IA, Evidente A (2013) Cyclopaldic acid, seiridin, and sphaeropsidin A as fungal phytotoxins, and larvicidal and biting deterrents against *Aedes aegypti* (Diptera: Culicidae): structure-activity relationships. Chem Biodivers 10:1239
330. Nelson PH, Carr SF, Devens BH, Eugui EM, Franco F, Gonzalez C, Hawley RC, Loughhead DG, Milan DJ, Papp E, Patterson JW, Rouhafza S, Sjogren EB, Smith DB, Stephenson RA, Talamas FX, Waltos AM, Weikert RJ, Wu JC (1996) Structure-activity relationships for inhibition of inosine monophosphate dehydrogenase by nuclear variants of mycophenolic acid. J Med Chem 39:4181
331. Rios MY, Delgado G, Espinosa-Pérez G (1998) Base-catalyzed intramolecular condensations of diligustilide. Tetrahedron Lett 39:6605
332. Quiroz-García B, Hernández-Ortega S, Sterner O, Delgado G (2004) Transformations of the natural dimeric phthalide diligustilide. Tetrahedron 60:3681
333. Quiroz-García B, Hernández L, Toscano RA, Sterner O, Delgado G (2003) Base-catalyzed intramolecular condensation of tokinolide B. Tetrahedron Lett 44:2509
334. León A, Cogordán JA, Sterner O, Delgado G (2012) Enantiomeric derivatives of tokinolide B: absolute configuration and biological properties. J Nat Prod 75:859
335. León A, Delgado G (2012) Diligustilide: enantiomeric derivatives, absolute configuration and cytotoxic properties. J Mex Chem Soc 56:222
336. Kitayama T (1997) Microbial asymmetric syntheses of 3-alkylphthalide derivatives. Tetrahedron Asymmetry 8:3765
337. He L, Sun J, Xu Y, Sun Z, Zheng C (2008) Novozyme 435-catalyzed efficient acylation of 3-*n*-butylphthalide in organic medium. Prep Biochem Biotechnol 38:376
338. He L, Sun J, Xu Y, Sun ZH (2008) A novel method to resolve (*R*,*S*)-3-*n*-butylphthalide catalyzed by Novozyme 435 in microaqueous medium. Process Biochem 43:1215
339. He L, Li C, Gao B (2009) Novozyme 435-catalyzed asymmetric acylation of (*R*,*S*)-3-*n*-butylphthalide in hexane. Prep Biochem Biotechnol 39:266
340. Li C, He L, Qiu B, Gao B (2010) An efficient system for the asymmetric acylation of (*R*,*S*)-3-*n*-butylphthalide catalyzed by Novozyme 435. Prep Biochem Biotechnol 40:354

341. Jekkel A, Barta I, Kónya A, Süto J, Boros S, Horváth G, Ambrus G (2001) Microbiological transformation of mycophenolic acid. J Mol Catal B Enzym 11:423
342. Jekkel A, Barta I, Boros S, Suto J, Horváth G, Szabó Z, Ambrus G (2002) Microbial transformation of mycophenolic acid. Part II. J Mol Catal B Enzym 19–20:209
343. Jones DF, Moore RH, Crawley GC (1970) Microbial modification of mycophenolic acid. J Chem Soc C 1725
344. Herath WHMW, Ferreira D, Khan IA (2003) Microbial transformation of the phthalideisoquinoline alkaloid, beta-hydrastine. Nat Prod Res 17:269
345. Nasini G, Bava A, Fronza G, Giannini G (2007) Microbial transformation of spirolaxine, a bioactive undecaketide fungal metabolite from the Basidiomycete *Sporotrichum laxum*. Chem Biodivers 4:2772
346. Bava A, Nasini G, Fronza G (2012) Biotransformation of spirolaxine by *Absidia cuneospora* and *Trametes hirsuta*: formation of β-glycosyl and β-xylosyl derivatives. J Mol Catal B Enzym 82:59
347. Mali RS, Babu KN (1998) Naturally occurring prenylated phthalides: first total synthesis of salfredin B11. J Chem Res 292
348. Alder K, Rickert HF (1936) Zur Kenntnis der Dien-synthese. I. Über eine Methode der Direkten Unterscheidung Cyclischer Penta- und Hexa-diene. Justus Liebigs Ann Chem 524:180
349. Patterson JW (1993) The synthesis of mycophenolic acid. Tetrahedron 49:4789
350. Brookes PA, Cordes J, White AJP, Barrett AGM (2013) Total synthesis of mycophenolic acid by a palladium-catalyzed decarboxylative allylation and biomimetic aromatization sequence. Eur J Org Chem 32:7313–7319
351. Hariprakasha HK, Subba Rao GSR (1998) Synthesis based on cyclohexadienes. Part 26. Total synthesis of some naturally occurring phthalides from *Alternaria* species. Indian J Chem B 37:851
352. Katoh N, Nakahata T, Kuwahara S (2008) Synthesis of novel antifungal phthalides produced by a wheat rhizosphere fungus. Tetrahedron 64:9073
353. Mal D, Pahari P, De SR (2007) Regiospecific synthesis of 3-(2,6-dihydroxyphenyl) phthalides: application to the synthesis of isopestacin and cryphonectric acid. Tetrahedron 63:11781
354. Ohzeki T, Mori K (2001) Synthesis of corollosporine, an antibacterial metabolite of the marine fungus *Corollospora maritima*. Biosci Biotechnol Biochem 65:172
355. Paradkar MV, Kulkarni A, Joseph AR, Ranade AA (2000) An efficient synthesis of dimethoxyphthalides. J Chem Res:364
356. Talapatra B, Roy MK, Talapatra SK (1983) Syntheses of methyl ether of anaphatol and three other natural phthalides. J Indian Chem Soc 60:1169
357. Bellina F, Ciucci D, Vergamini P, Rossi R (2000) Regioselective synthesis of natural and unnatural (*Z*)-3-(1-alkylidene) phthalides and 3-substituted isocoumarins starting from methyl 2-hydroxybenzoates. Tetrahedron 56:2533
358. Kanazawa C, Terada M (2007) Organic-base-catalyzed synthesis of phthalides via highly regioselective intramolecular cyclization reaction. Tetrahedron Lett 48:933
359. Kuethe JT, Maloney KM (2013) A concise synthesis of 3,4-fused spiro[isobenzofuran-3-ones], spiro[furo[3,4-*b*]pyridin-5(7*H*)-ones], 3-aryl-, and alkylphthalides. Tetrahedron 69:5248
360. Mondal M, Argade NP (2004) DBU-induced phenol-keto resonance in 3,5-dihydroxyphthalide: regioselectivities in condensations with α, β-unsaturated aldehydes - facile synthesis of bioactive natural and unnatural benzopyrans. Synlett 7:1243
361. Ogawa Y, Maruno M, Wakamatsu T (1994) Efficient synthesis of hydroxyphthalides. Heterocycles 1:47
362. Li S, Wang Z, Fang X, Li Y (1993) Synthesis of (*Z*)-ligustilide. Synth Commun 23:2909

363. Kobayashi K, Shimizu H, Itoh M, Sugimone H (1990) An efficient synthesis of 5,7-dihydroxy-4-methylisobenzofuran-1(3*H*)-one, a metabolite of *Aspergillus flavus* and a key intermediate in the synthesis of mycophenolic acid. Bull Chem Soc Jpn 63:2435
364. Asaoka M, Miyake K, Takei H (1977) Synthesis of 7-hydroxyphthalides starting from unsaturated lactones via 2-trialkylsiloxyfurans. Chem Lett:167
365. Allison WR, Newbold GT (1959) Lactones. Part VI. The preparation of 5,7-dihydroxyphthalide, its methyl ether and related compounds. J Chem Soc:3335
366. Canonica L, Rindone B, Santaniello E, Scolastico C (1972) A total synthesis of mycophenolic acid, some analogues and some biogenetic intermediates. Tetrahedron 28:4395
367. Mali RS, Patil SR (1990) Synthesis of 3-butylidene-7-hydroxyphthalide. Synth Commun 20:167
368. Petrignet J, Inack Ngi S, Abarbri M, Thibonnet J (2014) Short and convenient synthesis of two natural phthalides by a copper(I) catalysed Sonogashira/oxacyclisation copper (I) process. Tetrahedron Lett 55:982
369. Ohzeki T, Mori K (2003) Synthesis and absolute configuration of (-)-3-butyl-7-hydroxyphthalide, a cytotoxic metabolite of *Penicillium vulpinum*. Biosci Biotechnol Biochem 67:2240
370. Jimenez R, Maldonado LA, Salgado-Zamora H (2010) Synthesis of demethylated nidulol via an intramolecular Michael reaction. Nat Prod Res 24:1274
371. Reddy RS, Kiran INC, Sudalai A (2012) CN-assisted oxidative cyclization of cyano cinnamates and styrene derivatives: a facile entry to 3-substituted chiral phthalides. Org Biomol Chem 10:3655
372. Schwaben J, Cordes J, Harms K, Koert U (2011) Total syntheses of (+)-pestaphthalide A and (-)-pestaphthalide B. Synthesis 18:2929
373. Oguro D, Watanabe H (2011) Asymmetric synthesis and sensory evaluation of sedanenolide. Biosci Biotechnol Biochem 75:1502
374. Pedrosa R, Sayalero S, Vicente M (2006) A direct efficient diastereoselective synthesis of enantiopure 3-substituted-isobenzofuranones. Tetrahedron 62:10400
375. Choi PJ, Sperry J, Brimble MA (2010) Heteroatom-directed reverse Wacker oxidations. Synthesis of the reported structure of (-)-herbaric acid. J Org Chem 75:7388
376. Kitahara T, Uchida K, Watanabe H, Usui T, Osada H (1998) Syntheses and bioactivities of acetophthalidin and its derivatives. Heterocycles 48:2649
377. Lin L, He X, Lian L, King W, Elliott J (1998) Liquid chromatographic-electrospray mass spectrometric study of the phthalides of *Angelica sinensis* and chemical changes of *Z*-ligustilide. J Chromatogr A 810:71
378. Quiroz-García B, Figueroa R, Cogordan JA, Delgado G (2005) Photocyclodimers from (*Z*)-ligustilide. Experimental results and FMO analysis. Tetrahedron Lett 46:3003
379. Fang L, Xiao X, Liu C, He X (2012) Recent advance in studies on *Angelica sinensis*. Chin Herb Med 4:12
380. Sowbhagya HB (2014) Chemistry, technology and nutraceutical function of celery (*Apium graveolens* L.): an overview. Crit Rev Food Sci Nutr 54:389
381. Chen XP, Li W, Xiao XF, Zhang LL, Liu CX (2013) Phytochemical and pharmacological studies on radix *Angelica sinensis*. Chin J Nat Med 11:577
382. Yang J, Chen H, Wu J, Gong S (2012) Advances in studies on pharmacological functions of ligustilide and their mechanisms. Chin Herb Med 4:26
383. Chen X, Dang TT, Facchini PJ (2015) Noscapine comes of age. Phytochemistry 111:7
384. Neerupma D, Ankur S, Archana S (2013) Noscapine: an anti-mitotic agent. World J Pharm Pharm Sci 3:324
385. DeBono A, Capuano B, Scammells PJ (2015) Progress toward the development of noscapine and derivatives as anticancer agents. J Med Chem 58:5699
386. Tripathi M, Reddy PL, Rawat DS (2014) Noscapine and its analogues as anti-cancer agents. Chem Biol Interface 4:1

387. Li W, Wu Y, Liu X, Yan C, Liu D, Pan Y, Yang G, Yin F, Weng Z, Zhao D, Chen Z, Cai B (2013) Antioxidant properties of *cis*-(*Z*,*Z*′)-3a.7a′,7a.3a′-dihydroxy-ligustilide on human umbilical vein endothelial cells in vitro. Molecules 18:520
388. Dietz BM, Liu D, Hagos GK, Yao P, Schinkovitz A, Pro SM, Deng S, Farnsworth NR, Pauli GF, van Breemen RB, Bolton JL (2008) *Angelica sinensis* and its alkylphthalides induce the detoxification enzyme NAD(P)H:quinone oxidoreductase 1 by alkylating Keap1. Chem Res Toxicol 21:1939
389. Qi H, Siu SO, Chen Y, Han Y, Chu IK, Tong Y, Lau ASY, Rong J (2010) Senkyunolides reduce hydrogen peroxide-induced oxidative damage in human liver HepG2 cells via induction of heme oxygenase-1. Chem Biol Interact 183:380
390. Du J, Yu Y, Ke Y, Wang C, Zhu L, Qian ZM (2007) Ligustilide attenuates pain behavior induced by acetic acid or formalin. J Ethnopharmacol 112:211
391. Lin Q, Zhao AG, Chen JN, Lai XP, Gui SH, Fang CP (2011) Anti-inflammatory and analgesic effects of ligustilide. Chin J Exp Med Formulae 17:165
392. Juárez-Reyes K, Ángeles-López GE, Rivero-Cruz I, Bye R, Mata R (2014) Antinociceptive activity of *Ligusticum porteri* preparations and compounds. Pharm Biol 52:14
393. Brindis F, Rodríguez R, Bye R, González-Andrade M, Mata R (2011) (*Z*)-3-Butylidenephthalide from *Ligusticum porteri*, an α-glucosidase inhibitor. J Nat Prod 74:314
394. Xiao B, Yin J, Park M, Liu J, Li JL, La Kim E, Hong J, Chung HY, Jung JH (2012) Design and synthesis of marine fungal phthalide derivatives as PPAR-gamma agonists. Bioorg Med Chem 20:4954
395. Zhang L, Du J-R, Wang J, Yu D-K, Chen Y-S, He Y, Wang C-Y (2009) *Z*-Ligustilide extracted from Radix *Angelica sinensis* decreased platelet aggregation induced by ADP ex vivo and arterio-venous shunt thrombosis in vivo in rats. Yakugaku Zasshi 129:855
396. Teng CM, Chen WY, Ko WC, Ouyang CH (1987) Antiplatelet effect of butylidenephthalide. Biochim Biophys Acta 924:375
397. Xu H, Feng Y (2001) Effects of 3-*n*-butylphthalide on thrombosis formation and platelet function in rats. Acta Pharm Sin 36:329
398. Naito T, Kubota K, Shimoda Y, Sato T, Ikeya Y, Okada M, Maruno M (1995) Effects of constituents of Chinese crude drug, Ligustici Chuanxiong Rhizoma, on vasoconstriction and blood viscosity. Nat Med 49:288
399. Or TCT, Yang CLH, Law AHY, Li JCB, Lau ASY (2011) Isolation and identification of anti-inflammatory constituents from *Ligusticum chuanxiong* and their underlying mechanisms of action on microglia. Neuropharmacology 60:823
400. Peng H-Y, Du J-R, Zhang G-Y, Kuang X, Liu Y-X, Qian Z-M, Wang C-Y (2007) Neuroprotective effect of (*Z*)-ligustilide against permanent focal ischemic damage in rats. Biol Pharm Bull 30:309
401. Kuang X, Yao Y, Du JR, Liu YX, Wang CY, Qian ZM (2006) Neuroprotective role of (*Z*)-ligustilide against forebrain ischemic injury in ICR mice. Brain Res 1102:145
402. Wu XM, Qian ZM, Zhu L, Du F, Yung WH, Gong Q, Ke Y (2011) Neuroprotective effect of ligustilide against ischaemia-reperfusion injury via up-regulation of erythropoietin and down-regulation of RTP801. Br J Pharmacol 164:332
403. Qi H, Han Y, Rong J (2012) Potential roles of PI3K/Akt and Nrf2-Keap1 pathways in regulating hormesis of (*Z*)-ligustilide in PC12 cells against oxygen and glucose deprivation. Neuropharmacology 62:1659
404. Peng B, Zhao P, Lu YP, Chen MM, Sun H, Wu XM, Zhu L (2013) *Z*-Ligustilide activates the Nrf2/HO-1 pathway and protects against cerebral ischemia-reperfusion injury in vivo and in vitro. Brain Res 1520:168
405. Mahmoudian M, Mehrpour M, Benaissa F, Siadatpour Z (2003) A preliminary report on the application of noscapine in the treatment of stroke. Eur J Clin Pharmacol 59:579
406. Chen D, Tang J, Khatibi NH, Zhu M, Li Y, Wang C, Jiang R, Tu L, Wang S (2011) Treatment with *Z*-ligustilide, a component of *Angelica sinensis*, reduces brain injury after a subarachnoid hemorrhage in rats. J Pharmacol Exp Ther 337:663

407. Kuang X, Du JR, Liu YX, Zhang GY, Peng HY (2008) Postischemic administration of (*Z*)-ligustilide ameliorates cognitive dysfunction and brain damage induced by permanent forebrain ischemia in rats. Pharmacol Biochem Behav 88:213
408. Ho CC, Kumaran A, Hwang LS (2009) Bio-assay guided isolation and identification of anti-Alzheimer active compounds from the root of *Angelica sinensis*. Food Chem 114:246
409. Kuang X, Du JR, Chen YS, Wang J, Wang YN (2009) Protective effect of (*Z*)-ligustilide against amyloid B-induced neurotoxicity is associated with decreased pro-inflammatory markers in rat brains. Pharmacol Biochem Behav 92:635
410. Cheng LL, Chen XN, Wang Y, Yu L, Kuang X, Wang LL, Yang W, Du JR (2011) *Z*-Ligustilide isolated from Radix *Angelica sinensis* ameliorates the memory impairment induced by scopolamine in mice. Fitoterapia 82:1128
411. Li J-J, Zhu Q, Lu Y-P, Zhao P, Feng Z-B, Qian Z-M, Zhu L (2015) Ligustilide prevents cognitive impairment and attenuates neurotoxicity in D-galactose induced aging mice brain. Brain Res 1595:19
412. Qi H, Zhao J, Han Y, Lau ASY, Rong J (2012) *Z*-Ligustilide potentiates the cytotoxicity of dopamine in rat dopaminergic PC12 cells. Neurotoxic Res 22:345
413. Matsumoto K, Kohno S, Ojima K, Tezuka Y, Kadota S, Watanabe H (1998) Effects of methylene chloride-soluble fraction of Japanese *Angelica* root extract, ligustilide and butylidenephthalide, on pentobarbital sleep in group-housed and socially isolated mice. Life Sci 62:2073
414. Bjeldanes LF, Kim I-S (1978) Sedative activity of celery oil constituents. J Food Sci 43:143
415. Straughan DW, Neal MJ, Simmonds MA, Collins GG, Hill RG (1971) Evaluation of bicuculline as a GABA antagonist. Nature 233:352
416. Curtis DR, Duggan AW, Felix D, Johnston GAR (1970) GABA-[aminobutyric acid], bicuculline, and central inhibition. Nature 226:1222
417. Huang JH, Johnston GA (1990) (+)-Hydrastine, a potent competitive antagonist at mammalian $GABA_A$ receptors. Br J Pharmacol 99:727
418. Branco C dos S, Scola G, Rodrigues AD, Cesio V, Laprovitera M, Heinzen H, Telles MDS, Fank B, de Freitas SCV, Coitinho AS, Salvador M (2013) Anticonvulsant, neuroprotective and behavioral effects of organic and conventional yerba mate (*Ilex paraguariensis* St. Hil.) on pentylenetetrazol-induced seizures in Wistar rats. Brain Res Bull 92:60
419. Sadek B, Kuder K, Subramanian D, Shafiullah M, Stark H, Lazewska D, Adem A, Kiec-Kononowicz K (2014) Anticonvulsive effect of nonimidazole histamine H_3 receptor antagonists. Behav Pharmacol 25:245
420. Yu S, You S (1984) Anticonvulsant effect of 3-*n*-butylphthalide and 3-*n*-butyl-4,5-dihydrophthalide. Acta Pharm Sin 19:566
421. Yang J, Chen Y (1984) Isolation and identification of anticonvulsive constituents of *Apium graveolens*. Chin Pharm Bull 19:670
422. Yu SR, Gao NN, Li LL, Wang ZY, Chen Y, Wang WN (1988) The anticonvulsant effect of 3-butylphthalide in rats. Acta Pharm Sin 23:656
423. Yu S, Gao N, Li L, Wang Z, Chen Y, Wang W (1988) Facilitated performance of learning and memory in rats by 3-*n*-butylphthalide. Zhongguo Yaoli Xuebao 9:385
424. Dong G, Feng Y (1999) Anticonvulsant effects of 3-*n*-butylphthalide and its optical isomers. Chin Pharmacol Bull 15:88
425. Lee TF, Lin YL, Huang YT (2007) Studies on antiproliferative effects of phthalides from *Ligusticum chuanxiong* in hepatic stellate cells. Planta Med 73:527
426. Aneja R, Dhiman N, Idnani J, Awasthi A, Arora SK, Chandra R, Joshi HC (2007) Preclinical pharmacokinetics and bioavailability of noscapine, a tubulin-binding anticancer agent. Cancer Chemother Pharmacol 60:831
427. Yang Z-R, Liu M, Peng X-L, Lei X-F, Zhang J-X, Dong W-G (2012) Noscapine induces mitochondria-mediated apoptosis in human colon cancer cells in vivo and in vitro. Biochem Biophys Res Commun 421:627

428. Landen JW, Lang R, McMahon SJ, Rusan NM, Yvon A, Adams AW, Sorcinelli MD, Campbell R, Bonaccorsi P, Ansel JC, Archer DR, Wadsworth P, Armstrong CA, Joshi HC (2002) Noscapine alters microtubule dynamics in living cells and inhibits the progression of melanoma. Cancer Res 62:4109
429. Zhou J, Panda D, Landen JW, Wilson L, Joshi HC (2002) Minor alteration of microtubule dynamics causes loss of tension across kinetochore pairs and activates the spindle checkpoint. J Biol Chem 277:17200
430. Ye K, Ke Y, Keshava N, Shanks J, Kapp JA, Tekmal RR, Petros J, Joshi HC (1998) Opium alkaloid noscapine is an antitumor agent that arrests metaphase and induces apoptosis in dividing cells. Proc Natl Acad Sci USA 95:1601
431. Momin RA, Nair MG (2002) Antioxidant, cyclooxygenase and topoisomerase inhibitory compounds from *Apium graveolens* Linn. seeds. Phytomedicine 9:312
432. Kan WLT, Cho CH, Rudd JA, Lin G (2008) Study of the anti-proliferative effects and synergy of phthalides from *Angelica sinensis* on colon cancer cells. J Ethnopharmacol 120:36
433. Tsai NM, Chen YL, Lee CC, Lin PC, Cheng YL, Chang WL, Lin SZ, Harn HJ (2006) The natural compound *n*-butylidenephthalide derived from *Angelica sinensis* inhibits malignant brain tumor growth in vitro and in vivo. J Neurochem 99:1251
434. Guo H, Li Z-H, Feng T, Liu J-K (2014) One new ergostane-type steroid and three new phthalide derivatives from cultures of the basidiomycete *Albatrellus confluens*. J Asian Nat Prod Res 17:107
435. Huang F, Li SJ, Lu XH, Liu AL, Du GH, Shi GG (2011) Two glutathione *S*-transferase inhibitors from Radix *Angelica sinensis*. Phytother Res 25:284
436. Kobayashi S, Mimura Y, Notoya K, Kimura I, Kimura M (1992) Antiproliferative effects of the traditional Chinese medicine Shimotsu-to, its component Cnidium Rhizome and derived compounds on primary cultures of mouse aorta smooth muscle cells. Jpn J Pharmacol 60:397
437. Kobayashi S, Mimura Y, Naitoh T, Kimura I, Kimura M (1993) Chemical structure-activity of Cnidium Rhizoma-derived phthalides for the competence inhibition of proliferation in primary cultures of mouse aorta smooth muscle cells. Jpn J Pharmacol 63:353
438. Lu Q, Qiu T-Q, Yang H (2006) Ligustilide inhibits vascular smooth muscle cells proliferation. Eur J Pharmacol 542:136
439. Liang MJ, He LC (2006) Inhibitory effects of ligustilide and butylidenephthalide on bFGF-stimulated proliferation of rat smooth muscle cells. Acta Pharm Sin 41:161
440. Yang P, Zhang W, Rui Y (2004) Use of ligustilide for prevention and treatment of atherosclerosis. Chin Pat 1543859
441. Miyazawa M, Tsukamoto T, Anzai J, Ishikawa Y (2004) Insecticidal effect of phthalides and furanocoumarins from *Angelica acutiloba* against *Drosophila melanogaster*. J Agric Food Chem 52:4401
442. Wedge DE, Klun JA, Tabanca N, Demirci B, Ozek T, Baser KHC, Liu Z, Zhang S, Cantrell CL, Zhang J (2009) Bioactivity-guided fractionation and GC/MS fingerprinting of *Angelica sinensis* and *Angelica archangelica* root components for antifungal and mosquito deterrent activity. J Agric Food Chem 57:464
443. Chae SH, Kim S Il, Yeon SH, Lee SW, Ahn YJ (2011) Adulticidal activity of phthalides identified in *Cnidium officinale* rhizome to B- and Q-biotypes of *Bemisia tabaci*. J Agric Food Chem 59:8193
444. Noto T, Sawada M, Ando K, Koyama K (1969) Some biological properties of mycophenolic acid. J Antibiot 22:165
445. Abraham EP (1945) The effect of mycophenolic acid on the growth of *Staphylococcus aureus* in heart broth. Biochem J 39:398
446. Jones EL, Epinette WW, Hackney VC, Menendez L, Frost P (1975) Treatment of psoriasis with oral mycophenolic acid. J Invest Dermatol 65:537
447. Hodge EE (1996) The role of mycophenolate mofetil in clinical renal transplantation. World J Urol 14:249

448. Staatz CE, Tett SE (2007) Clinical pharmacokinetics and pharmacodynamics of mycophenolate in solid organ transplant recipients. Clin Pharmacokinet 46:13
449. Van Gelder T, Hesselink DA (2015) Mycophenolate revisited. Transpl Int 28:508
450. Cégiéla-Carlioz P, Bessière JM, David B, Mariotte AM, Gibbons S, Dijoux-Franca MG (2005) Modulation of multi-drug resistance (MDR) in *Staphylococcus aureus* by Osha (*Ligusticum porteri* L., Apiaceae) essential oil compounds. Flavour Fragr J 20:671
451. Radcliff FJ, Fraser JD, Wilson ZE, Heapy AM, Robinson JE, Bryant CJ, Flowers CL, Brimble MA (2008) Anti-*Helicobacter pylori* activity of derivatives of the phthalide-containing antibacterial agents spirolaxine methyl ether, CJ-12,954, CJ-13,013, CJ-13,102, CJ-13,104, CJ-13,108, and CJ-13,015. Bioorg Med Chem 16:6179
452. Awaad AS, El-Meligy RM, Soliman GA (2013) Natural products in treatment of ulcerative colitis and peptic ulcer. J Saudi Chem Soc 17:101
453. Guzman JD, Evangelopoulos D, Gupta A, Prieto JM, Gibbons S, Bhakta S (2013) Antimycobacterials from lovage root (*Ligusticum officinale* Koch). Phytother Res 27:993
454. Qin XD, Dong ZJ, Liu JK, Yang LM, Wang RR, Zheng YT, Lu Y, Wu YS, Zheng QT (2006) Concentricolide, an anti-HIV agent from the ascomycete *Daldinia concentrica*. Helv Chim Acta 89:127
455. Azuma M, Yoshida M, Horinouchi S, Beppu T (1990) Basidifferquinone, a new inducer for fruiting-body formation of a Basidiomycetes *Favolus arcularius* from a *Streptomyces* strain I. Screening and isolation. Agric Biol Chem 54:1441
456. Azuma M, Yoshida M, Horinouchi S, Beppu T (1993) Basidifferquinone analogues, basidifferquinone B and C, which induce fruiting-body formation of a basidiomycete, *Favolus arcularius*. Biosci Biotechnol Biochem 57:344
457. Sekiya K, Tezuka Y, Tanaka K, Prasain JK, Namba T, Katayama K, Koizumi T, Maeda M, Kondo T, Kadota S (2000) Distribution, metabolism and excretion of butylidenephthalide of Ligustici Chuanxiong Rhizoma in hairless mouse after dermal application. J Ethnopharmacol 71:401
458. Yan R, Nga LK, Li SL, Yun KT, Lin G (2008) Pharmacokinetics and metabolism of ligustilide, a major bioactive component in Rhizoma Chuanxiong, in the rat. Drug Metab Dispos 36:400
459. Ding C, Sheng Y, Zhang Y, Zhang J, Du C (2008) Identification and comparison of metabolites after oral administration of essential oil of *Ligusticum chuanxiong* or its major constituent ligustilide in rats. Planta Med 74:1684
460. Guo J, Duan JA, Shang EX, Tang Y, Qian D (2009) Determination of ligustilide in rat brain after nasal administration of essential oil from Rhizoma Chuanxiong. Fitoterapia 80:168
461. Ma Z, Bai L (2013) Anti-inflammatory effects of *Z*-ligustilide nanoemulsion. Inflammation 36:294
462. Lu Y, Liu S, Zhao Y, Zhu L, Yu S (2014) Complexation of *Z*-ligustilide with hydroxypropyl-β-cyclodextrin to improve stability and oral bioavailability. Acta Pharm 64:211

Alejandra León graduated with a B.Sc. degree in Chemical Pharmaceutical Biology at the Universidad Nacional Autónoma de México (2004), where she also obtained her Ph.D. with honors (2011) under the supervision of Dr. Guillermo Delgado, working on the isolation, semisynthesis, chemical reactivity, and bioactivity of natural products isolated from different plant sources. She performed part of her graduate work in the group of Prof. Olov Sterner (2008), in Lund, Sweden, carrying out chemical transformations of phthalides. From 2013 to 2015, she conducted postdoctoral work at the Universidad Autónoma del Estado de Morelos, Mexico, under the guidance of Dr. Laura Álvarez, isolating bioactive podophyllotoxin type-lignans and triterpenes, and working on their semisynthesis. Her research interests and experience include the chemistry and biology of natural products, as well as the development of NMR methodology. She has published ten research papers in international journals and is a member of the Mexican Chemical Society.

Mayela Del Ángel was born in Saltillo, Coahuila, México. She completed her B.Sc. degree in Chemical Pharmaceutical Biology with a specialization on Industrial Pharmacy at the Universidad Autónoma de Coahuila. Her B.Sc. thesis focused on the biomimetic synthesis of polyaniline, and was conducted at the Department of Advanced Materials of the Centro de Investigación en Química Aplicada (CIQA). She obtained her M.Sc. degree in Chemical Biological Sciences with a specialization in toxicology at the Department of Pharmacy of the Instituto Politécnico Nacional, in Mexico City. Her M.Sc. thesis dealt with the antiteratogenic effect of curcumin. Her Ph.D. degree was in Biomedical Sciences from the Universidad Nacional Autónoma de México, and she investigated the anti-inflammatory and antiteratogenic effect of some natural and semisynthetic products from *Ligusticum porteri*. Her research interests include the in vitro and in vivo evaluation of the biological activities of natural products and other compounds, as well as the investigation of natural and synthetic products in the neurosciences.

José Luis Ávila was born in Mexico City in 1989. He studied at the School of Chemistry, Universidad Nacional Autónoma de México (UNAM), where he obtained his B.Sc. (2012) and his M.Sc. degree (2015, with honors) in chemistry, working on the isolation, characterization, chemical reactivity, and biological properties of phthalides from *Ligusticum porteri*. He is currently doing his Ph. D. thesis at the Institute of Chemistry, UNAM, under the guidance of Dr. Guillermo Delgado, investigating the chemical reactivity, synthesis and biological properties of naturally occurring compounds found in selected Mexican plants used traditionally for medicinal and agronomical purposes. His main academic interests include the chemical reactivity, biological activity, synthesis, and structural determination of organic natural products.

Guillermo Delgado was born in Mexico City, and received his B.Sc., M.Sc., and Ph. D. degrees in Chemistry from the Universidad Nacional Autónoma de México, under the guidance of Professor Alfonso Romo de Vivar, followed by academic stays at the Swiss Federal Institute (ETH), Zürich, Switzerland and at the Skaggs Institute of Chemical Biology, Scripps Research Institute, La Jolla, CA, USA, with Professor Albert Eschenmoser. He has received the Award of the Mexican Academy of Sciences in Scientific Research, and the National Prize of Chemistry, awarded by the Mexican Chemical Society, among other accolades. His research interests are focused mainly on the exploration of both chemical and biological space, particularly on the structure, chemical reactivity, semisynthesis, and bioactivity of natural products, and their ecological significance. He is currently Professor of Chemistry at UNAM.